UNIVERSITAT DE VALÈNCIA

DOCTORADO EN BIOMEDICINA Y FARMACIA

“NT-3 IN CARDIOVASCULAR PATHOLOGIES”

ANDREA MARCELA ZAMBRANO COBOS

TESIS DOCTORAL

Valencia, 2019

DIRECTORAS:

Pilar D’Ocón Navaza

Ma. Dolores Ivorra Insa

Ma. Antonia Noguera Romero

Dña. **Pilar D'Ocón Navaza**, Dña. **Mª Dolores Ivorra Insa** y Dña. **Mª Antonia Noguera Romero**

CERTIFICAN:

Que el trabajo presentado por la Lda. **Andrea Marcela Zambrano Cobos**, titulado **"NT-3 in cardiovascular pathologies"**, para obtener el grado de Doctor, ha sido realizado en la Universitat de València en el Departamento de Farmacología, bajo nuestra dirección y asesoramiento. Concluido el trabajo experimental y bibliográfico, autorizamos la presentación de la Tesis, para que sea juzgado por el tribunal correspondiente.

Lo que firmamos en Valencia a 14 de febrero de 2019

Pilar D'Ocón Navaza *Mª Dolores Ivorra Insa* *Mª Antonia Noguera Romero*

“¡Oh quanta glòria és per a nosaltres haver

travessat tanta mar i haver arribat bé al

port desitjat de la nostra felicitat!”

Tirant lo Blanc

Joanot Martorell

A mis padres,

Quiero mostrar mi gratitud a todas aquellas personas que estuvieron presentes en la realización de esta meta tan importante para mí.

Primero, me gustaría expresar mi sincera gratitud a mis tres directoras, a Pilar D'Ocón, por su confianza y apoyo en la dirección de la tesis, a María Dolores Ivorra por guiarme y por lo mucho que he aprendido todo este tiempo de ella y a María Antonia Noguera por ser no solo mi directora sino una compañera.

Además de a mis directoras, me gustaría agradecer a mis compañeros del laboratorio, a Fermín por tenerme paciencia, por su inmenso apoyo y amabilidad para solucionarlo todo. A Cristina por guiarme y mostrarme el camino correcto dentro del laboratorio. A María, por todo el apoyo que he recibido durante estos años, las palabras no pueden expresar mis sentimientos ni mi agradecimiento por toda su ayuda. Sin el apoyo de mis compis no hubiera sido posible llevar a cabo esta investigación, fue un placer trabajar con ustedes.

A todos los profesores del departamento de farmacología, de manera especial a Terens y Nuria por sus consejos y conversaciones estimulantes. Así como, al personal de secretaría: a Mamen, Inés, Irene, Mati y Carlos por su ayuda recibida este tiempo.

También, me gustaría agradecer al grupo de "compis" de inflamación: Miguel, Carmen, Elena, Josep, Asun y María José por buenos momentos y experiencias que nos ha regalado el doctorado dentro y fuera del laboratorio. De manera especial a Laura C, por su confianza, apoyo y experiencias compartidas.

Mi agradecimiento también va para Cristina Espinosa, por motivarme, inspirarme y animarme a lo largo de la escritura de esta tesis.

La amistad es un gran valor muy importante para mí. Me gustaría agradecer a Lola y Laura V, por regalarme dosis de positivismo y alegría, por compartir conmigo buenos y no tan buenos momentos. A María Tecno, por esa amistad incondicional y ponerle color a mis días. A Patrice y Manu, por aportarme confianza y tenerme en cuenta para todo. A mi Enana, por esos años de amistad y de convivencia juntas, por ser mi familia en Valencia. A Héctor por regalarme siempre conversaciones provechosas y un bonito sentimiento. A gente linda que

he ido conociendo y que han hecho que mis días sean mejores: Juan Ramón, Oscar, Emilio, Andrea, Ángel, Juana y Blanca.

Por último, pero no menos importante, me gustaría agradecer a la base de todo esto, mi familia, que han entendido mi ausencia y me han apoyado siempre: a mis padres por ese amor incondicional, por ser mi norte y luz en el camino, por ser un ejemplo de superación y por todo su amor. A Mari y Luis por escucharme, comprenderme y apoyarme. A mi abuelita, tíos y primos gracias por regalarme siempre un mensaje de apoyo y felicidad.

¡Muchas gracias a todos ustedes por construir conmigo este logro!

This Thesis was supported by the following grants:

Fellowship:

Programa Santiago Grisolia funded by Generalitat Valenciana

Project:

The *Neurotrofina-3, nueva diana terapéutica en patología cardiovascular* Project was supported by Comisión Interministerial de Ciencia y Tecnología (CICYT) Proyecto SAF: 2013-45362-R

ABBREVIATIONS

ACE	Angiotensin-converting enzyme
ACH	Acetylcholine
ADCF	Adipocyte-derived contractile factors
ADRFs	Adipocyte-derived relaxing factors
AKT	Protein kinase B/Akt
Ang	Angiotensin
ANOVA	Analysis of variance
ANS	Autonomous enteric nervous system
APS	Ammonium persulfate
AR	Adrenergic receptors
ATP	Adenosine triphosphate
BAT	Brown adipose tissue
BDNF	brain-derived neurotrophic factor
BH_4	5,6,7,8-tetrahydrobiopterin
BMI	Body mass index
BP	Blood pressure
BSA	Bovine serum albumin
Ca^{2+}	Calcium ions
cAMP	Cyclic adenosine 3′,5′-monophosphate
cDNA	Complementary DNA
cGMP	Cyclic guanosine monophosphate
CO2	Carbon dioxide
CRC	Concentration-response curve
CRC2	Second CRC
Ct	Thereshold cycle
DC	Dilated cardiomyopathy
DEPEC	Diethylpyrocarbonate
DGXI	General Direction for the Environment
DMEM	Dulbecco's modified Eagle's
DMSO	Dimethyl sulfoxide
dNTP	Deoxinucleoside triphosphate
EC	Endothelial cell
EDRF	Endothelium-derived relaxation factor
EGF	Epidermal growth factor
Emax	Maximal relaxant response
eNOS	Endothelial NOS
$eNT3^-$	Knockout mice with NT-3 deleted from endothelium
$eNT3^+$	Control mice
Eph	Ephrin
ERK1/2	Extracellular signal-regulated kinases
ET-1	Endothelin

FCS	Fetal calf serum
FGFs	Fibroblast growth factors
GAPDH	Glyceraldehyde 3-phosphate dehydrogenase
GF	Growth factor
GOT	Glutamate oxaloacetate transaminase
GPT	Glutamate piruvate transaminase
HAoAF	Human aortic adventitial fibroblasts
HAoEC	Human aortic endothelial cells
HAoSMC	Human aortic smooth muscle cells
HCAEC	Human coronary artery endothelial cells
HCF	Human cardiac fibroblasts
HCM	Human cardiac myocytes
HCMEC	Human cardiac microvascular endothelial cells
HF	Heart failure
HTZ	Heterozygous mice
HUVEC	Human umbilical vein endothelial cells
IC	Ischemic cardiomyopathy
IGF-1	Insulin-like growth factor-1
iNOS	Enzyme inducible NOS
ISO	Isoprenaline hemisulfate
JNK	JUN N-terminal kinase
KCl	Potassium chloride
kDa	KiloDalton
L-NAME	L-N^G-Nitroargine methyl ester
L-NMMA	L-N^G-monomethyl-L-argenine
L-NMA	N^G-Nitroargine methyl ester
LV	Left ventricle
LVEF	Left ventricular ejection fraction
LVESD	Left ventricular end-systolic diameter
LVEDD	Left ventricular end-diastolic diameter
MAPK	Mitogen-activated protein kinase
MGB	Minor groove binder
mRNA	Messenger RNA
MTT	3-(4,5-Dimethyl-2-thiazolyl)-2,5-diphenyl-2H-tetrazolium bromide
NF	Neurotrophic factor
NFG	Nerve growth factor
NFQ	Nonfluorescence quencher
nNOS	Neuronal NOS
NO	Nitric oxide
NO_2	Nitrate
NO_3	Nitrite
NOS	Nitric oxide synthase
NPY	Neuropeptide Y

NSCs	Adult neural stem cells
NT	Neurotrophins
NTF3	Neurotrophin-3 gene
$NT3^{+/+}$	$Ntf3^{+/+}$ Wild-type mice
$NT3^{+/-}$	$Ntf3^{+/lacZneo}$ heterozygousmice
NT-3	Neurotrophin-3
NT-4	Neurotrophin-4/5
NTRK3	Neurothrophic receptor tyrosine kinase 3
NT-proBNP	N-terminal proB-type natriuretic peptide
NYHA	*New York Heart Association*
P1	First protocol
P2	Second protocol
P3	Third protocol
P4	Four protocol
$p75^{NTR}$	p75 neurotrophin receptor
PB	Phosphate buffered
PBS	Phosphate buffered saline
PBST	PBS containing 0.1% Tween 20
PDVF	Polyvinylidene fluoride
pEC50	-log of the agonist concentration needed to produce 50% of Emax
pEC_{50} (1)	Site high affinity
pEC_{50} (2)	Site low affinity
PGI2	Prostacyclin
PHE	Phenylephrine hydrocholoride
PI3K	Phosphoinositide 3-kinase
PKA	Cyclic AMP-protein kinase A
PKC	Protein kinase C
PNS	Parasympathetic nervous system
proNT	Pro-neurotrophins
PVAT	Perivascular adipose tissues
+PVAT	Thoracic aorta with PVAT
-PVAT	Thoracic aorta clean or without PVAT
qPCR	Quantitative polymerase chain reaction
RT	Reverse transcription
SDS	Sodium dodecyl sulfate
SEM	Standard Error of Mean
SHR	Spontaneously Hypertensive Rat
SNS	Sympathetic nervous system
SVZ	Stem cells in the ventricular zone
TEMED	N,N,N′,N′-tetramethylethylenediamine
TH	Tyrosine hydroxylase
TNF	Tumor necrosis factor
TNS	Trypsin neutralization solution
Trk	Tropomyosin-related kinase

TrkA	Tropomyosin-related kinase A
TrkB	Tropomyosin-related kinase B
TrkC	Tropomyosin-related kinase C
VSMCs	Vascular smooth muscle cells
VEGF	Vascular endothelial growth factor
WAT	White adipose tissue
WKY	Wistar Kyoto Rat
WT	Wild-type mice
α-AR	Alpha-adrenoceptors
β-AR	Beta-adrenoceptors

INDICE

I INTRODUCTION

1. THE CARDIOVASCULAR SYSTEM

1.1 INNERVATION IN THE CARDIOVASCULAR SYSTEM

The autonomic nervous system (ANS) consists of motor neurons that control smooth muscles, cardiac muscles, and glands. ANS is divided into sympathetic nervous system (SNS) and parasympathetic nervous system (PNS) with opposite effects on target organs by the activation of adrenergic and cholinergic receptors. (Femminella et al., 2016).

The heart is innervated by autonomic nerve fibres, both SNS and PNS, which form the cardiac plexus. The branches of the cardiac plexus innervate the conduction tissue, the coronary blood vessels, and the myocardium. Sympathetic and parasympathetic nerves provide the final common pathway for neural control of cardiovascular targets. SNS (adrenergic) releases catecholamine transmitters (noradrenaline and adrenaline) and neuropeptide Y (NPY) that promotes changes in vascular contractility, increases heart rate, enhances cardiac contractility, and promotes growth of vascular endothelial cells (ECs) and vascular smooth muscle cells (VSMCs). Conversely, parasympathetic nerves decrease heart rate through the release of acetylcholine (ACH) and also regulate vascular pressure (Damon, 2008; Femminella et al., 2016).

Blood vessels are richly innervated by sympathetic nerve and express adrenergic receptors (ARs) to promote vasoconstrictor or vasodilator responses induced by catecholamine transmitters or sympathomimetic drugs (Bradley et al., 2003; Damon, 2008; Femminella et al., 2016). The ARs are divided into α and β-receptors (α-ARs; β-ARs). The α-family was split into two subfamilies α_1 and α_2, with the α_1 subfamily comprising three members, α_{1A}, α_{1B}, and α_{1D}. α_1- are localized in VSMCs and induce blood vessel constriction. α_2-ARs (α_{2A}, α_{2B}, α_{2C}) can also modulate the vasoconstrictor response in smooth muscle. β-AR family consists of three subtypes such as β_1, β_2, and β_3. β-ARs increase heart rate, contraction force and vascular smooth muscle relaxation. The β_1 subtype predominates in the human heart and have a critical role in cardiopathologies including heart failure (HF) (Femminella et al., 2016).

1.2 HEART STRUCTURE

1.2.1 Pericardium

The pericardium is a membrane which surrounds and protects the heart. It is composed of an outer fibrous and an inner double-layered serous pericardium. Serous pericardium includes visceral layer and parietal layer that are separated by the pericardial cavity (Illustration 1). The parietal layer is considered the outer layer of heart wall (epicardium) (Sharma & Waymack, 2018).

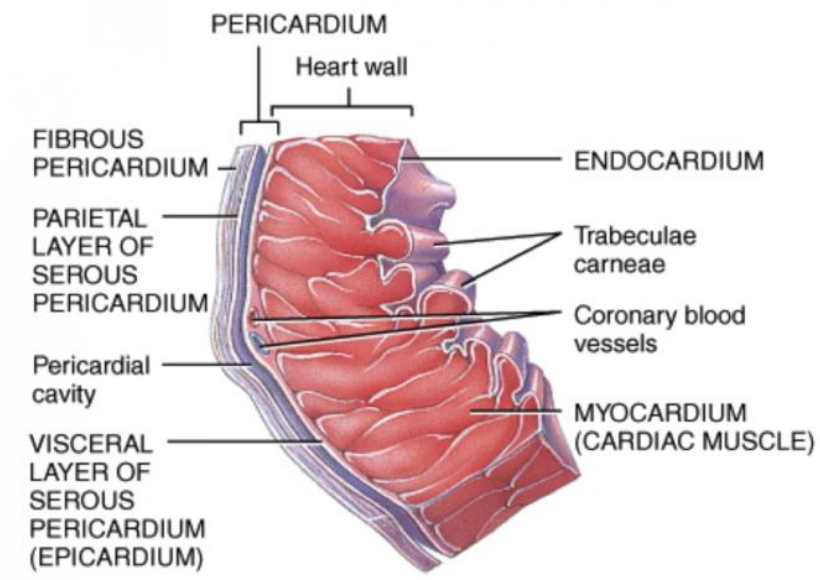

Illustration 1*. Section of the heart wall (Available from: http://www.piqqem.com/immaculate-layers-of-the-heart-wall-for-your-residence-concept/).*

1.2.2 Heart wall

The heart wall is composed of three layers: an outer layer, called the **epicardium** (visceral layer of serous pericardium), formed by an endothelium serous membrane and inner lining connective tissue, which enters in contact with the blood (Rodriguez & Tan, 2017). It includes elastic and collagen fibres, blood vessels, and specialized muscle fibres. An intermediate layer, called **myocardium**, which is a contractile muscle mass that contains connective tissue, blood capillaries, lymphatic capillaries, and nerve fibres. An inner layer, called the **endocardium**, which covers the inside of the heart and continues with the endothelium of the great thoracic vessels.

The heart is the first organ to develop and function. During cardiogenesis, the endothelium and endocardium transmit hemodynamic cues to the underlying cells: myocytes, fibroblasts, and smooth muscle cells. Accordingly, heart development engages not only the endothelial/endocardial inner lining, but also myocardial, epicardial, smooth muscle, and neuronal cells, and fibroblasts derived from their precursors (Poelmann & Gittenberger-de Groot, 2018).

1.3 BLOOD VESSELS STRUCTURE

The vasculature plays a critical role to uptake oxygen from the alveoli, distributes blood, and exchanges gas and nutrition between the blood and the surrounding tissue. Blood vessels are part of cardiovascular system; arteries are responsible for carrying blood from the heart to other parts of our body. This flows into small arteries, arterioles, which bind to the capillaries. The aorta is the main artery in human body and is originated from the left ventricle (LV) of the heart to the abdomen. Anatomically, the aorta is divided into four sections such as ascending aorta, aortic arch, thoracic aorta and abdominal aorta. On the venous side, venules are smallest vessels that progressively form the large veins until the venae cavae. Capillaries connect arterioles to venues. Venus have thinner wall than arteries even though veins are largest. (Zhao et al., 2015).

All blood vessels are composed of layers: tunica intima, media, and adventitia (Illustration 2). The **tunica adventitia or externa** consists of nerves endings, connective elements (fibroblasts and collagen), and perivascular adipose tissue (PVAT). A basic function of this layer is to protect and provide structural support to the vessels. The **tunica media** is the thickest layer of arterial tunics and includes collagen, elastin, and smooth muscle. This layer lends muscular support to the vessel and mediates the constrictions and dilatation of the blood vessels. The **tunica intima**, the thinnest and innermost layer of the blood vessels, consists of endothelial cells (ECs) and connective tissue composed of collagen and elastic fibres. It acts a barrier between the blood in the lumen and the surrounding tissues (Bouis 2001; Zhao et al., 2015).

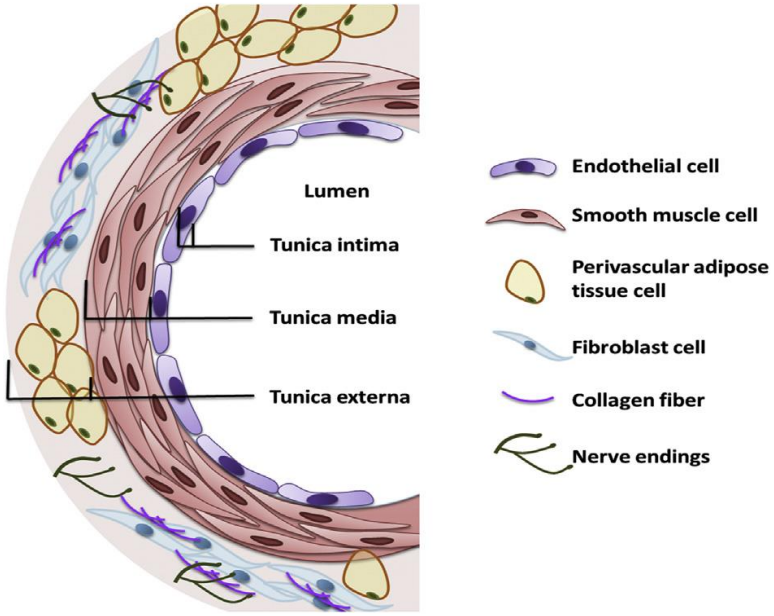

Illustration 2. Structure of arterial wall. *Tunica intima, tunica media, and tunica adventitia or externa (Zhao et al., 2015).*

1.3.1 Endothelium

The vascular endothelium, a structurally simple and functionally complex organ, is a monolayer of cells which forms the wall of capillaries. The microvascular circulation involves a network of capillary ECs that connects arterioles to venules and represents more than 95% of the total circulatory surface area (Paz & Amore, 2014). The wall of the largest blood vessels is lined across the innermost surface, by a thin layer of ECs, thereby the endothelium is considered as the guardian of the vascular wall. ECs play a critical role in the physiology of vascular integrity and tone; but their function also depends on the localization and size of their corresponding blood vessels.

ECs are different in morphology and are derived from mesodermal stem cells, which are the source of angioblasts and hematopoietic stem cells. Angioblasts differentiate into ECs. During the development, the endothelium includes dynamic processes that involve growth factors (GFs) in cell proliferation and migration (Aird, 2007; Chester et a., 2017; Paz & Amore, 2014). The human body contains 10 trillion-60 trillion ECs, with a total weight in an adult of 720 g (Bouïs et al., 2001; Rafii et al., 2016). ECs supply blood to the most tissues of our body and prevent diffusion of proteins, regulate passage of immune cells, and separate

blood from the tissues. In the circulatory system, the main physiological functions are to maintain the homeostasis, the control of vascular tone, migration, creation, and remodelling of the vasculature (Paz & Amore, 2014; Rajendran et al., 2013; Staton et al., 2009). The endothelium has also anti-coagulant and anti-thrombotic activity that regulates blood coagulation and platelet activation.

Due to lack of availability human endothelial tissues, endothelial physiology has been studied in cell cultures. The first culture of ECs from umbilical veins was described by Jaffe et al. (1973) which identified ECs according to morphologic and immunologic criteria.

ECs are pharmacology targets to investigate cardiovascular diseases. Abnormalities in the structure and function of vascular endothelium promote the development of atherosclerotic lesions. Endothelial dysfunction has become in the main focus of study in cardiovascular pathologies (Chester et al., 2017; Kermani et al., 2005; Rajendran et al., 2013).

1.3.1.1 Endothelial cells and NO

The endothelium modulates the vascular tone by releasing active molecules such as nitric oxide (NO), prostacyclin (PGI_2) and endothelin (ET-1), which have direct effects on the vessel wall. PGI2 is a vasodilator and anti-aggregating substance that is enhanced by the presence of NO, whereas ET-1 is a vasoconstrictor and a functional antagonist to the vasodilator effects of NO (Chester et al., 2017).

In 1980, a study demonstrated that ACH interacts with ECs to stimulate the formation of a factor called endothelium-derived relaxation factor (EDRF) (Furchgott & Zawadzki, 1980). This report has been important to guide the study of cardiovascular system. Seven years later, EDRF was described as NO (Furchgott, 1988; Ignarro et al., 1988; Moncada et al., 1988).

NO enzymatic production is generated upon the conversion of L-arginine to L-citrulline by three isoforms of nitric oxide synthase (NOS) (Table 1). Two constitutive forms: endothelial NOS (eNOS), produced mainly in ECs, and neuronal NOS (nNOS), mainly in neuronal cells, and the inducible isoform NOS (iNOS) in immune cells; for instance, in response to abnormal cell processes such as HF (Dias et al., 2011; Sukhovershin et al., 2015). The inhibitors of NOS,

including L-N^G-monomethyl-L-argenine (L-NMMA), L-N^G-Nitroargine methyl ester (L-NAME), and N^G-Nitroargine methyl ester (L-NMA) have allowed to determine the role of NO in the vascular system (Cannon, 1998; Chester et al., 2017).

All NOS bind calmodulin and utilise L-arginine and molecular oxygen as substrates. Enzymes contain haem and require the co-factors nicotinamide-adenine-dinucleotide phosphate, flavin adenine dinucleotide, flavin mononucleotide, and (6R-) 5,6,7,8-tetrahydrobiopterin (BH_4). Isoforms of NOS differ in dependence on calcium, amount of NO produced, distribution, structure and function (Chester et al., 2017).

Table 1. Characteristics NO isoforms (Chester et al., 2017)

Isoform	Chromosome locus	Main localization sites
nNOS (NOS I)	12q24.2	Neuronal tissue, skeletal muscle
iNOS (NOS II)	17cen-q12	Immune system, cardiovascular system
eNOS (NOS III)	7q35-36	Endothelium

NOS: Nitric oxide synthase; eNOS: Endothelial NOS; nNOS: Neuronal NOS; iNOS: Inducible NOS

NO is a reactive molecule with an unpaired electron in its nitrogen atom. This property is responsible for its ultrashort half-life (3-5 seconds) (Chester et al., 2017). NO is released from the endothelium as a gas and stimulates soluble guanylyl cyclase, elevating concentrations of cyclic GMP, to regulate physiological process including vascular tone, myocardial contractility, cell proliferation, inflammation, and oxidative stress among others (Tousoulis et al., 2012). For instance, in an inflammation environment, this molecule inhibits the synthesis and expression of cytokines and cell adhesion molecules that attract inflammatory cells.

1.3.1.2 Endothelial cells and angiogenesis

Angiogenesis and vasculogenesis are modes of formation of new vessels from endothelial progenitor cells; hence, they are responsible for the development of the vascular system (Illustration 3).

Vasculogenesis is a crucial process for blood vessel formation during embryonic development (Carmeliet, 2005; Carmeliet & Jain, 2011; Pepper, 1997; Risau & Flamme, 1995). Angiogenesis consists of the formation of new capillaries from pre-existing blood vessels, which results in new capillary networks and involves the migration and proliferation of differentiated ECs (Carmeliet, 2000; Emanueli et al., 2014; Pepper, 1997; Roskoski, 2007). These capillary networks consist of ECs tubes lacking additional structures, such as smooth muscle cells and cells of the adventitial layer. Additionally, this network is formed by extracellular matrix proteins, and angiogenic factors (Adair & Montani. 2010; Bowers & Baudino, 2010; Folkman, 1997; Heil et al., 200, Lazarovici et al., 2018; Sinha et al., 2011). Vasculogenesis is restricted to embryonic development, whereas angiogenesis occurs during development and continues in the postnatal period and adulthood.

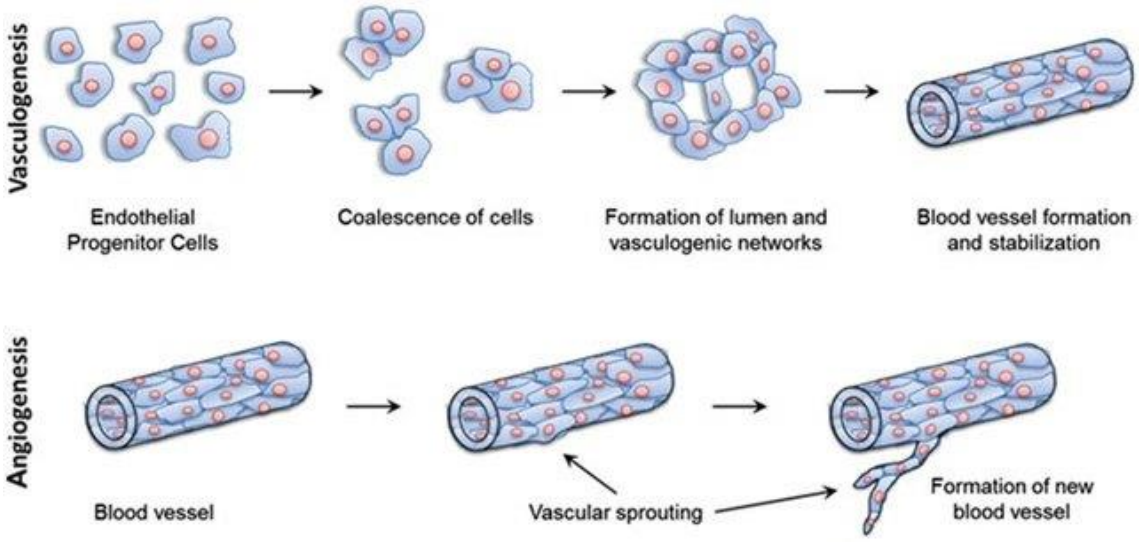

***Illustration 3**. **Vascular system.** New blood vessel formation occurs via vasculogenesis and angiogenesis (Peak et al., 2015).*

During angiogenesis, ECs exit blood vessels and migrate towards an angiogenic stimulus. Subsequent, ECs proliferate and provide a necessary number of cells for making a new vessel. Finally, the new population of ECs reorganizes into a tubular structure (Emanueli et al., 2002; Lazarovici et al., 2018). In capillaries growing and forming new vessels exist a regulated increase in vascular permeability. This vascular permeability can be increased during the angiogenesis and produce a pathological angiogenesis (Bates & Harper, 2002).

Two types of angiogenesis occur in utero and in adults (Illustration 4): (i) sprouting angiogenesis composed of emergent ECs which grow toward an angiogenic stimulus and can add blood vessels to portions of tissues previously barren of blood vessels; and (ii) intussusceptive angiogenesis involves the formation of blood vessels by a process of division in which elements of interstitial tissues invade existing vessels; therefore, this type is rapid and efficient compared with sprouting angiogenesis (Adair & Montani, 2010).

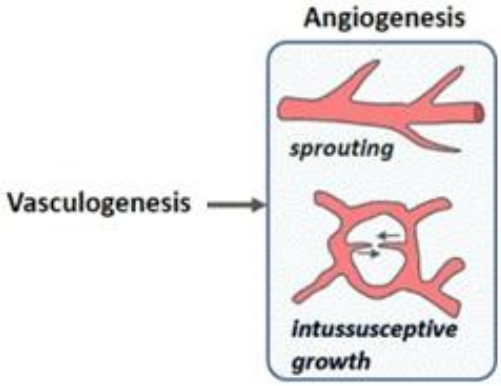

Illustration 4. Types of primary vascular growth. *Sprouting angiogenesis composed of emergent ECs, and intussusceptive angiogenesis involves the formation of blood vessels by a process of division in which elements of interstitial tissues invade existing vessels. This type is rapid and efficient compared with sprouting angiogenesis (Modified from Adair & Montani, 2010).*

Angiogenesis is subject to a complex control determined by a physiological balance between positive and negative regulators (pro-angiogenic and anti-angiogenic factors, respectively) (Hoeben et al., 2004; Pepper, 1997). Positive regulators predominate in the activated endothelium, whereas negative regulators predominate in the quiescent endothelium (Pepper, 1997). This is essential for the development of physiological processes such as wound healing, tissue regeneration, bone remodelling, formation of the corpus luteum and the placenta (Ebrahim & El Sayed, 2016; Hoeben et al., 2004; Roskoski, 2007). Moreover, angiogenesis restores blood perfusion of hypoxic tissue and promotes the development of collateral vasculature in the ischemic tissue. In addition, angiogenesis plays a critical role in pathological processes such as the progression of tumours and metastases, rheumatoid arthritis, retinopathies, and psoriasis (Ebrahim & El Sayed, 2016; Ferrara & Kerbel, 2005; Hoeben et al.,

2004). On the other hand, insufficient angiogenesis contributes to the development of cardiovascular pathologies because the poor circulation in tissue.

Angiogenesis is a complex process that comprises three sequential phases: quiescence, activation, and resolution. The first phase, **quiescence**, occurs when the ECs are in quiescence forming a monolayer of cells interconnected by binding molecules. In this state, ECs are coated with pericytes that suppress their proliferation and release survival signals (Carmeliet & Jain, 2011).

In **activation** phase, the onset of angiogenesis occurs by angiogenic stimulus that activate ECs, increases vascular permeability (Pepper, 1997), and produces pericytes detachment from the vessel wall (Carmeliet & Jain, 2011). Once activated, angiogenesis begins with the local destruction of the wall of the pre-existing blood vessels along with the activation, proliferation, and migration of ECs. This process begins to form tubular structures around the walls of the vessels that are continuously in formation. During the maturation of the vascular bed, the capillaries become large vessels, arteries, and veins (Carmeliet & Jain, 2011).

Finally, in **resolution** phase, the maturation of the vessels includes the inhibition of the proliferation and migration of the ECs, reconstitution of the basement membrane, and stabilization of the vessel wall by the recruitment and differentiation of pericytes and smooth muscle cells (Roskoski, 2007).

Angiogenesis is regulated by a variety of GFs and inhibitors (Freedman & Isner, 2001). GFs act through binding to a group of receptors belonging to the tyrosine kinases. They include vascular endothelial growth factor (VEGF), angiopoietin, ephrin families, fibroblast GF, the hypoxia-1 inducible factor, and NTs (Bates & Harper, 2002; Bir et al., 2012; Carmeliet & Jain, 2011; Emanueli et al., 2002; Heil et al., 2006). VEGF is the most potent angiogenic factor that can stimulate selectively ECs to secrete proteases, proliferate, and form new capillaries. Additionally, VEFG is involved in the maintenance and restoration of peripheral nerve integrity (Emanueli et al., 2002; Adair & Montani, 2010; Bianchi et al., 2013).

Moreover, there are molecules such as NO, which are also involved in the formation of new vessels (Bir et al., 2012). Previous studies have shown the role of NOS in angiogenesis (phosphorylation of eNOS at Ser-1179 regulates a proangiogenic response) and have suggested that the growth produced by NO is bonded to cGMP generation.

In cell culture, ECs form capillary tubes in presence of GFs and depend on an extracellular matrix in the environment (Lazarovici et al., 2018).

1.3.2 Perivascular adipose tissue

PVAT not only provides structural support in blood vessels, but now is recognized as a specialized endocrine organ that surrounds most blood vessels including small vessels, where adipocytes are an integral part and constitute the adventitial layer (Gil-Ortega et al., 2015).

Perivascular adipocytes are the main cellular component and often resemble white adipocytes, but display characteristics of both white and brown adipocytes. Adipocytes around rodent thoracic aorta and perivascular adipocytes of human coronary arteries are more similar to brown adipocytes (Chartterjee et al., 2009; Padilla et al., 2013). However, adipocytes from the abdominal aorta and mesenteric arteries in both rodents and humans are similar to white adipocytes (Henrichot et al., 2005; Padilla et al., 2013).

PVAT contains other important cell types such as macrophages, T-lymphocytes and fibroblasts, which may also contribute to its function (Illustration 5). Also, PVAT is innervated by sympathetic nerves (Bulloch & Daly, 2014; Darios et al., 2016).

Under physiological conditions, PVAT releases diffusible factors that modulate local vascular reactivity and inflammatory status and regulate the vascular tone. PVAT produces perivascular adipocyte derived relaxing factors (ADRFs) and adipocyte-derived contractile factors (ADCFs) (Gao, 2007; Meyer et al., 2013). Moreover, perivascular immune cells and sympathetic nerves might serve as additional sources of these molecules (Gao et al., 2006).

PVAT exerts a predominantly anti-contractile effect in humans (Ramirez et al., 2017). Adiponectin, leptin, angiotensin (Ang) 1-7, NO, hydrogen and peroxide are

the main ADRFs released by perivascular adipocytes (Dubrovska et al., 2004; Gao et al., 2007; Gil-Ortega et al., 2010; Lee et al., 2009; Payne et al., 2010; Schleifenbaum et al., 2010). ADRFs release from the adipose tissue can be modulated by changes in Ca^{2+} concentrations and its effects are regulated by diverse signalling mechanisms including endothelial NO release, cGMP generation, reactive oxygen species and opening of various K^+ channel subtypes (Gollasch, 2012; Withers et al., 2014).

The mechanism for the relaxation by PVAT, which attenuates the contractile response to noradrenaline in rats (Löhn et al., 2002; Soltis & Cassis, 1991; Zhao et al., 2015) and to phenylephrine in human arteries, activates calcium-dependent K^+ channels (Gao et al., 2005). In mesenteric arteries from spontaneously hypertensive rats (SHR), there is a loss of anti-contractile effect due to a down-regulation of K^+ channels or reduced PVAT-induced production of Ang 1–7 (Gálvez et al., 2006; Li et al., 2013).

Some studies have confirmed that the anti-contractile effect does not involve presynaptic neurons, it is independent of neuronal uptake and it is directly dependent on the amount of adipose tissue (Gollasch & Dubrovska, 2004).

Contrarily, adipocytes express a local renin–angiotensin–aldosterone system for the synthesis of the potent vasoconstrictor, Ang II (Cassis et al., 2008; Karlsson et al., 1998). The expression can vary depending on the location of adipose tissues (Cassis et al., 1988; Engeli et al., 1999; Riedel et al., 2016). PVAT-derived Ang II promotes contractions through the activation of its receptors (AT1) in rat mesenteric arteries (Lu et al., 2010). Ang II has also been shown to play a role in the local inflammation associated with hypertension and obesity.

Adipose tissues may also synthesize and release noradrenaline and adrenaline in thoracic aorta and superior mesenteric arteries, where PVAT enhances contraction via α_1-ARs (Ayala-Lopez et al., 2014). Another factor that may contribute to the contractile effects of PVAT is the adipokine chemerin (Watts et al., 2013). Direct application of chemerin to isolated aorta or mesenteric artery increases agonist-induced contraction and ERK activation (Lobato et al., 2012). In addition to chemerin, cytokines (TNF-α and IL-6) derived from PVAT might also enhance contractions, probably via upregulation of endothelin signalling or

reduction in NO production and in endothelium-dependent relaxation, especially in obese patients (Greenberg et al., 1985; Orshal & Khalil, 2004; Virdis et al., 2015). Aortic and small mesenteric PVAT also release contractile prostanoids, including TXA2 and PGE2 (Mendizábal et al., 2013; Meyer et al., 2013).

Indeed, a primary mechanism of contractile action for PVAT is to reduce NO production or bioavailability, although NO-independent signalling pathways may also be compromised. The inhibitory effect of PVAT on responses to endothelium-dependent relaxants could enhance vasocontraction and might be particularly relevant for hypertension.

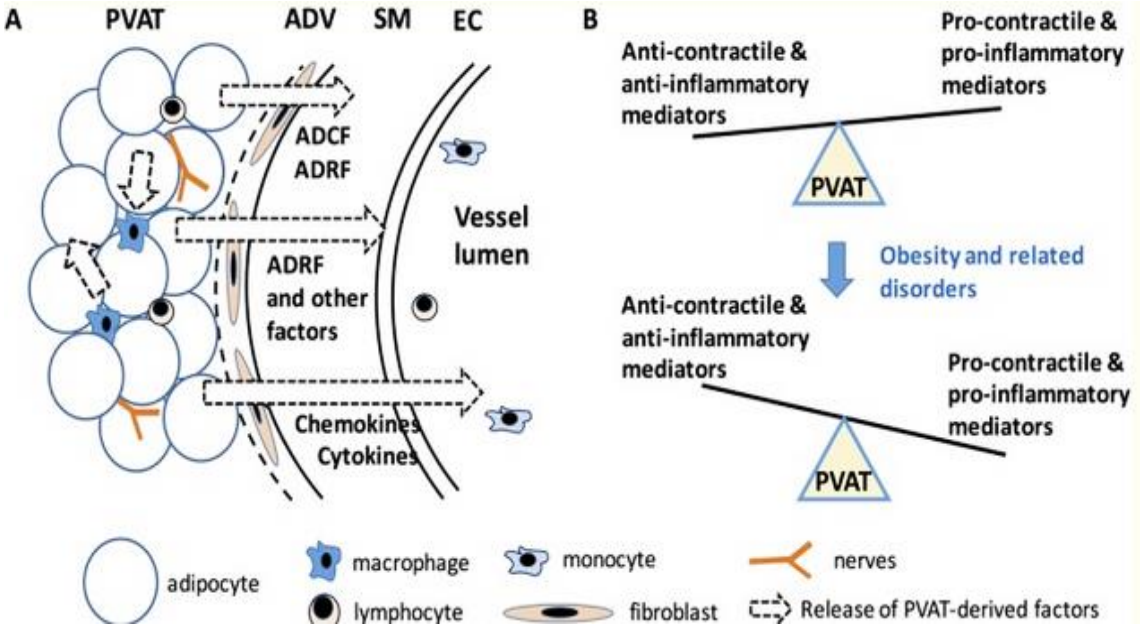

Illustration 5. Regulation of vascular tone by PVAT in health and disease. (A) *PVAT releases a diverse group of bioactive and diffusible substances. These mediators modulate vascular tone through a paracrine action on the endothelium, vascular smooth muscle and immune cells. The chemokines and cytokines regulate the migration of immune cells into PVAT, and activated macrophages and lymphocytes within PVAT can also release additional cytokines.* ***(B)*** *In healthy conditions, PVAT tends to exert a net anti-contractile effect. Pathophysiological stimuli (obesity, hypertension and diabetes) increase pro-contractile and decrease anti-contractile actions. This imbalance is characteristic of PVAT dysfunction in disease states. Other changes in PVAT composition and function include adipocyte hypertrophy, infiltration of macrophages and lymphocytes, and inflammation within PVAT and vascular cells. ADV, adventitia; EC, endothelium; SM, smooth muscle (Ramirez et al., 2017).*

Dysfunctional PVAT release cytokines, adipokynes, contractile factors (such as prostaglandins, Ang II, chemerin) and adrenalin to enhance vascular contractility. Thus, dysfunctional PVAT favor the arterial remodeling and endothelial dysfunction.

Both relaxant and contractile actions of PVAT effects are detectable in healthy conditions, at least in thoracic aorta and mesenteric and coronary artery (Dubrovska et al., 2004; Payne et al., 2010; Soltis & Cassis, 1991; Verlohren et al., 2004). Many studies have proposed a predominantly anti-contractile action in health (Illustration 5), although it is possible that the net effect on vascular tone depends on the anatomical location and experimental conditions used. In humans, the loss of the anti-contractile effect of PVAT in obese patients could contribute to the local oxidative stress and inflammation. These processes might modulate endothelial function (Gollasch & Dubrovska, 2004).

One of the functional role of PVAT is to protect vessels against neighboring tissues (Guzik et al., 2007; Villacorta et al., 2015). The loss of PVAT-derived anti-contractile factors such as prostacyclin and adiponectin reduces the anti-contractile ability of PVAT, leading to arterial stiffness, hypertension, and the development of vascular lesion formation, vascular calcification, or aneurysmal formation (Villacorta et al., 2015).

The evidence suggests that a pro-inflammatory phenotype of PVAT is common in pathologies (Illustration 5) such as hypertension, obesity, insulin resistance and atherosclerosis (Almabrouk et al., 2014; Chartterjee et al., 2009; Mikolajczyk et al., 2016). There is an up-regulation of pro-inflammatory mediators (e.g. TNF-α and IL-6), and a down-regulation of anti-inflammatory mediators (e.g. adiponectin and IL-10) from adipocytes and macrophages (Chartterjee et al., 2009; Greenstein et al., 2009; Lumeng et al., 2007). In rats, thoracic PVAT is more prone to inflammation than abdominal PVAT. Hence, the metabolic activity and mechanisms such as the anti-contractile effect of PVAT vary depending on the anatomical location (Ozen et al., 2013; Padilla et al., 2013).

2. NEUROTROPHINS

During the development, different cell types and extracellular matrix regulate gene expression, migration, differentiation, proliferation, and apoptosis. In these processes participate a group of neurotrophic factors (NFs) which are present in survival and regeneration of neurons and are studied for novel therapies. In mammals, NFs can be secreted by neurons, glial cells, ECs, epithelial cells, muscle cells, adipocytes, and immune cells. These factors are grouped in three families according to biochemistry: neurotrophin (NT) family, glial cell line-derived NF, and cerebral dopamine neurotrophic/Mesencephalic astrocyte-derived NF family (Illustration 6) (Martinelli & Ribeiro, 2016; Sornelli et al., 2009).

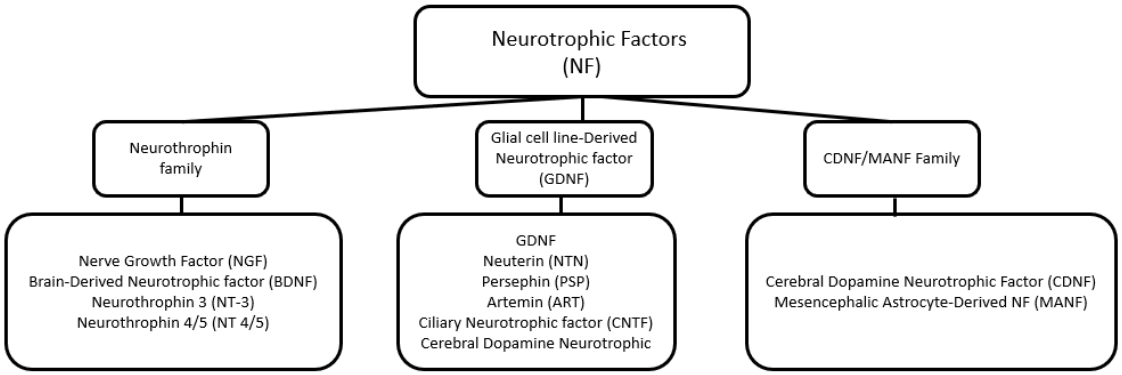

Illustration 6. *Neurotrophic factors (Modified from Martinelli and Ribeiro, 2016).*

NTs are a family of proteins that promote proliferation, survival and differentiation of different cell population. This family includes nerve growth factor (NGF), brain-derived neurotrophic factor (BDNF), neurotrophin-3 (NT-3), and neurotrophin-4/5 (NT-4) (Caporali & Emanueli, 2009; Tessarollo, 1998).

In the early 1950s, Rita Levi-Montalchini discovered the first member of the family, the protein NGF, followed by BDNF. These NTs were closely related proteins and led to identify NT-3 and NT-4. Originally, NTs are highly conserved and share an overall structure with similar molecular mass (13.2-15.9 kDa), isoelectric points, and 50% identity in primary structure. NTs are able to form homodimers but some subunits may form heterodimers with others NTs subunits (Caporali & Emanueli, 2009; Chaldakov et al., 2014; Ernfors et al., 1990; Gibon & Barker, 2017a; Hohn et al., 1990; Kolbecket al., 1994; Lee et al., 2001; Longo & Massa, 2013; Zanin et al., 2016).

NTs are highly expressed in mammalian nervous system and are known for their roles during different stages of development. However, there are evidences that NTs and their receptors enhance survival and activity of a large of non-neuronal cells including immune cells, pancreatic β cells, VSMCs, cardiomyocites, ECs, epithelial cells, and adipocytes (Caporali & Emanueli, 2009; Chaldakov et al., 2009; Meloni et al., 2015).

2.1 NEUROTROPHIN SYNTHESIS AND SECRETION

All NTs are initially synthesized in the rough endoplasmatic reticulum as pro-proteins of approximately 35 kDa, where they are subsequently converted into pro-neurotrophins (proNTs), the uncleaved NT precursors. ProNTs range from about 210 to 270 amino acid residues in length, named proNGF, proBDNF, proNT-3, and proNT-4, that are transported to the Golgi apparatus (Bothwel, 2014; Caporali & Emanueli, 2009). ProNTs can dimerize into homodimers and stable (BDNF and NT-3) or not stable (NGF) heterodimers (Farhadi et al., 2000). Post-translational modifications occur during proNT translocation from Golgi apparatus to trans-Golgi network. ProNTs are processed by proteases of the pro-protein convertase family producing the mature proteins which are about 120 residues in length and weighing 13 kDa. This cleavage event may occur either within the secretory pathway or following secretion (Bothwell, 2014; Caporali & Emanueli, 2009).

Two secretory vesicles are responsible for the regulated secretion of NTs. The first vesicles represent the constitutive pathway of secretion (Ca-independent pathway) in the absence of any triggering stimulus, and the second type represent the regulated pathway of secretion (Ca-dependent pathway) in response to an extracellular triggering stimulus. Both pathways depend on several factors including the localization of protein convertases and the optimum pH in different compartments of the cells (Al-Qudah & Al-Dwairi, 2016). In the secretory pathway, ProNTs can release an N-terminal pro-domain peptide and a C-terminal mature NT, so that receptor may be exposed to both ProNTs and mature NTs (Mark Bothwell, 2016).

Neurons and neuroendocrine cells have regulated and constitutive secretory pathways, whereas non-neuronal cell types typically have only the constitutive

secretory pathway (Farhadi et al., 2000; Reichardt, 2006). In brain, the secretion of NGF, NT-3, and NT-4 occurs mainly through the constitutive secretory pathway, whereas BDNF selectively traffics through the regulated secretory pathway (Reichardt, 2006).

2.2 NEUROTROPHIN FAMILY

2.2.1 NGF

NGF, a glycoprotein of 118 amino acids, has been the pioneer in studies of NTs. During early studies, this protein has been considered as the prototypic member of the family to study properties of NTs (Gibon & Barker, 2017a; Kolbeck et al., 1994). NGF has been studied in both central and peripheral tissues; indeed high levels of NGF mRNA and protein have been reported in hippocampus and neocortex (Gibon & Barker, 2017), with low levels of expression in most peripheral tissues including the heart and vasculature, although large molecular weight NGF precursors are abundant (Bierl et al., 2005).

In early studies, the synthesis of human NGF led to construct a human genomic library. The human NGF gene encodes a precursor of 241 amino acids with proteolytic and glycosylation sites conserved (Nikolics, 1993)

NGF is synthesized from two transcripts corresponding to 34 and 27 kDa, then glycosylated forms of NGF are cleaved to mature form. Interestingly, proNGF (32 kDa) is more predominant than the mature NGF (13 kDa) in sympathetic neurons and in its peripheral tissues (Bierl et al., 2005).

2.2.2 BDNF

BDNF has been studied since 1990s in brain and is involved in hippocampal neuronal synaptic plasticity, learning and memory (Mark Bothwell, 2016; Gibon & Barker, 2017b). BNDF is also implicated in the central control of fluid balance (Black et al., 2018). The regulated secretory vesicles are most efficient in BDNF and involve receptor-mediated mechanisms (Al-Qudah & Al-Dwairi, 2016).

BDNF controls different functions depending on the receptor, with TrkB promotes synaptic long-term potentiation and with $p75^{NTR}$ promotes synaptic long term depression (Bothwell, 2016).

2.2.3 NT-3

In 1990s, a protein with a similar sequence to both NGF and BDNF was discovered by researchers from different laboratories. Since then, NT-3 has been studied in neuronal tissues during development, but the expression decreases dramatically as they mature (Ernfors et al., 1990; Hohn et al., 1990; Lamballe et al., 1994; Maisonpierre et al., 1990). In neuronal tissues, NT-3 acts as regulator of neurogenesis and also has a neuroprotector effect in ischemic brain (Gibon & Barker, 2017; Zhang et al., 2012). NT-3 is also widespread distributed in peripheral tissues incluiding skeletal muscle, heart, lung, liver, and gut (Donovan et al., 1995; Hohn et al., 1990; Su et al., 2016; Tessarollo et al., 1994).

NT-3 binds to two types of cell surface receptors according to the biological process: NT-3 binding to TrkC can control critical functions in development, whereas NT-3 activates $p75^{NTR}$ to induce cell death (Gibon & Barker, 2017; Yano at al., 2009; Zanin et al., 2016). NT-3, through TrkC activation, is able to control the proliferation and differentiation of neural cells, and the migration of Schwann cells (Yamauchi et al., 2004), melanoma cells (Truzzi et al., 2008) mesenchymal stem cells (Shen et al., 2013) and marrow stromal cells (Birnbaum et al., 2007).

NT-3 is synthesized as proNT-3 and both proteins can elicit different biological events in both neuronal and non-neuronal tissues. Indeed, some findings have revealed that proNT-3 can be an apoptotic factor for specific neuronal populations or a regulator of neuronal proliferation and neurogenesis (Gibon & Barker, 2017; Yano at al., 2009). In western-blot analyses, NT-3 exists in either a dimer (40 kDa) or a monomer form (21 kDa) protein. The biological activity of NT-3 monomers are 100–1000 times less when compared with dimers, presumably from a much reduced ability of the monomers to interact with their cognate receptor TrkC, as shown by comparing the ability to promote the survival of cultured sensory neurons and in a TrkC phosphorylation assay in TrkC transfected fibroblasts (Kolbeck et al., 1994). More recently, in a rat model of experimental cerebral infarction, Chung et al. (2017) found that the expression of NT-3 monomer was less than that of NT-3 dimers in the focal cerebral ischemia.

2.2.4 NT-4

NT-4 was reported by Hallbök et al. (1991) in Xenopus and viper using molecular techniques. DNAs from human, rat, snake, frog, and fish were used to analyze the NTs, and a very highly conserved NT was found. NT-4 is a 236-amino acid protein (Nikolics, 1993) that induces TrkB phosphorylation and promotes survival and differentiation of hippocampal (Gibon & Barker, 2017)

2.2.5 NT-5

NT-5 was characterized by Berkemeier et al. (1991). This NT is a 13.5 kDa protein, highly homologous, and present the same basic structure as the others NTs. NT-5 is expressed at low levels in many peripheral organs and actives TrkB promoting the cell survival (Berkemeier et al., 1991).

2.3. NEUROTROPHIN RECEPTORS

In order to understand the role of NTs, it is important to know the function of their receptors. NTs bind preferentially to two types of cell surface receptors with different selectivity: Tropomyosin-related kinase (Trk) family and p75 NT receptor ($p75^{NTR}$) (Table 2; Illustration 7) (Al-Qudah & Al-Dwairi, 2016; Chaldakov et al., 2014; Gibon & Barker, 2017; Keeler & Deppmann, 2017; Lee et al., 2001; Longo & Massa, 2013; Zanin et al., 2013; 2016). Mature NTs can bind and activate Trk receptors, whereas $p75^{NTR}$ is activated by both mature and proNT, although is more effectively proNT form (Bothwell, 2006).

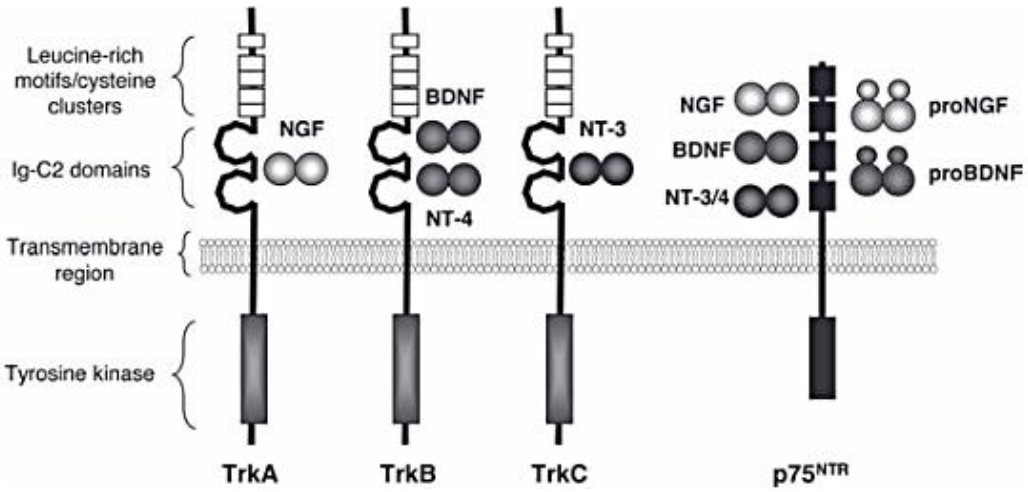

Illustration 7. Neurotrophins and their receptors. *NTs bind to specific Trk receptors and $p75^{NTR}$. Trk receptors dimerize and become active upon NT ligand binding. NTs are synthesized as proNTs that also bind to $p75^{NTR}$ (Arévalo &Wu, 2006).*

Table 2. Main NTs and their selectivity for the receptors.

NEUROTROPHIN	RECEPTOR	
	High affinity	Low affinity
NGF	TrkA	$p75^{NTR}$
BDNF	TrkB	$p75^{NTR}$
NT-3	TrkC	TrkB, TrkA, $p75^{NTR}$

2.3.1 Trk receptors

The Trk receptors are transmembrane glycoproteins of approximately 140 kDa with an intracellular tyrosine kinase domain and an extracellular ligand-binding domain (Deinhardt & Chao, 2014). The phosphorylated tyrosine residues are found in the autoregulatory loop of the tyrosine kinase domain and initiate downstream signalling pathways (Barbacid, 1994; Deinhardt & Chao, 2014). They are tyrosine kinase receptors that include epidermal growth factor (EGF) and insulin-like growth factor-1 (IGF-1) receptors (Barbacid, 1994; Kawaguchi-Manabe et al., 2007; Longo & Massa, 2013).

Trk family consists of three different domains including TRKA (NTRK1), TRKB (NTRK2), and TRKC (NTRK3), which selectively bind to NGF, BDNF, or NT-3 respectively, with affinities of 10^{-9}–10^{-10} M to their respective Trk receptors. In addition, there is an heterologous low affinity binding of NT-3 to TrkA, TrkB, and $p75^{NTR}$ (Table 2) (Barbacid, 1994; Donovan et al., 2000; Gibon & Barker, 2017; Ivanov et al., 2013; Lamballe et al., 1994; Longo & Massa, 2013; Tessarollo et al., 1997).

Trk isoforms lacking large parts of the intracellular domain are truncated Trk receptors, which are expressed at high levels throughout the mature nervous system and are active signalling molecules (Deinhardt & Chao, 2014, Fenner, 2012). TrkB and TrkC encodes at least three and eight isoforms, respectively. These isoforms are different in their intracellular regions and exhibit different biological properties. Given the complexity of Trk family, with differences in their domains, Trk isoforms are generated by alternative splicing, which can occur in

the cytoplasmic domain (Deinhardt & Chao, 2014; Menn et al.,1998). Truncated isoforms of TrkB and TrkC may have dominant negative effect compared to full-length Trk receptors because of the lack the tyrosine kinase domain (Longo & Massa, 2013).

K252a is a natural alkaloid which selectively inhibits all Trk isoforms by competing with the binding of ATP to the catalytic domain, and acting as a kinase inhibitor. It has also been described as a partial inhibitor of the platelet-derived growth factor receptor (Morotti et al., 2002).

TrkC, the third member of Trk family, is the primary receptor for NT-3. TrkC has multiple receptor isoforms (Beltaifa et al., 2005). In humans, at least three isoforms have been detected by Western blot analysis. A band around 145–150 kDa with variable glycosylation, which corresponds to the full-length TrkC. This isoform contains a kinase domain with catalytic activity responsible for the main signaling pathways (Elkabes et al., 1995; Menn et al., 2000; Tesarollo et al., 1997; Tsoulfas et al., 1993). Another band corresponding to a truncated, non-catalytic isoform of 50-60 kDa, which lacks the tyrosine kinase domain (Shelton et al., 1995; Menn et al., 1998) and finally, a third band of approximately 110 kDa which corresponds to another truncated isoform of TrkC with lack of portions in the cytoplasmic domain (Donovan et al., 1995; Tesarollo et al., 1997).

In addition, several TrkC protein variants of the isoforms, with a wide range of sizes (80 kDa, 120 kDa and 150 kDa) have also been described (Lamballe et al., 1993; Quartu et al., 2003; Rudge et al., 1994; Tsoulfas et al., 1993, 1996; Valenzuela et al., 1993).

Many studies have demonstrated that TrkC is expressed in the developing central and peripheral nervous system, and in the enteric nervous system (Lamballe et al., 1994). TrkC expression is also observed in non-neuronal tissues including lung, heart, kidney, urogenital mesenchyme, dental papillae, brown adipose tissue (Donovan et al., 1995; Tessarollo et al., 1997; Youn et al., 2003; Lin et al., 2000), and in cells types, such as cells of the submandibular gland and subendothelial mesenchyme in arteries in developing embryo, where other Trk genes are not active (Tessarollo et al., 1993).

NT-3 binding results in TrkC kinase activation, leading to the recruitment and phosphorylation of signalling proteins which regulate neuronal proliferation, growth, differentiation, and survival of nervous and non-neuronal systems. The truncated TrkC isoforms with lack of kinase domain inhibit signalling triggered by catalytic receptors when both catalytic and truncated isoforms are co-expressed (Arévalo & Wu, 2006; Bartkowska et al., 2013; Das et al., 2000; Lin et al., 2000; Palko et al., 1999; Youn et al., 2003). These non-catalytic receptors are well conserved among species. Overexpression of truncated TrkC in a transgenic mouse model leads to a phenotype similar to that observed in TrkC or NT-3 null mutant animals, suggesting that the truncated TrkC receptors negatively modulate signalling by TrkC with kinase activity (Lin et al., 2000).

2.3.2 p75^{NTR} receptor

The p75^{NTR} is a tumor necrosis factor (TNF) superfamily member which contains an extracellular domain with four cysteine-rich motifs, a single transmembrane domain, and a death cytoplasmic domain to induce distinct cellular responses. The p75^{NTR} unselectively binds all of the NTs with low affinity, depending on the concentration of ligand, receptors ratio, cell type, and differentiation. This receptor is also involved in the affinity and the specificity of NTs to Trk receptors; indeed, it can influence NT/Trk receptor interactions (Illustration 8) (Al-Qudah & Al-Dwairi, 2016; Huang & Reichardt, 2003).

Mature NTs bind preferentially to Trk receptors promoting survival and differentiation of cells, which can be modulated by p75^{NTR}, either inhibiting or promoting signalling depending on the case (Caporali & Emanueli, 2009). Contrarily, all proNT bind a complex composed of the co-receptor sortilin and p75^{NTR} promoting cell death (Song et al., 2010).

In addition, high doses of NTs induce apoptosis through p75^{NTR} receptor given that this receptor signalling is relatively limited in comparison with other receptors of the TNF receptor superfamily (Lee et al., 2001).

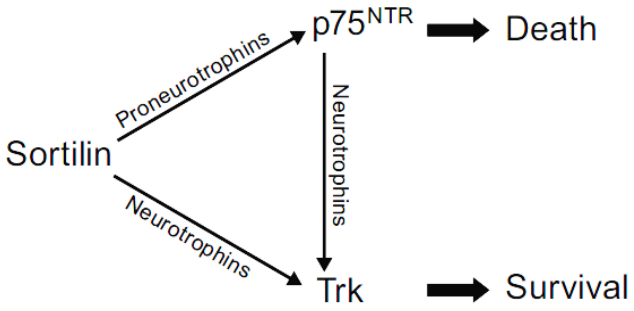

Illustration 8. The neurotrophin triangle. *Sortilin and key receptors in survival and death signaling by mature/pro-NTs (Glerup et al., 2014).*

2.4 NEUROTROPHIN SIGNALLING PATHWAYS

The two NTs receptors present independent signalling properties and downstream signalling can generate individual responses. In addition, both receptors participate in the formation of signalling endosomes (Chao, 2003; Longo & Massa, 2013).

2.4.1 Trk-mediated signalling

TrkC activation is mediated by dimerization, phosphorylation and endocytosis of the receptor-ligand complexes (Illustration 9) (Deinhardt & Chao, 2014). The cytoplasmic domain of these receptors contains five tyrosines essential for signalling. The tyrosine kinase domain (Tyr670, Tyr674, and Tyr675) promotes kinase activity and can recruit adaptor proteins after phosphorylation which act as intermediaries in signalling cascades (Barbacid, 1994; Deinhardt & Chao, 2014; Huang & Reichardt, 2003; Kawaguchi-Manabe et al., 2007; Longo & Massa, 2013). There are major phosphorylated tyrosines which are not in the kinase activation loop (Tyr490 and Tyr785) and serve as main docking sites to initiate signalling pathways (Deinhardt & Chao, 2014; Reichardt, 2006). The efficiency and duration of Trk signalling depend on endocytosis and transfer of Trk receptors to specific membrane compartments (Reichardt, 2006).

The mature NTs bind to Trk receptors and activate three intercellular signalling pathways (Illustration 10): (i) the mitogen-activated protein kinases (MAPK) / extracellular signal-regulated kinase (ERK1/2) pathway, (ii) the phosphatidylinositol-3-kinase (PI3K) / protein kinase B (Akt) pathway, and (iii) the phospholipase Cγ1(PLCγ1)- protein kinase C (PKC) pathway (Chao, 2003; Longo & Massa, 2013).

Thus, Trk signalling plays diverse functions, including cell survival and differentiation, govern of several neuronal functions, and control of synaptic plasticity (Al-Qudah & Al-Dwairi, 2016; Barbacid, 1994; Caporali & Emanueli, 2009; Deinhardt & Chao, 2014; Kawaguchi-Manabe et al., 2007; Longo & Massa, 2013).

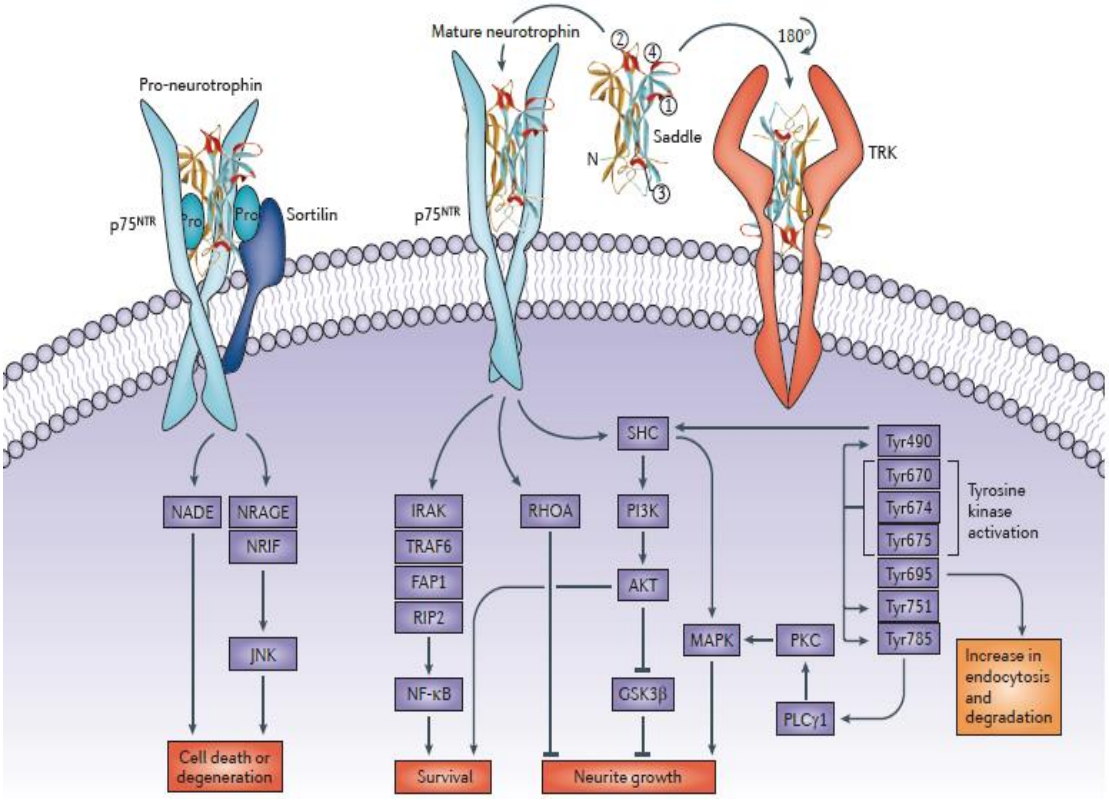

***Illustration 9. Neurotrophins and their signalling pathways**. NTs bind to two receptors: Trk and p75NTR. NTs signalling proceeds through preformed or induced receptor dimers. NTs bind to Trk results in the phosphorylation of an array intracellular tyrosine residues which promotes kinase activity (Tyr 670, Tyr647, and Tyr675). Phosphorylation at Tyr490, Tyr875 and Tyr751 forms adaptor binding sites that couple the receptor to mitogen-activated protein kinases (MAPKs), phosphoinositide 3-kinase (PI3K), and phospholipase Cγ1 (PLCγ1) pathways, which may act locally and/or via signalling endosomes that are transported to the nucleus, to promote neurite outgrowth, differentiation and cell survival. Mature NTs binding to p75^{NTR} may augment NTs binding to TRK receptors, reinforce TRK signalling through AKT and MAPKs and further promote survival through NF-κB pathway, or antagonize the actions of TRK through the activation of JUN N-terminal kinase (JNK) and RHOA pathways. Pro-NTs binding in complex with sortilin selectively activates cell-death-related pathways. FAS-associated phosphatase 1 (FAP1); glycogen synthase kinase 3β (GSK3β); interleukin-1 receptor-associated kinase (IRAK); p75^{NTR}-associated cell death executor (NADE); neurotrophin receptor-interacting MAGE homologue (NRAGE); neurotrophin receptor-interacting factor (NRIF); receptor interacting protein 2 (RIP2); SRC homology domain-containing protein (SHC); TNF receptor-associated factor 6 (TRAF6) (Longo & Massa, 2013).*

Via MAPK / ERK1/2

NGF induces the phosphorylation of TrkA, which provides a recruiting site for the binding of an adapter protein, which activates Ras cascade signalling (Illustration 10). First, Ras activates Raf (MAPK), which in turns activates ERK1/2 phosphorylation. Once activated, ERK1/2 enters the nucleus and modifies the phosphorylation of proteins that are transcription factors, to regulate transcription and to modulate the expression of different genes (Krishna & Narang, 2008). Overall, the MAPK complex is deactivated by ERK1/2 that inactivates Raf through negative feedback. In some cases, phosphatases intervene to inactivate the complex by eliminating the phosphate groups.

Via PI3K / Akt

The PI3K / Akt pathway is initiated through the recruitment of the protein PI3K to the plasma membrane through its binding to tyrosine phosphorylated Trk receptors (Illustration 10). PI3K is activated and is responsible for transferring a phosphate group to phosphatidyl inositol, 4,5-bisphosphate, generating phosphatidyl inositol, 3,4,5-triphosphate. PI3K also phosphorylates and generates lipid products that serve as ligands to recruit the serine/threonine kinase protein Akt to the plasma membrane. Subsequently, on the inner side of the membrane, Akt is phosphorylated and activated by a phosphatidyl inositol-3-dependent kinase. Then, Akt phosphorylates some proteins implicated in the control of survival, proliferation, growth, cell migration, and angiogenesis. In the absence of phosphorylation, these proteins promote apoptosis (Manning & Cantley, 2007). Activation of the PI3K / Akt pathway also leads to the phosphorylation of the eNOS and production of NO by the ECs (Caporali & Emanueli, 2009).

Via PLC

In response to the activation of the kinase receptor by the NTs, phospholipase C-γ (PLC-γ) is recruited to cut near the phosphorylated Tyr785 site of TrkA, TrkB or TrkC. The activation of PLC-γ takes place through the hydrolysis of phosphatidylinositol 4,5-bisphosphate generating inositol 1,4,5-triphosphate and diacylglycerol, which results in the activation of PLC and in the stimulation of the different isoforms of PKC, as PKC-δ which is necessary for the induction by NGF

of the MEK1 and ERK1/2 pathway (Illustration 10). The PLC-γ pathway plays an important role in the migration of VSMCs (Caporali & Emanueli, 2009).

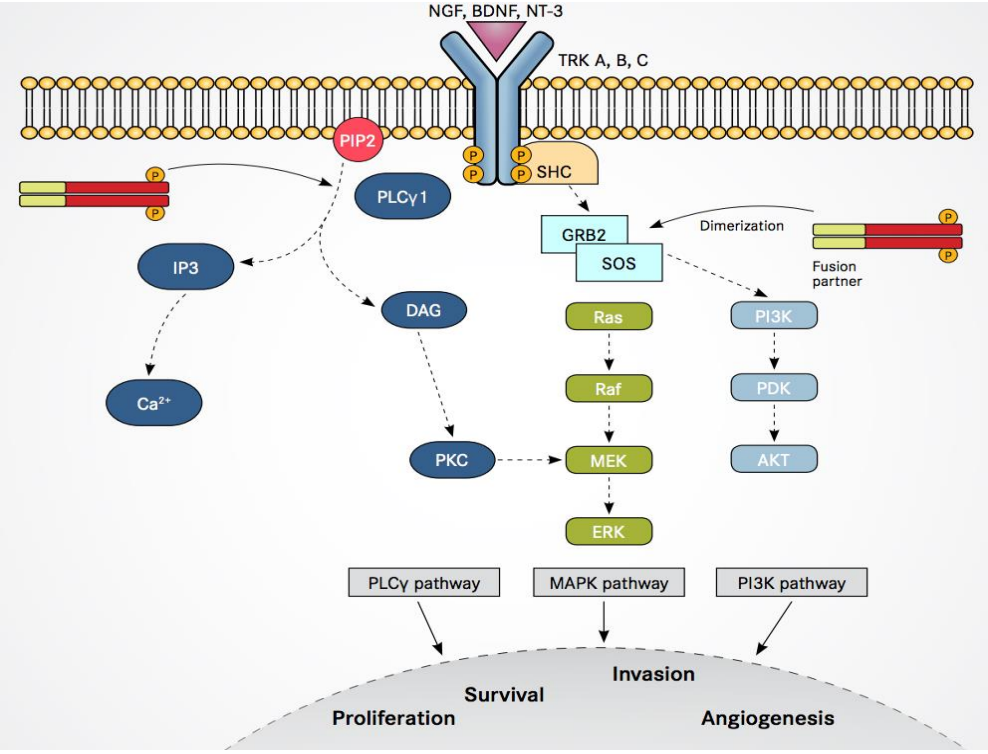

Illustration 10. Neurotrophin actions and Trk signalling pathways*. Three major pathways may be activated as a result of TRK receptor signalling. NGF, BDNF, and NT-3 promote activation of TrkA, TrkB, and TrkC, respectively* (Lartigue, 2017).

2.4.2 p75-meadiated signalling

Several signalling pathways are activated by $p75^{NTR}$ through adaptor proteins (Reichardt, 2006). Among the numerous pathways are PI3K-Akt pathway, MAPK, JUN N-terminal kinase (JNK), the cyclic AMP-protein kinase A (PKA) pathways, and the ceramide signalling pathway (Longo & Massa, 2013). The major pathway activated is JNK kinase-signalling cascade which causes cell death. In addition, JNK can lead to the release of cytochrome c from mitochondria and caspase-dependent apoptosis (Kraemer et al., 2014). The modulatory action of proNT binding to $p75^{NTR}$ is dependent on association of $p75^{NTR}$ with sortilin. An interesting fact is that the molecular composition of a cell may determinate the cell responses to proNT by apoptosis signalling or unknown activities (Al-Qudah & Al-Dwairi, 2016; Caporali & Emanueli, 2009; Gibon & Barker, 2017b; Lee et al., 2001; Leßmann & Brigadski, 2009; Lewin & Nykjaer, 2014; Longo & Massa, 2013; Zanin et al., 2016).

3. ROLE OF NEUROTROPHINS IN THE CARDIOVASCULAR SYSTEM

NTs are involved in several functions of the nervous system; in addition, new findings have also demonstrated NT effects on the cardiovascular system development and maturation, a complex process that includes cell proliferation, migration, and invasion (Emanueli et al., 2014). Production or secretion of NGF from vascular cells and myocytes, and the expression of TrkB and TrkA in endothelial progenitor cells from bone marrow and peripheral blood, suggest an autocrine control of cardiovascular cell functions by NTs (Caporali & Emanueli, 2009). For instance, NGF promotes survival, proliferation and migration of ECs (Lazarovici et al., 2018), and BDNF enhances the proliferation and vascularization of the hematopoietic stem cells, improves the process of embryonic stem cells differentiation to ECs, and regulates the proliferation of embryonic cardiomyocytes (Descamps et al., 2018).

Trk and $p75^{NTR}$ receptors also play a crucial role in the development of the cardiovascular system. It is reported that Trk is expressed during the early stages of neurogenesis (Martin-Zanca et al., 1990), but Trk receptors are also present on vascular ECs, VSMCs, and cardiomyocytes.

Different studies have demonstrated that cardiovascular cells and stem cells express NT receptors which are activated by different NTs to regulate myocyte proliferation. Moreover, early *in vitro* studies demonstrated that NTs and Trk receptors are expressed and promote innervation in VSMCs in normal vasculature and during embryogenesis (Emanueli et al., 2014; Donovan et al., 1995; Scarisbrick et al., 1993) and $p75^{NTR}$ regulates both the growth and the stability of cardiac sympathetic fibres (Habecker et al., 2008).

Studies using mouse models that lack or overexpress NTs have also shown that receptor activation by BDNF, NGF or NT-3 has a direct effect on cardiovascular development and plays an important role in the formation of the heart and vascularization (Caporali & Emanueli, 2009; Donovan et al., 1995; Hassankhani et al., 1995; Tessarollo et al., 1997). Overexpression of NGF induces cardiac repair following myocardial infarction in mice (Caporali & Emanueli, 2009; Meloni

et al., 2010; 2012). The lack of BDNF impairs the survival of ECs in intramyocardial arteries and capillaries in the early postnatal period, produces a reduction in endothelial cell-cell contacts and in ECs apoptosis, and leads to intraventricular haemorrhage and reduction of cardiac contractility (Donovan et al., 2000). The lack of NT-3 induces ventricular septal defects, tetralogy of Fallot, impaired cardiac morphogenesis or abnormalities in the large blood vessels (Donovan et al., 1996).

NTs and their receptors are also involved in heart and blood vessels functionality under both physiological and pathological conditions. Multiple studies have demonstrated that changes in the expression or activity of NTs are involved in pathogenesis of several diseases such as myocardial infarction (Meloni et al., 2010, 2012), hypertension (Ricci et al., 2004) allergic asthma (Nockher & Renz, 2002), respiratory syncytial virus infection (Nockher & Renz, 2002), chronic pulmonary disease (Arcamone et al., 2005; Groneberg et al., 2005), lung fibrosis (Hoyle, 2003), and lung cancer (Ricci et al., 2004). NTs may promote therapeutic neovascularization in ischemic muscles and diabetic skin ulcers, reduce diabetes-induced apoptosis of ECs or promote vascular regeneration in response to vascular injury. For instance, NGF stimulates therapeutic neovascularization in the ischemic muscle of the hind limbs and BDNF induces angiogenesis in mice with limb ischemia. BDNF and NGF, and their receptors play a critical role in migration of VSCMs during a lesion in vasculature (Caporali & Emanueli, 2009; Donovan et al., 1995; Emanueli et al., 2002; Meloni et al., 2010). Additionally, there is evidence to suggest that NTs exert pleotropic responses in different cell types (Caporali & Emanueli, 2009; Cristofaro et al., 2010; Donovan et al., 1995, 2000; Ly et al., 2014; Meloni et al., 2010).

These studies allow us to understand the physiological functions of NTs during development and the role of NTs in pathologies in order to develop different therapeutic objectives. However, the precise role of NT-3 in heart and vessels during the adult life remains unknown.

3.1 NGF

Several reports indicate that NGF influences on peripheral tissues including the vasculature. Heart cells secrete NGF and express TrkA in normal conditions. The

proangiogenic effect of NGF promotes survival, proliferation and migration of cardiomyocytes and ECs. The interaction between NGF and its receptor in cardiomyocytes triggers a prosurvival signal which involves the PI3K/Akt pathway implicating transcriptional factors (Govoni et al., 2011).

At the endothelial level, NGF via TrkA, and pro-NGF acting on $p75^{NTR}$, seem to produce opposite effects. NGF was the first NT reported in postnatal angiogenesis and repair processes, and its proliferative action mediated by ERK1/2 activation was described on human dermal microvascular ECs, human umbilical vein endothelial cells (HUVEC), human choroidal ECs, and rat brain ECs. Additionally, NGF and its receptor play a role in survival, angiogenic response, migration in VSMCs, and neovascularization mediated by the activation PI3K/Akt and ERK1/2 signalling pathways. In fact, the findings in a mouse model of limb ischemia show that NGF is an autocrine proangiogenic factor acting through TrkA. In mice, NGF is abundantly expressed in the heart, increases the capillary density in heart and promotes angiogenesis in healing wounds (Caporali & Emanueli, 2012; Dolle et al., 2005; Donovan et al., 1995; Ieda et al., 2006). Cardiovascular actions of NGF have demonstrated therapeutic potential for ischemic heart diseases (Caporali & Emanueli, 2009). On the contrary, the interaction of pro-NGF with $p75^{NTR}$, which is scarcely expressed in ECs, leads to cellular apoptosis and inhibits angiogenesis (Caporali et al., 2008).

3.2 BDNF

BDNF and its receptor TrkB are synthesized in many non-neuronal tissues and cell types including the developing heart, ECs, VSMCs, macrophages, and atherosclerotic vessels, which may explain the involvement of this peptide in the mechanisms of loss and gain of function within cardiovascular niche (Illustration 11). It is evident that BDNF is essential for cardiovascular development (Pius-Sadowska & Machaliński, 2017). The recent findings emphasize the crucial cooperation between sympathetic nerve endings, cardiomyocytes and cardiac fibroblasts in the functionality of the neurocardiac synapses (Pius-Sadowska & Machaliński, 2017).

BDNF and its receptor are expressed in the ECs lining the coronary arteries (Kermani & Hempstead, 2007), and are known to be associated with the

development of capillaries and cardiac endothelium formation in the heart tissue during the late gestation period (Fulgenzi et al., 2015). On the other hand, activation of BDNF/TrkB is involved in vascular remodelling of giant cell arteries and is required for survival ECs during development of the cardiac vasculature (Donovan et al., 1995; Ly et al., 2014).

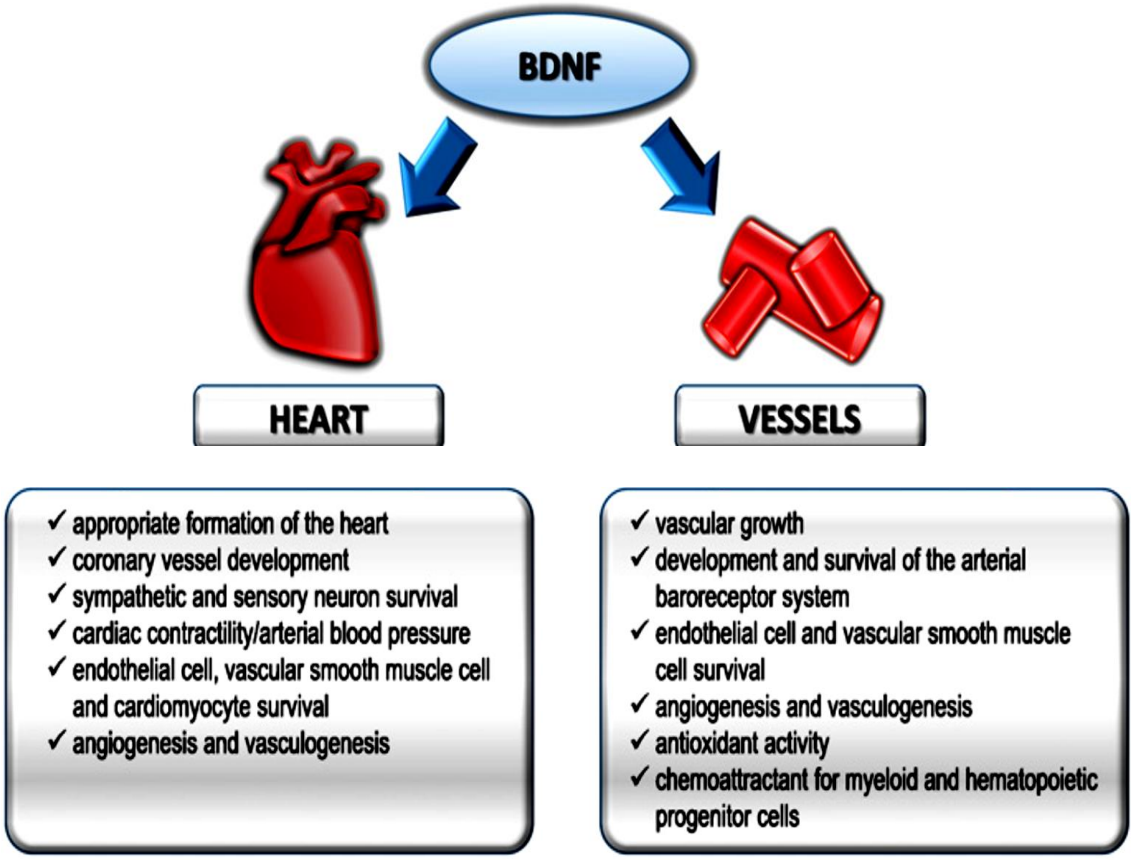

Illustration 11. Effects of BDNF on the cardiovascular system. *BDNF is required for the regulation of cardiovascular system development, viability and function, and the induction of the response to vascular injury (Pius-Sadowska & Machaliński, 2017).*

In adult mammals, BDNF has a critical role in maintaining the integrity of the vascular system. Studies have demonstrated that BDNF promotes ECs survival through TrkB and provides a proangiogenic action mediated by PI3K/AKT (Donovan et al., 2000). BDNF/TrkB and NGF/TrkA play a critical role in migration of VSCMs during a lesion. Also, BDNF binds to $p75^{NTR}$ to induce VSMCs apoptosis (Caporali & Emanueli, 2009; Donovan et al., 1995; Emanueli et al., 2002; Meloni et al., 2010).

3.3 NT-3

The growing interest in the role of NT-3 in non-neuronal tissues has led to the study of NT-3 and its receptor in the cardiovascular system.

Several preliminary studies have focused on NT-3 in cardiogenesis (Table 3). An early study in rats displayed high NT-3 expression in the densely innervated heart during development (Maisonpierre et al., 1990). Posterior studies in rats and mice showed that all three NTs, including NT-3, are expressed within the tunica media of major thoracic arteries and their branches from development to adulthood, as well as in the heart (Scarisbrick et al., 1993). TrkC expression was detected in aortic arch arteries, dorsal aorta, aorta, and lung arteries in the mouse embryo (Tessarollo et al., 1993). In addition, a relevant study indicated that NT-3 and TrkC are present in VSMCs during human adult life and also demonstrated their involvement in vascular resistance and cardiovascular regulation from the development to adulthood (Donovan et al., 1995). Studies in chicken cardiogenesis showed that NT-3 and TrkC were expressed in cardiomyocytes, but truncated TrkC was not detected (Lin et al., 2000). The inability to detect NT-3 and TrkC mRNA at later stages of heart development in rats was consistent with the observations of decreased TrkC expression during later stages (Lin et al., 2000).

These findings suggest that NTs promote abundant innervation and have given rise to study the involvement of NT-3 on cardiovascular system.

Takeo et al. (2003) found that TrkC mRNA is dominantly expressed in rat cerebral, but not aortic, ECs. These authors also found that TrkB, a receptor for BDNF, is dominantly expressed in rat aortic ECs. Other studies showed that NT-3 is highly expressed in both rat heart and vasculature, although TrkC mRNA is expressed more abundantly in rat heart than aorta and can mediate the cardiomyocyte hypertrophy (Kawaguchi-Manabe et al., 2007; Tessarollo et al., 1993). Additionally, BDNF, NT-3, and Trk receptors are particularly expressed in the intima of human pulmonary artery (Ricci et al., 2000) but also in smooth muscle as well as the endothelium in human pulmonary artery (Meuchel et al, 2011). In mouse pulmonary arteries, $p75^{NTR}$ is also expressed in both endothelium and smooth muscle (Xu et al., 2008).

However, the role of NT-3 remains unknown in the field of vascular biology. *In vitro* assays have demonstrated the ability of NT-3 to promote angiogenesis in ischemic disease (Caporali et al., 2012; Cristofaro et al., 2010; Donovan et al., 1996; Tessarollo et al., 1997). In skeletal tissues, NT-3 induced osteogenesis and vascularization during bone healing in rats. Increased expression in the injury site was observed for NTs and their Trk receptors and NT-3 and its receptor TrkC showed the highest induction. Consistent with its angiogenic effect *in vivo*, NT-3 promoted angiogenesis in metatarsal bone explants, suggesting that NT-3 may be an osteogenic and angiogenic factor with a possible application in bone repair (Su et al., 2016).

In chicken and murine heart, NT-3 is a potent physiologic mitogen for cardiac myocytes, regulates vessels and cardiac myocyte proliferation and plays an important role in the development of the heart, cardiac innervation, and vascular system during early development (Lin et al., 2000; Saygili et al., 2010).

Changes in expression or activity of NTs or their receptors in heart vasculature or innervation can contribute to the development of pathologies including HF, hypertension, and atherosclerosis. Therefore, NT-3 expression can be involved in acute myocardial infarction and hypertrophy (Palko et al., 1999; Donovan et al., 1996). The biological actions of TrkC on the proliferation of cardiomyocytes is likely to be the basis for defects in cardiac ventricular septation and, possibly, in the thinning of the ventricular wall observed in mice lacking NT-3 or TrkC (Donovan et al., 1996; Tessarollo et al., 1997). These studies have revealed cardiac abnormalities including atria and ventricular septa defects, valvulogenesis, and abnormal valvular architecture suggesting an essential function of NT-3 and TrkC in cardiac development of the atria, ventricles, and cardiac outflow tracts (Donovan et al., 1996; Lin et al., 2000; Tessarollo et al., 1997).

The lack or overexpression of NT-3 and its receptor induces the development of the cardiovascular abnormalities, including septal defects and Tetralogy of Fallot (Illustration 12). In human paediatric patients, the defects in neural crest development may lead to these types of abnormalities (Donovan et al., 1996; Palko et al., 1999; Srivastava & Olson, 1996).

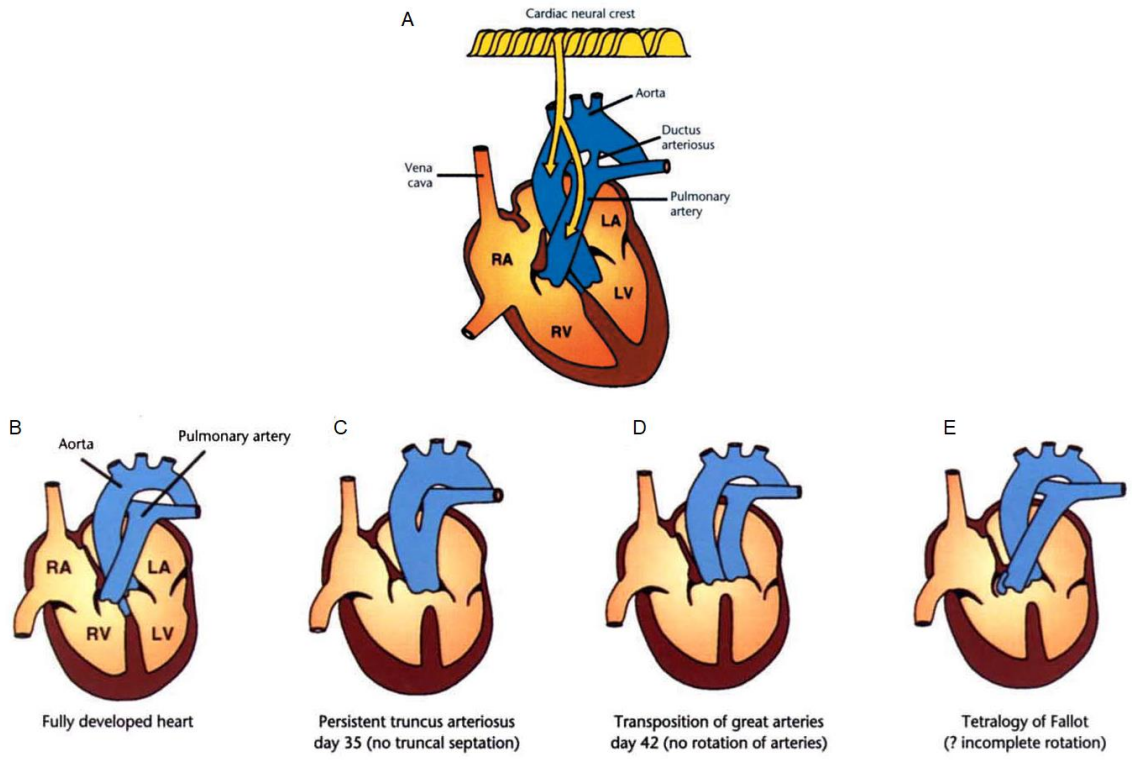

Illustration 12. Cardiac defects of neural crest-derived structures. A*, Cardiac neural crest cells migrate to the heart from the neural folds and populate the aortic arch, proximal pulmonary arteries, ductus arteriosus, and the upper portion of the ventricular septum.* ***B****, Normal adult heart with the aorta arising from the LV and the pulmonary artery arising from the right ventricle.* ***C****, Persistent truncus arteriosus represents an arrest around day 35 of human gestation due to a lack of truncal septation into a pulmonary artery and aorta.* ***D****, Lack of rotation of the great vessels after septation gives rise to transposition of the great arteries.* ***E****, Incomplete rotation of the great arteries associated with Tetralogy of Fallot. (as seen in some NT-3 deficient mice). RA=Right atrium; LA= Left atrium; RV= Right ventricle; LV= Left ventricle (Srivastava & Olson, 1996).*

Conversely, $p75^{NTR}$ is scarcely expressed by ECs or VSMCs under culture conditions. Vascular cells express $p75^{NTR}$ in pathological conditions, such as ischemia, atherosclerosis, and diabetes (Caporali & Emanueli, 2009). In the absence of Trk receptors, $p75^{NTR}$ promotes apoptosis in oligodendrocytes, neurons, and VSMCs; and has apoptotic effects on endothelial lineage. In some cases, the binding of mature NTs to $p75^{NTR}$ may exert effects such as cell survival, proliferation, and inhibition of neurite outgrowth (Caporali & Emanueli, 2009; Brodeur et al., 2009; Lee et al., 2001; Zanin et al., 2016). Unlike TrkC, $p75^{NTR}$ receptor can induce pathologies such as ischemic, atherosclerosis and diabetes (Caporali & Emanueli, 2009).

Table 3. *Main findings in NT-3 and TrkC expression detected on cardiovascular system.*

References	Specie	Cell/Tissue	Gene		Main findings in expression	Methodology
Maisonpierre et al., 1990	Rat [a]	Perinatal and adult heart	*NT-3*		NT-3 increases in the densely innervated heart during development and decreases in adulthood	*Northern blot*
Scarisbrick et al., 1993	Rat *	Arteries	*NT-3*		NT-3 mRNA is particularly prominent in SMCs.	*In situ* hibridazation
Tesarollo et al.,1993	Mouse	Aortic and arteries during mouse development		*TrkC*	TrkC is expressed in dorsal aorta, branchial arch arteries, and aorta.	*In situ* hibridazation
Donovan et al., 1995	Human	Neonatal and adult aortic tissues sections and SMCs cells	*NT-3*	*TrkC*	NT-3 is detected in aorta. NT-3 and TrkC are expressed in SMCs from explants of atherosclerotic lesions The full length and truncated TrkC is detected in human SMC extracts and also in SMC arteries, large veins and in low levels in EC and adventitia from human neonate.	Immunohistochemistry, RT-PCR, and WB
	Rat [a]	Aortic tissues sections and SMCs and ECs	*NT-3*	*TrkC*	Rat VSMCs and ECs express NT-3 and truncated TrkC. However, NT-3 mRNA was no specific in rat aorta after balloon injury. High levels of TrkC expression are detected in SMCs in rat aorta after balloon injury.	Immunohistochemistry, RT-PCR, and WB
Shibayama & Koizumi, 1996	Human	Cardiac muscles		*TrkC*	Trk receptors are not detected in heart.	Inmunoreactivity
Lin et al., 2000	Chicken	Developing heart	*NT-3*	*TrkC*	NT-3 and TrkC are expressed in cardiac myocytes, but not in epicardial and endocardial cells. However, truncated Trk C expression is not detectable in the developing heart.	Immunohistochemistry
Zhang & Rush, 2001	Rat [+]	Heart and blood	*NT-3*		Developing heart express NT-3 for both SHR and WKY rats. At all ages, SHR express higher levels of NT-3 than WKY rats. In neonate serum, NT-3 is expressed very low for both rats.	Inmunoassay

Takeo et al., 2003	Rat *	RCEC and RAEC		*TrkC*	TrkC mRNA is expressed in RCEC, but not in RAEC.	RT-PCR
Kawaguchi-Manabe et al., 2007	Rat *	Adult rat heart and thoracic aorta	*NT-3*	*TrkC*	Aorta and heart express NT-3. NT-3 is downregulated in cardiac hypertrophy. TrkC mRNA is more abundant in heart than the aorta.	qPCR
Damon, 2008	Rat [a]	VSMCs and the corresponding explants of aorta and tail arteries of neonatal and adult rats	*NT-3*		NT-3 in the adult aorta was considerably less than that in VSMCs, neonatal arteries, and adult tail artery.	Immunohistochemistry and WB
Saygili et al., 2010	Rat [a]	Neonatal atrial myocyte cultures	*NT-3*		NT-3 is more abundant in sympathetic neurons than in atrial myocytes. NT-3 increases when neonatal atrial myocytes are subjected to high frequency bipolar electrical field stimulation.	ELISA, WB
Cristofaro et al., 2010	Mouse - Human	Mouse SMEC and Human cells: HUVEC, HVSMC, and microvascular	*NT-3*	*TrkC*	Only SMEC express TrkC gene and protein. NT-3 mRNA expression was increased after ischemia. In contrast, ischemia did not modulate TrkC mRNA or protein levels, but phoshporylated TrkC was enhanced in ischemic muscles.	RT-PCR
Ly et al., 2014	Human	TASMCs from patients with GCA	*NT-3*	*TrkC*	Protein levels of NT-3 was detected in patients, whereas TrkC was detected in both patients and controls. NT-3 and TrkC mRNA were overexpressed in TASMCs from patients compared to control.	WB, qPCR
Yao et al., 2015	Human	AVICs	*NT-3*	*TrkC*	AVICs express NT-3 in control subjects and overexpress NT-3 in diseased valves. TrkC was detectable in both normal and diseased valves.	Microarray analysis

AVICs: Aortic valve interstitial cells; ECs: Endothelial cells; GCA: giant cell arteritis; *HUVEC: Human umbilical vein ECs; HVSMCs: Human VSMCs; RCEC: Rat cerebral ECs; RAEC: Rat aortic ECs; SMC: Smooth muscle cells; SMEC: skeletal muscle ECs; TASMCs: Temporal artery VSMCs.*

**Wistar Rat; [+]SHR and WKY Rats; [a] Sprague-Dawley Rat.*

3.3.1 NT-3 and the adrenergic cardiovascular innervation

In cardiovascular homeostasis, NTs are involved in the development and maintenance of several different aspects of neural control of cardiovascular function. NTs have direct effects on cardiovascular cells that express Trk receptors. NT-3 and TrkC are co-expressed in the developing cardiomyocytes to mediate their proliferation. However, some findings have demonstrated that NTs can also influence cardiovascular development through nerve-mediated actions (Caporali & Emanueli, 2009).

NTs play an important role in the development of the autonomic circuits that provide neural control to the cardiovascular system (Caporalli & Emanuelli, 2009). It is known that target tissues can modulate neurotransmitter and neuropeptide expression in postganglionic neurons. NT-3 expression is highly detected in sympathetic effector tissues (iris, heart, kidney, salivary gland, and blood vessels in developing and adult rat) with dense sympathetic innervation.

Postganglionic sympathetic neurons innervating blood vessels express NPY and tyrosine hydroxylase (TH), a limiting enzyme for catecholamine synthesis. NT-3 receptors are expressed in cardiac sympathetic and parasympathetic neurons. According to this, NT-3, synthesized in sympathetic effector tissues and detected in vascular smooth muscle, has been reported to maintain TH and NPY expression in postganglionic sympathetic neurons that innervate them. (Damon, 2008).

In addition, NTs can contribute for the survival of neurons which are required to change arterial pressure, oxygenation, peripheral resistance, heart rate, and stroke volume. Therefore, the lack of specific NTs or their cognate Trk receptors results in the loss of different types of neurons. For instance, NT-3, NT-4, and BDNF are all involved in the development of chemo-afferent sensory neurons that innervate the carotid body, and postganglionic sympathetic neurons require NT-3 for their initial survival and axon outgrowth to targets (Emanueli et al., 2014).

NT-3 plays an important biological role throughout the life cycle of the sympathetic neuron. Zhou and Rush (1996) explained the role of NT-3 in the developing and mature SNS. Sympathetic neuroblasts express both NT3 and

TrkC, and require NT3 for their proliferation, differentiation, and survival. Moreover, it has been proposed that this factor acts at the developmental stage as an autocrine or paracrine factor. To begin, Shawn cells are a source of NT-3 and express TrkC, which decline during development (Illustration 13), therefore, sympathetic neurons express mRNA of NT-3, implying the possibility of autocrine/paracrine actions (Belliveau et al., 1997; Zhou & Rush, 1996).

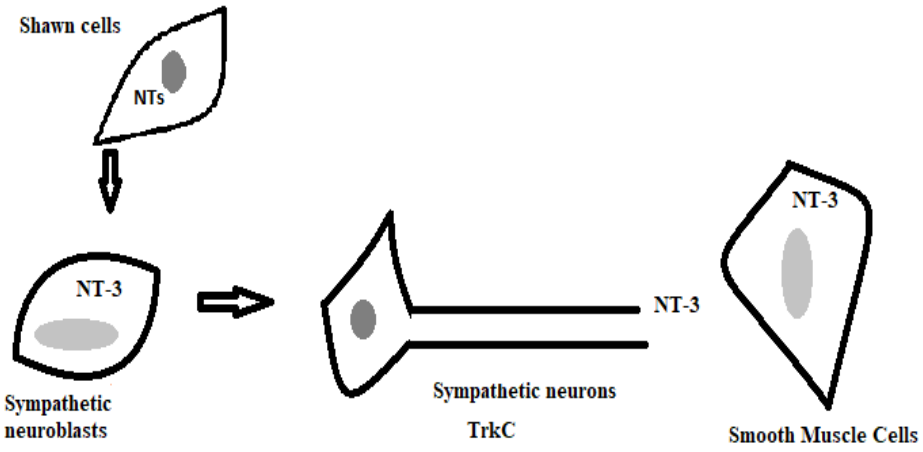

Illustration 13. The influence of NT-3 and its receptor in development of sympathetic neurons*. Shawn cells are a source of NT-3; therefore, expression of NT3 and TrkC in sympathetic neuroblasts and non-neuronal cells implies an autocrine and paracrine mechanism operating within sympathetic ganglia. NT3 acts as a survival factor for proliferating sympathoblasts and promotes differentiation and dependence on NT3 for survival (modified from Zhou & Rush, 1996).*

The catecholamine synthesizing enzymes appear early in development and NT-3 also influences the survival of neuroblasts by regulating the expression of catecholamine synthesizing enzymes (Elshamy et al., 1996). Studies have displayed that NT-3$^{-/-}$ mice have half sympathetic neurons and show deficits in sympathetic innervation of selective organs in these animals, which can be caused by apoptosis of sympathetic neuroblasts, and can be rescued by exogenous NT-3. Exogenous NT-3 is known to bind specifically to mature sympathetic neurons (Belliveau et al., 1997; Elshamy et al., 1996; Zhou & Rush, 1996).

Besides their role as a model system for the regulation of neuronal survival, sympathetic neurons of mammals have also been used extensively to study

another developmental phenomenon controlled by diffusible GFs: neurotransmitter plasticity. To promote cholinergic differentiation, sympathetic neurons express TrkC activated by NT-3 and this effect of NT-3 on cholinergic marker gene expression is abolished by NGF. The cells interpret signals originated from NT-3 and TrkC different to NGF and TrkA signals, which initiate neuronal survival and the accumulation of noradrenergic markers. Thus, functional antagonism between NGF and NT-3 might play an important role in the effects of NTs. NT-3 seems to have first a function in catecholaminergic differentiation at early stages and subsequently in cholinergic differentiation at later stages of sympathetic development (Brodski et al., 2000).

3.3.2 NT-3 and nitric oxide

To understanding the functions of NT-3 in vasculature, this section involves its relationship with NO, given that this molecule exerts functions similar to NTs as a differentiation factor or a survival-promoting factor (Xiong et al., 1999).

It has been reported that NTs may control the formation of the vessels in the central nervous system and may regulate the maintenance of the functions of the brain microvasculature through the regulation of cerebral ECs. It has also been reported that NT-3 increases the protein expression of eNOS and the production of NO in a dose-dependent manner in rat brain vasculature, and inhibits the proliferation of cerebral ECs. Therefore, NT-3 may promote the differentiation of rat cerebral ECs and maintain the environment of the cerebral microvasculature (Takeo et al., 2003).

Previous studies have revealed that NO and NTs play a critical role in the development and function in the cardiovascular system. Several works have suggested a role for NT-3 in local control of vascular responses, particularly on the vascular endothelium modulating vasodilator function (Meuchel et al, 2011). In isolated ECs from the human pulmonary artery, exogenous NT-3 releases NO and increases cGMP in a similar level to ACH. This effect is mediated by previously established cascades of elevated [Ca^{2+}], and eNOS and Akt phosphorylation and activation (Illustration 14) (Meuchel et al, 2011). NO production induced by NT-3 appears to largely involve Trk receptors. However, $p75^{NTR}$ interactions with Trk receptors could facilitate rapid NTs effects.

The PI3K-Akt-eNOS signalling pathway is well-known to promote ECs survival, migration and angiogenesis (Caporali & Emanueli, 2009). Activation of the PI3K-Akt-eNOS pathway is critical for NT-3–induced angiogenesis both *in vitro* and *in vivo* in a mouse model of limb ischemia (Cristofaro et al., 2010). Furthermore, studies have reported that PI3K inhibition by LY294002 and NOS inhibition by L-NAME inhibited NT-3–induced network formation on Matrigel. All these data provide evidence that the PI3K-Akt-eNOS pathway mediates the proangiogenic responses of ECs to NT-3 stimulation.

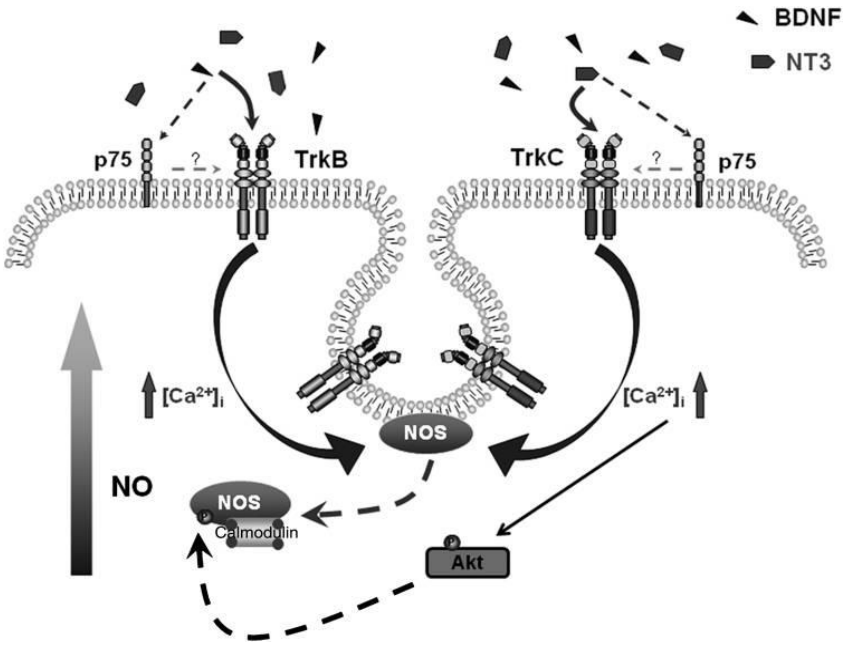

Illustration 14. Schematic representation of NTs effects on ECs-derived NO. *NTs (such as BDNF and NT3) increase Ca^{2+} in pulmonary artery ECs and Akt phosphorylation, which then induces dissociation (and activation) of eNOS from caveolae, with subsequent production of NO. Such NT-induced NO production involves activation of Trk receptors (TrkB) for BDNF and to a lesser extent TrkC for NT3, but may also involve the low-affinity $p75^{NTR}$ (Meuchel et al., 2011).*

NT-3 also induces the rapid phosphorylation and activation of eNOS present in the neural stem cells resulting in NO production and NO-dependent cytostasis. In addition, the release of NO mediated by NT-3 in ECs of the brain vasculature, modulates the proliferation of neural stem cells, and maintains a quiescent population of these cells (Delgado et al., 2014).

3.3.3 NT-3 and angiogenesis

NTs play a role in adult neovascularization, for instance NGF, BDNF or NT-3 induce capillarization, thereby accelerating wound healing or hemodynamic recovery of ischemic tissues. NGF promotes reparative angiogenesis produced in the ischemic limb muscles through a VEGF-Akt-NO-mediated mechanism in the setting of ischemia (Emanueli et al., 2002; Meloni et al., 2010; Shen et al., 2013). NTs also modulate the cutaneous microvascular network and are highly potent angiogenic factors. This angiogenic effect is mediated directly through binding to the Trk receptors (Blais et al., 2013).

Studies evidence that NT-3 stimulates ECs proliferation, survival, migration and angiogenesis in skeletal muscle ECs, VSMCs, and TrkC-transduced HUVEC. In an angiogenesis assay using mesenteric rings, exogenous NT-3 produced neovascularization and increased the number and size of functional vessels. Microvascular responses induced by NT-3 were accompanied by TrkC phosphorylation and involved the PI3K-Akt-eNOS pathway both *in vitro* and *in vivo* (Cristofaro et al., 2010b).

In the diabetic foot and other ischemic ulcers, NT-3 promotes cell proliferation and migration to accelerate wound healing by inducing angiogenesis through activation of vascular ECs (Shen et al., 2013). NT-3 released in malignant glioma has the capacity to attract bone marrow-derived stroma cells, which may have implications for tumour vasculogenesis (Caporali & Emanueli, 2012).

Additional studies have shown that NT-3 treatment promoted bony repair with increased vascularization and mRNA expression for VEGF at the injured growth plate. After injury, prominent induction of NT-3 and its receptor TrkC were observed at the injury site. NT-3 induced endothelial sprouting comparable to that induced by VEGF treatment in foetal mouse metatarsal bone explants, and inhibition of VEGF by anti-VEGF antibody blocked NT-3-induced angiogenesis (Su et al., 2016).

Contrarily, studies have demonstrated that $p75^{NTR}$ inhibits neovascularization in a mouse model of limb ischemia (Cristofaro et al., 2008).

4. NT-3 IN CARDIOVASCULAR PATHOPHYSIOLOGY

Cardiovascular diseases represent a major healthcare problem in the world and are the main cause of morbidity and mortality. These pathologies also represent a high impact in the economy in the world (Benjamin et al., 2018). Cardiovascular diseases are disorders of the heart and blood vessels including coronary heart diseases, atherosclerosis, hypertension, cardiac ischemic, peripheral arterial disease, HF, and other pathologies. In the last year, statistical update of the American Heart Association showed that the leading cause of cardiovascular diseases death in United States is coronary heart disease followed by hypertension, HF, and others. The factors associated with cardiovascular diseases are obesity, sedentary lifestyle, diabetes, high blood pressure, and cholesterol (Phillips & Guazzi, 2015).

Several pathologies that affect cardiovascular function involve changes in the expression or activity of NTs. It has been seen that NT-3 and TrkC are expressed in heart and vessels from embryonic development to maturity (Scarisbrick et al., 1993, Kawaguchi-Manabe et al., 2007). Neurons, cardiomyocytes, ECs, VSMCs, and pericytes are all targets for NTs action during development and in the mature system.

Activation of TrkC by NT-3 is required for the development of the atria, ventricles, and cardiac output tracts, so that genetic deletion of either NT-3 or TrkC results in impaired cardiac morphogenesis (Meuchel et al., 2011). The lack of NT-3 leads to defects that resemble some of the congenital malformations in humans. Overexpression of a dominant negative version of TrkC also leads to the development of cardiovascular abnormalities (Emanueli et al., 2014). Moreover, mutations in NTRK3 (TrkC) contribute to the aetiology of congenital heart defects including Tetralogy of Fallot and ventricular septal defects (Werner et al., 2014)

NTs also act by regulating several processes that include the stimulation of angiogenesis in situations of hypoxia, regulation of neurotransmission at the level of the synapses (Lockhart et al., 2000; Sharma et al., 2010), control of neuronal excitability (Luther & Birren, 2009), production of neurotransmitters (Thoenen, 1972) and synthesis of neuropeptides (Shadiack et al., 2001)

On the other hand, the expression of $p75^{NTR}$ is induced in pathological situations such as ischemia, atherosclerosis and diabetes (Caporali & Emanueli, 2009). However, the consequences of its activation have not been deeply studied at this level.

These evidences suggest not only a relevant role of NT-3 in the development and function of the cardiovascular system, but also its relationship with pathological situations in the mature cardiovascular system. In many of these conditions, the impaired expression of NTs and / or NT receptors has direct effects on vascular and smooth muscle ECs, besides the effects on nerves that modulate vascular resistance and cardiac function (Emanueli et al., 2014).

4.1 HEART FAILURE AND NT-3

HF is a chronic cardiovascular disease that results from structural or functional cardiac disorders caused by numerous underlying cardiac etiologies and varying clinical settings. The most common underlying causes of systolic HF are ischemic heart disease, cardiomyopathies, and heart valve diseases. An impaired ventricle relaxation is the result in a diastolic HF syndrome (Sayago-Silva et al, 2013). HF is frequently associated with chronic hypertension, ischemic heart disease or hypertrophic cardiomyopathies. Different mechanisms can produce a reduction in cardiac output due to a decrease in cardiac frequency or in stroke volume (Sayago-Silva et al., 2013; Tanai & Frantz, 2015).

Little is known about the relation between HF and NT-3 Studies in cardiac hypertrophy have displayed that NT-3 is highly expressed in heart and vasculature while TrkC is highly expressed in heart so that NT-3 induces cardiomyocyte hypertrophy via TrkC (Kawaguchi-Manabe, et al, 2007).

In rat cardiomyocyte cultures, exogenous or endogenous NT-3 exerted a hypertrophic action, activating MAPKs (p38, ERK1/2, and JNK) and increasing the expression of hypertrophy markers and the size of cardiomyocytes (Kawaguchi-Manabe et al., 2007; Saygili et al., 2010). However, NT-3 was downregulated in cardiac hypertrophy induced by endothelin-1 stimulation (*in vitro*) or evoked by pressure overload (*in vivo*) in rat (Kawaguchi-Manabe et al., 2007).

4.2 ISCHEMIC CARDIOMYOPATHY AND NT-3

Cardiomyopathies are associated structural and functional abnormalities in the myocardium and are classified according to morphological and functional criteria: Dilated cardiomyopathy (DC), ischemic cardiomyopathy (IC), hypertrophic cardiomyopathy, restrictive cardiomyopathy, and arrhythmogenic right ventricular cardiomyopathy. In IC, ischemic regions have abnormalities in myocardial contractility.

It has been observed a protective vascular action of exogenously NT-3 and a decrease in NT-3 expression during cerebral ischemia, but this process has not been studied in IC (Galvin & Oorschot, 2003; Lindvall et al., 1992; Zhang et al., 1999). There have been few studies of the role of NT-3 in cardiac ischemic processes. It has been observed that, after an acute myocardial infarction, NT-3 mRNA levels do not change with respect to those existing in a non-pathological situation (Hiltunen et al., 1996).

4.3 HYPERTENSION AND NT-3

Hypertension is one of the leading causes of death and the most treatable. This pathology increases incidence of HF, atherothrombotic and hemorrhagic stroke (Cressman et al., 1983).

Studies in SHR rats, a genetic hypertension model from Wistar-Kyoto rats, showed that the underlying cause of hypertension was the existence of a sympathetic hyperinnervation of VSMCs (Head, 1989). Other studies have demonstrated that NT-3 expression is higher in SHR rats than in the normotensive WKY strain during the first weeks and NT-3 levels in heart of SHR rats are elevated compared to their controls (Zhang & Rush, 2001). These results suggest that NT-3 could be related with the establishment of noradrenergic hyperinnervation.

Additionally, increased mRNA and protein expression levels of NT-3 were detected in lung from SHR which could be implicated in the development of pulmonary hypertension and pulmonary vascular remodelling (Ricci et al., 2004).

4.4 ATHEROSCLEROSIS AND NT-3

Atherosclerosis is a complex chronic inflammatory process of the arterial wall that involves the activation of ECs by inflammatory cytokines, followed by increased adhesion of circulating monocytes to the endothelium, and the migration of VSMCs to the neointima layer in developing.

NT-3, TrkC, and $p75^{NTR}$ are present in VSMCs from human atherosclerotic lesions (Donovan et al., 1995; Kraemer et al., 1999), suggesting that NTs can regulate the responses of VSMCs to vascular injury. Alternatively, $p75^{NTR}$ activation induces apoptosis of these cells during remodelling of the established vascular lesion, whereas TrkA activation stimulates VSMCs migration (Wang et al., 2000). Therefore, NTs can contribute to the development and remodelling of atherosclerotic plaques.

4.5 METABOLIC SYNDROME AND NT-3

The metabolic syndrome is a group of conditions that increase the risk of developing heart disease and type 2 diabetes. These conditions are: high blood pressure, high glucose and triglycerides levels in the blood, low HDL blood levels and excess fat. NTs have been recognized as metabokines and are implicated in the control of glucose, lipid, and antioxidant metabolism. Therefore, NTs could also be implicated in the pathogenesis of cardiometabolic and immune-inflammatory diseases. The alteration of BDNF and TrkA in heterozygous mice leads to hyperphagia and obesity, and BNDF acts synergistically with leptin to modulate food intake (Chaldakov et al., 2004). In patients with metabolic syndrome and with acute coronary syndromes, BDNF and NGF levels are reduced. Moreover, the high-fat/high-carbohydrate diet reduces BDNF content which is an atherogenic risk factor (Chaldakov et al., 2009; 2003).

4.6 NT-3 AND THERAPEUTIC PERSPECTIVES

NTs share poor pharmacokinetic characteristics and the blood-brain barrier presents a major hurdle in the use of peptide therapeutics in case the target is the brain to prevent neuronal degeneration (Caporali and Emanueli, 2010). Moreover, NTs can still activate the proapoptotic $p75^{NTR}$ although with lower affinity than proNTs. Thus, NTs are not considered good drug candidates. Alternative strategies for use of NTs proteins may consist in molecule activators of Trk receptors. Recently, cell-permeable small compounds able to activate TrkA (but not $p75^{NTR}$) in the absence of NGF have been developed and could have potential utility in the treatment of neurodegenerative diseases (Lin et al., 2007). Similarly, agonists for TrkB and TrkC could be developed for anti-apoptotic and proangiogenic therapies.

Another alternative could be to develop antagonist compounds capable of blocking NT-induced activation of Trk receptors. Overall, drugs able to block Trk signalling at receptor or post-receptor level might have a role in inhibiting angiogenesis (Caporali & Emanueli, 2010). In this case, the compounds could be used to treat pathological angiogenesis associated with inflammatory pathologies such as arthritis and psoriasis, or cancer (Caporali & Emanueli, 2010). Conversely, it could also be interesting molecules able to sequestrate NTs, thus impeding interaction with their receptors.

On the other hand, molecules that partially activate distinct patterns of intracellular signalling cascades could also be useful. For instance, small molecules capable to act selectively at $p75^{NTR}$ or TrkA receptors, and to activate partially distinct patterns of intracellular signalling cascades, have been shown to prevent neuronal degeneration *in vitro* (Longo & Massa, 2004). Thus, selective TrkA activation may promote angiogenesis in ischemic tissues. Additionally, Trk function could also be improved by inhibition of protein-tyrosine phosphatase, leading to augmentation of receptor activation, downstream signalling, and neurotrophic effects (Xie et al., 2016).

II OBJECTIVES

The aim of the present Thesis is to determine the expression of NT-3 and TrkC in the cardiovascular system of human and rodents, to further study the role of NT-3/TrkC pathway as modulator of the cardiovascular functions and their relation to cardiovascular diseases.

This general objective is developed on the following specific objectives:

- To determine the gene and/or protein expression of NT-3 and TrkC in left ventricle, kidney, brain and vessels from human or rodents as well as in aortic and heart human cell lines or primary cell cultures from rat.
- To study the role of NT-3/TrkC in the migration process in three different human endothelial cells (ECs) lines: aortic, coronary artery, and coronary microvasculature ECs.
- To analyse the role of NT-3/TrkC in the angiogenic process both in *in vitro* models in human EC lines, and in *ex vivo* models in isolated rat aortic rings.
- To examine the role of NT-3 in the contractile tone of rat aortic and tail artery rings, and the involvement of NO in its mechanism of action, determining the influence of endothelium and perivascular adipose tissue.
- To determine the cardiovascular consequences of changes in the expression of NT-3, by using genetically engineered mice with partial expression or endothelial deletion of NT-3.
- To evaluate the changes in the expression of NT-3/TrkC that occur in the myocardium of patients with heart failure and different pharmacological treatments, and in cardiovascular tissues from animal models with hypertension or obesity, to establish whether there is a parallelism between these changes and those determined in human pathologies.

III. MATERIALS AND METHODS

1. MODELS FOR EXPERIMENTATION

1.1 HUMAN MODEL

Adult patients were recruited, diagnosed, and treated in the Cardiology Service at the Hospital La Fe (Valencia). All patients signed written consent before their inclusion in the study. The protocols (clinical assessment, treatment, and biochemical assays) were approved by the Ethics Committee of the Hospital La Fe and the University of Valencia and conducted in accordance with the Declaration of Helsinki.

1.1.1 Study population and patient selection

All the patients had severe HF, which was classified according to the New York Heart Association's functional classes IV. Subjects with HF were divided into two groups according to their aetiology: patients with dilated cardiomyopathy (DC) or ischemic cardiomyopathy (IC), and patients with other forms of cardiomyopathy (non-ischemic, non-dilated). They all were on a pharmacological therapy for HF with diuretics, β-blockers (Rengo et al, 2011), angiotensin-converting enzyme (ACE) inhibitors (Ramos-Ruiz et al., 2000), intravenous β-agonist drugs (Belmonte & Blaxall, 2011), antiarrhythmic or digoxin (Agüero et al., 2009), according to hemodynamic status. Clinical data were obtained from the echocardiographic study, within 24 hours of sampling, and hemodynamic parameters were carried out in the same moment previous to the taking of sample. Anthropometric variables as well as biochemistry profile were determined in this patients.

Control subjects were normotensive, with normal values in biochemistry profile and none of them developed cardiovascular diseases.

1.1.2 Sample collection

Myocardial samples from 38 HF patients and from 4 organ donors, when the heart was not used for transplant (control subjects), were collected. Immediately, after the heart extraction, in the first 8 h after the explant, the sample is deposited in physiological saline solution at 4°C. Transmural samples of the explanted heart were obtained from the posterior part of the LV adjacent to the interventricular

septum. The areas containing grossly visible scar tissue were avoided in patients with HF.

The human aorta was obtained from 4 patients who had undergone prior aortic surgery.

All samples were immediately frozen in liquid nitrogen and stored at -80ºC until processed.

1.2 ANIMAL MODEL

Care and treatment of animals and all the experimental procedures complied with guidelines established in the Spanish legislation (Royal Decree RD 53/2013) about "Protection of animals used for experimental and other scientific purposes" which transposes and implements Directive of the European Union (2010/63 / EU). In addition, all procedures were approved by the Experimental Animal Ethic Committee of the University of Valencia.

The study was performed in animals housed in clean cages (five animals per cage), maintained with a normal 12-hour light/dark cycle at 22ºC and 60% relative humidity. The animals were provided with standard chow and water *ad libitum* until they were used for the study.

1.2.1. Rats

1.2.1.1 Wistar rats

Male Wistar rats (250-300g) from 16-20 weeks (Harlan Interfauna Ibérica, Barcelona, Spain), bred in the Animal Production service of the SCSIE of the University of Valencia, were used in our study.

One group of 12-week-old Wistar rats received L-NAME (80 mg/kg per day in drinking water for 4 weeks) until the age of 16 weeks to induce hypertension. This treated group is named L-NAME-induced hypertensive rat (LNAME-HR).

L-NAME (NG-nitro-L-arginine methyl ester) is an inhibitor of NOS, responsible for the synthesis of NO, an important vasodilator agent. In this model of animal hypertension, the disease is induced by the lack of NO production (Ribeiro et al.,

1992). The average increase in weight of the animals as well as the liquid intake were taken into consideration for the dosage of L-NAME.

1.2.1.2 Spontaneously Hypertensive Rat

16-Week-old male rats (250-325 g) of two strains were used: Spontaneously Hypertensive Rat (SHR) and their normotensive controls Wistar Kyoto Rats (WKY) (Harlan Interfauna Ibérica, Barcelona, Spain).

SHR is a model of genetic animal hypertension widely used since 1963. Okamoto and Aoki developed a genetic line of hypertensive rats based on male rats of Wistar-Kyoto strain that had spontaneously developed hypertension arterial, and crossing them with females of the same strain that had previously been selected with high blood pressure.

1.2.1.3 Zucker rats

Zucker obese rat (fa/fa) is an animal model with metabolic syndrome that develop obesity, hyperlipidaemia, and hypercholesterolemia. The mutation in the *Lepr*^{fa} gene was discovered in 1961 by Lois and Theodore Zucker, in the population of 13 M inbred rats. Male obese Zucker rats (Charles River Laboratories, Barcelona, Spain) of 15 weeks of age (550- 680 g) and their control lean rats (430- 480 g) were used in the present study.

1.2.2 Mice

Genetically engineered mice were used as a tool for the analyses of NT-3 in cardiovascular system. Two mouse models were utilized:

-Mice of 40-50 weeks of age (160-240mg) with partial expression of NT-3 (*Ntf3*^{lacZneo}) by homologous recombination; the coding region of NT-3 gene has been replaced by *lacZ* which codes for β-galactosidase. The generation of the NT-3 mutant mice has been described by Fariñas et al. (1994).

- *Ntf3*$^{+/lacZneo}$ heterozygous mice (**NT3**$^{+/-}$)
- *Ntf3*$^{+/+}$ wild-type mice (**NT3**$^{+/+}$)

-Male mice of 55-65 weeks of age (140-210mg) with deleted expression of NT-3 in the endothelium (*Ntf3*$^{flo1/lox2}$) (Delgado et al., 2014), obtained by crossing mice carrying loxP sites flanking the Ntf3 exon (*Ntf3*$^{flox1/flox2}$) (Shimazu et al., 2006) with mice expressing the Cre-recombinase under the control of the endothelium-

specific angiopoietin receptor tyrosine kinase receptor-2 (Tie2/Tek) promoter (Tie2-cre$^{+/0}$) (Kisanuki et al., 2001):

- *Ntf3*$^{flox1/lox2}$; Tie2-cre$^{+/0}$ knockout mice with NT-3 deleted from endothelium, (**eNT3^{-}**)
- *Ntf3*$^{flox1/lox2}$; Tie2-cre$^{0/0}$ control mice (**eNT3^{+}**)

The two mouse models were kindly provided by Dra. Isabel Fariñas (Department of Cell Biology, University of Valencia).

1.2.3 Systolic blood pressure determination

Several methods have been applied for the measurement of systolic blood pressure (BP) in animals. The non-invasive blood pressure methodology consists of placing a cuff on the animal's tail to occlude the blood flow, recording the hemodynamic constants (Plehm et al., 2006).

Systolic BP was monitored using this non-invasive method of plethysmographic measurement by *tail-cuff* (NIPREM 645; Cibertec, Barcelona, Spain) in unanaesthetized animals. The measurements were made each day during a month. Systolic BP measurements involve the observation of animals for long periods. Therefore, in order to reduce animal stress and enhance blood flow through its tail, the animals were placed on a warm blanket at 37ºC for at least 30 min. The pressure cuff was fixed in the same position around the tail of rats as it has been previously described (Gisbert et al., 2000).

The software registered the signal of three measurements and documented constant BP (mmHg) in each animal. For each animal, the average of 10-15 measures was taken into account. Systolic BP was determined weekly, taking the last measure the day before the animals were sacrificed.

1.2.4 Sacrifice and sample collection

Animals were anaesthetized with isofluorane (IsoFlo® Esteve, Spain); mice were sacrificed by cervical dislocation and rats were sacrificed by decapitation, taking into account the recommendations for the euthanasia of animals, from the General Direction for the Environment (DGXI) of the European Commission, for sacrifice with the minimum physical and mental suffering of the animal (Close et al., 1996).

Sample collection was as follows:

Thoracic aorta: after the thoracotomy, the lungs and heart were separated, leaving the artery uncovered, which was carefully removed with fine microdissecting forceps and iridectomy scissors. In most cases, PVAT which surrounds the aorta was removed avoiding damaging the muscle layer and losing capacity to contract and relax.

Tail artery: the tail artery was carefully isolated from the animal with fine microdissecting forceps and scalpel to remove epithelial, tendinous, and cartilaginous tissues. The section used for the study was isolated from the area near the beginning of the tail.

Heart: after the thoracotomy, the heart was extracted with tweezers and scissors, sectioning the pulmonary artery and aorta, and the pulmonary veins and cava, and depositing it in a Petri dish in sterile physiological saline medium. The heart was immediately cleaned of any blood remnant and the possible existing adipose tissue was eliminated. The heart was dried and weighed for further analysis. Then, the right and left atria were separated and the LV was carefully dissected from the right ventricle and the interventricular wall.

Brain: Once the animal is exsanguinated, the extraction and dissection of the brain, and separation of the cerebral cortex was carried out. The whole process was quickly done at 4°C.

Kidney: The abdomen of the animal was opened by laparotomy and the intestinal pack moved to the side, leaving visible the left kidney, which is protected by peritoneal fat and joined to the aorta by the renal artery. A unilateral radical nephrectomy was performed sectioning the artery and vein to extract the kidney that was dissected and cleaned of any remaining adipose tissue.

Once tissues of interest were removed from the animal, they were placed in aerated *Krebs solution* (118mM NaCl, 4.75mM KCl; 1.8 mM $CaCl_2$; 1.2 mM MgCl2; 25mM NaHCO3; 1.2 mM KH2PO4; 11 glucose pH=7.4).

The tissues, that were used for RNA and / or protein extraction experiments, were immediately frozen in liquid nitrogen and then stored at -80 ° C until processed.

1.3 *IN VITRO* MODEL

1.3.1 Human cell lines

The use of *in vitro* models can provide insight of physiological or pathological process in cardiovascular system. We employed human cells including human aortic ECs (**HAoEC**), human coronary artery ECs (**HCAEC**), human cardiac microvascular ECs (**HCMEC**), human aortic smooth muscle cells (**HAoSMC**), human aortic adventitial fibroblasts (**HAoAF**), human cardiac myocytes (**HCM**), and human cardiac fibroblasts (**HCF**), and were grown in the corresponding medium. The cells were used in passage 5-6.

ECs were grown in Endothelial Cell Growth Medium MV2 supplemented with 0.05 ml/ml (5%) Fetal Calf Serum (FCS) and GFs: 5 ng/ml Epidermal GF, 10 ng/ml Basic Fibroblast GF, 20 ng/ml insulin-like GF, 0.5ng/ml Vascular Endothelial GF, 1µg/ml ascorbic acid and 0.2µg/ml hydrocortisone. For better compression, this medium will be named *complete medium*. Some experiments required the use of the Endothelial Cell Growth Medium MV2 without GFs and FCS; this medium will be named *basal medium*. Thus, the basal medium supplemented with 0.5% FCS will be called *basal medium with 0.5% FCS.*

HAoSMC were grown in Smooth Muscle Cell Growth Medium 2 supplemented with 0.05 ml/ml (5%) FCS, 0.5 ng/ml Epidermal GF, 2 ng/ml Basic Fibroblast GF and 5 µg/ml Insulin.

HAoAF were grown in Fibroblast Growth Medium 2 supplemented with 0.02 ml/ml (2%) FCS, 1ng/ml Basic Fibroblast GF and 5 µg/ml Insulin.

HCM were grown in Myocyte Growth Medium supplemented with 0.05 ml/ml (5%) FCS, 0.5 ng/ml Epidermal GF, 2ng/ml Basic Fibroblast GF, and 5µg/ml insulin.

HCF were grown in Fibroblast Growth Medium 3 supplemented with 0.1 ml/ml (10%) FCS, 1 ng/ml Basic Fibroblast GF, and 5 µg/ml Insulin.

All culture media were added 50 µg/ml gentamicin (Genta-Gobens®; Normon) as antibiotic and 50ng/ml amphotericin B (Biowhittaker®; Cambrex) as antimycotic.

The cell lines, as well as culture media and SupplementPack were purchased from PromoCell (Heidelberg, Germany).

1.3.1.1 Thawing cryopreserved cells

Briefly, the frozen vials (cryovials) were thawed in a water bath at 37ºC for 2 min (Promocell protocol). The cells were transferred to a centrifuge tube (Falcon, USA), containing 1 ml pre-warmed phosphate buffered saline (PBS, GIBCO, USA) and were centrifuged at 8000 x *g* for 5 min. The supernatant was discarded and pre-warmed complete medium was added to the pellet, the cells were plated in 25cm^2 cell culture flasks (T25 flask) (Falcon, USA) and were placed in an incubator at 37ºC in 5% CO_2 for cell attachment. The medium was changed every two or three days and the cell density was checked each day.

1.3.1.2 Cell subculture

The cells were subcultivated according to the Promocell protocol, once they reached 80% confluence. First, Detachkit from Promocell, which consists of Hepes-BSS solution, Trypsin/EDTA solution, and Trypsin neutralization solution (TNS), was pre-warmed for at least 30 min. Then, the medium was aspirated from the culture vessel and Hepes BSS solution (100 µl/cm^2 flask surface) was added to plate for several seconds. Carefully, the Hepes BSS solution was removed and Trysin/EDTA solution (100 µl/cm^2 flask surface) was added for 5 min at 37ºC in 5% CO_2. When the cells started to detach, TNS (100 µl/cm^2 flask surface) was added to the flask to neutralize the trypsin and gently agitated. The cells were collected and centrifuged for 5 min at 800 x *g.* The cells were resuspended in 1 ml of the appropriated cell growth medium and then counted using a haemocytometer. The average of three different measures was used to calculate cell number in a 1 ml cell suspension. After cell counting, the cells were resuspended in the appropriate cell growth medium and seeded into T25 flask or plated according to the experiment. The cells were placed in an incubator at 37ºC in 5% CO_2 until reach 80-90% confluence, and the medium was renewed every two days. Experiments were performed between passage 5 and 6.

1.3.1.3 Cryopreservation

The cells were periodically cryopreserved in each cell passaging to maintain a stock of cell lines. The cells were detached with trypsin/EDTA solution and centrifuged as described above. Then, the cells were frozen with 1 ml Cryo-SFM (Promocell) in cryovials (cell density of 10^5 or $2x10^5$ cells/ml) and were placed in

an isopropanol box at -80ºC. The next day, the frozen cells were immediately transferred to liquid nitrogen for future use.

1.3.2 Primary rat cultures

Primary cultures were performed with fibroblasts from rat heart and smooth muscle cells from rat aorta. The isolation was carried out according to the protocol described below:

1.3.2.1 Fibroblasts isolation

The rat heart was crushed with a scalpel until obtaining a homogeneous paste, which was poured into 5 ml of DMEM F-12 Ham´s medium (Dulbecco's modified Eagle's minimum essential medium, Sigma St. Louis MO, USA) and 5-7.5 mg of collagenase II (1-1.5 mg/ml, Sigma Aldrich). This mixture was incubated at 37ºC for 45 min in a shaking incubator and then, centrifuged at 390 g for 5 min. The supernatant was removed and the resulting pellet was resuspended in DMEM supplemented with 12% FCS (Gibco BRL, Gaithersburg MD, USA), 100 U/ml penicillin, and 100µg/ml streptomycin. The cells were seeded in plates of 35 mm diameter and incubated at 37°C and 5% CO_2. The medium was renewed every 3 days until 75% confluence was achieved, around 5-7 days. Then, the medium was removed and the cells were harvested in Tripure Isolation Reagent (800 µl/plate) (Roche Applied Science). This isolation method does not guarantee a pure fibroblasts culture, although it must be mainly composed of fibroblasts.

In another group of experiments, the same protocol was performed but instead of cultivating the fibroblasts, they were stored at -80°C for subsequent RNA extraction. In the results, this isolation has been called "fresh" cells.

1.3.2.2 Aortic smooth muscle cells isolation

The endothelium was mechanically scraped from the aorta using a blunt Pasteur pipette, to remove the endothelium. Then, the tissue was cut up with a scalpel. The homogenous mass was poured into 2.5 ml of DMEM F12- Ham´s medium (Sigma St. Louis MO, USA), supplemented with: 180U/ml penicillin 180µg/ml streptomycin, 20nM L-glutamine, fungizone 2.5 U/ml and gentamicin 4mg / ml. Subsequently, it was centrifuged at 180g for 4 min and the pellet was resuspended in 2.5ml of a collagenase solution (2.5mg / ml Sigma St Louis MO, USA) in this medium. The tissue was incubated for 90 min in the collagenase

solution at a constant temperature of 37ºC and under stirring. In order to obtain an efficient disintegration, the solution was strongly agitated every 10 min and a mechanical disintegration was performed every 30 min using a Pasteur pipette whose tip was narrowed by flaming.

Subsequently, the disintegrated tissue was centrifuged at 390 *g* for 10 min; the pellet was resuspended in the same medium and the centrifugation was repeated once again. The final pellet was resuspended in supplemented DMEM F12-Ham´s medium and 12 % FCS. The cells isolated from tissue were seeded in plates of 35 mm diameter and the medium was renewed every 3 days. The culture was incubated at 37ºC and 5% CO_2 around 15 days, until 70-75%% of confluence.

In another group of experiments, the same protocol was performed but instead of cultivating the cells, they were frozen directly at -80 ° C after isolation. In the results, this isolation has been called "fresh" cells.

2. REAGENTS, DRUGS, AND ANTIBODIES

The recombinant human **NT-3** was obtained from *PeproTech, Inc (*Rocky Hill, NJ, USA), prepared according to manufactur's instructions, and stored aliquots of stock concentration (10 µg/ml) at -80ºC ready for use. We used a final concentration of 32 ng/ml in all experiments. The Trk receptors inhibitor **K252a** was purchased from Calbiochem (San Diego, CA), was dissolved in dimethyl sulfoxide (DMSO), and was divided into aliquots. The final concentration of K252a was 0.20 µM in DMSO (0.01%) in all experiments.

Many drugs were purchased to Sigma-Aldrich (St Louis MO, USA): **Acetylcholine** (ACH), (R)-(−)-**Phenylephrine** hydrochloride (PHE), **Isoprenaline** hemisulfate (ISO), N(ω)-nitro-l-arginine methyl ester (**L-NAME**), **SR58611A** [[(7S)-7-[[(2R)-2-(3-Chlorophenyl)-2-hydroxyethyl] amino]-5,6,7,8 - tetrahydro - 2 -naphthalenyl] oxy acetic acid ethyl ester hydrochloride. PHE and L-NAME were prepared in distilled water, ISO was diluted in 0.01% ascorbic acid, and SR58611A in 20% ethanol.

NT-3 antibody was purchased from Abcam (Cambridge, MA), TrkC antibody was obtained from Cell Signalling (Beverly, MA), and Glyceraldehyde 3-phosphate

dehydrogenase (GAPDH) antibody was obtained from Sigma (Table 1). Antibodies were used for Western blot analysis.

Table 1. Antibodies used in Western Blot.

Protein	WM (kDa)	Antibody	Dilution
NT-3	29	Rabbit polyclonal (ab65804; Abcam)	1:1000
TrkC	145.1	Rabbit monoclonal (3376S; Cell signaling)	1:1000
GAPDH	36	Rabbit polyclonal (G9545; Sigma Aldrich)	1:10000

3. EXPERIMENTAL PROCEDURES

3.1 β-GALACTOSIDASE HISTOCHEMISTRY

A rapid and visual assay of *LacZ* activity was used to detect reporter gene expression, where the bacterial *LacZ* is knocked into our gene of interest (NT-3). The bacterial *LacZ* gene encodes the β-galactosidase enzyme which catalyses the hydrolysis of β-galactosides including X-gal (5-bromo-4-chloro-3-indolyl-beta-D-galactopyranoside). X-gal is separated into galactose and 5-bromo-4-chloro-3-hydroxyindole; then, it is oxidized and the final product is a dark blue stain. Therefore, the cells stain blue to show the *LacZ* gene is expressed under NT-3 promoter.

Mouse expressing the *LacZ* reporter gene, encoding the enzyme β-galactosidase from the NT-3 locus (*Ntf3*$^{+/lacZneo}$) were used. Organs (aorta, tail artery, LV, kidney and brain) were dissected and were immediately incubated in 0,1M PO_4 with 2 mM $MgCl_2$, 5 mM $K_3Fe(CN)_6$, 5 mM $K_4Fe(CN)_6$, 0.01% sodium deoxycholate, 0.02% NP-40, and 1 mg/ml X-gal during 1 h for vessels and 2 h for the rest of tissues to increase stain penetration. The tissues were washed with phosphate buffer (PB) and sodium azide 0.05% for three times at room temperature on a shaker in the dark and stored at 4ºC. Images were obtained in a LEICA M165 stereo microscope.

Aorta samples were embedded in LR-White resin, cut in 2 µm sections (Ultracut UC6, Leica), and visualized in Leica DM IL LED microscope in the Microscopy Service of the SCSIE of the University of Valencia

3.2 QUANTIFICATION OF GENE EXPRESSION

3.2.1 Total RNA extraction

Human and animal tissues were disrupted by grinding the frozen tissue with a mortar or pestle to generate very small particles. During the grinding of the tissues, the samples were kept frozen with liquid nitrogen to prevent their degradation. Once the cells reached the confluence, the medium was removed and the cells were stored at -80ºC until their use.

Then, 1 ml of TriPure Isolation Reagent (Roche Applied Science) was added to tissues or cells. Total RNA from samples was isolated in appropriate RNAase free conditions to analyse gene expression of NT-3, TrkC, and β-ARs (Oliver et al., 2010). The samples were homogenized by vigorously shaking at 3 cycles for 15 seconds at room temperature in vortex. Subsequently, the mixture was centrifuged at 12.000 *g* during 10 min at 4ºC. Following centrifugation, the supernatant was transferred into a new tube and 200 µl chlorophormo was added in the supernatant and shaken for 15 seconds in vortex. In order to be separated in three phases (red phenol phase, interphase, and aqueous phase), the mixture was incubated for 10 min at room temperature.

RNA, in aqueous phase, was carefully transferred into a fresh tube. A second centrifugation was performed at 12.000 *g* for 15 min at 4 °C to facilitate separation and precipitation of genomic DNA. In order to precipitate the RNA, 500µl of isopropranol were added in the aqueous phase during 10 min at room temperature. To collect total RNA, we centrifuged at 12.000 *g* at 4ºC for 10 min and removed the supernatant. Total RNA pellet was washed with 1 ml of 70 % ethanol DEPC (diethyl pyrocarbonate)-treated water, subsequent, centrifugation at 8.000 *g* at 4ºC for 5 min. DEPC-treated water was added into the RNA pellet and the pellet was subjected to drying under the light of a lamp the necessary time. Total RNA was quantified and stored at -80ºC until use.

The accuracy of gene expression is influenced by the quantity and quality of RNA. After RNA extraction, it was necessary determined the RNA concentration in each sample. Total RNA was quantified using a spectrophotometer Biophotometer® (Eppendorf) which measures wave lengths at 260 nm (specific for nucleic acids) and 280 nm (specific for proteins); the 260/280 ratio is an indicator of purity, and a value greater than 1.8 is indicator of good RNA quality. To analyse RNA integrity, total RNA was diluted 1/250 in a volume of 500 µl and was transferred into a cuvette to be measured.

3.2.2 Reverse transcription

A high sensitivity enzyme, Improm-II was used for the Reverse Transcription or Retrotranscription (RT) reaction of the RNA obtained from each sample, which allows starting from lower amounts of total RNA (0, 1-1 µg).

To perform the reverse transcription (RT), total RNA was incubated with oligo $(dT)_{16}$ primer (250ng) in DEPC-treated water at 70ºC. RT reaction was adjusted to 20 µl with the master mix: Buffer-RT 5X, 3mM MgCl2, 20 U ribonuclease inhibitor RNAsin® (Promega Corp., Madison USA), 0.5 mM of each deoxinucleoside triphosphate (dNTP), and 1 µl of reverse transcriptase ImProm-II™ (Promega Corp. Madison, USA). The reaction was carried out at 42ºC for 1 h. Then, the enzyme was inactivated at 70ºC during 15 min; synthetized cDNA was stored at -20ºC or directly proceed to qPCR.

3.2.3 Quantitative real-time polymerase chain reaction (qPCR)

In quantitative gene expression analysis, mRNA coding for NT-3, TrkC and GAPDH as endogenous control, were analysed using TaqMan® RT-PCR (Gene Expression Assays, Applied Biosystems), and were run on a GeneAmp 7500 fast system thermocycler (Applied Biosystems, Carlsbad, CA, USA) as described by Montó et al., (2012).

To perform TaqMan® assay, cDNA was diluted 1/10 before adding to the PCR reaction. Master mix was set up with 20X primers and TaqMan probe labelled with 6-FAM™fluorochrome on the 5' end and minor groove binder (MGB) and nonfluorescence quencher (NFQ) on the 3' end designed to detection and quantification of gene sequence.

The reactions were carried out with 25µl of TaqMan® Universal Master Mix (AmpliTaq Gold® DNA Polymerase; Applied Biosystems, US) including 5 µl cDNA diluted, 1.2 µl of 20X probe (250nM nmol/L), and primers (900 nmol/L) mix (TaqMan® Gene Expression Assay). The cDNA was amplified following the manufacture's conditions: one initial Hold-step at 95ºC for 10 min, a second step with 40 cycles including 15 seconds at 95°C (denaturation) and 1 min at 60°C (annealing/extension). The targets and reference (GAPDH) were amplified in parallel reactions.

Table 2. Probes gene expression assay

Gene symbol	Gene name	Specie	Assay ID
NTF3	Neurothrophin-3	Human	Hs00267375_s1
		Rat	Rn00579280_m1
		Mouse	Mm01182924_m1
NTRK3	Neurothrophic receptor tyrosine kinase 3	Human	Hs00176797_m1
		Rat	Rn00570389_m1
		Mouse	Mm00456222_m1
ADRAB1	β_1-AR	Human	Hs00265096_s1
		Rat	Rn 00824536_s1
ADRAB2	β_2-AR	Human	Hs00240532_s1
		Rat	Rn00560650_s1
ADRAB3	β_3-AR	Human	Hs00609046_m1
		Rat	Rn00565393_m1
GAPDH	Glyceraldehyde-3-phosphate dehydrogenase	Human	Hs99999905_m1
		Rat	Rn99999916_s1
		Mouse	Mm99999915_g1

Resource provided by Applied Biosystem.

3.2.4 Analysis of results

Threshold cycle (Ct) values were calculated by 7500 fast sequence-detection system software (Applied Biosystems, US). We normalized the gene expression with the levels of GAPDH mRNA; therefore, CT values obtained from each gene were referenced to GAPDH and calculated ΔCt as the difference between gene of interest Ct value and the reference gene Ct value. ΔCt value was converted into the linear form using the term $2^{-\Delta Ct}$ as a value directly proportional to the initial mRNA copy number (Livak & Schmittgen, 2001).

3.3 QUANTIFICATION OF PROTEIN EXPRESSION

Analysis of protein expression of NT-3 and TrkC was performed in rat and human tissues by Western blot, using specific antibodies and followed by a densitometry analysis as described below.

Immunoblotting involves numerous steps such as protein isolation, total protein quantification, protein separation, protein transfer, antibody incubation, protein detection, and densitometry analysis.

3.3.1 Samples preparation for Western blot

Once tissues were pulverized in nitrogen liquid as detailed in **section 3.2.1** of this Thesis, the samples were homogenized in RIPA lysis buffer (50 mM HEPES pH=7.5, 150 mM NaCl, 10% glycerol, 1 mM EGTA, 1% Triton X-100), containing protease inhibitor cocktail (Complete®, Roche Applied Science, Germany) and phosphatase inhibitor cocktail (PhosSTOP®, Roche Applied Science, Germany). Then, the samples were sonicated (Microson™ XL 2000 ultrasonic liquid Processor) three times for 5 seconds at 4ºC in 3 cycles of 3 pulsed. Subsequently, the samples were centrifuged at 16.100 *g* for 20 min at 4ºC; the supernatant, which contained the soluble proteins, was stored at 80ºC until use.

3.3.2 Protein concentration

The protein content was measured by Bradford method (Bio-Rad, Hercules, CA). In this instance, bovine serum albumin (BSA, Sigma) was used to establish the standard curve, because this assay provides a linear signal in the range of 32-1000 µg/ml BSA.

The samples and BSA curve were loaded for duplicate using a multilabel plate reader (ViCTOR™X, PerkinElmer, Inc). The absorbance was measured at 595 nm. Subsequently, the obtained values were extrapolated to achieve the concentration of protein in each sample.

3.3.3 Western blot

Western blot technique is used to separate specific proteins. Poliacrylamide gels were prepared using 40% acrylamide/bis-acrilamide solution (Bio-Rad Laboratories, Inc). The running gel was prepared using a buffer containing 10% polyacrylamide submerged in 125 mM Tris-HCl pH 8.8 and 0.1% SDS. The

stacking gel was prepared with a low concentration of acrylamide (3%) diluted in a buffer 125mM Tris-HCl pH 6.8 and 0.1% SDS. Ammonium persulfate (APS, Bio-Rad) and N,N,N′,N′-tetramethylethylenediamine (TEMED, Sigma) were used for the preparation of polyacrylamide gels.

Once protein concentration (20 µg) was determined by Bradford, total protein was prepared with loading buffer (60 mM Tris-HCl pH=6.8, 10% glycerol, 2% SDS, 5% β-mercaptoethanol, and 0.01% bromophenol blue) and was denatured by boiling the mixture at 95ºC for 5 min. The protein samples were loaded in each well using a protein marker (PanReac) to be monitored during the protein separation. The electrophoresis allowed to separate the proteins using 10% SDS-polyacrylamide gel and was filled with running buffer 1 X Tris-Glicina-SDS (25mM Tris pH8.3, 192 mM glycine and 0.01% SDS). The gel was run at 60V for 30 min and then gone up at 110V for 90 min at 4ºC.

After electrophoresis, the proteins were transferred from the gel to the membrane with the transfer sandwich. All reagents were obtained from GE Healthcare (Piscataway, NJ).

Prior to assemble the sandwich, polyvinylidene fluoride (PDVF) membrane was wet in methanol for 1 min and washed with transfer buffer 1X Tris-Glycine-Methanol (25mM Tris pH8.3, 192 mM glycine and 20% methanol SDS), the filter papers and sponges were soaked in transfer buffer. The sandwich was assembled according to the charge, the membrane was at the positive electrode and the gel was at the negative electrode. The sandwich was placed into tank transfer system. The transfer ran for 2 hours at 360mA at 4ºC. Mini-Transfer-Blot® Electrophoretic Transfer Cell System (Bio-Rad Hercules CA, USA) was used for both electrophoresis and transfer.

To prevent non-specific background binding, once proteins transferred, the membranes were blocked in 3% BSA in PBS containing 0.1% Tween 20 (PBST) for 1 h at room temperature with gentle agitation. The membranes were incubated with the primary antibody diluted in 3% BSA overnight at 4ºC. The antibodies used in immunoblotting are described in the table 1. The next day, the membranes, which were washed three times with PBST to remove the remains of primary antibody, were incubated with anti-rabbit IgG (Cell signalling) 1:2500

as secondary antibody for 90 min at room temperature, and were extensively washed before developing by incubation with ECL™ western blotting detection reagent (Amersham Biosciences).

In case of proteins of very similar molecular weights, the antibody was removed from the membrane with a stripping buffer (100 mM 2-mercaptoethanol, 2% SDS, 62,5 mM Tris-HCl pH=6,7) for 10 min, to eliminate the primary and secondary antibodies and reincubate the membranes with other antibodies of similar molecular weight. Then, the membrane was washed three times with PBST, blocked with 3% BSA for 1 h, and incubated with a primary antibody. Before reincubation, absence of signal from previous antibody was proved by chemiluminescence detection of the membranes.

3.3.4 Analysis of results

The membranes were immediately documented and quantified with an Autochemi™ BioImaging System using the Labworks 4.6 capture software (Ultra-Violet Products Ltd., Cambridge, UK). Densitometric analysis was performed with ImageJ software (NHI image - Bethesda, Maryland, USA). The protein band of interest was quantified and normalized by GAPDH. The result was expressed as arbitrary units of immunodetectable protein.

3.4 CELL VIABILITY TEST

To study the cell viability, we used 3-(4,5-Dimethyl-2-thiazolyl)-2,5-diphenyl-2H-tetrazolium bromide (MTT) assay described by Mossman (1983), which measures the viability in a cell population and is used for citotoxity test drugs. The yellow MTT is reduced in the mitochondria of active cells through the action of dehydrogenase enzyme to form an insoluble purple formazan crystal. The number of viable cells is directly proportional to the formazan produced (purple colour). Purple colour shows higher cell viability.

To assess the cell viability, ECs were seeded on 24-well plate and incubated under cell culture conditions (37ºC and 5%CO_2). Once cells reached confluence, NT-3 (32ng/ml), K252a (0.2µM) or their combination were added to the corresponding well as described in **section 3.5.4** and the plate was incubated for 48 h. Additionally, MTT stock solution (5 mg/ml) was prepared in PBS. 100µl of

MTT were added in each well to a final concentration of 0.5mg/ml for 1 h at 37ºC. After incubation, the supernatant was carefully removed and discarded; formazan products were dissolved in 100µl of DMSO and protected from light.

3.4.1 Analysis of results

The absorbance was measured at 490 nm using a multilabel plate reader *VICTOR™X3* (Perkin Elmer, UK). The absorbance value of untreated cells was compared with the absorbance values of treated cells with K252a and NT-3.

3.5 CELL MIGRATION

There are many different methods to study cell migration. One of them is wound closure assay, which is a simple technique and useful to determine the migration ability of whole cell masses. Measuring the closed distance over time when comparing to a control may reveal specific migration changes (Justus et al, 2014; Liang et al., 2007).

The scratch technique was used to perform the *in vitro* two-dimentional migration assay in ECs cultures. In this technique, a scratch is created in a confluent monolayer of ECs by physical exclusion and then, ECs migrate to fill the scratch area. The scratch assay may be used to analyse and characterize the key regulators of cell migration and the effect of drugs on cell migration.

3.5.1 Setting up scratch assay

The entire process described below was carried out under the highest sterility conditions. The HAoEC were seeded on 24-well culture plate (5.10^4 cells/well, according to the size of well; Promocell) to allow the cells to adhere and spread on the well completely. Then, after 24h incubation at 37ºC and 5% CO_2 in complete medium, the cells reach 90% confluence to form a monolayer.

First, the optimal conditions (FCS concentration and migration time) were tested in four different protocols (P1, P2, P3, and P4; Table 3) to analyse spontaneous migration on HAoEC and to prevent the cell proliferation and stress response based on the literature (Chen, 2013; Guo et al., 2014; Murohara et al., 1999).

In the first protocol (**P1**), the complete medium was removed and the cells were serum starved 12h before and after the scratch, without GFs.

In the second protocol (**P2**), the complete medium was removed from the plate and basal medium supplemented with 0.5% FCS, without GFs, was added 12h before and after the scratch.

In the third protocol (**P3**), the medium was replaced with basal medium supplemented with 0.5% FCS, without GFs, for 12h. Next, the scratch was created and basal medium supplemented with 5% FCS and without GFs was added.

The fourth protocol (**P4**) did not need previous serum starvation; therefore, the cells were serum starved, without GFs, after the scratch.

Table 3. Comparison of different migration assay protocols

	P1	**P2**	**P3**	**P4**
FCS concentration at 12h before scratch	0%	0.5%	0.5%	5%
Medium	Basal	Basal	Basal	Complete
FCS concentration after scratch	0%	0.5%	5%	0%
Medium	Basal	Basal	Basal	Basal

P1=Protocol 1; P2= Protocol; P3=Protocol 3; P4= Protocol 4

According to the obtained data (Results: **section 3.1**), P4 is the most appropriate protocol for studying cell migration in HAoEC and HCAEC, or modified P4 (0.5% FCS after the scratch) in HCMEC to avoid cellular damage.

3.5.2 Scratch technique

A new p1000 pipette tip was used to scrape the cell monolayer in a straight line, pressing firmly against the top of the cell culture plate. It is important not use

excessive force against the cell culture plate with the pipette tip to prevent surface damage.

To remove death cells and prevent the cells from sticking to the center of the scratch, the cells were gently washed with 2 ml of pre-warmed PBS, avoiding the cells detaching. Then, the medium was replaced with 400 µl of appropriate media for each protocol. To track the wound an initial picture was captured at 0 h. The plate was incubated at 37ºC for 8 and 24 h. After the incubation, the plate was placed under an inverted microscope to capture an image, to determine an adequate time frame of incubation which allows cell migration.

3.5.3 Analysis of images

A reference point (line or point in the center of the well) was created to capture images of the same area at different times (0, 8, and 24 h). Two images of different areas were acquired for each well. The images were recorded with a Leica DM IL LED inverted microscope (Leica, Buffalo Grove, IL) and a 2.5X objective. The cell scratch area was measured using Leica Microsystems software (Leica, Buffalo Grove, IL) at 0h, 8h, and 24h, tracing manually a rectangle around the cell-free area.

The cell migration was calculated as cell-free area decreased over time:

$$Area\ decrease\ (\%\ 0h)\ = \frac{\mathrm{A0h} - \mathrm{A}x\mathrm{h}}{\mathrm{A0h}} * 100\%$$

A0h= area at time zero (scratch)

A*x*h= area at x hours after the scratch (8h or 24h)

The results were expressed as percentage respect to 0h.

3.5.4 Experimental procedure to study the role of NT-3 on endothelial cell migration

The effect of NT-3 on cell migration was analysed in cardiac (HCAEC, HCMEC) and aortic (HAoEC) ECs using the appropriate protocol described above. The entire process was carried out under the highest sterility conditions.

Once a monolayer of confluent ECs was reached in 24-well culture plate, the complete medium was removed and was replaced by the basal medium (HAoEC and HCAEC) or the basal medium supplemented with 0.5% FCS (HCMEC). The involvement of TrkC was studied using K252a (Trk inhibitor) in some experiments. Thus, K252a (0.20 µM) or vehicle (DMSO 0.01%) were added in cell cultures for 1h before scratch. The wound (scratch) was then performed and the basal medium (or the basal medium with 0.5% FCS) was applied for 8h in the presence of NT-3 (32ng/ml), K252a (0.20 µM) or NT-3 and K252a (final volume 400 µl/well). The control and NT-3-treated cells were incubated in presence of DMSO 0.01%.

All treatments were performed for duplicate and incubated at 37ºC and 5% CO_2. Figure 1 shows a scheme of the experimental design.

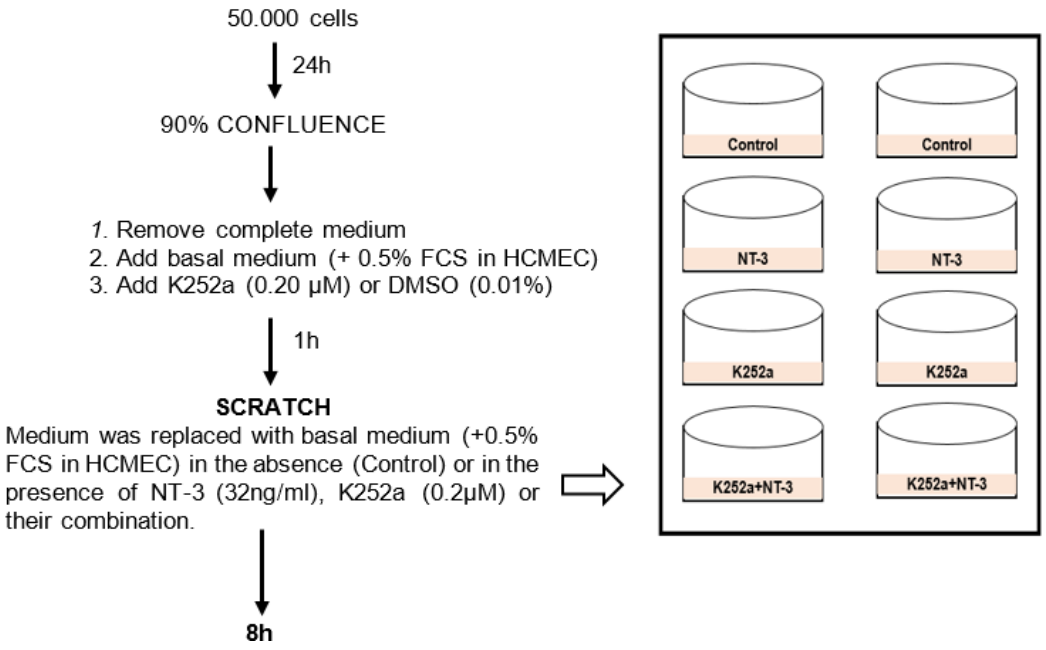

Figure 1. *Experimental design to study the role of exogenous NT-3 in an in vitro model.*

3.5.5 Analysis of images

The cell migration was analyzed at 0h and 8h of migration as described above and calculated as cell-free area decreased at 8h:

$$Area\ decrease\ (\%\ control) = \frac{(\mathrm{A0h} - \mathrm{A8h})\ treated}{(\mathrm{A0h} - \mathrm{A8h})\ control} * 100\%$$

The results were expressed as percentage respect to the control.

3.6 ANGIOGENESIS

Angiogenesis, the sprouting of blood vessels from pre-existing vasculature is associated with both natural and pathological processes. In 1983, Montesano *et al*., reported that ECs inside a three-dimentional matrix have the capacity to form vessel-like structures to study the ECs behaviour. One method used to quantify angiogenesis is to measure the ability to form tubes when placed on an extracellular matrix. The ECs tube formation assay is one of the most widely used *in vitro* methods. It is a simple assay, requiring relatively few components and a short culture period. The process of angiogenesis is important to study of proangiogenic and antiangiogenic molecules. The formation of these tubes is a critical early step in angiogenesis, therefore testing molecules that can stimulate or inhibit tube formation provide good insight (Xie et al., 2016).

An example for the use of the tube formation assay involves comparing the development of tubes from vascular ECs grown on extracellular matrix. Other assays that are commonly used to determine the effects of compounds on angiogenesis are *ex vivo* methods. In 1990, Nicosia and Ottinetti reported angiogenesis in rings of rat aorta as a quantitative assay. The aortic ring assay is an angiogenesis model that is based on organ culture. In this assay, angiogenic vessels grow from a segment of the aorta (Nicosia, 2009).

In this Thesis, ECs tube formation assay and rat aortic ring assay were selected as *in vitro* and *ex vivo* assay, respectively.

3.6.1 Endothelial tube formation assay

In order to study the role of NT-3 on the angiogenesis in tube formation assay, we used HAoEC, HCAEC, and HCMEC. The entire process described below was carried out under the highest sterility conditions.

The Matrigel® was thawed at 4ºC for 24 h until liquid and kept on ice. Then, a 96-well culture plate was coated with 50 µl/well Matrigel® al 37ºC for 20 minutes until solidify. ECs were seeded (6.10^4 cells/well) on basement membrane matrix with complete medium and incubated at 37ºC and 5% CO_2 for 20 min. The involvement of TrkC was studied using K252a (TrkC inhibitor) in some

experiments. Thus, to induce a pro-angiogenic or antiangiogenic response (formation of tube-like structures), NT-3 (32 ng/ml), K252a (0.2 µM) or their combination were added to the corresponding well as described in **section 3.5.4**, with a final volume of 200 µl/well. ECs attach and form tubes within 4 h. Finally, the number of tubes are measured after 18 h of incubation

3.6.2 Angiogenesis *ex vivo* in rat aortic rings

The entire process described below was carried out under the highest sterility conditions. The Matrigel® was thawed at 4ºC for 24 h until liquid and kept on ice. Rat aorta was excised and cleaned, the fat layer was removed avoiding damage the endothelium. The rings (approximately 1 mm in length) were prepared and washed in PBS containing 50µg/ml gentamicin and 50ng/ml amphotericin B. Briefly, the Matrigel® was placed onto each well (50µl/well) of a 96-well plate avoiding bubbles formation. Subsequently, individual aortic rings were embedded in each well and the plate was incubated at room temperature for 20 min until solidification of Matrigel® (Vicente et al., 2013). The basal medium, supplemented with 5% FCS, 50µg/ml gentamicin, and 50ng/ml amphotericin B, was added onto each well. NT-3 (32ng/ml), K252a (0.2µM) or their combination were added to the corresponding well as described in **section 3.5.4.** The experiment was performed in duplicate. Finally, the plate was incubated for seven days in cell culture conditions. The medium was removed and replaced every two days and neovessel outgrowth was monitored first, third, fifth, sixth, and seventh day.

3.6.3 Analysis of results

After the incubation, cells and aortic ring cultures were observed under a microscope to evaluate angiogenic potential of NT-3. The images were captured using the inverted microscope Leica DM IL LED Leica (objective 2,5X) and analysis of images were carried out by Leica Microsystems. In cells, we counted the new tubes at 18 h of incubation. The results were expressed as percentage respect to the control.

In aortic rings, the vessels were photographed among third and seventh days and the images were captured in 4 axes. The length of new vessel was measured

daily from the centre of the ring until the final end of each vessel formed, to analyse the kinetics of growth of new vessels. The results were expressed in µ length.

3.7. QUIESCENT RAT AORTIC RINGS

In quiescence, the spontaneous angiogenic activity is abolished in the rings while preserving the capacity to grow new vessels in response to angiogenic factors or vascular damage. For this instance, aorta was carefully removed from animal, cleaned of perivascular adipose tissues and blood, and divided into two segments in each vessel (Nicosia, 2009).

One segment, fresh vessel, was rapidly stored at -80ºC and the other segment, quiescent vessel, was incubated with basal medium containing 50 µg/ml gentamicin and 50 ng/ml amphotericin B during 7 days, changing the incubation medium every two days. After 7 days, mRNA levels of TrkC were analysed by qPCR in quiescent and fresh vessels.

3.8 FUNCTIONAL STUDY IN ISOLATED ORGAN BATH

To a better understanding of the role of NT-3 on vascular tone, we used the isolated organ bath technique.

3.8.1 Tissues preparation

Thoracic aorta and tail artery from rat and mouse were isolated following the specifications described in **section 1.2.4.**

In some experiments, the influence of PVAT on vascular tone in rat aorta was analysed: thoracic aorta with PVAT (+PVAT) and thoracic aorta clean or without PVAT (-PVAT). In this case, aorta was sectioned into two parts with or without PVAT and then, the vessels were cut into 4 mm rings. In the rest of the experiments, the PVAT that surround the vessels was removed (Figure 2A), as described in **section 1.2.4**.

When experimental protocol required, mechanical removal of the endothelium was carried out, introducing a cannula of appropriate calibre in the lumen of the vessel repeatedly, taking care not to damage the muscular layer.

Then, the rings were placed into organ bath (Figure 2B) with 10 ml of Krebs solution aerated with 95%O_2 and 5% CO_2 (37ºC; pH= 7,4). Two fine stainless steel wires were introduced through the lumen of each arterial segment, one was fixed to the organ bath and the other was connected to an isometric force-displacement transducer. The preparations were subjected to an initial tension of 1 g and were maintained during a stabilization period of 60 minutes, changing the Krebs solution every 20-30 minutes and adjusting the tension of the different preparations until obtaining a stable baseline. Isometric tension was acquired using an isometric force transducer (Grass FT03), connected to an acquisition system (PowerLab/8SP; ADInstruments) and recorded the tension with software Chart v5.0.2 (ADInstruments, New South Wales, Australia).

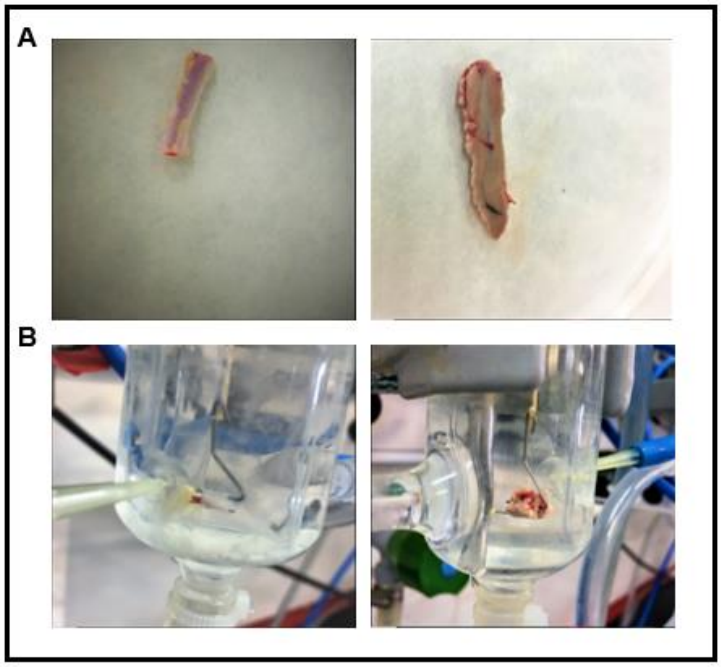

Figure 2. *Thoracic aorta without PVAT (left) and with PVAT (right) (A). Aorta rings mounted in an organ bath (B).*

3.8.2 Description of experimental protocols

3.8.2.1 Effect of NT-3 on vascular tone of rats

After a 1h stabilization period, the tail and aortic rings were contracted with a depolarizing solution (80 mM KCl-Krebs obtained by an isotonic replacement of NaCl by KCl) to check the vessels' functionality. The magnitude of this contraction will be used as reference in the analysis of the results and vessels that contracted less than 3mN to KCl were discarded. After the washout and the return of a stable

baseline, vessels were contracted with the α_1-AR agonist PHE (aorta: 1µM, tail artery 10µM) and endothelium integrity was tested with concentration-response curve (CRC) of relaxation to ACH (10nM-100µM) which causes endothelium-dependent relaxation in rings (Scheme 1). Only the rings that relaxed by more than 60% to ACH were considered to have an intact endothelium; those that failed to relax (<10%) to ACH were considered to have the endothelium removed.

Influence of endothelium

After washing the tissue and a resting period; addition of PHE (aorta: 1µM, tail artery 10µM) induced a maximal contractile response. Then, a CRC of relaxation to NT-3 (2, 4, 8, 16 and 32 ng/ml) was performed on PHE-pre-contracted rings (Scheme 1). The involvement of the endothelium and NO was studied using vessels without endothelium or after exposure to the non-selective NOS inhibitor L-NAME (100 µM) which was added 30 min prior to addition of PHE.

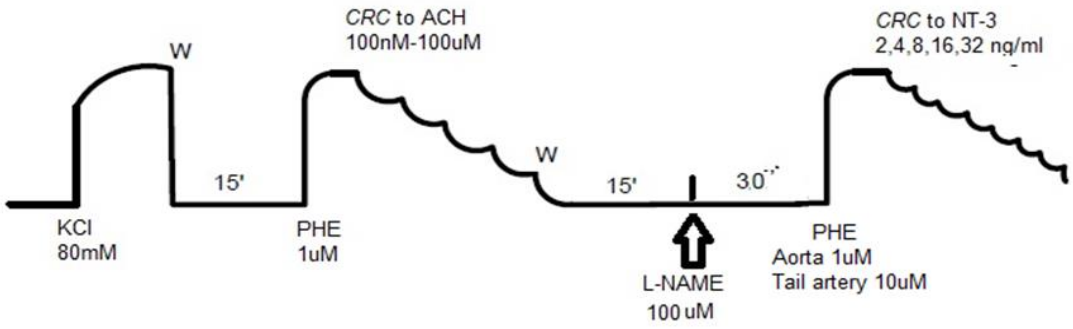

Scheme 1. *Schematic drawing showing the experimental procedure used in rat vessels to study the role of NT-3 on vascular tone in the presence or absence of L-NAME. PHE: Phenylephrine, ACH: Acetylcholine. CRC: concentration response curves, W: washing.*

Role of TrkC

In another set of experiments, after washing the tissue and incubating during a resting period, a CRC of contraction to PHE (aorta: 10nM–1µM; tail artery: 10nM-10 µM) was performed by the addition of cumulative concentrations of the agonist every 7 min (Scheme 2). The involvement of TrkC was studied using K252a (0.2 µM) (Trk inhibitor) in some experiments, which was added 30min prior to CRC to PHE. After the maximal sustained contractile response to PHE, a CRC of

relaxation to NT-3 (2, 4, 8, 16, and 32 ng/ml) was performed in pre-contracted vessels.

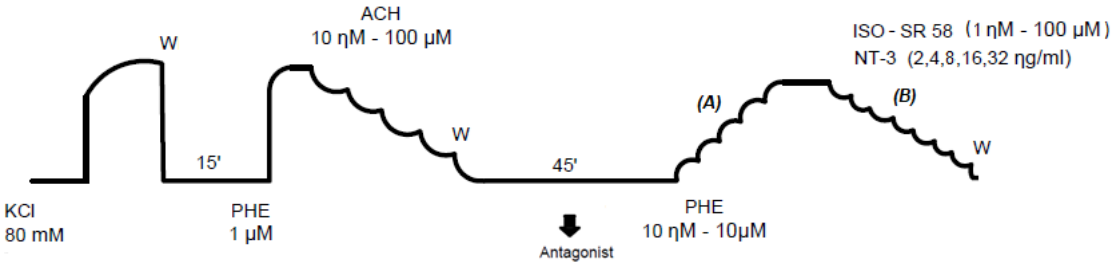

Scheme 2. *Schematic drawing showing the experimental procedure used to study the role of NT-3 and β-adrenergic receptors in vessels of animals. PHE: Phenylephrine, ACH: Acetylcholine, ISO: Isoprenaline, SR58: SR5811A. (A) CRC to PHE, (B) CRC to NT-3, ISO, or SR58*

Influence of aorta perivascular adipose tissue (PVAT)

The influence of PVAT on NT-3-induced relaxation was determined in endothelium-intact aortic rings with (+PVAT) or without PVAT (-PVAT) following a protocol similar to that described in Scheme 2.

In another group of experiments, after washing the tissue, the role of β-AR subtypes (β_1, β_2, β_3) was also investigated by using the non-selective β_1 and β_2 agonist isoprenaline (ISO,1nM-100µM) and a selective agonist for β_3 subtype (SR58611A, 1nM-100µM). CRC of relaxation were obtained by addition of the agonists on the maximal contractile response obtained in CRC to PHE (Scheme 2).

3.8.2.2 Influence of the lack of endothelial NT-3 expression in genetically modified mice on vascular tone

Genetically engineered mice in which the endothelial expression of NT-3 was supressed (**eNT3$^-$**) and the corresponding wild type (WT) mice with a normal NT-3 expression levels (**eNT3$^+$**) were selected, as described in the **section 1.2.2.**

In mouse aortic rings with endothelium, the responses to an α agonist (PHE) and the role of β-AR subtypes (β_1, β_2, β_3) were analysed by using a non-selective β_1 and β_2 agonist (ISO; 0.1nM-100µM) and a selective agonist for β_3 subtype (SR58611A, 0.1nM-100µM), following the experimental procedure shown in

Scheme 2. CRC of relaxation were obtained by addition of the agonists on the maximal contractile response obtained in CRC to PHE.

3.8.3 Analysis of results

The CRC of contraction to PHE are expressed as a percentage of KCl-induced contraction. CRC of relaxation to the different compounds were expressed as a percentage of relaxation with respect to the maximum contractile response induced by PHE. Contractile or relaxing CRC were plotted using the Graph Pad Software version 4.0 (San Diego, CA, USA), with sigmoid curve fitting (variable slope) performed by non-linear regression.

The following characteristic parameters were obtained: E_{max} (maximal contractile or relaxing response) and pEC50 (-log of the agonist concentration needed to produce 50% of E_{max}). In case the curve adjustment is significant for two sites, pEC_{50} (1) and pEC_{50}(2) were calculated, for high and low affinity, respectively. In this case, the percentage of receptors in each site was also calculated.

3.9 STATISTICAL ANALYSIS

The obtained results were analysed by *GraphPad Prism 4.0* (GraphPad Software, Inc., San Diego, CA, USA) software. All results were expressed as mean ± Standard Error of Mean (SEM) for *n* determinations obtained from samples different.

Comparison between two groups was analysed using *Student's t-test* (paired and unpaired). Comparison among three or more groups was analyzed using one-way analysis of variance (ANOVA) test followed by the Newman Keuls correction and Tukey post-test. In all cases, $p<0.05$, $p<0.01$, and $p<0.001$ were interpreted to denote statistical significance.

To determine if there are correlations between variables analysed, linear regression analysis was used and the Pearson correlation coefficient (GraphPad Software) was evaluated, which informs about the existence or not of linear relationship ($P <0.05$), the intensity of correlation (according to the absolute value

of the Pearson coefficient between 0 and 1) and its sense (inverse or direct relationship).

IV RESULTS

1. NT-3 AND TrkC EXPRESSION IN ADULT CARDIOVASCULAR SYSTEM

Gene expression and protein levels of NT-3 and its receptor, TrkC, were determined in different human and rat cardiovascular tissues as well as in different human cells isolated from heart and aorta.

1.1 HUMAN SAMPLES

The expression of NT-3 and TrkC was analysed in:

- Left ventricle (LV) from the heart donors which have not been finally considered suitable for transplantation,
- Aorta samples from individuals who underwent surgery
- Different types of human cardiac and aortic cells

As shown in Figure 1, mRNA levels of NT-3 and TrkC were detected in human aorta and LV, being the expression of both genes more abundant in aorta than LV.

In cardiac cells, the results obtained show the presence of NT-3 and TrkC mRNA levels in cardiomyocytes (HCM) and cardiac fibroblasts (HCF) (Figure 2A and B) that were in the same range of values as well as the obtained in heart tissue (see Figure 1). A high expression of TrkC was found in HCM as compared with HCF (Figure 2B).

In aortic cells, NT-3 and TrkC were expressed at low levels in all cell types analysed: adventitial fibroblasts (HAoAF), smooth muscle (HAoSMC), and ECs (HAoEC) (Figure 2C and D). NT-3 expression was significantly higher in HAoSMC and HAoAF respect to HAoEC (Figure 2C), whereas TrkC expression was significantly higher in HAoAF than in HAoEC and HAoSMC (Figure 2D). Moreover, the mRNA levels were remarkably lower than the obtained in human aorta (see Figure 1), suggesting a loss of NT-3 and its receptor in these cells and/or in the experimental conditions used.

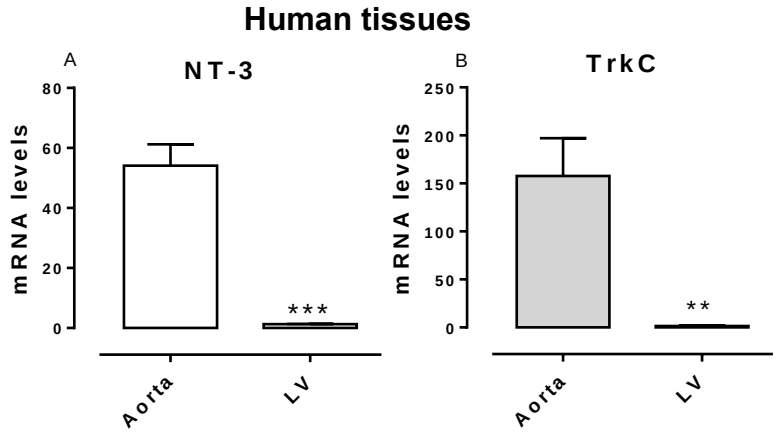

Figure 1. NT-3 and TrkC gene expression in human tissues. *mRNA levels of NTF3 (NT-3; A) and NTRK3 (TrkC; B) in aorta and left ventricle (LV). Values are expressed as $2^{-\Delta Ct}$ x10^4 using GAPDH as housekeeping gene and represent the mean ± SEM of n=4. **p<0.01, ***p<0.001 vs aorta. Student's t-test for unpaired samples.*

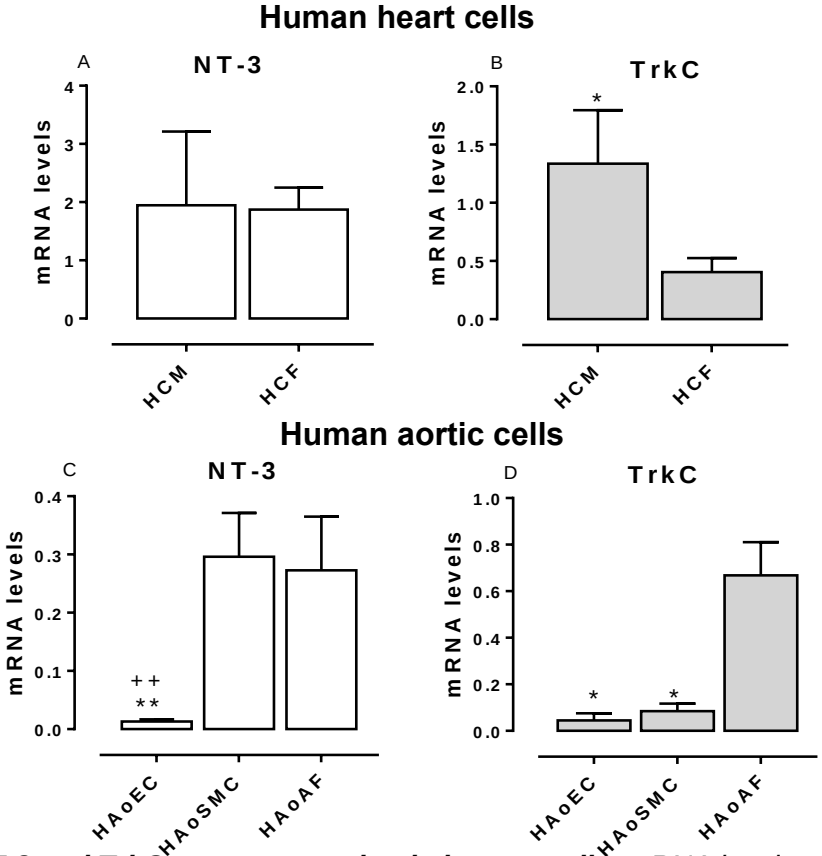

Figure 2. NT-3 and TrkC gene expression in human cells. *mRNA levels of NTF3 (NT-3) and NTRK3 (TrkC) in heart cells (A, B) including cardiomyocytes (HCM, n=3) and fibroblasts (HCF, n=7) and aortic cells (C, D) including ECs (HAoEC, n=9-3), smooth muscle cells (HAoSMC, n=4), and adventitial fibroblasts (HAoAF, n=5-6). Values are expressed as $2^{-\Delta Ct}$ x10^4 using GAPDH as housekeeping gene and represent the mean ± SEM. *p<0.05, **p<0.01 vs fibroblasts (HCF or HAoAF); ++p<0.01 vs HAoSMC. Student's t-test for unpaired samples or one-way ANOVA and Tukey post-test.*

1.2 RAT SAMPLES

We explored gene and protein pattern expression of NT-3 and TrkC in adult Wistar rats, using different cardiovascular tissues such aorta, tail artery and LV, as well as kidney, and comparing with a neural tissue (cerebral cortex).

The mRNA of both genes were detected in all tissues but in a different proportion (Figure 3). According to the results obtained in human tissue, NT-3 and TrkC levels were higher in rat aorta than LV. As shown in Figure 3A, NT-3 is highly expressed in vessels including aorta and tail artery compared to LV, kidney, and cerebral cortex. Furthermore, high mRNA levels of TrkC were found in vessels and cerebral cortex, whereas very low levels of this gene were present in LV and kidney (Figure 3B).

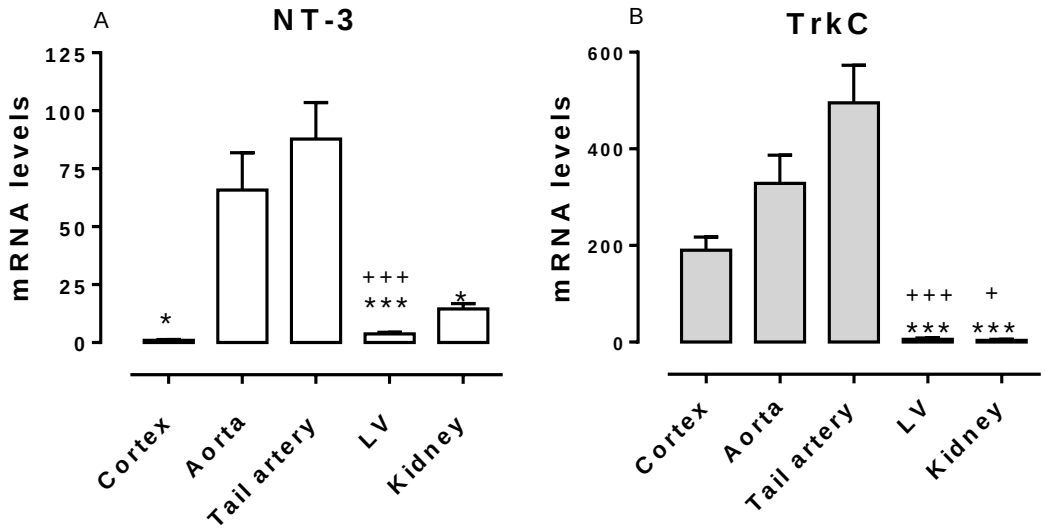

Figure 3. NT-3 and TrkC mRNA expression in Wistar rat tissues. *mRNA levels of Ntf3 (NT-3; A) and Ntrk3 (TrkC; B) in cerebral cortex (n=3), aorta (n=15), tail artery (n=7), left ventricle (LV) (n=17), and kidney (n=5). Values are expressed as $2^{-\Delta Ct}$ x10^4 using Gapdh as housekeeping gene and represent the mean ± SEM of n animals. +++p<0.001 vs aorta; *p<0.05, ***p<0.001 vs Tail artery. One-way ANOVA and Tukey post-test.*

According to mRNA levels, an abundant protein expression of TrkC was found in cerebral cortex and vessels (Figure 4). In cerebral cortex two bands were detected by TrkC antibody corresponding to the full length (145 kDa) and truncated isoforms (110 kDa) of TrkC as described in the literature (Donovan et al., 1995). In aorta and tail artery, only the truncated isoform of receptor was detected. In LV and kidney, undetectable protein levels were found at 145 or 110 kDa, but a band at around 50 kDa was observed (Figure 4B).

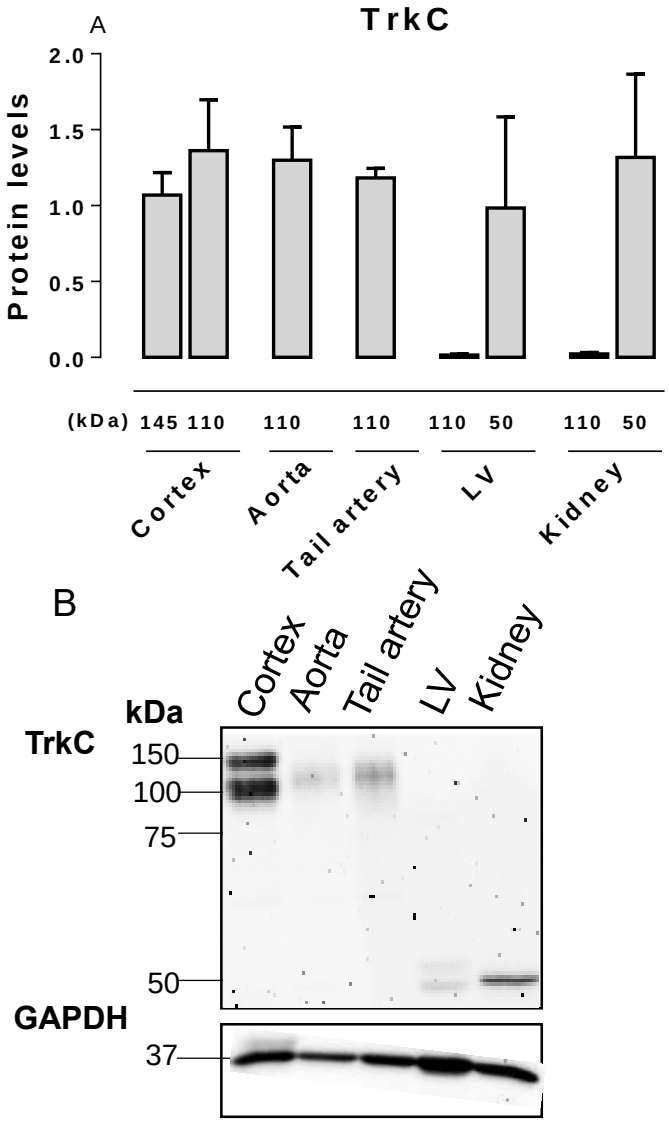

Figure 4. TrkC protein levels in Wistar rat tissues. *Relative protein quantification of TrkC/GAPDH (A) in cerebral cortex, aorta, tail artery, left ventricle (LV), and kidney. Representative immunoblot of TrkC (B). Data represent the mean ± SEM of n=4 animals.*

At the protein level, different isoforms of NT-3 were detected in the neural and non-neural tissues. These isoforms of the protein consist of NT-3 monomer (mature protein) with a size around 20 kDa and a proNT-3 or a NT-3 dimer that appears around 30 kDa. A 60 kDa band was also detected (Figure 5).

The expression profile of the isoforms was different depending on tissues (Figure 5). The expression of mature NT-3 form (20 kDa) was abundant in vessels (aorta and tail artery) as well as in LV and kidney, whereas a lower expression of this form was detected in cerebral cortex that was significant versus aorta (Figure

5A). Contrarily, an abundant expression of 30 kDa band was detected in cerebral cortex, whereas non-neural tissues expressed significant lower levels of this specie (Figure 5A). NT-3 form at 60 kDa was detected in smaller proportion in the vast majority of tissues (Figure 5).

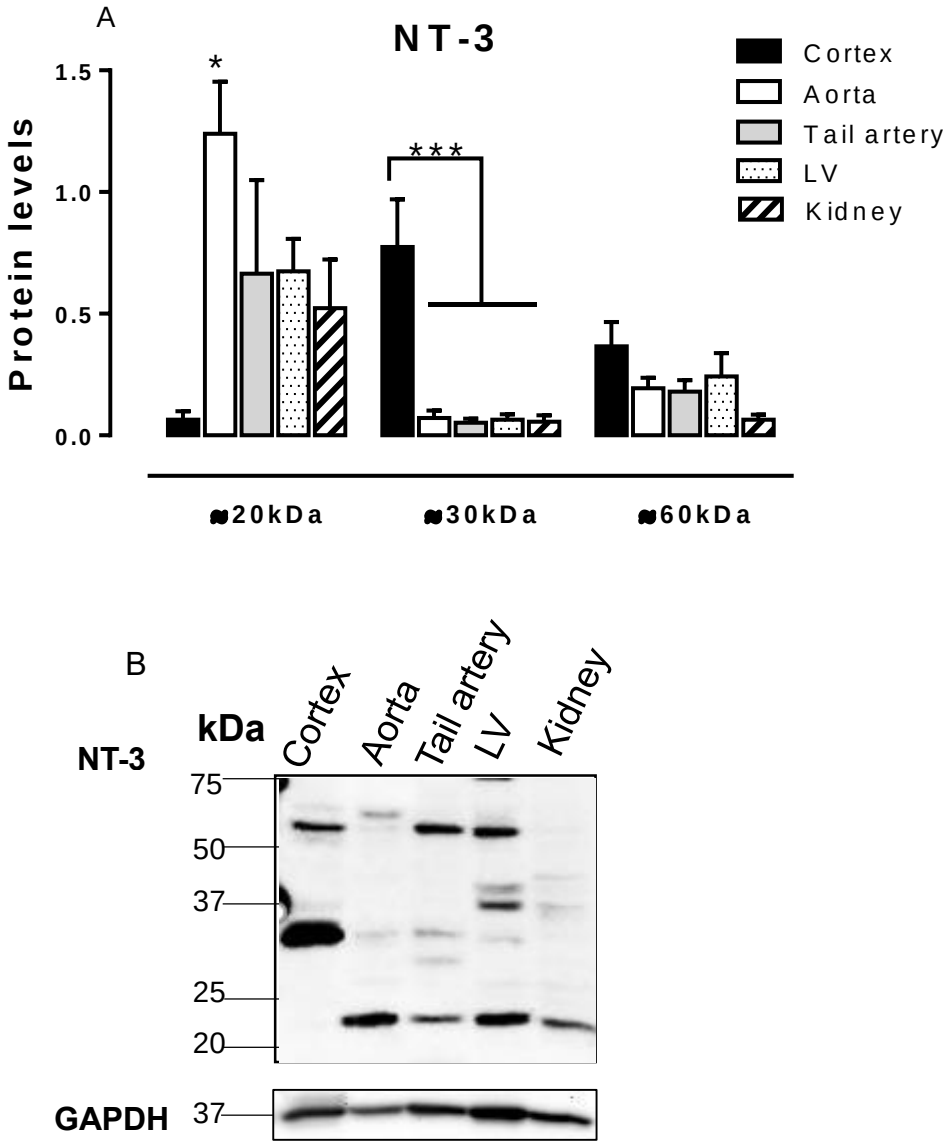

Figure 5. NT-3 protein levels in Wistar rat tissues. *Relative protein quantification of NT-3/GAPDH (A) in cerebral cortex, aorta, tail artery, left ventricle (LV), and kidney. Representative immunoblot bands for NT-3 species (B). Data represent the mean ± SEM of n=4.* *p<0.05. ***p<0.0001 vs cortex. *One-way ANOVA and Tukey post-test.*

2. LOCALIZATION OF NT-3 EXPRESSION IN DIFFERENT TISSUES

To obtain insights into the expression and localization of NT-3 in the cardiovascular tissues, we have utilized mice in which the *Escherichia coli lacZ* gene is integrated into the NT-3 locus (*Ntf3*$^{+/lacZneo}$: NT3$^{+/-}$) (Fariñas et al., 1994). In this mouse strain, β-galactosidase production is under control of the NT-3 promoter in its normal chromosomal environment, and histochemical measurement of β-galactosidase provides a simple and sensitive method to determine which cells express NT-3. The wild-type mice (NT3$^{+/+}$) was used as a negative control.

Firstly, we have analyzed the gene expression of NT-3 and TrkC in the heterozygous mice (NT3$^{+/-}$) in aorta and LV. The results obtained shown a significant decrease of NT-3 mRNA levels in both tissues from NT3$^{+/-}$ mice respect to NT3$^{+/+}$ (Figure 6A). There are no significant differences in TrkC expression (Figure 6B). As expected, these results evidenced a significant loss of NT-3 expression in this model of heterozygous mice; however, these reduced of neurotrophic expression did not modify the receptor expression levels. As described in Wistar rats, low expression levels of NT-3 (Figure 6A) and TrkC (Figure 6B) were found in LV.

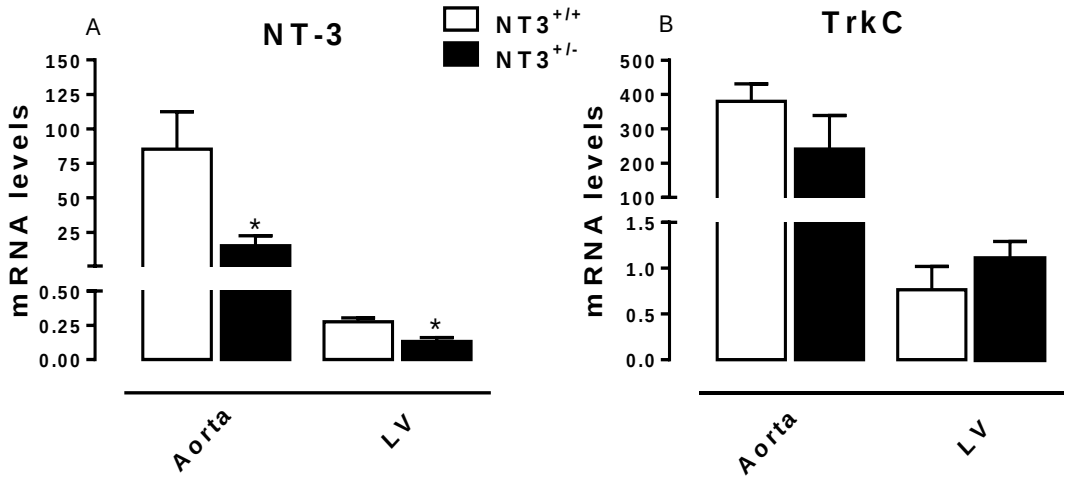

Figure 6. Gene expression of NT-3 and TrkC in genetically modified mice. *mRNA levels of Ntf3 (A) and Ntrk3 (B) in aorta and left ventricle (LV) obtained from heterozygous (NT3$^{+/-}$) and Wild-type (NT3$^{+/+}$) mice. Values are expressed as $2^{-\Delta Ct}$ x10^4 using Gapdh as housekeeping gene and represent the mean ± SEM of 5 different animals. *p<0.05 vs NT3$^{+/+}$. Student's t-test for unpaired samples.*

X-gal reaction gave a blue stain in cells expressing β-galactosidase. Therefore, in $NT3^{+/-}$ mice, blue staining will indicate that the NT-3 promoter is being expressed and, consequently that the *Ntf3* gene would be present. This staining could not be detected in $NT3^{+/+}$ mice because the NT-3 gene has not been genetically engineered.

Figure 7 shows X-gal staining of whole brain. As Vigers et al. described (2000) β-galactosidase is found in several areas of the cerebellum and cerebral cortex in $NT3^{+/-}$ mice (Figure 7A and C) but not in $NT3^{+/+}$ (Figure 7D y E). High levels of labeling are in the visual cortex (VS) and in blood vessels (bv) of cerebral cortex (Figure 7B). A ventral view of brain shows the diffuse presence of NT-3 in some areas and in the blood vessels (bv) (Figure 7C).

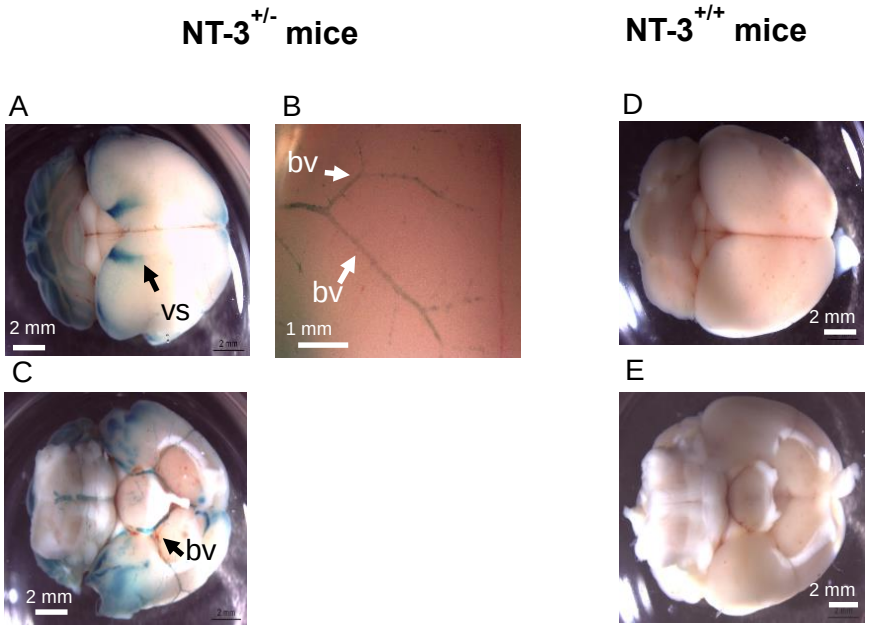

Figure 7. Expression pattern of NT-3 in whole brain. *Representative images of β-galactosidase staining in whole brain. X-gal staining in $NT3^{+/-}$ (A, B, C) and $NT3^{+/+}$ (D, E) mice. Dorsal views are shown in A and D, ventral views in C and E and, a dorsal higher magnification in B. Blue staining indicates the expression of NT-3. n=3 experiments in different animals.Arrowheads show the of β-galactosidase activity in visual cortex (VS) and blood vessels (bv).*

As Figure 8 shows, analysis of β-galactosidase histochemistry revealed high levels of NT-3 expression in aorta and tail artery from adult $NT3^{+/-}$ mice (Figure 8A-D and Figure 8I) but not in control mice ($NT3^{+/+}$) (Figure 8E-H and Figure 8J). These results confirm the high expression of this NT in vascular tissues. More in-depth analysis of magnification image of 2 µm aorta sections (Figure 8C and D), showed a robust expression of NT-3 in the medial layer, where smooth muscle cells are located.

In addition, the presence of NT-3 was also detected in blood vessels of LV (Figure 8K and L) and kidney (Figure 8N and O) of heterozygous mice. NT-3 was also detected in renal pelvis and ureter in $NT3^{+/-}$ mice (Figure 8N). No staining of LV or kidney was observed in control mice (Figure 8M and P).

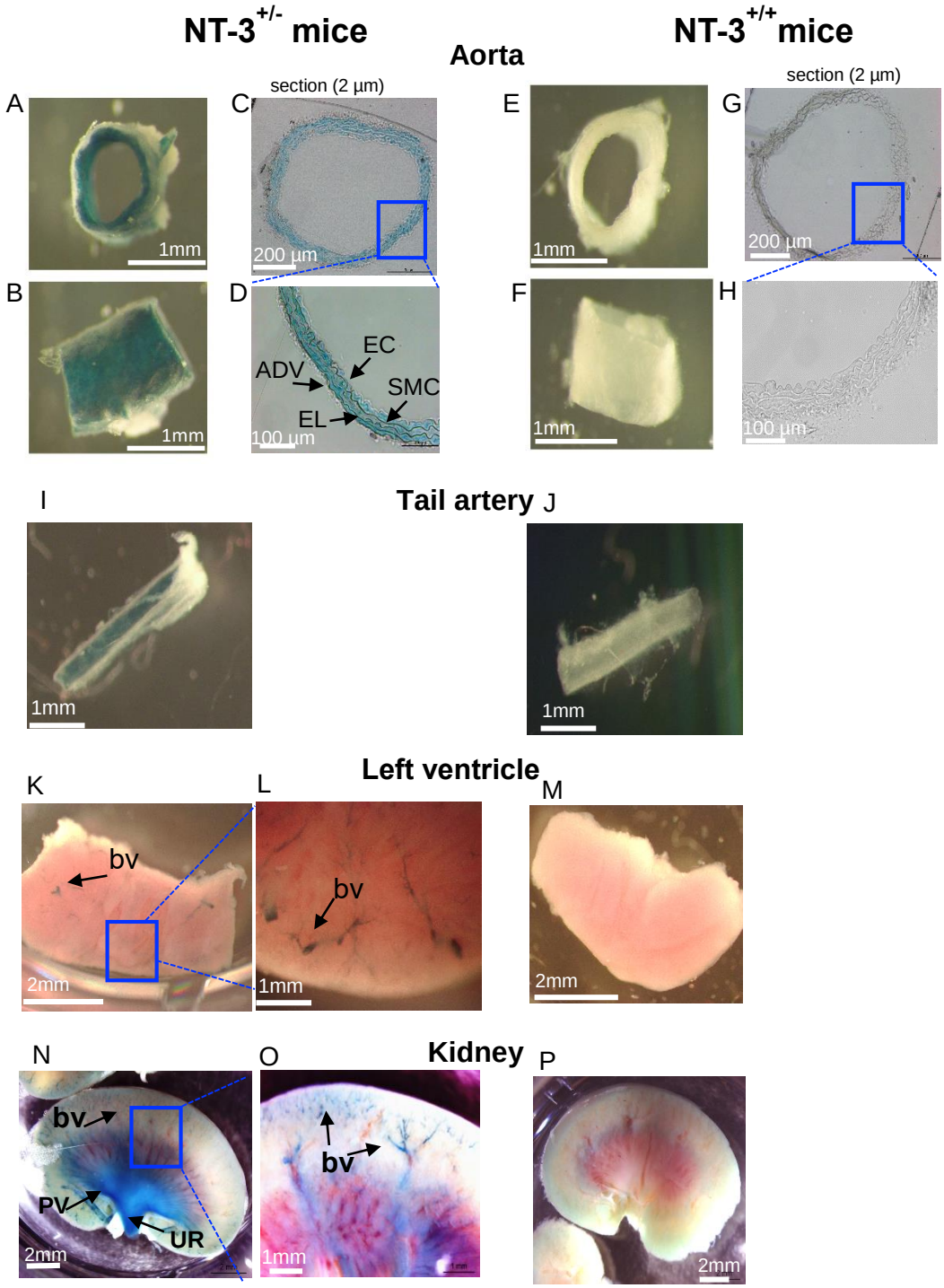

Figure 8. Expression pattern of NT-3 in different tissues. *Representative images of β-galactosidase staining in aorta (A-H), tail artery (I-J), LV (K-M), and kidney (N-P) from NT-3$^{+/-}$ and NT-3$^{+/+}$ mice. Higher magnification images showing aorta (D and H), left ventricle (LV; L), and kidney (O). Blue staining indicates the expression of NT-3. n=3 experiments in different animals. ADV: Adventitia; EL: Elastic lamina; SMC: Smooth muscle cells; EC: endothelial cells. Arrowheads show the of β-galactosidase activity in blood vessels (bv), pelvis (PV) and ureter (UR).*

3. EFFECT OF NT-3 ON VASCULAR FUNCTIONS

Altogether, the present results evidenced a strong presence of NT-3 and its receptor TrkC in blood vessels where NT-3 may act as an autocrine/paracrine factor. Therefore, we investigated the effect of exogenous NT-3 in different vascular functions, i.e. migration, angiogenesis, and vascular tone.

3.1 EFFECT OF NT-3 ON HUMAN ECS MIGRATION

We study the effect of recombinant NT-3 (32 ng/ml) on the migration process in different types of ECs from human aorta (HAoEC), coronary artery (HCAEC), and coronary microvasculature (HCMEC). To determine the implication of TrkC receptor in NT-3-mediated effects, an inhibitor of Trk (K252a) has been used at a concentration (0.2 µM) that has been described to inhibit Trk activity (Meuchel et al., 2011). ECs were also incubated with K252a to observe if it has an effect *per se*. In untreated cells (control), DMSO was added as a vehicle.

Firstly, to exclude a cytotoxic effect of the compounds, we used MTT assay to evaluate the cell viability in NT-3-treated HCMEC incubated for 48h, in the presence or absence of K252a. As shown in Figure 9, absorbance levels observed in untreated cells (control) were indicative of the maximum cell viability in our experimental conditions. These absorbance levels remained unchanged after treatment with NT-3 (32 ng/ml), K252a (0.2 µM), or their combination, indicating the absence of cytotoxic effect at the concentration assayed.

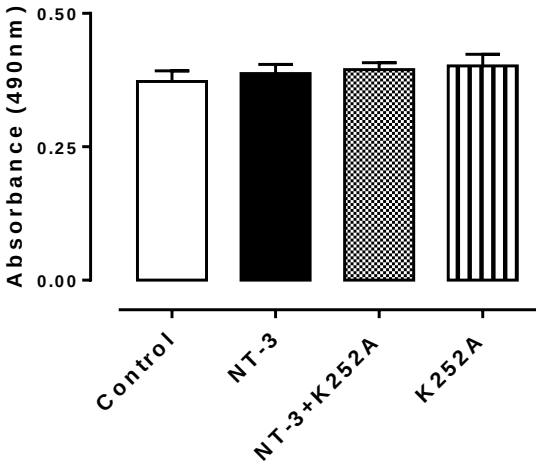

Figure 9. ***Effect of NT-3 and Trk inhibitor on cell viability****. Values of absorbance of HCMEC after 48h incubation in absence (control), or presence of NT-3 (32 ng/ml), K252a (0.20 µM), or NT-3 with K252a (NT-3+K252a). Data represent the mean ± SEM of n=4 independent experiments.*

Subsequently, we evaluated the ***migration of ECs*** using the scratch assay which allows tracing the migration of individual cells at the edge of the scratch. In the present Thesis, the optimal experimental conditions to study cells migration (FCS concentration, incubation medium, and migration time) were established, since different conditions have been described in the literature (Chen, 2013; Guo et al., 2014; Murohara et al., 1999). As described in *Methods (3.5.1)*, we analyzed spontaneous migration in HAoEC using the four protocols (P1, P2, P3, and P4) (Table 1). In P1, P2, and P3, the cells were incubated in basal medium (without GFs) before and after the scratch; whereas in P4, complete medium was used before scratch and basal medium was used after the scratch. In P1, the cells were serum starved for 12h before and after the scratch. In P2, the serum was reduced to 0.5% for 12h before and after the scratch. In P3, the serum was reduced to 0.5% for 12 h before the experiment, then, 5% FCS was added during the migration. In P4, the cells were serum starved after the scratch. The time frame for analysis of cell migration was determined at 8h and 24h in all protocols.

As shown in Table 1, in P1, a prolonged starvation led to cell damage and cell detachment. In P2, a low percentage of FCS (0.5%) during all experiment promoted cell detachment. In P3 and P4, the presence of 5% FCS (during the migration or until the scratch, respectively) avoids cell detachment at 8h after the scratch. In all experimental conditions, cellular damage was observed at 24h.

Therefore, P1 and P2 were discarded and we selected “8h” as the optimal time to just analyse the migration (Table 1).

Figure 10 compares the levels of spontaneous migration at 8 h using the four different protocols. We observed high levels of spontaneous migration in P4, being significantly different respect to P1 and P2 (Figure 10A). Moreover, in P4, the magnitude of cell-free zone after migration during 8h allows to determine the inhibitory or stimulating effect of drugs (Figure 10B).

Overall, we concluded that, in HAoEC, the optimal conditions to obtain spontaneous migration suitable to analyse the possible inhibitory or stimulant effects of compounds was achieved using the P4 protocol with a time of 8h migration.

Table 1. Comparison of the four different protocols used to analyse HAoEC migration using the experimental conditions described in the literature.

	P1	**P2**	**P3**	**P4**
FCS concentration at 12h before scratch	***0%***	***0.5%***	***0.5%***	***5%***
Medium	***Basal***	***Basal***	***Basal***	***Complete***
Cell damage before creating the scratch	*Yes*	*No*	*No*	*No*
FCS concentration after scratch	***0%***	***0.5%***	***5%***	***0%***
Medium	***Basal***	***Basal***	***Basal***	***Basal***
At 8h after scratch *Cell detachment during the migration*	*Yes*	*Yes*	*No*	*No*
Migration in cell-free zone respected to the reference point at time 0h	*Poor*	*Poor*	*Poor*	*Good*
At 24h after scratch *Cell detachment after cell migration*	*Yes*	*Yes*	*Yes*	*Yes*
Difficult to track migration	*Yes*	*Yes*	*Yes*	*Yes*

P1=Protocol 1 (Guo el al., 2014); P2=Protocol 2; P3=Protocol 3 (Murohara et al., 1999) P4=Protocol 4 (Chen, 2013)

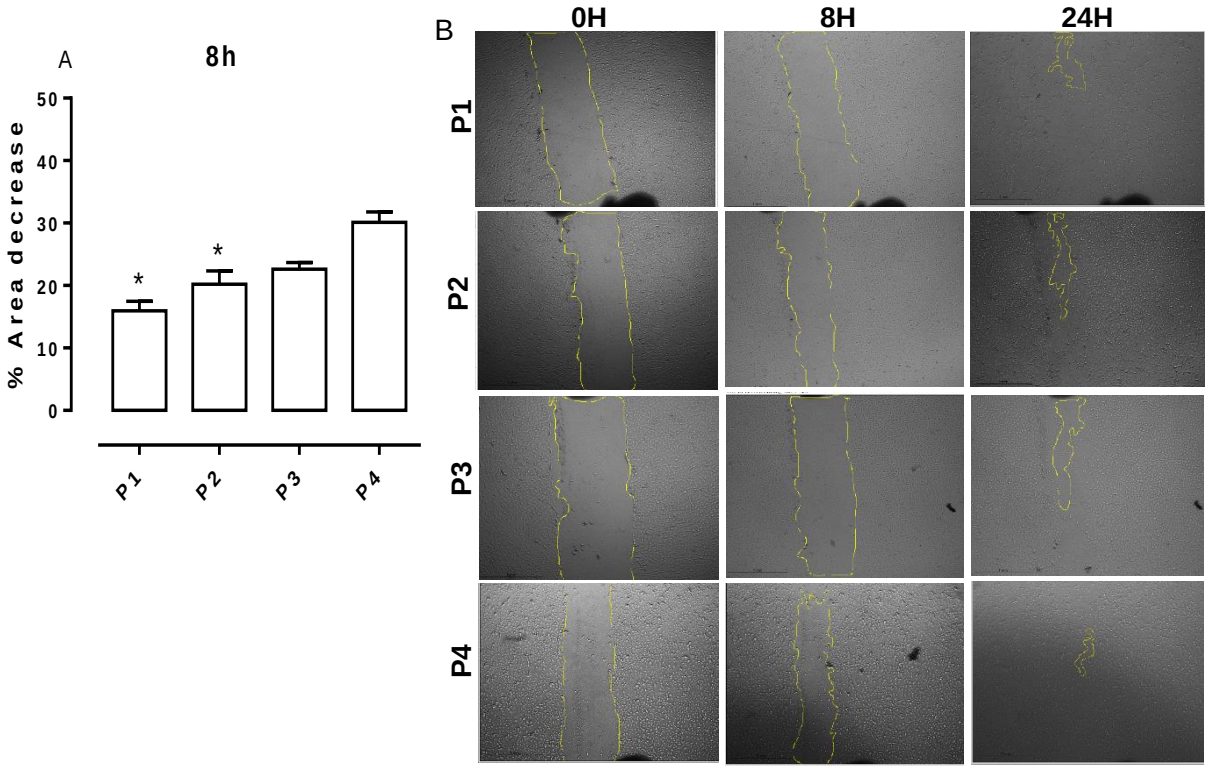

***Figure 10**. **Spontaneous HAoEC migration using different protocols.** Quantification of HAoEC migration at 8h (A). Values are represented as the percentage of area decrease at 8h respect to area at 0h. Representative images of ECs migration at different time in scratch assay (B). The edge of the scratch (yellow) was monitored at 0h, 8h, and 24h. Data represent the mean ± SEM of n=3 independent experiments. *p<0.05 vs P4. One-way Anova and Tukey post-test. P1, P2, P3, and P4: Protocol 1, 2, 3, and 4.*

According to the obtained results, P4 has been selected to determine the ***effect of NT-3 on human cells migration*** at 8 h in aortic (HAoEC) and coronary (HCAEC) ECs. However, in these experimental conditions, a cellular damage was observed in ECs from human coronary microvasculature (HCMEC), therefore 0.5% FCS was added in the medium after scratch of ECs.

As described in *Methods (3.5.4)*, cardiac (HCAEC, HCMEC) and aortic (HAoEC) ECs were pre-treated or not with K252a (0.20µM) for 1 h followed by incubation with NT-3 (32ng/ml) for 8h.

As shown in Table 2 and Figure 11, NT-3, K252a or NT-3 in the presence of K252a did not significantly modify migration in any of the three EC lines tested.

Table 2. Effect of NT-3 on migration of different types of ECs

Area decrease (μm^2)	HCAEC	*n*	HCMEC	*n*	HAoEC	*n*
Control	391597 ± 30522	*4*	482925 ± 103435	*4*	451156 ± 66375	*4*
NT-3	459306 ± 95308	*4*	495292 ± 60853	*3*	465567 ± 69585	*4*
NT-3+K252a	413276 ± 23585	*4*	495233 ± 2257	*2*	383452 ± 54912	*4*
K252a	359805 ± 41117	*4*	454319 ± 92567	*4*	365516 ± 107884	*4*

Values represent the mean ± SEM obtained from n different animals.
Data expressed as area decrease (μm^2) at 8h respect 0h.
HCAEC: Human coronary artery ECs, HCMEC: Human cardiac microvascular ECs, HAoEC: Human aorta ECs

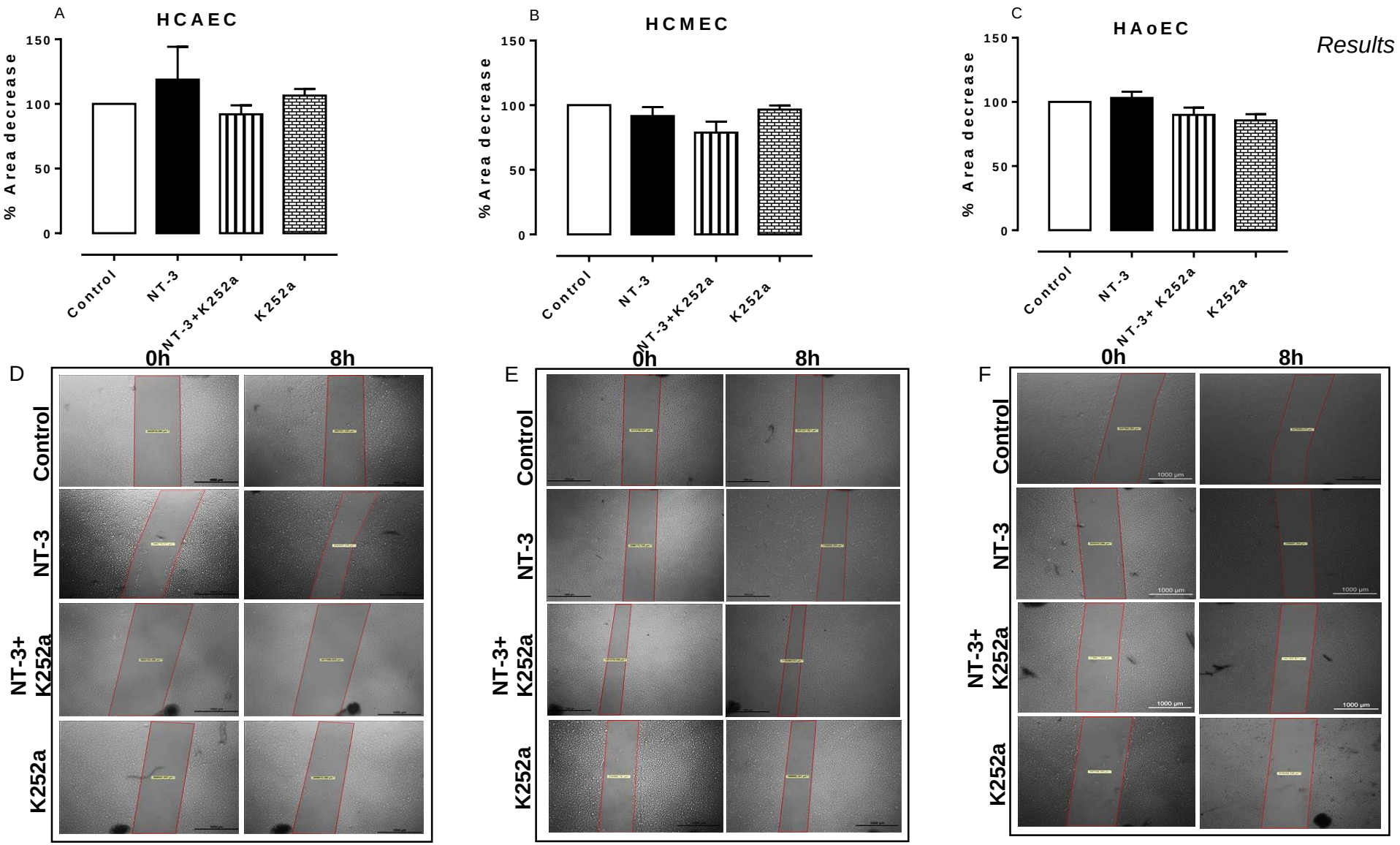

Figure 11. Effect of NT-3 and TrkC receptor on ECs migration*. Cell migration was determined by scratch assay in the presence of NT-3 (32 ng/ml), K252a (0.20 µM) or NT-3 after the treatment with K252a (NT-3+K252a). Values represent the area decrease at 8h expressed as percentage respect to control migration in, HCAEC (A), HCMEC (B), and HAoEC (C). Data represent the mean ± SEM of n=3 independent experiments. Representative cell migration images captured at 0h and 8 h after scratch in HCAEC (D), HCMEC (E), and HAoEC (F).*

3.2 EFFECT OF NT-3 ON HUMAN ECS TUBE-LIKE NETWORK FORMATION

As described in *Methods* (3.6.1), ECs were seeded on Matrigel® to promote the formation of tubular structures and were incubated in the absence (control) or presence of NT-3 (32 ng/ml) for 18h. To test the participation of TrkC receptors, in some experiments, K252a (0.20 µM) was added for 1h before NT-3. The effect of K252a (0.20 µM) was also evaluated.

The effect of NT-3, K252a or NT-3 in the presence of K252a was not significant on tube formation in the three types of ECs (Table 3, Figure 12). These results are similar to results obtained on cell migration.

Table 3. Effect of NT-3 on ECs tube-like network formation

	HCAEC	*n*	HCMEC	*n*	HAoEC	*n*
Control	51.50 ± 7.35	*4*	101.5 ± 13.65	*3*	64.30 ± 3.62	*5*
NT-3	62.50 ± 8.00	*4*	105.00 ±8.97	*3*	58.30 ± 6.28	*5*
NT-3+K252a	56.13 ± 7.92	*4*	98.33 ± 7.58	*3*	61.00 ± 7.15	*5*
K252a	56.25± 3.88	*4*	87.5 ± 8.64	*3*	53.30 ± 3.31	*5*

Values are expressed as number of tube formation
Data represent the mean ± SEM obtained from n different animals.
HCAEC: Human coronary artery EC, HCMEC: Human cardiac microvascular ECs
HAoEC: Human aorta ECs

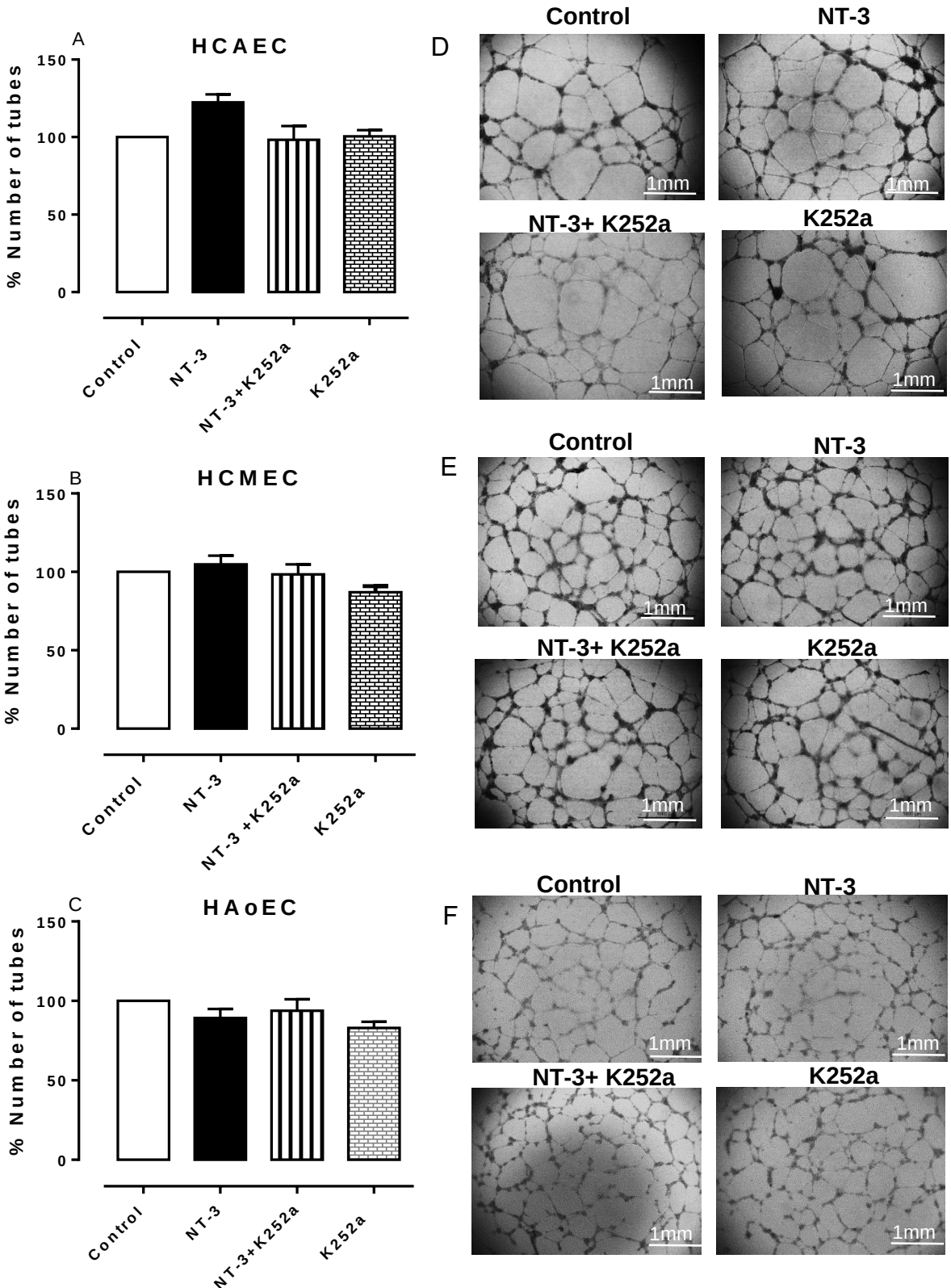

Figure 12. Effect of NT-3 on ECs tube-like network formation. *Quantitative analysis of the tube formation in HCAEC (A), HCMEC (B), and HAoEC (C), plated on Matrigel matrix and incubated for 18h in absence (control) or presence of NT-3 (32 ng/ml), K252a (0.20 μM) or NT-3 after the treatment with K252a (NT-3+K252a) Bars represent the new tube formation expressed as percentage respect to control. Data represent the mean ± SEM of n=4 independent experiments. Representative images captured after 18h in HCAEC (D), HCMEC (E), and HAoEC (F).*

3.3 EFFECT OF NT-3 ON ANGIOGENESIS IN RAT AORTIC RINGS

The effect of NT-3, in the presence or absence of K252a, was tested along the angiogenic process, in aortic rings embedded in Matrigel®, as described in *Methods* section (3.6.2). The new vessel growth was controlled and measured from day 3, in which the vessels begin to adopt differentiated tubular structures, until day 7. The angiogenic process was not significantly modified by NT-3, K252a or NT-3 after the treatment with K252a (Figure 13).

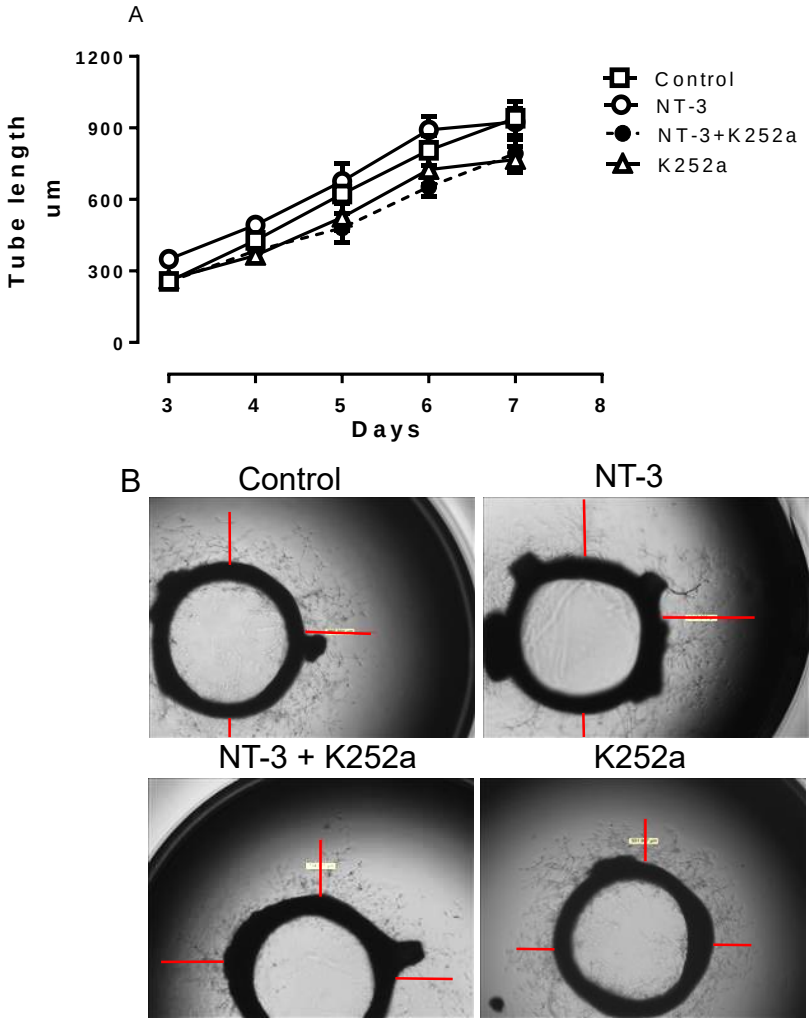

Figure 13. Effect of NT-3 on angiogenesis using the rat aortic ring assay*. Mean length (µm) of the new vessel growth from day 3 until day 7 in rat aorta explants in absence (control) or presence of NT-3 (32 ng/ml), K252a (0.20 µM) or NT-3 after the treatment with K252a (NT-3+K252a) (A). Data represent mean ± SEM of n=3 different animals. Representative images (microscopy Leica DM IL LED Leica camera, objective 2.5X) of aorta rings embedded in Matrigel® on day 7(B). Red lines show the measure for each axis.*

3.4 CHANGES IN THE EXPRESSION LEVELS OF TRKC IN CULTURED CELLS ISOLATED FROM RAT AORTA AND IN QUIESCENT AORTA RINGS

Taking account, the lack of response to NT-3, on human ECs migration and tubule formation as well as on rat aorta angiogenesis, we have analyzed the TrkC gene expression in:

- the different types of human ECs used in the performed assays,
- smooth muscle cells and fibroblasts isolated from rat aorta and heart, respectively (fresh and cultured until confluence is reached)
- isolated rat aorta (fresh and quiescent rings).

As described above, the results obtained show the presence of TrkC mRNA at very low levels in aortic ECs (HAoEC). In addition, undetectable levels of TrkC were found in coronary artery cells (HCAEC) and coronary microvasculature (HCMEC) ECs (Figure 14A).

Moreover, a robust decrease in TrkC expression was produced in cultivated SMCs and fibroblasts vs freshly isolated cells from rat aorta (Figure 14B), and on quiescent vs freshly isolated rat aorta (Figure 14C).

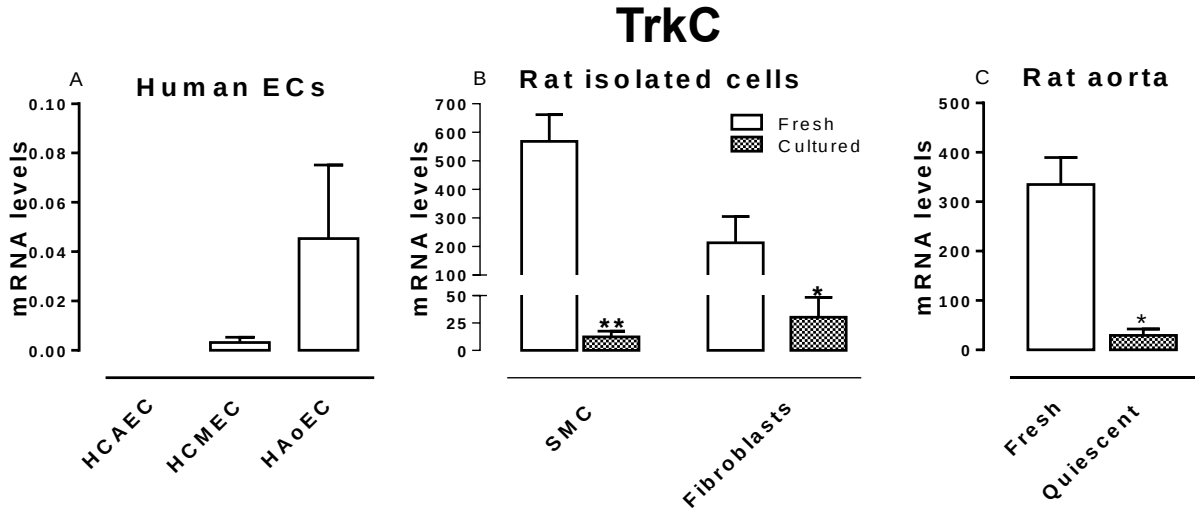

Figure 14. Changes in gene expression of TrkC. *mRNA levels of NTRK3 (TrkC) in human endothelial cells (HCAEC, n=5; HCMEC, n=4; HAoEC, n=3) (A), isolated rat aorta SMCs (fresh, n=2; cultivated, n=3) and cardiac fibroblasts (fresh, n=7 ; cultivated, n=5) (B), and rat aorta (fresh, n=21; and quiescent, n=3) (C). Values are expressed as* $2^{-\Delta Ct}$ *x* 10^4 *using GAPDH as housekeeping gene and represent the mean ± SEM of n different experiment. *p<0.05, **p<0.01 vs Fresh. Student's t-test for unpaired samples.*

3.5 EFFECT OF NT-3 ON VASCULAR TONE

The effect of NT-3 on vascular tone was tested in two types of vessels, aorta (conductance) and tail artery (distributing) isolated from adult Wistar rats, and the influence of endothelium and PVAT was evaluated.

A) Influence of endothelium

The effect of NT-3 on vascular tone has been tested using isolated thoracic aorta and tail artery rings, in the absence or presence of endothelium. To test the participation of NO, some experiments were performed in the presence of an inhibitor of NOS (L-NAME, 100 µM) that has been added to the bath 30 min before PHE induced contractile response (Scheme 1). In these set of experiments, the perivascular adipose tissue (PVAT) surrounding the vessels has been eliminated.

The following protocol, which has been described in *Methods (3.8.2*), has been used in this section:

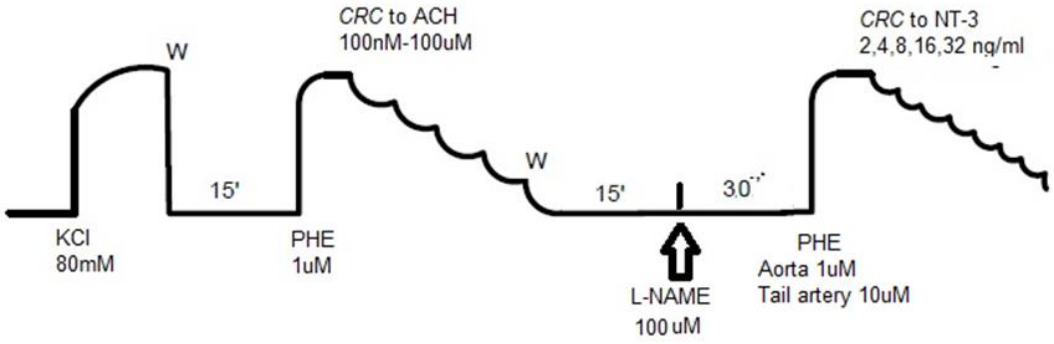

Scheme 1. *Schematic drawing showing the experimental procedure used in rat vessels to study the role of NT-3 on vascular tone in the presence or absence of L-NAME. PHE: Phenylephrine, ACH: Acetylcholine. CRC: concentration response curves, W: washing.*

The addition of KCl (80mM) induced a contractile response in aorta and tail artery. A sustained contractile response was also observed after addition of a concentration of PHE that induce a maximal response (aorta: 1µM, tail artery 10µM) (Table 4).

Table 4. Magnitude of vascular contraction induced by KCl or PHE.

	Aorta (mN)		Tail artery (mN)	
		n		***n***
KCl	7.72 ± 0.46	10	9.75 ± 1.00	12
PHE	7.14 ± 0.48	10	8.70 ± 0.81	12

Values represent the mean ± SEM obtained from n animals.

The endothelium integrity was tested by performing CRCs to ACH on PHE-induced maximal contraction since this agonist induces a relaxant response due to endothelial-derived NO (Furchgott & Zawadzki, 1980). In aorta, cumulative addition of ACH induced a concentration-dependent relaxation (Emax= 64.66 ± 3.46% vs PHE-induced contraction; pEC50= 6.33 ± 0.09, n=6) evidencing the presence of an intact endothelium. However, in tail artery, low relaxant response to ACH was observed (Emax= 24.3± 6.42% vs PHE, n= 6) suggesting that the endothelium has been damage or the absence of an endothelial response mediated by ACH in this vessel. In aorta, some experiments were done in the absence of endothelium, and then a relaxant response to ACH less than 10% was obtained.

CRCs to NT-3 (2, 4, 8, 16, and 32ng/ml) were performed on maximal PHE-pre-contracted rings. In aorta, NT-3 induced a relaxant response that was abolished in the presence of L-NAME or when endothelium has been removed (Figure 15A, Table 5). However, in tail artery, only a slight relaxant response to NT-3 was observed, and the pre-incubation with L-NAME did not modify this response (Figure 15B, Table 5). Altogether, these results suggest that NT-3 induces a NO endothelium-dependent relaxation in rat aorta but not in tail artery.

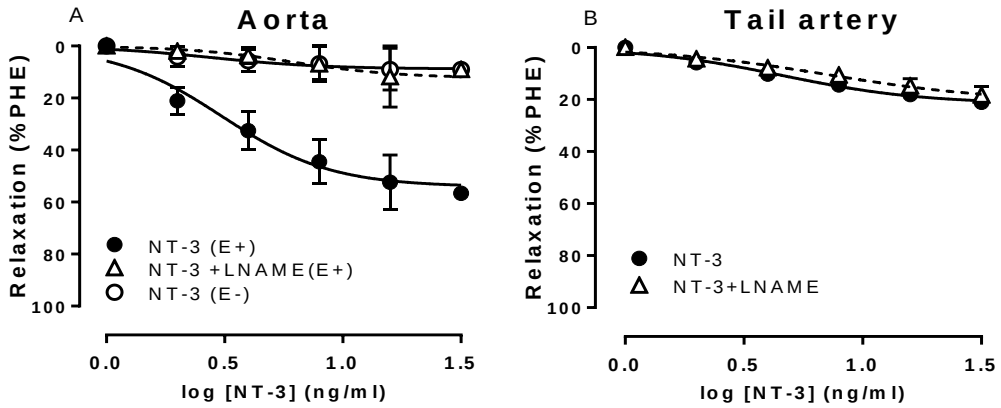

Figure 15. Effect of NT-3 on vascular tone. *CRCs of relaxation of NT-3 in the presence or absence of L-NAME (100 µM) in aorta (A) or tail artery (B) from Wistar rat. CRCs of relaxation of NT-3 in the presence (E+) or absence (E-) of endothelium in aorta. Values are expressed as percentage respect to the contraction induced by PHE. Data represent the mean ± SEM of n=4-5 animals*

Table 5. Parameters obtained from the CRCs of relaxation to NT-3 (2,4,8,16,32 ng/ml) in aorta and tail artery rings from Wistar rat.

	Aorta			Tail artery	
	Emax (%PHE)	**pEC50**	***n***	**Emax (%PHE)**	***n***
NT-3 (E+)	54.14 ± 8.44	0.49 ± 0.13	4	21.09 ± 1.42^{++}	5
NT-3+L-NAME	12.31 ± 12.32*		4	18.28 ± 3.35	5
NT-3 (E-)	8.80 ± 5.81**		4		

Values represent the mean ± SEM of n different animals.
E_{max}: Maximum effect expressed as % with respect to the contraction induced by PHE.
pEC50: Negative logarithm of the molar concentration of agonist that produces half of E_{max}.
**p<0.05, **p<0.01 vs E (+). $^{++}$p<0.01 vs aorta E (+). Student's t-test for unpaired samples.*

In another set of experiments, the effect of NT-3 on vascular tone has been tested in aorta and tail artery in the presence or absence of K252a (0.2 µM) to block the activity of Trk receptor. This inhibitor has been added for 30 min before PHE induced CRCs of contraction (10 nM- 1 µM or 10 µM, in rat aorta or tail artery, respectively), and then cumulative concentrations of NT-3 were added as previously described. Figure 16 and Table 6 show that K252a did not modify the CRCs of relaxation to NT-3 in rat aorta nor in tail artery. These results exclude the participation of TrkC in NT-3-induced relaxant response.

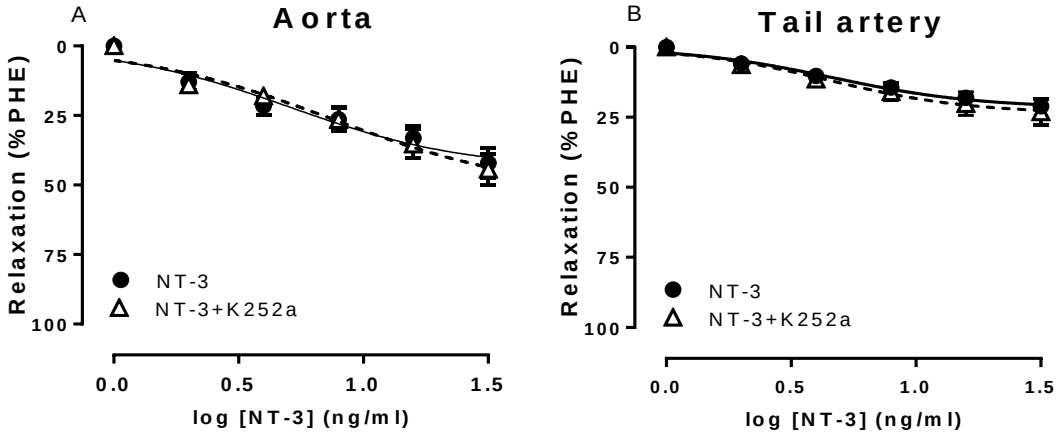

Figure 16. Effect of TkrC on NT-3 relaxant response. *CRCs of relaxation to NT-3 on aorta (A) or tail artery (B) in the presence or absence of K252a (0.2µM). Values are expressed as percentage respect to the contraction induced by PHE. Data represent the mean ± SEM of n=5-9 animals*

Table 6. Parameters obtained from the CRCs of relaxation to NT-3 (2,4,8,16,32 ng/ml) in aorta and tail artery rings from Wistar rats.

	Aorta			**Tail artery**	
	Emax (%KCl)	**pEC50**	***n***	**Emax (%KCl)**	***n***
NT3	42.04 ± 5.36	0.70 ± 0.18	8	21.09 ± 1.42	5
NT-3+K252a	44.40 ± 5.50	0.87 ± 0.25	9	23.12 ± 4.54	5

Values represent the mean ± SEM of n different animals.
E_{max}: Maximum effect expressed as % with respect to the contraction induced by PHE.
pEC50: Negative logarithm of the molar concentration of agonist that produces half of E_{max}.

We have also assessed that Trk inhibitor (K252a) did not modify the contractile response to α_1-AR stimulation. Thus, the CRCs of contraction to PHE were similar in the absence or presence of K252a, in both aorta and tail artery rings (Figure 17). The parameters (Emax and pEC50) of these curves are detailed in Table 7.

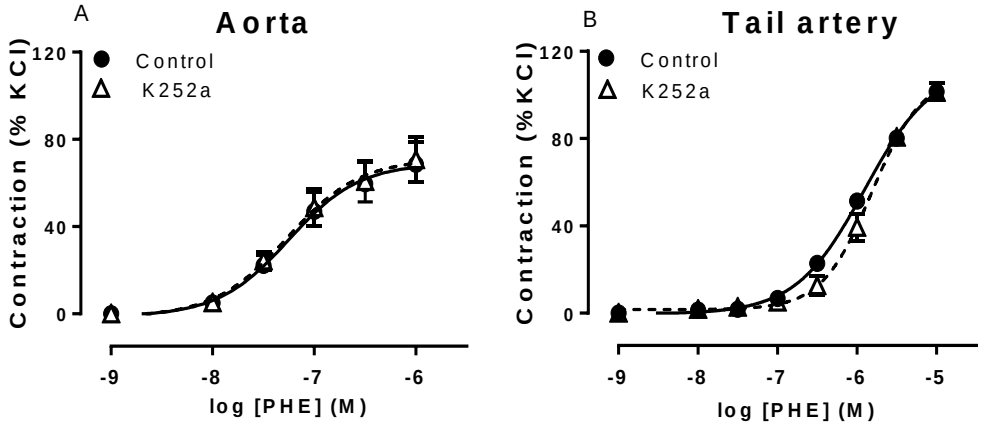

Figure 17. Effect of K252a on PHE-induced contractions in vessel rings. *CRCs to PHE in the absence or presence of K252a (0.2 μM) in aorta (A) and tail artery (B) obtained from Wistar rats. Data are expressed as percentage respect to the contraction induced by 8 0mM KCl. Data represent the mean ± SEM of n=8-9 (aorta) or n=5 (tail artery) different animals.*

Table 7. Parameters obtained from the CRCs to PHE in aorta and tail artery rings from Wistar rats in the absence or presence of K252a (0.2 μM).

	Aorta			Tail artery		
	Emax (%KCl)	**pEC50**	**n**	**Emax (%KCl)**	**pEC50**	**n**
Control	69.08 ± 8.66	7.25 ± 0.17	8	113.16 ± 5.72	5.90 ± 0.06	5
K252a	71.10 ± 8.74	7.27 ± 0.17	9	108.83 ± 6.11	5.82 ± 0.06	5

Values represent the mean ± SEM obtained of n different animals
E_{max}: Maximum effect expressed as % vs the contraction induced by 80 mM KCl.
pEC50: Negative logarithm of the molar concentration of agonist that produces half of E_{max}.

B) Influence of aorta perivascular adipose tissue (PVAT)

The influence of PVAT on NT-3-induced relaxation was determined in aortic rings with (+PVAT) or without PVAT (-PVAT) following a protocol similar to that described in Scheme 1. All experiments were performed in the presence of endothelium, and only aorta rings that relaxed >60% to ACH were considered.

Firstly, we characterized this preparation analysing the effect of PVAT on KCl- and α_1-AR-induced contraction and ACH- and β-AR-induced relaxation.

We observed a significant diminished KCl (80mM)-induced contraction in aorta rings with PVAT (6.07 ± 0.32mN, n=20) compared with non-PVAT aorta rings (7.28 ± 0.31 mN, n=19) (Figure 18A). Similar results were obtained when maximal PHE (1 µM) contractile response were evaluated (4.20 ± 0.31mN, n=20, in +PVAT aorta vs 6.74 ± 0.31 mN, n=19, in –PVAT aorta) (Figure 18B).

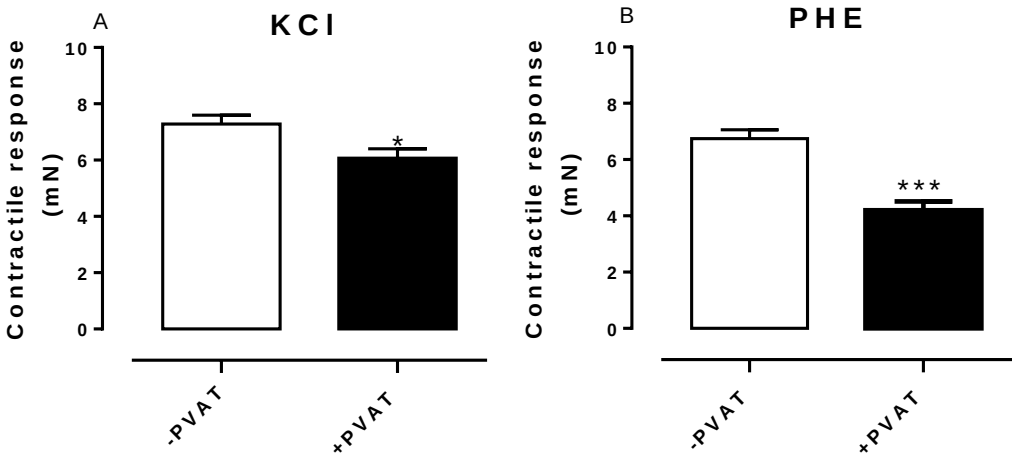

Figure 18. Anti-contractile effect of PVAT. *Magnitude of the contractile response induced by KCl (A) and PHE (B) in aorta with (+PVAT) or without PVAT (-PVAT). Data represent the media ± SEM of n=19-20 animals. *p<0.05, ***p<0.001 vs –PVAT. Student's t-test for unpaired samples*

As expected, in +PVAT aorta rings, CRCs of contraction to α_1-AR agonist (PHE, 10 nM-10 µM) were significantly reduced (Figure 19), and significant decreases were obtained in the maximal effect (Emax) and in the potency (pEC50) compared to -PVAT aortic rings, as shown in Table 8. These results suggest that PVAT exerts a modulatory effect reducing the contractile response to α_1-ARs stimulation.

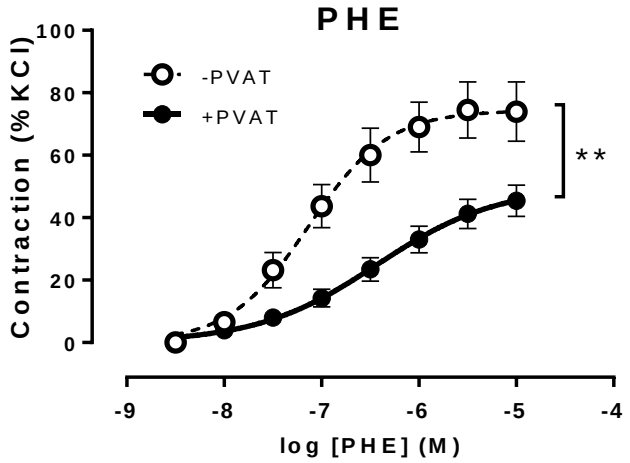

Figure 19. Anti-contractile effect of PVAT on PHE induced contraction. *CRCs to PHE (10nM-10μM) in aorta with (+PVAT; n=12) or without PVAT (-PVAT; n=10). Values are expressed as percentage respect to the contraction induced by 80 mM KCl. Data represent the mean ± SEM of n different animals. **p<0.01 vs –PVAT. Student's t-test for unpaired samples*

Table 8. Parameters obtained from the CRCs to PHE (10nM to 10μM) in aortic rings with (+PVAT) or without PVAT (-PVAT).

	PHE		
	Emax	**pEC50**	***n***
-PVAT	74.34 ± 4.90	7.13 ± 0.12	10
+PVAT	49.94 ± 6.21**	6.42 ± 0.22*	12

Values represent the mean ± SEM of n animals.
E_{max}: Maximum effect expressed as % with respect to the contraction induced by KCl. pEC50: Negative logarithm of the molar concentration of agonist that produces half of E_{max}.
*$^{+}$p<0.05; **p<0.01 vs -PVAT. Student's t-test for unpaired samples*

To determinate the role of PVAT on β-AR-induced relaxation, we assessed the effect of isoprenaline (ISO) (non-selective β_1-, β_2-AR agonist) and SR58611A (β_3 -selective agonist) in aorta rings with and without PVAT. CRCs of relaxation were performed by addition of cumulative concentrations of ISO (1nM-100μM) or SR58611A (1nM-100μM) on maximal PHE-pre-contracted rings.

The results obtained show a slight but significant reduction on ISO-induced relaxant response in aorta with PVAT (+PVAT) respect to aorta without PVAT (-PVAT) (Figure 20A, Table 9A).

In the case of SR58611A, biphasic curves were obtained in aorta with and without PVAT (Figure 20B). Analysis of these curves provided two receptor populations: one of high potency (1) that corresponds to β_3 subtype and whose percentage was about 47% or 56% (+PVAT or –PVAT, respectively) and another of low potency (2) that corresponds to β_1- and/or β_2 -ARs (Table 9B). A slight decrease in the relaxing response to SR58611A could be observed in +PVAT aortic rings although the difference *vs* -PVAT rings did not reach statistical significance (Figure 20B, Table 9 B).

The NO-dependent endothelium relaxation induced by ACH was also analyzed. Figure 19C shows that the ACH-induced relaxant response was significantly reduced in aorta with PVAT compared to aorta without PVAT and a significant decreased in Emax and pEC50 was obtained (Table 9C).

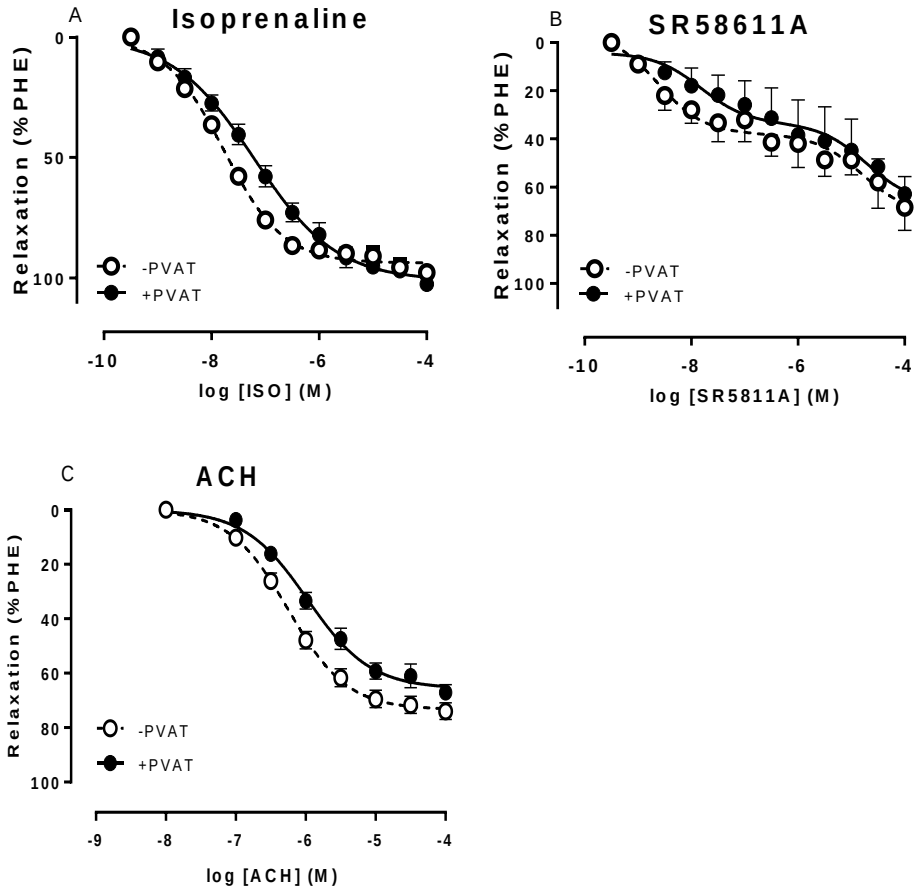

Figure 20. Pro-contractile effect of PVAT on the relaxant response induced by β-ARs and ACH. *CRCs to isoprenaline (1nM-100μM, n= 7) (A), SR58611A (1nM-100μM; n=3) (B), and ACH (10nM-100 μM, n=19-20) (C) in aortic rings pre-contracted with PHE (1μM). Values are expressed as percentage respect to the contraction induced by PHE. data represent the mean ± SEM of n different animals.*

Table 9. Parameters obtained from the CRCs of relaxation to isoprenaline, SR5811A, and ACH in aortic ring with (+PVAT) or without (–PVAT).

A

ISOPRENALINE			
	Emax	**pEC50**	***n***
-PVAT	93.68 ± 1.24	7.77 ± 0.04	7
+PVAT	101.02 ± 2.55	7.20 ± 0.07***	7

B

SR58611A				
	Emax	**pEC50**	**% (1)** [a]	***n***
-PVAT	71.24±10.94	8.62 ± 0.37 (1) 4.79 ± 0.49 (2)	55.9 ± 0.10	3
+PVAT	66.76±15.55	7.81 ± 0.54 (1) 4.71 ± 0.79 (2)	46.8 ±0.13	3

C

ACH			
	Emax	**pEC50**	***n***
-PVAT	73.34 ± 1.97	6.24 ± 0.05	19
+PVAT	65.70 ± 2.52*	5.97 ± 0.07**	20

Values represent the mean ± SEM of n animals
E_{max}: Maximum effect expressed as % with respect to the contraction induced by PHE
pEC50: Negative logarithm of the molar concentration of agonist that produces half of E_{max}.
pEC50 (1) and (2): pEC50 for high and low potency site
a: percentage of high potency site
**p<0.05; **p<0.01; ***p<0.001 vs -PVAT; Student's t-test for unpaired samples.*

These results evidence a pro-contractile activity of PVAT on β-ARs- and ACH-induced relaxant response. Similar results were obtained when NT-3 was used as vasodilator agent. In fact, a slight decrease in the CRCs of relaxation to NT-3 was observed in aorta with PVAT (+PVAT) *vs* aorta without PVAT (-PVAT) although the difference did not reach statistical significance (Figure 21, Table 10).

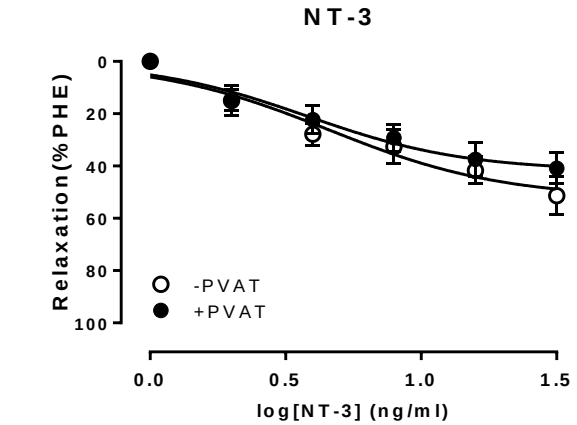

,

Figure 21. ***Effect of PVAT on NT-3-induced relaxation responses.*** *CRCs to NT-3 (2,4,8,16,32 ng/ml) in aortic rings with (+PVAT) or without (-PVAT). Values are expressed as percentage respect to the contraction induced by PHE. Data represent the mean ± SEM of n=4-6 animals.*

Table 10. Parameters obtained from the CRCs to relaxation to NT-3 (2,4,8,16,32 ng/ml) in aortic ring with (+PVAT) or without (–PVAT).

	NT-3		
	Emax	**pEC50**	**n**
- PVAT	51.36 ± 7.26	0.66 ± 0.17	4
+ PVAT	41.83 ± 6.74	0.57 ± 0.15	6

Values represent the mean ± SEM of n animals
E_{max}: Maximum effect expressed as % with respect to the contraction induced by PHE.
pEC50: Negative logarithm of the molar concentration of agonist that produces half of E_{max}.

4. CONSEQUENCES OF A REDUCED ENDOGENOUS NT-3 EXPRESSION IN GENETICALLY ENGINEERED MICE ON CARDIOVASCULAR FUNCTIONS

Two models of genetically engineered mice with deficient expression of NT-3 were selected:

- Heterozygous mice for NT-3 (NT-$3^{+/-}$), as described previously in the section 2.
- Mice in which the endothelial expression of NT-3 was supressed (*Ntf3*$^{flox1/lox2}$;*Tie2-cre*$^{+/0}$: eNT3^{-}) (Delgado et al., 2014).

In both models, the corresponding wild type (WT) mice with a normal NT-3 expression levels were used (NT-$3^{+/+}$ and *Ntf3*$^{flox1/flox2}$;*Tie2-cre*$^{0/0}$: eNT3^{+}, respectively).

The changes observed in anthropometric and hemodynamic parameters as well as in the regulation of vascular tone mediated by the stimulation of α_1- and β-adrenergic receptors are detailed below.

4.1 ANTHROPOMETRIC AND HEMODYNAMIC PARAMETERS

As shown in Table 11, no significantly changes were observed in ***body weight***, ***heart weight*** and ***heart/body weight ratio*** when comparing NT$3^{+/-}$ or eNT3^{-} mice vs corresponding WT mice.

Table 11. Anthropometric data in genetically modified mice

	NT3$^{+/+}$ ***n=12***	***NT3$^{+/-}$*** ***n =14***	***eNT3^{+}*** ***n =7***	***eNT3^{-}*** ***n =7***
Age (week)	37.21±2.21	39.52±1.89	58.61±5.51	53.74±2.10
Body weight (g)	39.61±2.06	41.22±1.57	33.09±0.54	33.95±1.40
Heart weight (g)	0.23±0.01	0.23±0.01	0.22±0.03	0.18±0.01
Heart/Body weight Ratio (mg/g)	5.99±0.25	5.74±0.28	6.65±0.81	5.28±0.61

.

Values represent the mean ± SEM of n different animals

Systolic blood pressure (BP) was determined by the tail-cuff measurement as described in *Methods (1.2.3).* The results obtained shown a significant decrease in BP in both strains of mice with deficient expression of NT-3 (NT-$3^{+/-}$, $eNT3^{-}$) in comparison with the corresponding WT mice (NT-$3^{+/+}$, $eNT3^{+}$, respectively) (Table 12, Figure 22).

Table 12. Systolic BP in genetically modified mice

	$NT3^{+/+}$ ***N=7***	***$NT3^{+/-}$*** ***n =10***	***$eNT3^{+}$*** ***n =11***	***$eNT3^{--}$*** ***n =11***
Age (week)	45.78±1.77	43.73±1.43	66.95±3.85	62.2±3.56
Blood pressure (BP) (mmHg)	135.00±2.54	127.30±2.16*	108.80±2.61	101.61±1.69*

Values represent the mean ± SEM of n different animals
**p<0.05 vs $NT3^{+/+}$ or $eNT3^{+}$*

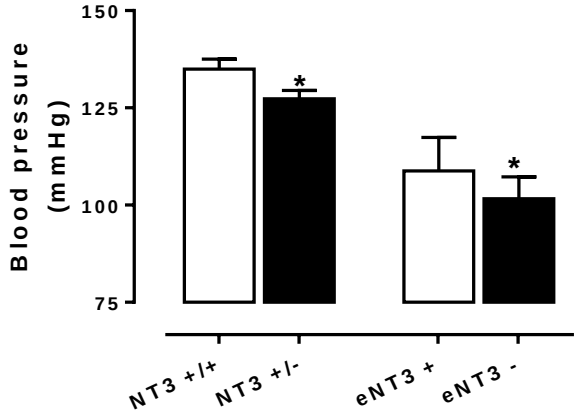

Figure 22. ***Arterial blood pressure in genetically modified mice.*** *Systolic blood pressure (BP) in mice with reduced expression of NT-3 ($NT3^{+/-}$) and in mice without endothelial expression of NT-3 ($eNT3^{-}$) compared to its corresponding controls mice ($NT3^{+/+}$, $eNT3^{+}$, respectively). Data represent the mean ± SEM of n different animals. p<0.05 vs $NT3^{+/+}$ or $eNT3^{+}$. Student's t-test for unpaired samples.*

4.2 VASCULAR TONE MEDIATED BY ADRENERGIC STIMULATION

We analysed the responses to α_1- (PHE) and β-AR agonists (isoprenaline, non-selective β_1 and β_2, and SR58611A, selective β_3). For this purpose, PHE-induced CRCs of contraction and β agonists-induced CRCs of relaxation have been performed, following a protocol similar to that described in Scheme 1. All experiments have been done in endothelium-covered aorta in which the surrounding PVAT was eliminated. To ensure the presence of an intact endothelium, ACH-induced CRCs of relaxation was performed on the contraction plateau of PHE, and rings with a relaxant response >60% were used, as previously indicated. The contractile response to KCl was also analysed.

In a previous work performed in our laboratory, the changes in vascular tone in heterozygous mice for NT-3 ($NT3^{+/-}$) were investigated. Therefore, in the present Thesis, we extend these results and we analyzed the vascular responses in mice without endothelial expression of NT-3 ($eNT3^{-}$) compared to control mice ($eNT3^{+}$).

Firstly, we observed no significant differences on KCl (80mM)-induced contraction in aorta from $eNT3^{+}$ (4.47 ± 0.44 mN, n=11) compared to aorta from $eNT3^{-}$ mice (3.73 ± 0.27 mN, n=19).

Furthermore, the results obtained show similar PHE-induced CRCs (10 nM-10 μM) in both strains of mice ($eNT3^{-}$ and $eNT3^{+}$) (Figure 23, Tabla 13). These results evidence that endothelial NT-3 deletion does not modify the contractile response induced by a despolarizing agent (KCl) or by α_1-AR stimulation.

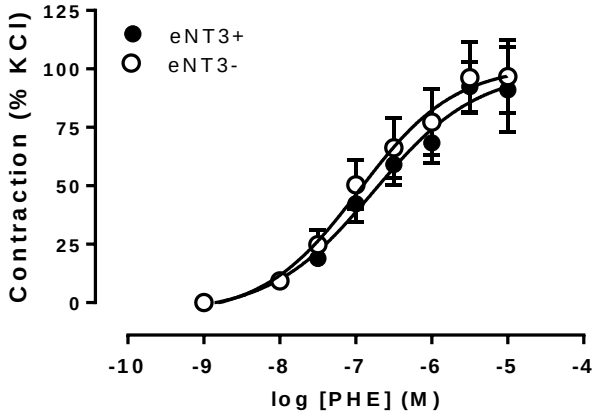

Figure 23. Effect of endothelial NT-3 on vasoconstrictor responses. *CRCs to PHE on aortic rings from mice without endothelial expression of NT-3 (eNT3$^-$; n=4) and control (eNT3$^+$; n=5) mice. Values are expressed as percentage respect to contraction induced by KCl (80mM). Data represent the mean ± SEM of n different animals.*

Table 13. Parameters obtained from the CRCs to PHE in eNT3$^+$ and eNT3$^-$ mice.

PHE			
	Emax	**pEC50**	**n**
eNT3$^+$	96.54 ± 11.36	6.74 ± 0.21	5
eNT3$^-$	99.05 ± 11.65	6.91 ± 0.22	4

Values represent the mean ± SEM obtained from n different animals.
Emax: Maximum effect expressed as % with respect to contraction induced by KCl.
pEC50: Negative logarithm of the molar concentration of agonist that produces half of Emax.

To investigate the relaxant capacity of β-ARs, vasodilator CRCs to ISO (1 nM-100 μM) and SR58611A (1 nM-100 μM) were performed in maximal PHE pre-contracted aorta, from eNT3- and eNT3+ mice. As Figure 24A and Table 14A shown, ISO induced a similar relaxation in both mice strains.

Similarly, to that happen in rat aorta, the β_3-selective agonist, SR58611A, induced biphasic CRCs of relaxation in eNT3$^+$ and eNT3$^-$mice (Figure 24B). Two β-AR populations were evidenced which correspond to β_3-AR subtype with high potency value [pEC50(1)] and β_1- and/or β_2-AR subtypes with low potency values [pEC50(2)] (Table 14B). However, a robust decrease in the proportion of high

potency sites [% (1)], corresponding to β_3-ARs, can be observed in eNT3$^-$ mice (Figure 24B, Table 14B).

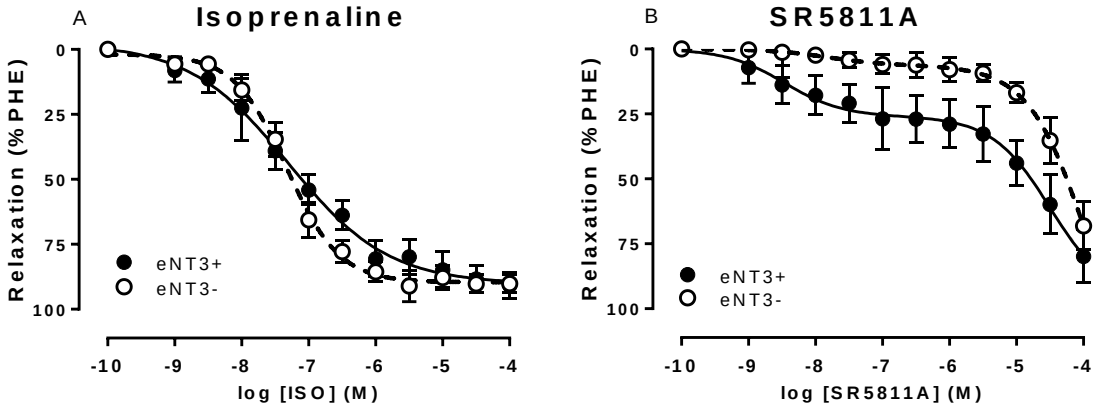

Figure 24. Changes in* the relaxant responses to β-AR stimulation in genetically modified mice. CRCs to ISO (1nM-100μM) (A) and to SR5811A (1nM-100μM) (B) on aortic rings from mice without endothelial expression of NT-3 (eNT3$^-$; n=4) and control mice (eNT3$^+$; n=5-6). Values are expressed as percentage respect to the contraction induced by PHE. Data represent the mean ± SEM of n different animals.*

Table 14. Parameters obtained from the CRCs of relaxation to isoprenaline and SR5811A in aortic rings from genetically modified mice.

A

	ISOPRENALINE		
	Emax	**pEC50**	**n**
eNT3$^+$	90.32 ± 4.52	7.29 ± 0.18	5
eNT3$^-$	89.65 ± 2.07	7.33 ± 0.07	4

B

	SR5811A			
	Emax	**pEC50**	**% (1)[a]**	**n**
eNT3$^+$	79.88 ± 10.12	8.47 ± 0.43 (1) 4.49 ± 0.36 (2)	26 ± 6%	5
eNT3$^-$	68.06 ± 9.25	7.82 ± 0.92 (1) 3.95 ± 0.30 (2)	4 ± 1%**	5

Values represent the mean ± SEM of n animals.
E_{max}: Maximum effect expressed as % with respect to the contraction induced by PHE
pEC50: Negative logarithm of the molar concentration of agonist that produces half of Emax.
(1) and (2): pEC50 for high and low potency site
a: Percentage of high potency site
***p<0.01 vs eNT3$^+$. Student's test for unpaired samples.*

Previous results obtained in our laboratory have shown that the relaxing response induced by β_3-ARs depends on the NO derived from the endothelium (Flacco et al., 2013). To assess whether there is an alteration in this pathway in NT3- mice, we analysed the relaxant CRCs to ACH and no differences between $eNT3^+$ and $NT3^-$ mice, were detected (Figure 25, Table 15).

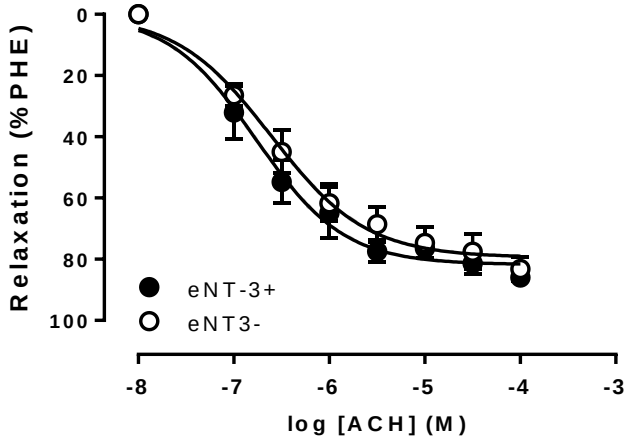

Figure 25. Endothelium dependent relaxation in genetically modified mice. *CRCs to ACH (10nM-100 µM) on aortic rings from mice without endothelial expression of NT-3 ($eNT3^-$; n=4) and control mice ($eNT3^+$; n=5). Values are expressed as percentage respect to the contraction induced by PHE. Data represent the media ± SEM of n different animals.*

Table 15. Parameters obtained from CRCs of relaxation to ACH in aortic rings from genetically modified mice.

	ACH		
	Emax	**pEC50**	**n**
$eNT3^+$	81.75 ± 3.25	6.76 ± 0.09	5
$eNT3^-$	79.41 ± 3.30	6.60 ± 0.10	4

Values represent the mean ± SEM obtained from n animals.
E_{max}: Maximum effect expressed as % with respect to the contraction induced by PHE.
pEC50: Negative logarithm of the molar concentration of agonist that produces half of Emax.

Taken together, these results suggest that the lack of endogenous NT-3 in the endothelium leads to a strong decrease on the β_3-AR vascular functionality, whereas the endothelium-dependent NO relaxation is not altered in $eNT3^-$ compared to $eNT3^+$ mice. Similar results were obtained in our laboratory in mice

with reduced expression of endogenous NT-3 ($NT3^{+/-}$) where a lack of the β_3-ARs functionality was evidenced compared to $NT3^{+/+}$ mice.

4.3 CHANGES IN NT-3, TRKC AND B-ARS SUBTYPES GENE EXPRESSION IN LEFT VENTRICLE OF GENETICALLY ENGINEERED MICE

To asses if the loss of vascular β_3-ARs funcionality in genetically modified mice, with either reduced expression of NT-3 ($NT3^{+/-}$) or without NT-3 expression in the endothelium ($eNT3^{-}$), could be due to a decrease in β_3-ARs expression, we determined the mRNA levels of NT-3, TrkC and β-AR subtypes (β_1, β_2 and β_3) in LV.

As previously described, a significant decrease in mRNA levels of NT-3 in $NT3^{+/-}$ compared with $NT3^{+/+}$ mice can be observed (Figure 26A). In $eNT3^{-}$ mice, the NT-3 gene expression is also reduced compared with $eNT3^{+}$ mice, but the difference did not reach statistical significance (Figure 26A). In any case, no significant changes in TrkC gene expression can be detected (Figure 26B).

A significant decrease in β_3-AR gene expression in $NT3^{+/-}$ compared with $NT\text{-}3^{+/+}$ mice was also evidenced (Figure 26C), without changes on the expression of β_1- and β_2-ARs (Figure 26D and E).

We have not observed significant modification on β_{1-}, β_{2-} or β_3-AR subtypes in $eNT3^{-}$ mice respect to $eNT\text{-}3^{+}$ mice (Figure 26C, D and E).

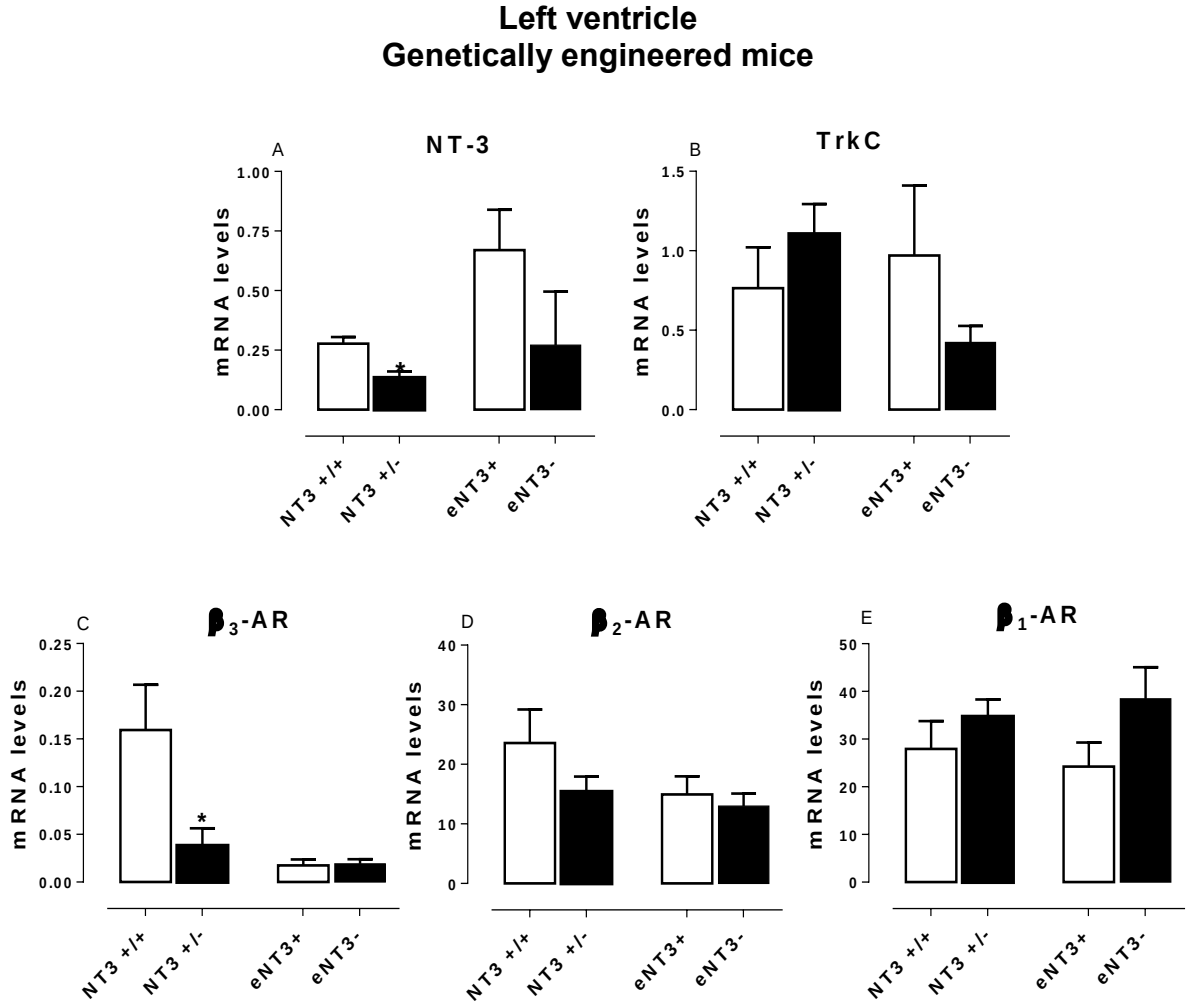

Figure 26. Changes in the NT-3 and β_3-ARs gene expression in left ventricle from genetically engineered mice. *mRNA levels of Ntf3 (NT-3; A), Ntrk3 (TrkC; B) Adrb3 (β_3-AR; C); Adrb2 (β_2-AR; D); Adrb1 (β_1-AR; E); in mice with reduced expression of NT-3 ($NT3^{+/}$; n=3-5), and in mice without endothelial expression of NT-3 ($eNT3^-$; n= 4-10) compared to its corresponding controls mice ($NT3^{+/+}$, n=3-5; $eNT3^+$, n=6-11; respectively). Values are expressed as $2^{-\Delta Ct}$ x10^4 using Gapdh as housekeeping gene and represent the mean ± SEM of n different animals. *p<0.05 vs $NT3^{+/+}$. Student's t-test for unpaired samples.*

5. CHANGES ON THE NT-3/TrkC PATHWAY IN CARDIOVASCULAR DISEASES

To determine the role of NT-3 on cardiovascular diseases, a quantitative analysis of NT-3 and TrkC expression was carried out in LV from explanted failing hearts from human patients. The results were compared with those obtained in LV from donor hearts, which could not be transplanted for technical reasons and had no apparent signs of cardiac failure (they were normotensive subjects with biochemistry profile within normality) (controls). Correlations of NT-3 gene expression with some clinical data of the patients were made to assess the functional significance of the changes.

Furthermore, we quantified NT-3 and TrkC expression in rat models of hypertension and obesity.

The expression levels of β-AR subtypes (β_1, β_2, and β_3) were also analysed to examine if there is a positive correlation between NT-3 and β-AR subtypes.

5.1 ANALYSIS OF NT-3/TRKC PATHWAY IN HUMAN HEART FAILURE

A) Clinical data of patients with heart failure

The group of patients with heart failure (HF) included patients with dilated cardiomyopathy (DC) or ischemic cardiomyopathy (IC) and patients with other forms of cardiomyopathy (non-ischemic, non-dilated) (Table 16).

The characteristics of these patients as well as their clinical variables and their pharmacological treatments are shown in Table 16.

Table16. Clinical variables in patients with heart failure (HF).

Sex, M/F	29/6
Age, yr	51.1±2.16
Body weight, kg	74.9±2.4
Height, m	168.2±1.6
Body mass index, kg/m^2	26.5±0.8
NYHA [I/II/III/III-IV/IV]	0/2/19/7/7
Ischemic cardiopathy (IC) [%]	8 [23%]
Dilated cardiopathy (DC) [%]	19 [54%]
Other cardiopathies [%]	8 [23%]
Hypertension [%]	9 [26%]
Diabetes mellitus [%]	4 [11%]
Left ventricular ejection fraction (LVEF), %	18.4±1.4
Left ventricle end-systolic diameter (LVESD), mm	58.16±2.5
Left ventricle end-diastolic diameter (LVEDD), mm	67.3±3.2
Pulmonary systolic arterial pressure, mmHg	53.4±2.8
Pulmonary diastolic arterial pressure, mmHg	30.4±1.7
Pulmonary capillary pressure, mmHg	29.7±1.6
Pulmonary vascular resistence, U Wood	3.07±0.31
NT-ProBNP, pg/ml	8773±2340
Bilirubin, mg/dL	1.25±0.133
GOT, UI/L	50.1±14.5
GTP, UI/L	63.3±22.7
Dopamine, noradrenaline, dobutamine [%]	11 [31.4%]
Angiotensin converting enzyme inhibitors [%]	23 [66%]
Carvedilol [%]	17 [49%]
Amiodarone [%]	6 [17%]
Furosemide [%]	30 [86%]
Spironolactone [%]	23 [66%]
Digoxin [%]	9 [26%]

M/F = male/female
Quantitative variables are expressed as the mean ± SEM.
Categorical variables are expressed as absolute value and percentage [%]

B) Gene and protein expression of NT-3, TrkC and β-AR subtypes in LV from heart failure patients

A significant increase in the mRNA levels of NT-3 and TrkC was observed in LV from HF patients compared to controls (Figure 27A and B, respectively).

NT-3 and TrkC protein expression levels determined by Western blot are shown in Figure 27. Two forms of NT-3, at 20 and 25 kDa, were detected in LV. Densitometry analysis show that there is a significant increase in the 25 kDa band in LV from HF patients compared to human controls, whereas non changes were detected in the 20 kDa band (Figure 27F, H). In addition, a significant increase in the TrkC protein, detected at 50 KDa and about 110 kDa, is found in LV from HF patient *vs* controls (Figure 27G, I). The increased NT-3 (25 kDa) and TrkC protein expression in LV from HF patients reproduces the observed changes in mRNA levels.

β-AR subtypes gene expression was also analysed and the results obtained show a significant decrease in β_1-AR subtype expression in LV from HF patients compared to controls, whereas β_2- and β_3-AR expression slightly increased; nevertheless, the differences were not significant (Figure 27C, D, E)

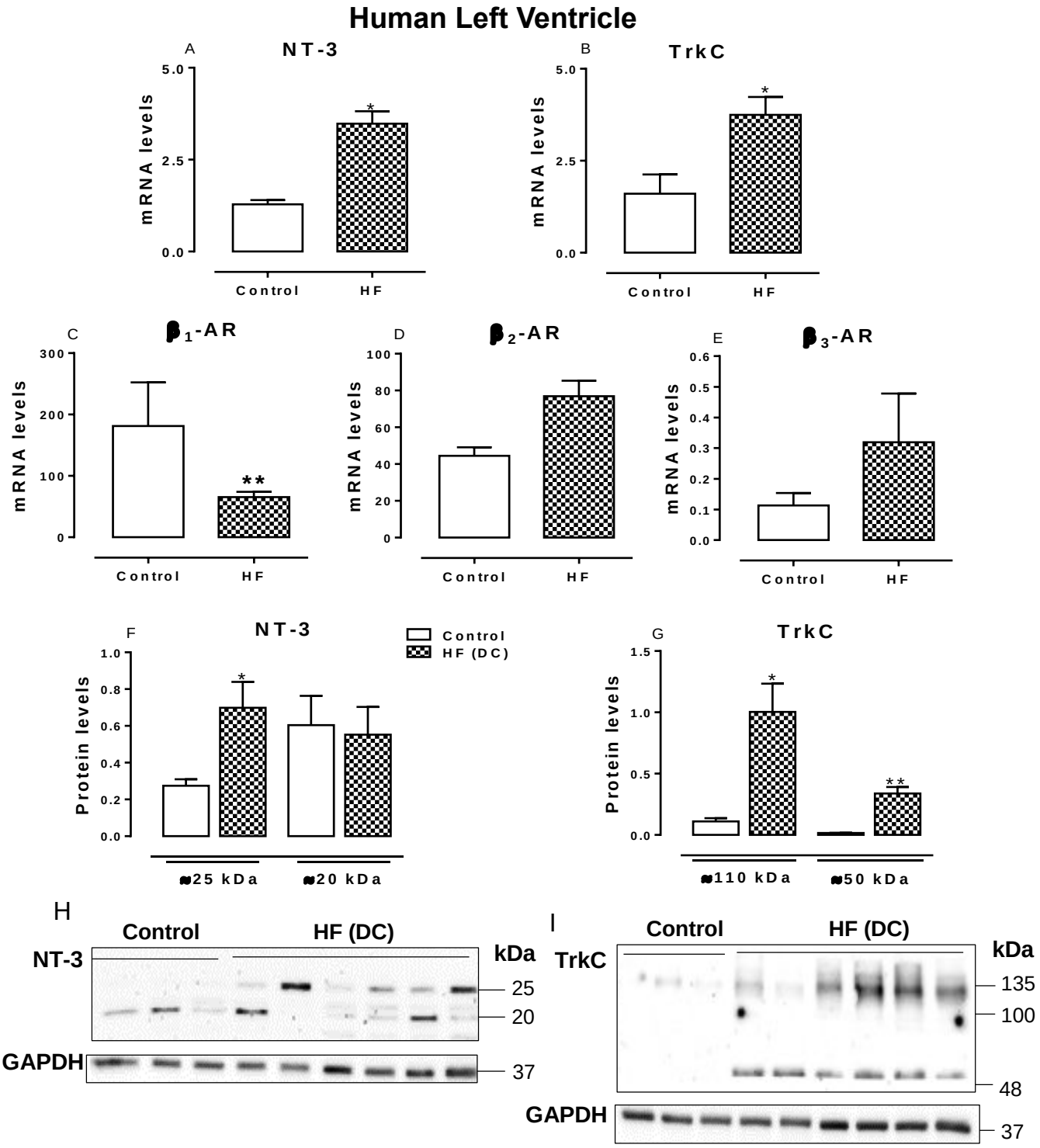

Figure 27. Changes in the NT-3, TrkC and β_3-ARs gene expression in left ventricle from heart failure patients. *mRNA levels of NTF3 (NT-3; n= 39) (A) and NTRK3 (TrkC; n= 14) (B), ADRB1 (β_1-AR; n= 41) (C), ADRB2 (β_2-AR; n= 40), (D); ADRB3 (β_3-AR; n= 34) (E) in left ventricle (LV) from failing hearts compared to controls (n=4). Values are expressed as $2^{-\Delta Ct}$ $X10^4$ using GAPDH as housekeeping gene. Relative protein quantification of NT3/GAPDH (F) around 20 and 25 kDa, and TRKC/GAPDH (G) around 50 and 110 kDa, in dilated cardiomyopathy (DC) patients (n=6) compared to controls (n=3). Representative immunoblots of NT-3 (H) and TrkC (I). Data represent the mean ± SEM. *p<0.05, **p<0.01 vs control patients. Student's t-test for unpaired samples.*

C) Correlation among the mRNA expression levels of NT-3, TrkC and β-AR subtypes in LV from human heart failure

Pearson's correlation tests were performed to establish statistical association between the gene expression levels of TrkC or β-AR subtypes and those of NT-3 obtained in the LV from HF patients. As shown in Figure 28, a significant and positive correlation between mRNA levels of NT-3 and TrkC (Figure 28A) as well as among mRNA levels of NT-3 and β_1-, β_2- or β_3-ARs (Figure 28B, C and D, respectively) was observed.

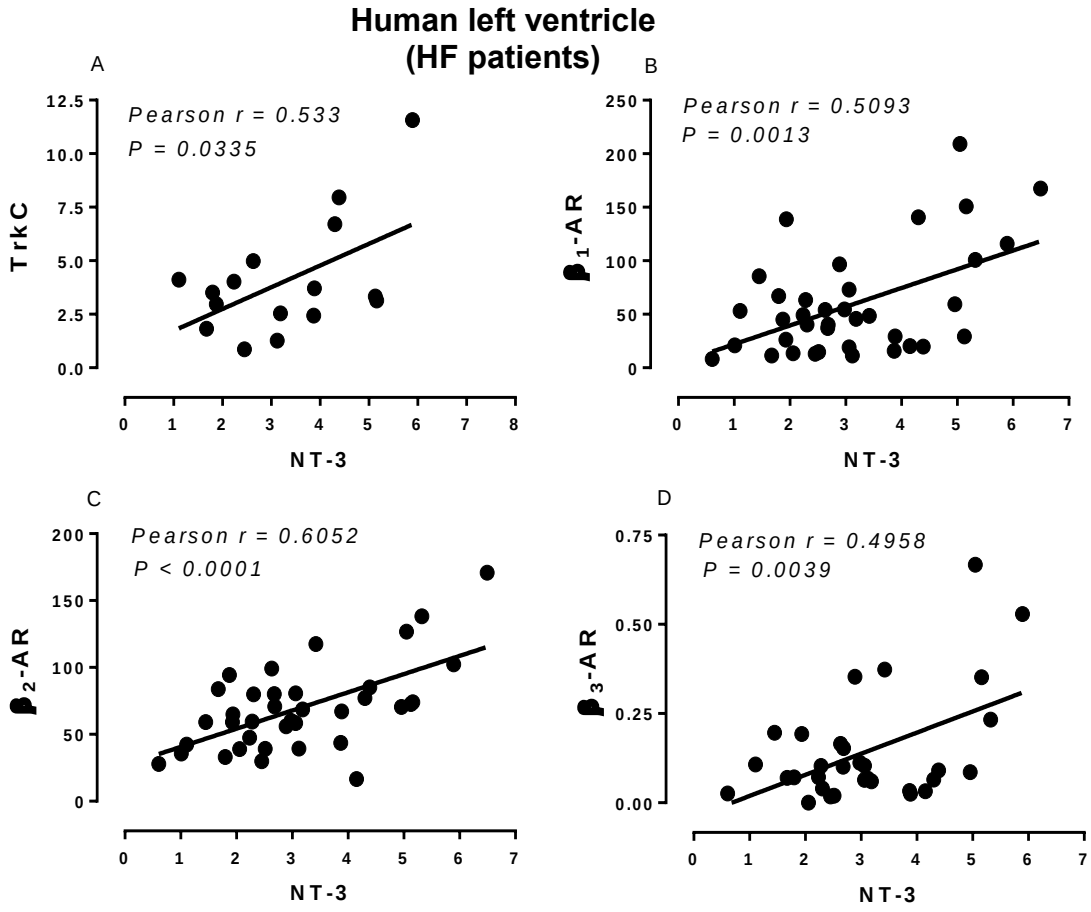

Figure 28. *Graphical representation of the correlation between the mRNA levels of NTF3 (NT-3) and NTRK3 (TrkC) (A) and, NTF3 (NT-3) and ADRB subtypes: ADRB1 (β_1-AR) (B), ADRB2 (β_2-AR) (C), ADRB3 (β_3-AR) (D) in the left ventricle (LV) of explanted failing hearts. Line fits were generated using linear regression.*

D) Comparative analysis of gene expression levels of NT-3 and TrkC in LV from heart failure patients depending on gender and hypertension and correlation of NT-3 expression levels with clinical variables

Firstly, we demonstrated that the changes in gene expression of NT-3 and TrkC observed in LV from HF patients do not depend on gender. Therefore, similar mRNA values of both genes were obtained in LV from HF woman or men (Figure 29A and B).

Since a group of HF patients are hypertensive, we also analysed the influence of hypertension in NT-3 and TrkC expression. As shown in the Figure 29C and D, there were no significant differences in the gene expression levels between patients with HF who were hypertensive with respect those who were not (control).

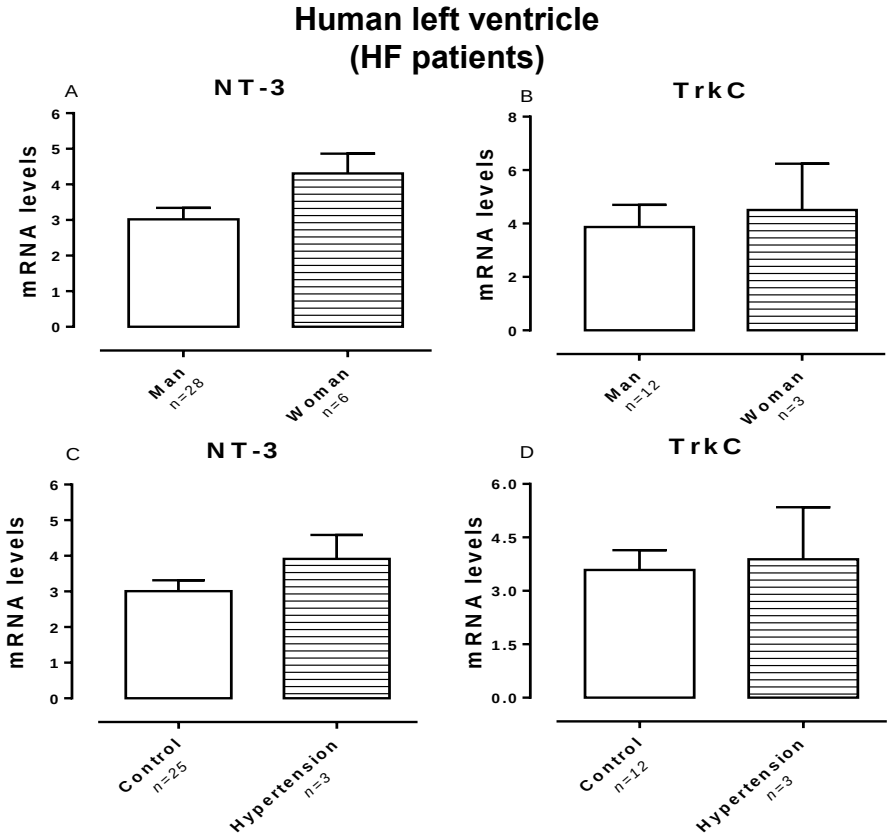

Figure 29. Comparison of NT-3 and TrkC gene expression in LV from heart failure (HF) patients depending on gender or hypertension. *mRNA levels of NTF3 (NT-3) (A and C) and NTRK3 (TrkC) (B and D) obtained in LV from heart failure patients distributed according to gender (A and B) or hypertension (C and D). Values are expressed as* $2^{-\Delta Ct}$ $x10^4$ *using GAPDH as housekeeping gene and represent the mean ± SEM of n patients.*

Furthermore, Pearson's correlation evidenced a significant and positive association between the mRNA levels of NT-3 and LVEF of HF patients (Figure 30A). However, the NT-3 gene expression levels significantly and inversely correlated with BMI (Figure 30B).

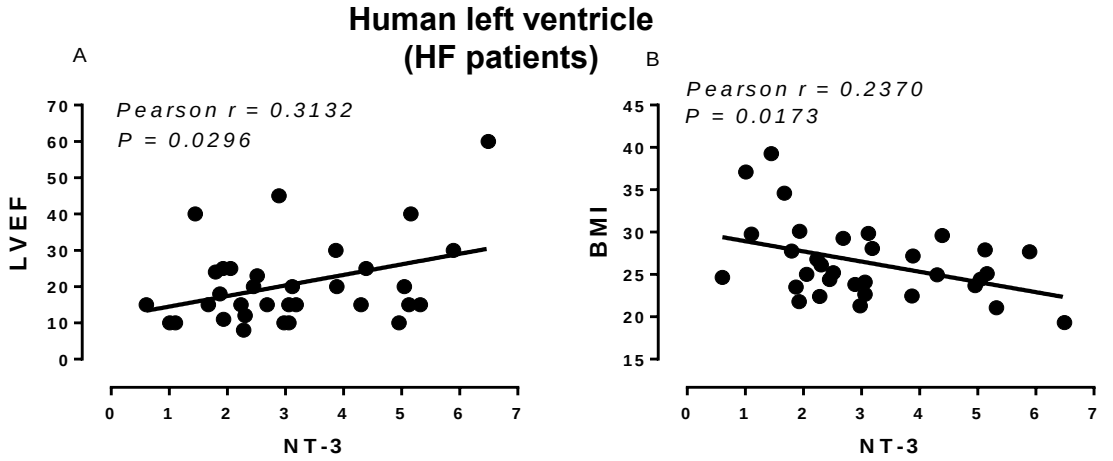

Figure 30. *Graphical representation of the correlation between the mRNA levels of NTF3 (NT-3) in the left ventricle of explanted failing hearts and left ventricular ejection fraction (LVEF) (A) or BMI (B) of the heart failure patients. Line fits were generated using linear regression.*

No significant correlations were found among mRNA levels of NT-3 and other clinical variables as LVESD, LVEDD, pulmonary systolic arterial pressure, pulmonary diastolic arterial pressure, pulmonary capillary pressure and pulmonary vascular resistence. Neither was observed an association between mRNA levels of NT-3 and GOT or GTP levels.

E) Effect of pharmacological treatments of heart failure patients on the expression levels of NT-3 and TrkC

To asses if the different pharmacological treatments could affect the gene expression levels of NT-3 and TrkC in LV from heart failure patients, we have performed a comparative analysis of the expression levels of both genes between the subgroups of patients receiving or not each of the different treatment. The results obtained were shown in Figure 31.

In the group of HF patients treated with the α_1/β-AR antagonist, carvedilol, a significant decrease of NT-3 expression levels was observed (Figure 31A). In addition, in this group of patients, a slight decrease (not significant) was also detected in TrkC expression levels. (Figure 31B). The treatment with ACE

inhibitors (Figure 31C and D), spironolactone (Figure 31E and F) or dobutamine (Figure 31G and H) did not significantly modify the mRNA levels of NT-3 or TrkC.

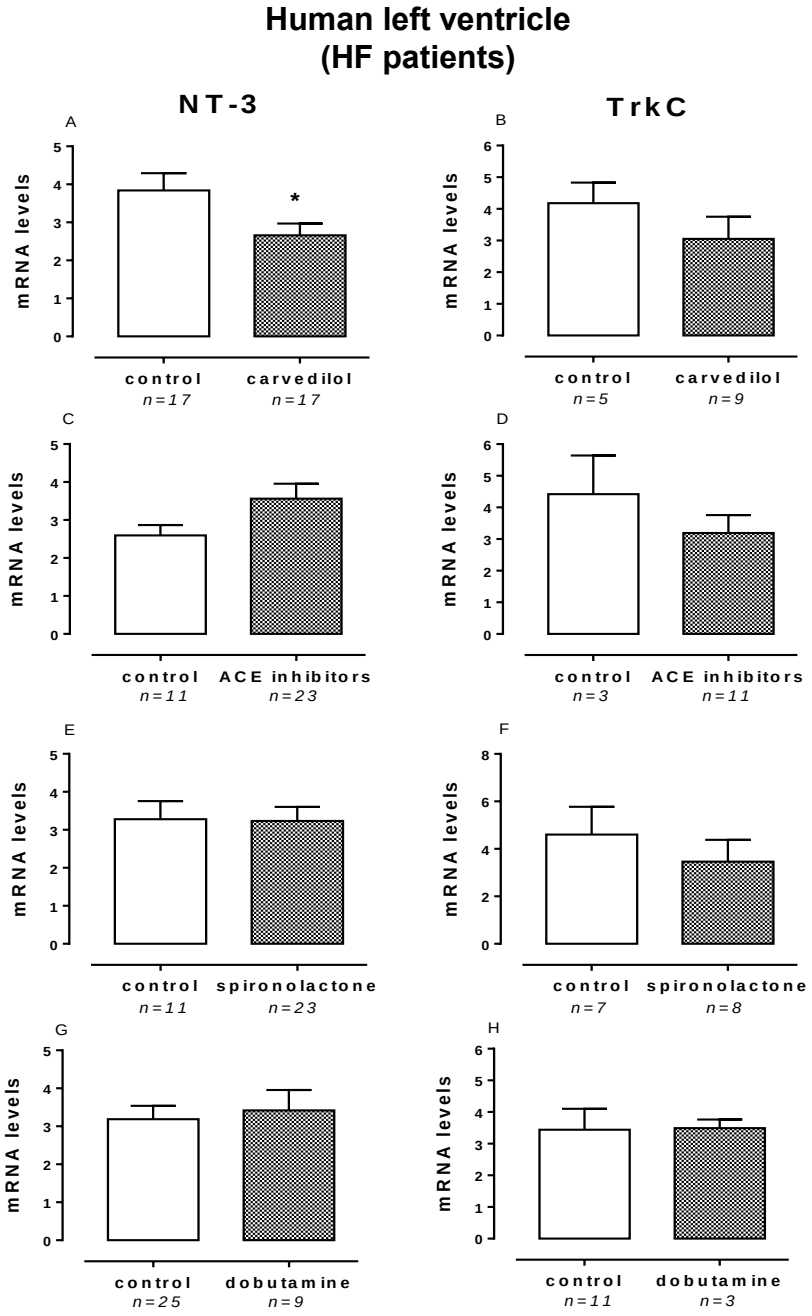

Figure 31. Comparison of NT-3 and TrkC gene expression in left ventricle (LV) from heart failure patients depending on the pharmacological treatment. *mRNA levels of NTF3 (NT-3) (A, C, E, G) and NTRK3 (TrkC) (B, D, F and H) obtained in LV from heart failure patients distributed according to the treatment with carvedilol (A and B), ACE inhibitors (C and D), spironolactone (E and F), and dobutamine (G and H). Control: patients without each of the different treatment analysed. Values are expressed as* $2^{-\Delta Ct}$ *x* 10^4 *using GAPDH as housekeeping gene and represent the mean ± SEM of n patients. *p<0.05 vs control. Student's t-test for unpaired samples.*

5.2 ANALYSIS OF NT-3/TRKC PATHWAY IN DIFFERENT MODELS OF HYPERTENSIVE RATS

We analysed changes in the NT-3 and TrkC gene and protein expression in two models of hypertensive animals: genetically induced hypertension (spontaneously hypertensive rats; SHR) and hypertension induced by endothelial dysfunction after chronic L-NAME treatment (L-NAME-induced hypertensive rats: LNAME-HR) as described in *Methods (1.2.1.1)* section.

Firstly, systolic blood pressure (BP) was measured in SHR and LNAME hypertensive animals (LNAME-HR) and compared to its respective controls (Wistar Kyoto rats, WKY, or Wistar rats) using the tail-cuff method. As expected, the results obtained show an increase in BP in both groups of hypertensive animals compared to controls (Table 17)

Table 17. Systolic blood pressure determined in the two models of hypertensive rats

Rat	BP (mmHg)	n
Control (WKY)	135.4 ± 2.8	4
SHR	213.45 ± 5.5***	4
Control (Wistar)	107.8 ± 1.5	9
LNAME-HR	188.1 ± 3.1***	24

BP: Systolic blood pressure
WKY: Wistar Kyoto Rats
SHR: Spontaneously Hypertensive Rat
LNAME-HR: L-NAME-induced hypertensive rats
****p<0.001 vs control. Student's t-test for unpaired samples.*

A) Spontaneously hypertensive rats

Figure 32 (A and B) shows the mRNA levels of NT3 and TrkC in LV from SHR and its controls (Wistar Kyoto rats, WKY) and it can be seen that similar expression levels were obtained in SHR compared with WKY, for NT-3 and TrkC.

Similar results were obtained when the protein levels were analysed by western blot in SHR and WKY. No significant changes were observed in protein NT-3 expression (bands at 30 and 20kDa) (Figure 32C and E) nor in TrkC expression, detected as a band at 50 kDa, between strains (Figure 32D and F).

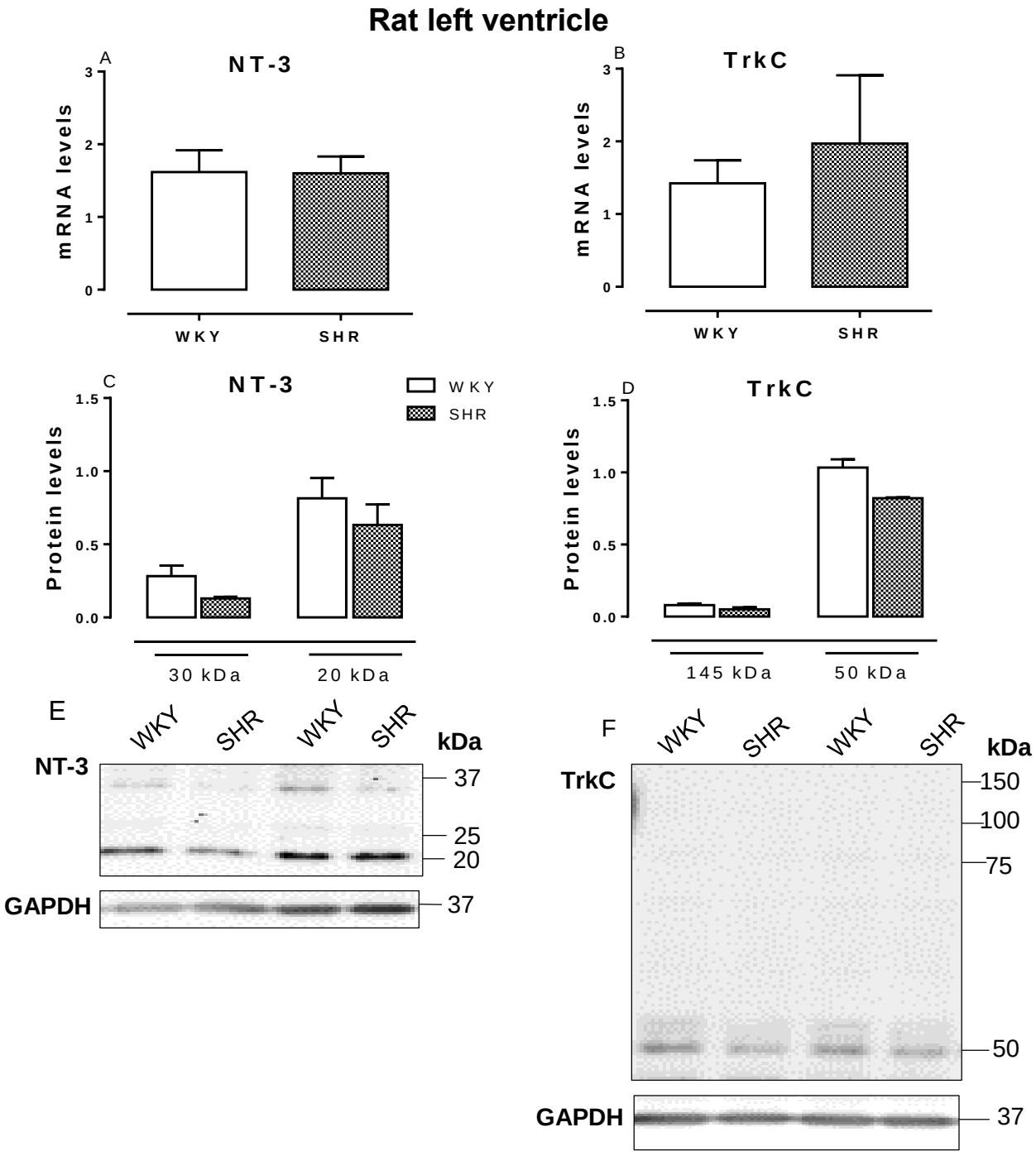

Figure 32. Gene and protein expression of NT-3 and TrkC in hypertensive rats*. mRNA levels of Ntf3 (NT-3; n=5) (A) and Ntrk3 (TrkC, n=3) (B) and relative protein quantification of NT-3 /GAPDH (n=2; C) and TrkC/GAPDH (n=2; D) in left ventricle (LV) obtained from spontaneously hypertensive rats (SHR) and their controls WKY. Representative immunoblots of NT-3 (E) and TrkC (F). mRNA values are expressed as* $2^{-\Delta Ct}$ $X10^4$ *using Gapdh as housekeeping gene. Data represent the mean ± SEM of n different animals.*

B) L-NAME-induced hypertensive rats

In this model of hypertension, we also observed similar levels of NT-3 gene expression in LV from hypertensive (LNAME-HR) and normotensive rats (control) (Figure 33A). However, a significantly increase in TrkC expression was found in LV from LNAME-HR *vs* normotensive animals (Figure 33B).

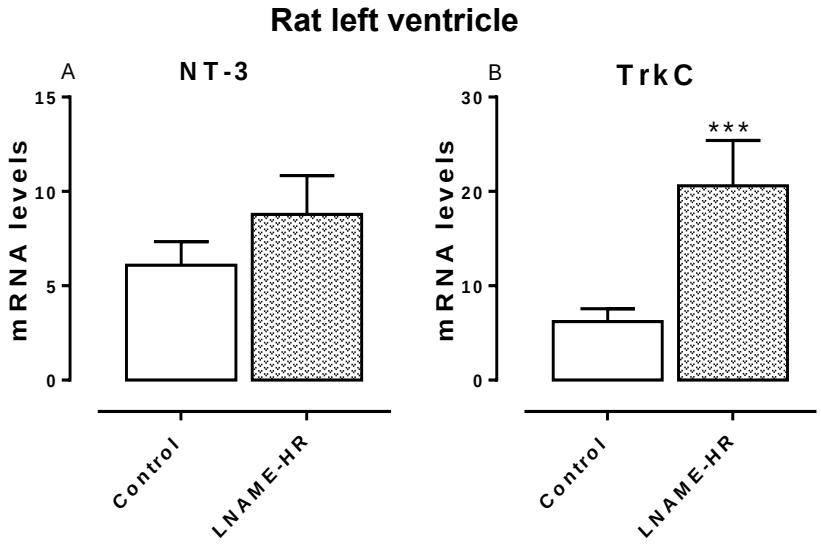

Figure 33. ***Changes on NT-3 and TrkC gene expression levels in L-NAME-induced hypertensive rats.*** *mRNA levels of Nt3 (NT-3; A) and Ntrk3 (TrkC; B) in left ventricle (LV) obtained from L-NAME-treated rats (LNAME-HR; n=6-9) and their controls (Wistar rats; n=17-26). Data represent the mean ± SEM of n different animals. ***p<0.001 vs control. Student`s t test for unpaired samples.*

5.3 ANALYSIS OF NT-3/ TRKC PATHWAY IN A RAT MODEL OF OBESITY

Since we found a significant negative correlation between NT-3 gene expression in the LV of heart failure patients and BMI, we also analysed if this occurs in Zucker obese rats, a characteristic model of rat genetic obesity.

The body weight was measured in obese Zucker rats and their lean littermates; a significant increase of body weight ($p<0.01$) was observed in Zucker rats (612.3 ± 36.22g; *n=3*) compared to their controls (455.2 ± 8.67g; *n=5*).

A robust significant decrease in the expression of NT-3 in kidney was observed in obese Zucker rats compared to the control lean rats. In LV, NT-3 mRNA

expression also diminished, but did not reach statistical significance. mRNA expression levels of TrkC were similar between control and obese rats in LV but significantly increased in kidney of obese rats (Figure 34A and B).

To study if there is a parallelism between NT-3 and β_3-AR gene expressions, the mRNA expression levels of β-AR subtypes were also determined. The results obtained show that there is a decrease in mRNA levels of β_3-AR in LV and kidney from obese rats respect to controls that was significant in kidney. No change in β_1- and β_2-AR subtype expression was found in LV neither kidney.

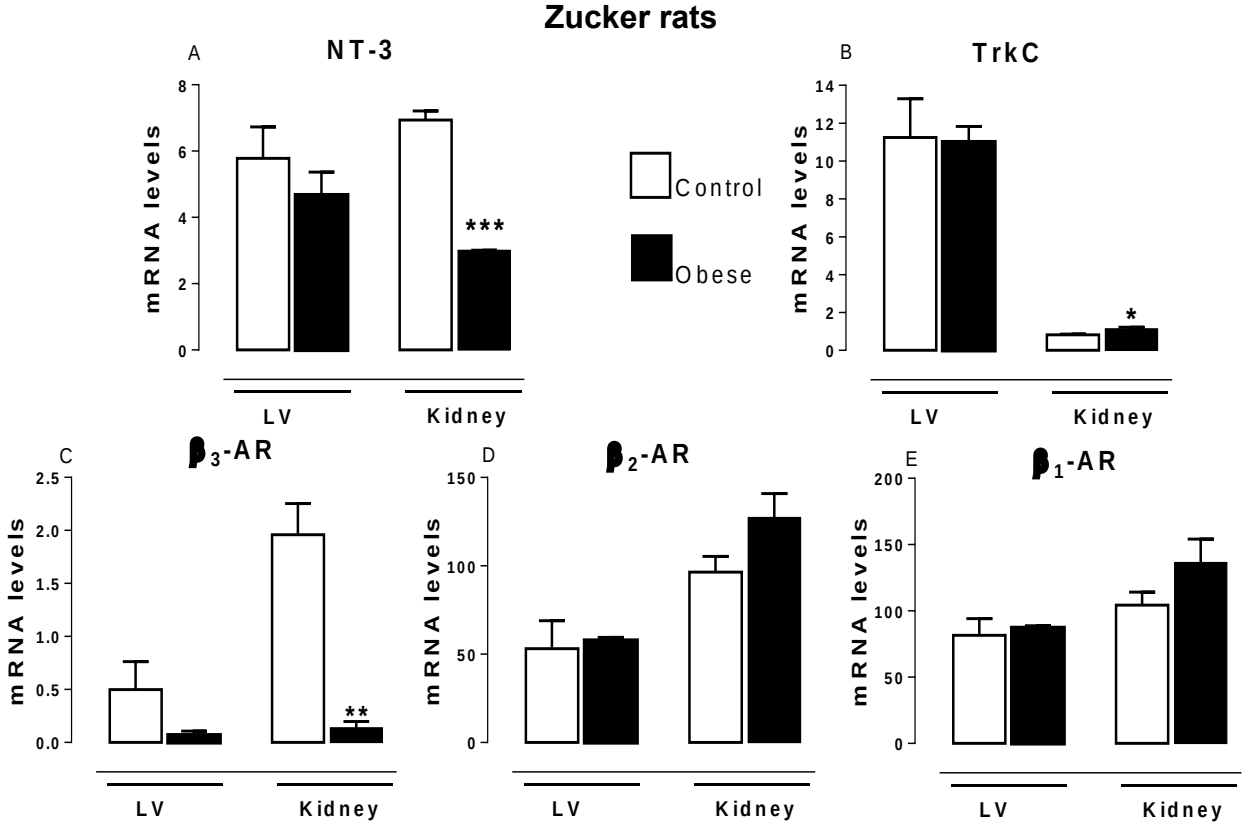

Figure 34. ***Decreased genic expression of NT-3 and β₃-ARs in obese Zucker rats****. mRNA levels of Ntf3 (NT-3; A), Ntrk3 (TrkC; B), Adrb3 (β₃-AR; C), Adrb2 (β₂-AR; D), and Adrb1 (β₁-AR; E) in left ventricle (LV; n=5-3) and kidney (n=3) obtained from obese and lean Zucker rats (control). Data represent the mean ± SEM of n different animals. *p<0.05, **p<0.01, ***p<0.001 vs control. Student`s t test for unpaired samples.*

V DISCUSSION

NT-3, encoded by the *NTf3* gene, intervenes on the development and maturation of the nervous system including neural differentiation, growth of neural extensions, neuronal survival, programmed cell death, and control of synaptic transmission (Zhou & Rush, 1996). NT-3 exerts these actions by binding to the low-affinity p75 neurotrophin receptor ($p75^{NTR}$) and, more selectively, to the high affinity tropomyosin-related kinase receptor C (TrkC) (Tessarollo et al., 1997).

Although NT-3 action was clasically studied in the nervous system, initial studies on the phenotype of *Ntf3* mutant mice demonstrated that this NT was also involved in cardiac development (Donovan et al., 1996). The best-known activity of NT-3 is related to their ability to modulate development and neuronal survival of sympathetic neurons during embryonic development (Fariñas et al., 1994; Francis et al., 1999; Zhou & Rush, 1995) but genetic deletion of NT-3 or TrkC results in impaired cardiac morphogenesis (Donovan et al., 1996; Tessarollo et al., 1997). In the same way, overexpression of a dominant negative version of TrkC also leads to development of cardiovascular abnormalities (Palko et al., 1999). The fact that some of these cardiac alterations appear before the onset of cardiac innervation in mice suggests a direct action of NT-3 on cardiac morphogenesis, independent of its action on neuronal development (Tessarollo, 1998). It is remarkable that NT-3 expression decreases in the adult central nervous system, being reduced to certain areas (Vigers et al., 2000), whereas NT-3 expression and its main TrkC receptor remains constant in the cardiovascular system from development to maturity (Kawaguchi-Manabe et al., 2007; Scarisbrick et al., 1993). Despite these early findings at cardiovascular level, NT-3 expression in vessels and heart and its potential functions in the context of cardiovascular function have begun to emerge only recently (Caporali & Emanueli 2009; Emanueli et al., 2014).

It has been described that the vascular bed produces large amounts of NT-3 which facilitates the growth of axons. Indeed, NT-3 is expressed in large proportion in regions where there has been growing axons of sympathetic neurons, and in NT-3-deficient mice which have a lower number of sympathetic axons compared to their controls (Howe & Mobley, 2005). It has also been observed that the sympathetic postganglionic neurons extend their axons through

regions of vessels producing NT-3, but it is not known if, in addition, NT-3 can also play a role on the functionality of the vessels or the heart.

NT-3 was expressed in rat aortic rings (Delgado et al., 2014), rat brain ECs (Delgado et al., 2014) and VSMCs (Damon, 2008; Scarisbrick et al., 1993). The NT-3, secreted by VSMCs, modulates the function of sympathetic neurons (Damon, 2008). TrkC has been detected in mouse skeletal muscle ECs (Cristofaro et al., 2010), mouse aortic ECs (Delgado et al., 2014), rat cerebral, and aortic ECs (Takeo et al., 2003), and human pulmonary artery ECs (Meuchel et al., 2011). However, TrkC has not been detected in HUVEC or microvascular ECs (Cristofaro et al., 2010). TrkC is also present in other cells such as rat and human aortic smooth muscle cells (Donovan et al., 1995), and human aortic valve interstitial cells (Yao et al., 2015).

Some recent evidences support a direct role of NT-3 on function and growth of heart and/or vessels: i) NT-3 exerts a hypertrophic action on cardiomyocytes (Kawaguchi-Manabe et al., 2007; Saygili et al., 2010); ii) NT-3 acts as an angiogenic factor and promotes therapeutic neovascularization in a mouse model of limb ischemia (Cristofaro et al., 2010); iii) NT-3 induces NO generation in human pulmonary artery ECs (Meuchel et al., 2011), brain ECs, neural stem cells, and aortic rings from mouse (Delgado et al., 2014) and rat cerebral and aortic ECs (Takeo et al., 2003). However, the potential role of NT-3 as a modulator of cardiovascular function at different levels has not been investigated in detail.

Therefore, the objective of this study was to determine the regions of the cardiovascular system where NT-3 is expressed in greater proportion and study its function at that level

1. EXPRESSION OF NT-3 AND TRKC IN THE CARDIOVASCULAR SYSTEM

We analysed the expression of NT-3 and its receptor TrkC in cardiovascular territories as heart and vessels obtained from human or rodents.

Our results show gene expression of NT-3 and TrkC in LV from donors, and in aortic sections from subjects who had undergone aortic surgery. The elevated

expression of NT-3 in human aorta vs human LV corroborates previous evidences obtained in rodents which indicate that the vascular bed produces large amounts of NT-3 that facilitates the growth of axons (Emanueli et al., 2014). Furthermore, the higher NT-3 expression in aorta was accompanied by an elevated TrkC expression, and TrkC expression in human heart also followed the same pattern of NT-3 expression, being significantly lower than in human aorta. These observations suggest that NT-3 in vessels not only facilitates the neuronal development but also acts locally in an autocrine or paracrine fashion. This may explain why the receptors for NT-3 exhibit a widespread distribution in tissues outside the developing nervous system as occurs in aorta and heart.

The elevated expression of NT-3 and TrkC in vessels supports the idea that NT-3 binds to TrkC to regulate physiological processes in vascular territories from adult humans. Therefore, it could be interesting to determine the cell type that mainly expresses NT-3 and TrkC in this vessel and compare it to what happens in heart. With this purpose, we determine the expression of both genes in primary cultures of different human cellular types as ECs (HAoEC), smooth muscle cells (HAoSMC) and fibroblasts (HAoAF) from human aorta, or cardiomyocites (HCM) and fibroblasts (HCF) from human heart.

NT-3 is expressed in smooth muscle cells of the tunica media of the elastic arteries and, to a lesser extent, in the subendothelial layer, suggesting smooth muscle cells as the source for this NT (Donovan et al., 1995; Ly et al., 2014; Scarisbrick et al., 1993). These results are confirmed in cultures of VSMCs that are able to secrete NTs on a regular basis, modulating the function of postganglionic sympathetic neurons (Damon, 2008; Nemoto et al., 1998). In ECs, NT-3 expression has also been described, but TrkC receptor expression does not appear in all of them: HUVEC and human microvasculature ECs do not express TrkC (Caporali & Emanueli, 2009) but it is present in ECs from mouse skeletal muscle from rat cerebral vessels, or from human pulmonary artery (Cristofaro et al., 2010; Meuchel et al., 2011; Takeo et al., 2003).

Our results indicate that NT-3 and TrkC were expressed in HAoSMC, HAoAF and HAoECs. NT-3 expression was higher in smooth muscle cells and fibroblasts than in ECs, being TrkC expression higher in fibroblasts than the other two cell types.

In human cardiac cell lines, gene expression of NT-3 and TrkC was observed, being TrkC expression higher in cardiomyocytes than fibroblasts.

It is remarkable that the mRNA levels of NT-3 and TrkC in human aortic cells lines were very low compared with expression of these genes in the vessel, suggesting a loss in the expression derived of the isolation of the cells or the culture procedure. This discrepancy could also be explained if we suppose that other aortic cells have the higher expression of both genes, but this hypothesis is not plausible if we consider that the cell types analysed were the most abundant in aorta. This point was more deeply studied by using rodent vessels and will be discussed later.

In rats, previous studies have demonstrated that NT-3 is expressed in the wall of aorta and pulmonary artery of embryonic and postnatal rat as well as in heart (Scarisbrick et al., 1993). The level of NT-3 in vessels is relatively constant from the embryonic to the adult stage (Scarisbrick et al., 1993), whereas the levels of NT-3 and truncated TrkC are detected on cardiac myocyte during the development, but the expression was diminished at later stages (Lin et al., 2000). Most previous studies in rats have found higher levels of NT-3 expression in vessels and a weak NT-3 expression in heart (Maisonpierre et al., 1990; Scarisbrick et al., 1993). However, other authors (Kawaguchi-Manabe et al., 2007) found that NT-3 mRNA is expressed at the same level in aorta and heart, whereas TrkC mRNA is expressed in a higher proportion in heart than in aorta.

To clarify these disparate observations, we analysed NT-3 and TrkC expression in different organs and tissues of adult rats and mice.

In line with previous studies, we also reported endogenous NT-3 in different territories from Wistar rats by mRNA analysis and protein level. We found NT-3 expression in cerebral cortex, conductance (aorta) and distributing (tail) arteries, LV, and kidney from Wistar rats. mRNA levels of NT-3 were higher in aorta and tail artery respect to the other tissues. TrkC mRNA was found in cortex, aorta, and tail artery in a similar level, but was almost undetectable in LV and kidney.

We analysed the protein expression of NT-3 and TrkC in the same tissues by immunoblotting. NT-3 was expressed as a monomeric (15-20 kDa) or dimeric (30-35 kDa) protein which interact with TrkC (Kolbeck et al., 1994; Chung et al.,

2017). In our immunoblot, NT-3 protein migrated as different forms, and the proportion of each form depends on the tissue studied. A band corresponding to 20 kDa (monomer) was mainly expressed in vessels, LV, and kidney, whereas a band at around 30 kDa (dimer) was mainly detected in cerebral cortex. We also found a third band at 60 kDa which was expressed at similar level in the majority of tissues.

The existence of these different bands difficult to establish a correlation between gene and protein expression of NT-3, but in any case, according to Kaisho, et al., (1994), there is no always a good correlation between NT-3 protein and NT-3 mRNA levels in peripheral tissues. Indeed, temporal and spatial differences between mRNA and protein levels for NTs have been reported in the literature (Narisawa-Saito & Nawa, 1996; Nawa et al., 1995), and previous studies (Narisawa-Saito & Nawa, 1996) have demonstrated that NT expression at the mRNA and protein levels is independently regulated during ageing in rats. In particular, NT-3 mRNA levels are reduced with advancing age whereas NT-3 protein levels remain elevated in the aged group.

The TrkC gene locus encodes multiple receptor isoforms and at least three TrkC splice variants exist in humans (Beltaifa et al., 2005) The major variants described are: (i) the full-length, catalytic form of 145–150 kDa, containing a kinase domain that is considered to be the signaling form of the receptor (Elkabes et al., 1995; Menn et al., 2000; Tessarollo et al., 1997; Tsoulfas et al., 1993); (ii) a truncated, non-catalytic form of 50–60 kDa, without the kinase domain (Menn et al., 1998; Shelton et al., 1995); iii) a truncated form of 110 kDa which lack portions of the cytoplasmic domain (Donovan et al., 1995; Tessarollo et al., 1997). These shorter isoforms are expressed at high levels throughout the mature nervous system. Several TrkC protein variants with a wide range of sizes for TrkC isoforms, including an 80, 120 and 150 kDa size (Quartu et al., 2003; Tsoulfas et al., 1993; Valenzuela et al., 1993), with inserts of variable amino acid sequences in one of the protein subdomains and with different biological effects have also been described (Lamballe et al., 1993; Rudge et al., 1994; Tsoulfas et al., 1993; 1996; Valenzuela et al., 1993).

The main function attributed to the kinase-deficient truncated Trk isoforms is inhibition of the kinase-active receptor isoforms, which is achieved by acting as a

dominant-negative inhibitor of the full-length receptor or by a ligand-sequestering mechanism, which limits the neurotrophic factor available to bind the kinase-active receptor (Huang & Reichardt, 2001; Tessarollo, 1998) or may recruit ligand (Tsoulfas et al., 1993) and sequester free NT ligands away from the active full-length receptors (Palko et al., 1999). However, the high degree of sequence conservation of the intracellular domains of truncated receptors among species suggests the potential for other functions, such as interaction with cytoplasmic adaptor proteins and activation of signaling pathways (Baxter et al., 1997; Hapner et al., 1998).

More recently, it has become clear that the truncated versions are not just NT sinks, but are also actively signaling molecules (Fenner, 2012) involved in neuronal differentiation and synaptic plasticity (Hapner et al., 1998; Menn et al., 1998). However, compared to their full-length counterparts, relatively little is known about the biological function of the truncated isoforms. For example, NT-3 activates TrkC-full length to maintain motor neuron health and function and TrkC-truncated to produce neurotoxic TNF-α; hence resulting in opposing pathways (Brahimi et al., 2016).

Our results show that TrkC antibody revealed full length (150 kDa) and truncated isoform (110 kDa) of TrkC in cerebral cortex, whereas aorta and tail artery only exhibited 110 kDa truncated isoform, as has been previously shown in rat vascular SMC (Donovan et al., 1995). The LV and kidney were the only tissues that express 50-60 kDa truncated isoform, both territories where the mRNA for TrkC was almost undetectable.

Given the variability in the isoforms described in the literature, the truncated TrkC detected by our antibody in LV and kidney at about 50 kDa may correspond to an isoform with a complete extracellular domain, with a transmembrane domain, and with or without a short cytoplasmic domain that lacks the tyrosine kinase sequence, in which case the protein size would range between 49 and 53 kDa (Beltaifa et al., 2005; Shelton et al., 1995).

Mismatch between protein and mRNA levels detected in LV and kidney, could be reconciled if the steady-state TrkC mRNA and protein have distinct points of

regulation or, if we suppose that the primer probes used to detect mRNA does not amplify the truncated portion of the receptor.

A similar discrepancy in TrkC protein and TrkC mRNA was found at two different time points when was evaluated in human lifespan (Beltaifa et al., 2005). As mentioned above, temporal and spatial differences between mRNA and protein levels for NTs have been reported in the literature (Narisawa-Saito & Nawa, 1996; Nawa et al., 1995). This could be also the reason of the discrepancy exhibited by our results for TrkC in rat tissues.

Taking together, these findings support our hypothesis that vascular territories express NT-3 which effectively function in a paracrine or autocrine manner through TrkC receptor in human and animal models.

2. FUNCTIONAL ROLE OF THE NT-3/TRKC PATHWAY IN VESSELS.

Co-expression of NT-3 and TrkC receptor in vascular cells suggested that NT-3 could act to modulate the activity of vessels. To clarify this point, we analyse the potential role of the NT-3/TrkC pathway in two functional scenarios:

- Since NT-3 is a neuronal growth factor capable of inducing proliferation, and migration of different cellular types (Caporali & Emanueli, 2009), it can act by promoting cell migration and angiogenesis.

- As NT-3 induces a rapid phosphorylation of eNOS an NO release in ECs (Meuchel et al., 2011; Delgado et al., 2014), it can modulate vascular tone.

2.1 NT-3 AS AN ANGIOGENIC FACTOR

Therapeutic neovascularization is an ambitious strategy for improving the prognosis of patients with cardiovascular ischemic disease. The driving force of angiogenesis is hypoxia in the surrounding tissues. Thus, ischemia provides a potent stimulus to angiogenesis and the subsequent development of collateral vasculature in part maintains and revitalizes the ischemic tissue. Sprouting of capillaries from a vessel, leads to an increase of their density improving blood

perfusion of hypoxic tissue which is necessary to maintain or restore local oxygen and nutrition supply.

The differentiation, migration, and organization of ECs into vascular tubes are critical steps in the process of angiogenesis. In fact, migration of vascular ECs is required for tube formation. Previous reports have shown that NT-3 is able to control not only the proliferation and differentiation of neural cells, but also the migration of mesenchymal stem cells (Shen et al., 2013) and marrow stromal cells (Birnbaum et al., 2007). It has been also reported that NT-3, through TrkC activation, stimulates migration of Schwann cells (Yamauchi et al., 2004), and melanoma cells (Truzzi et al., 2008).

The role of NT-3 in blood vessel formation was firstly described by Cristofaro et al (2010) using *in vitro* (cultured mouse skeletal muscle ECs and TrkC transduced HUVEC), and *in vivo* models (overexpression of NT-3 induces neovascularization in a rat mesenteric angiogenesis assay and a mouse model of hind limb ischemia). In the rat mesentery, the newly formed vessels show an enhanced branch point density and diameter compared to the control group, and they also display increased coverage by mural cells. Adenovirus-mediated NT-3 gene transfer to murine ischemic hind limbs stimulates the proliferation of capillary ECs, thus increasing capillary density and promoting blood flow recovery of the ischemic foot (Cristofaro et al., 2010).

NT-3 has also been shown to be an angiogenic factor who promote bone fracture healing and vascularization (Su et al., 2016). Indeed, after a drill-hole injury was made in the tibial growth plate and bone of rats, increased mRNA expression in the injury site was observed for NTs: NGF, BDNF, NT-3, and NT-4 and their Trk receptors. NT-3 and its receptor TrkC showed the highest induction. NT-3 was localized to repairing cells, whereas TrkC was observed in stromal cells, osteoblasts, and blood vessel cells at the injury site. Moreover, systemic NT-3 immunoneutralization reduced bone volume at injury sites and also reduced vascularization at the injured growth plate, whereas recombinant NT-3 treatment promoted bony repair with elevated levels of mRNA for osteogenic markers and bone morphogenetic protein (BMP-2) and increased vascularization and mRNA for VEGF and endothelial cell marker CD31 at the injured growth plate. Consistent with its angiogenic effect *in vivo*, NT-3 promoted angiogenesis in

metatarsal bone explants, an effect abolished by co-treatment with anti-VEGF. This study suggests that NT-3 may be an osteogenic and angiogenic factor upstream of BMP-2 and VEGF with a possible application in bone repair.

Therefore, to analyse the possible role of NT-3/TrkC in angiogenesis, we first studied the migration process using the scratch assay in three different types of ECs from human aorta (HAoEC), coronary artery (HCAEC), and coronary microvasculature (HCMEC).

The scratch assay was set up in our laboratory because is a straightforward, easy, and rapid method to study cell migration (Subalakshmi et al., 2014). In this Thesis, we established the adequate experimental conditions following the experimental protocol described by Chen (2011), but introducing little modifications to optimize the procedure.

In line with previous studies using this technique, serum starvation procedure was an important question to avoid that cell proliferation would introduce a confounding factor during the migration process (Chen, 2013; Guo et al, 2014; Murohara et al., 1999) . However, serum starvation could have dramatic consequences depending on the EC type. Aortic and coronary human ECs maintain their integrity after a serum starvation period of 12h before and during the migration assay but this did not occur with ECs from human coronary microvasculature. For this reason, we assayed different procedures in HAoECs, described in the methods section, and choose the protocol that ensures the best conditions to preserve cellular integrity in the three cell lines together to avoid cell detachment and harm underlying edges but at the same time, to avoid cell proliferation. According to these objectives, we do not perform a previous period of serum starvation but eliminate serum during the scratch assay of aortic and coronary ECs and add 0,5% FBS in the medium of ECs from coronary microvasculature.

The incubation time is another key aspect on cell migration to avoid cellular stress (Tremel et al., 2009). To optimize the experimental conditions, we measured migration at different times after scratching cells, therefore the optimal time to determine migration in the three EC lines was at 8h.

When analysing our results, we can conclude that exogenous NT-3, K252a or NT-3 in presence of K252a did not significantly affect the migration process in any of the three EC lines studied.

To complete these results on ECs migration, we evaluated the *in vitro* proangiogenic capacity of NT-3 in the same cell lines. We performed new experiments by culture of the human EC lines in Matrigel® to promote the formation of tubular structures. The results obtained reproduce that observed in the migration assays, so that none of the EC lines respond with tube formation when incubated with NT-3.

Revascularization of tissues is a complex process, modulated by the collaboration of multiple factors, and the *in vitro* angiogenic model using cultured ECs is very limited to reproduce the physiological conditions. To analyse the influence of the NT-3/TrkC pathway in this complex process, we developed a new experimental approach using the *ex vivo* angiogenic model of isolated aortic rings incubated in Matrigel ® that has been previously introduced by the Nicosia's group (Aplin et al., 2008) and was optimized in our laboratory (Vicente et al., 2016). The *ex vivo* aortic ring model combines advantages of both *in vivo* and *in vitro* assays. Neovessel growth occurs in a defined environment and the culture system can be easily adapted to different conditions (Aplin et al., 2008). The native endothelium of the explants has not been modified by repeated passaged in culture and, supposedly, behaves as EC do *in vivo*, as well as fibroblasts and pericytes, also involved in the process (Aplin et al., 2008; Vicente et al., 2016).

However, using this method, we realize that angiogenic growth, of the isolated aortic rings incubated in Matrigel ®, was not significantly modified by incubation with NT-3, nor K252a or NT-3 after the treatment with K252a.

Previous studies observed that quiescent aortic rings produced neovessels in response to VEGF, but lost their ability to respond to cytokines that were instead angiogenic in cultures of freshly cut explants (Gelati et al., 2008). This change in angiogenic behaviour is correlated with depletion of near complete VEGF production in response to cytokines. Therefore, the lack of a modulatory role for NT-3 in the angiogenic growth of rat aorta, that correlates to the lack of response of human aortic ECs, could be due to a loss of TrkC expression during culture.

At this point, it is interesting to remark that, as previously described, the high expression of NT-3 and TrkC found in human aorta did not correlate with the low level of expression of both genes in isolated human aortic ECs, smooth muscle cells, or fibroblasts. Therefore, to explain the lack of activity of NT-3 in rat aorta, we hypothesize that TrkC expression could be affected by culture conditions.

To test this hypothesis, we prepared quiescent aortic rings and determined the TrkC mRNA levels in this tissue. The results obtained indicate that a significant loss of TrkC expression was observed in quiescent *vs* freshly isolated vessels. The results obtained in rat aortic rings were corroborated by using rat aortic smooth muscle cells and rat cardiac fibroblasts, freshly isolated and until cultured reached confluence. A significant reduction in the expression of NT-3 and TrkC was observed after culture.

This observation explains the low expression of NT-3 and TrkC in human cultured cells, and makes it difficult the *in vitro* study of NT-3 activity.

According to this, the activity of NT-3 on angiogenesis must be confirmed in new and more complex experimental models.

2.2 NT-3 AS MODULATOR OF VASCULAR TONE

There is now some evidence that NT signalling may be important in the control of vascular structure and function (Caporali & Emanueli, 2009; Prakash et al., 2010). NT-3 can induce NO production within 5 min, an effect that was blunted by inhibition of eNOS, Trk or $p75^{NTR}$ receptors (Prakash et al., 2010). In human pulmonary artery rings, this NT induce acute vasodilation that is blunted by removal of the endothelium (Meuchel et al., 2011). Therefore, NT-3 appears to be important in endothelial function and vascular tone in pulmonary vessels. Conversely, alteration in NT signaling may contribute to EC dysfunction in pulmonary circulation (Prakash et al., 2011). However, the importance of such effects in extra-pulmonary vessels has not been examined.

Present work analyses the effect of exogenous NT-3 on vascular tone of rat aorta and tail artery, two vessels representative of conductance (aorta) or distributing (tail artery) vessels. Furthermore, we conducted experimental procedures to

determine the influence of endothelium or the perivascular adipose tissue (PVAT) in the activity of the NT-3/TrkC pathway in vessels.

Influence of endothelium

In isolated aorta, addition of cumulative concentrations of NT-3 elicited a concentration-response curve of vasodilatation that was not observed in de-endothelized vessels or in vessels preincubated with the NOS inhibitor L-NAME. These results in aorta, agree with similar NO-dependent vasodilator activity of NT-3 in pulmonary artery (Meuchel et al., 2010). However, in tail artery, changes in tone were not observed in response to NT-3 addition, nor in vessels incubated with L-NAME. These results show a clear difference in vascular responses to NT-3 depending on the type of vessel, and their dependence of NO-release to modulate the contractile tone. In aorta, a conductance vessel with a high modulation of the contractile response by different NO-dependent mechanisms (Arce et al., 2017), the activity of NT-3 on the endothelium promotes the synthesis and release of NO who induces vasodilatation as occurs with ACH. In tail artery, NT-3 fails to exert any vasodilator activity, as also occurs with ACH.

However, the intervention of Trk receptors in the modulation of vascular tone of aorta or tail artery could be discarded since it was not modified by incubation with K252a. Indeed, the vasodilator response to NT-3 in aorta, or the vasoconstrictor response to phenylephrine in aorta or tail artery, were not modified by pre-incubation with the Trk inhibitor which indicates that exogenous NT-3 or endogenous NTs does not activate these receptors to modulate vascular tone.

Influence of perivascular adipose tissue

PVAT was routinely removed in vessel contractility studies. However, the growing prevalence of obesity, and the realization that adipose tissue acts as a complex paracrine and endocrine organ (Ahima & Flier, 2000; Gustafson et al., 2007) have drawn attention to a functional role for PVAT, which might also provide a mechanistic link between obesity and vascular dysfunction (Ramirez et al., 2017). PVAT is now recognized as a specialized fat depot that surrounds most blood vessels, releasing diffusible factors that modulate local vascular reactivity and inflammatory status and, as a result, may contribute to the pathophysiological

changes seen in cardiovascular diseases, diabetes and obesity (Ramirez et al., 2017).

Indeed, the Framingham Heart Study shows that a higher volume of PVAT around thoracic aorta is associated with metabolic risk factors and a higher prevalence of cardiovascular disease in volunteers (Britton et al., 2012; Lehman et al., 2010).

Previous research has focused on identifying the relaxing factors involved in the modulatory role of PVAT, and on establishing their vascular actions (Gollasch, 2012; Withers et al., 2014). However, there is also evidence that PVAT produces contractile factors, (Gao et al., 2007; Meyer et al., 2013). This adds to the complex scenario of anti-contractile versus pro-contractile properties of PVAT (Ramirez et al., 2017), and makes essential to analyse the influence that PVAT can exerts in the activity of NT-3 to give an accurate picture of the physiological activity of this NT in vessels.

For this reason, we analysed NT-3 activity in aortic rings with or without PVAT, with a previous study of the modulatory role of PVAT in the aortic responses mediated by different agonists with contractile or relaxant activities.

We first studied the influence of PVAT on the sustained contractile response elicited by a depolarizing solution (KCl 80 mM) in rat aorta or a maximal concentration of the α_1-adrenergic agonist phenylephrine, and observe that, in both cases, the contraction obtained in presence of PVAT (+PVAT) was significantly lower than that obtained in vessels deprived of it (-PVAT). The same occurs when a concentration-response curve to phenylephrine was performed in -PVAT or +PVAT aortic rings. In this case, the parameters characteristics of the curve (Emax and pEC50) were significantly decreased in +PVAT rings. Therefore, our data corroborate the existence of a vasorelaxant mechanism mediated by PVAT in rat aorta.

The exact mechanism by which PVAT exerts this effect was the subject of numerous investigations, and what is clear already from organ bath studies is that perivascular adipocytes release transferable relaxing factors as adiponectin, omentin, leptin, Ang 1–7, hydrogen peroxide, hydrogen sulphide and NO (Dubrovska et al., 2004; Gao et al., 2007; Gil-Ortega et al., 2010; Lee et al., 2009;

Payne et al., 2010; Schleifenbaum et al., 2010). Diverse signalling mechanisms have been proposed, including endothelial NO release, cGMP generation, reactive oxygen species and opening of various K^+ channel subtypes (Ramirez et al., 2017). The objective of the present work was not to investigate these mechanisms but to confirm the adequate function of PVAT as a counter-regulator of the contractile responses induced by contractile agonists in rat aorta.

However, it has been proved that PVAT also releases diffusible factors which can induce direct vasocontraction. Much of the evidence comes from contractility studies using isolated arteries with and without PVAT, as present study does.

Adipocytes are known to express a local renin– angiotensin–aldosterone system for the synthesis of the potent vasoconstrictor, Ang II (Cassis et al., 2008; Karlsson et al., 1998) that promotes contractions through the activation of AT1 receptors in rat mesenteric arteries (Lu et al., 2010). Gao and co-workers proposed that Ang II acts indirectly by stimulating superoxide radical production from NADPH oxidase in PVAT adipocytes or the vascular wall itself (Gao et al., 2006; Lu et al., 2008).

A primary mechanism of action for PVAT is to reduce NO production or bioavailability. Given the physical distance between PVAT and the endothelium particularly in conduit arteries, it is thought that mediators released by PVAT are involved. They include NADPH oxidase-derived reactive oxygen species (superoxide and hydrogen peroxide) and pro-inflammatory cytokines (Aghamohammadzadeh et al., 2015; Greenstein et al., 2009; Ketonen et al., 2010; Marchesi et al., 2009; Payne et al., 2010; Vallejo et al., 2011). Importantly, targeting dysregulation of these PVAT factors, which accompanies adipocyte hypertrophy in obesity and metabolic syndrome, can improve endothelial function (Aghamohammadzadeh et al., 2016; Marchesi et al., 2009).

To clarify the vasoconstrictor role of PVAT, we tested its effect on the vasorelaxant activity induced by activation of endothelial NO release mediated by acetylcholine and the vasodilatory response induced by activation of β-ARs.

As has been previously shown by other authors in rat (Lee et al., 2014; Ma et al., 2010) or mouse aorta (Mikolajczyk et al., 2016), rat coronary artery (Aalbaek et al., 2015) and rat and human resistance mesenteric arteries (Vallejo et al., 2011),

our results confirm that PVAT negatively affects the endothelium–dependent relaxation induced by ACH. Additionally, we found that PVAT has a similar inhibitory effect on the vasodilatation induced by isoprenaline, an agonist that acts selectively on β_1 and β_2-ARs or SR58611A, a β_3-adrenoceptor agonist, although in this latter case, the inhibition induced by PVAT did not reach statistical significance.

Curves of relaxation to the selective β_3-AR agonist SR58611A were biphasic and discriminated two populations of β-ARs with a high and low potency, indicating that a mixed population of β_3- (high potency) and β_1-/ β_2-ARs (low potency) play a functional role in the rat aorta. No significant changes in the fraction of high or low potency were observed in PVAT+ vs PVAT- aortic rings.

Taken together, our findings indicate that the balance between vasodilator and vasoconstrictor mediators released by PVAT was favorable for vasodilator mediators since the effect on the contractile responses was more marked than those observed on the vasodilator agents.

It is well known the implication of NO release in the vasodilator activity induced by ACH (Furchgott & Zawadzki, 1980) and β-ARs in vessels (Flacco et al., 2013). Therefore, we can suppose that a mechanism related to an impaired NO release or bioavailability was involved in the lower vasodilatation observed in presence of PVAT. The opposite activity showed by PVAT against vasodilatation mediated by ACH or β-agonists was observed when relaxation was promoted by addition of NT-3, although the differences did not reach statistical significance.

In any case, the relaxant activity of NT-3 in aorta is not remarkable whereas it lacks in tail artery but was more evident in pulmonary artery (Meuchel et al., 2010) indicating that it depends of vessel type. Considering these results, the existence of an abundant expression of NT-3 and TrkC in vessels cannot be always explained by a significant role of this NT on vascular tone and open new questions about the physiological role of NT-3 in vessels. To clarify this point, the next step in our work was to propose a study with a different approach, we analysed the consequences of an NT-3 deficit at the vascular level, and for this purpose, we worked with two models of genetically modified mice.

3. GENETICALLY ENGINEERED MICE AS A TOOL FOR INVESTIGATING THE NT-3 LOCALIZATION AND FUNCTION ON CARDIOVASCULAR SYSTEM

Studies that utilized targeted inactivation of NT-3/TrkC genes focused primarily on the impact of a complete absence of these factors in mice. Early studies have provided evidence for the essential function of NT-3 in cardiac development (Donovan et al., 1996; Tessarollo et al., 1997). Previous findings with NT-3 null mice have reported extensive abnormalities of the great vessels and impaired cardiac morphogenesis (Caporali & Emanueli, 2009; Palko, Coppola, & Tessarollo, 1999; Tessarollo, 1998). NT-3 activation of TrkC is required for the development of the atria, ventricles, and cardiac outflow tracts, so that genetic deletion of either NT-3 or TrkC results in impaired cardiac morphogenesis (Donovan et al., 1996; Emanueli et al., 2014; Tesarollo et al., 1997). The lack of NT-3 leads to cardiac defects similar to tetralogy of Fallot, which resemble some of the most common congenital malformations in humans (Donovan et al., 1996). Overexpression of a dominant negative version of TrkC also leads to development of cardiovascular abnormalities, highlighting its essential role in the adequate cardiac development (Emanueli et al., 2014; Palko et al., 1999). Moreover, NT-3$^{-/-}$ mice develop abnormalities of the great vessels, including developmental delay in the primitive myofibril organization of the truncus arteriosus (Donovan et al., 1996; Tesarollo, 1998). Some of these developmental defects appear before the onset of cardiac innervation in mice, thus suggesting the existence of a direct control of NT-3 on cardiovascular development (Tesarollo, 1998).

A major limitation of this type of study is that mice with total deletion of NT-3 or TrkC die at birth or shortly thereafter due to pleiotropic effects on different organs or a failure to thrive (Story et al., 2000). Therefore, the premature mortality of these mice limits their usefulness for investigating the function of the NT in postnatal mice. For this reason, to evaluate the role of NT-3 in cardiovascular system behaviour, we analysed two different models of genetically engineered mice with partial expression of NT-3:

a) Mice with a targeted mutation in the NT-3 gene, in which the coding region of the *lacZ* gene replaces the coding exon for NT-3 (heterozygous Ntf3+/lacZneo mice, CD1 genetic background, referred to as $NT3^{+/-}$). As has been previously shown (Fariñas et al., 1994, 1996; Delgado et al., 2014) and present results confirm, these mice express reduced levels of NT-3, without changes in the TrkC expression compared to their controls (referred to as $NT3^{+/+}$). This model was useful to localize NT-3 expression by immunohistochemistry, and to determine the consequences of a deficit in NT-3 expression on hemodynamic parameters and functional response of vessels.

b) Mice with deleted expression of NT-3 in the endothelium ($Ntf3^{flox1/lox2}$) (Delgado et al., 2014), obtained by crossing mice carrying loxP sites flanking the *Ntf3* exon ($Ntf3^{flox1/flox2}$; Shimazu et al., 2006) with mice expressing the Cre-recombinase under the control of the endothelium-specific angiopoietin receptor tyrosine kinase receptor-2 (Tie2/Tek) promoter ($Tie2\text{-}cre^{+/0}$; Kisanuki et al., 2001). This resulted in elimination of NT-3 produced by endothelium in blood vessels of $NTf3^{flox1/flox2}$; $Tie2\text{-}cre^{+/0}$ (referred to as $eNT3^{-}$) compared to $NTf3^{flox1/flox2}$; $Tie2\text{-}cre^{0/0}$ mice (referred to as $eNT3^{+}$) with no changes in vasculature overall growth or morphometry (Delgado et al., 2014). This model was useful to determine the importance of endothelial NT-3 on hemodynamic parameters and functional response of vessels.

Localization of NT-3 expression in vascular territories

Analysis of NT-3 expression, as assessed using the *lacZ* reporter inserted in the *NT-3* gene, has indicated that there is a remarkable association between regions of high NT-3 expression and determined areas of the cerebral cortex, but, specially, in vessels as aorta or tail artery, or in the most irrigated regions of peripheral tissues as heart and kidney. The observation, that NT-3 is mainly expressed in vessels from mice, confirms the results in rats and human vessels obtained in the present Thesis as well as the results previously described by other authors (Cristofaro et al., 2010; Damon, 2008; Delgado et al., 2014; Fox & McAdams, 2010; Meuchel et al., 2011; Scarisbrick et al., 1993; Takeo et al., 2003; Yao et al., 2015).

All together present data strongly support our working hypothesis that blood vessels are the major source of NT-3 in peripheral tissues during adult life.

Consequence of deficient expression of NT-3 on anthropometric and hemodynamic parameters

We investigate the consequences of partial ($NT3^{+/-}$) or endothelial ($eNT3^{-}$) deletion of NT-3 in anthropometric parameters and observe that no significant changes were found among body weight, heart weight, or the ratio heart/body weight compared to their respective controls. Therefore, mice with partial or endothelial deletion of NT-3 do not exhibit alterations in heart size, nor symptoms of cardiac hypertrophy. These results confirm previous evidences indicating that heterozygous mice, in which a single copy of the NT3 gene has been inactivated, are visually indistinguishable from wild-type and reproduce well (Story et al., 2000).

According to previous data weights of $NT3^{+/+}$ and $NT3^{+/-}$ mice were equivalent at birth, weaning, and adulthood whereas $NT3^{-/-}$ mice weighed 20% less than the other two genotypes at birth (Story et al., 2000). Delgado et al., (2014) showed no significant differences in body weight of mice with endothelial deletion of NT-3 vs controls, as occurs in the present Thesis.

In the case of hearts from $NT3^{-/-}$ mice, Story et al. (2000) found that they were proportionately smaller in $NT3^{-/-}$ mice that exhibit a lower body weight; however, heart/body weight ratios were equivalent among $NT3^{+/+}$, $NT3^{+/-}$ and $NT3^{-/-}$ mice at birth. Likewise, heart/body weight ratios between $NT3^{+/+}$ and $NT3^{+/-}$ mice were equivalent at weaning and adulthood (Story et al., 2000), and the data obtained by these authors ranged into a similar interval than values obtained in the present work.

The sympathetic nervous system is critical for maintaining both resting and stressed cardiac function based on its dominant role in regulating cardiac inotropism and chronotropism, and the arterial pressure due to its activity on heart and vessels. In a previous study in conscious and unrestrained mice, deletion of a single copy of the NT-3 gene results in a lower resting heart rate as well as a lower sympathetic nerve activity and norepinephrine levels, without changes in arterial pressure (Story et al., 2000). However, it is surprising that blood pressure

was not affected by a lowered heart rate and a decrease in norepinephrine levels and sympathetic tone. For this reason, in the present study, we newly analysed the effect of partial deletion of NT-3 on blood pressure, and complete this study with the same determination in animals with endothelial NT-3 deletion. Our results showed a significant decrease in blood pressure in both genetically engineered strains *vs* their respective controls. These results explain the functional consequences on the hemodynamic parameters of deficient expression of NT-3, but also the importance of the disruption of endothelial expression of NT-3, focusing on the importance of the endothelium as a source of NT-3, then release of NT-3 by ECs could be a new interesting modulatory mechanism of the cardiovascular function.

Consequence of deficient expression of NT-3 on vascular responses to adrenergic stimulus

The next objective of our study was to analyse the influence of deficient expression of NT-3 on the vascular response of mouse aorta to different agents which modulate vascular tone, including agents that induce depolarization as KCl 80 mM, agents that induce endothelial NO release as ACH, or agents that activate AR as phenylephrine or β-AR agonists (Arce et al., 2017).

Changes in the vascular responses related to partial deletion of NT-3 in mice have been yet analysed in a previous work of our laboratory; herein, we analysed the vascular responses in mice without endothelial expression of NT-3 ($eNT3^-$) compared to control mice ($eNT3^+$).

We determined that endothelial deletion of NT-3 does not evoke differences in the contractile responses elicited by a depolarizing solution, or by activation of α_1-AR, then, the contractile machinery as well as the response to vasoconstrictors acting through ARs was not altered in $eNT3^-$ mice. The same occurs when we analysed the concentration-response curves of relaxation to ACH, who promotes endothelial NO release and could be considered as a referent of the endothelial function (Furchgott & Zawadzki, 1980), or the relaxant response to isoprenaline, who acts by activation of β_1- and β_2-ARs (Flacco et al., 2013).

These results indicate that in absence of endothelial expression of NT-3, the endothelial function as well as the capacity of SMC to respond to the opening of

voltage operated calcium channels and the activation of α_1-, β_1- or β_2-ARs, remain intact. Similar results have been previously found in mice with partial deletion of NT-3 ($NT3^{+/-}$ *vs* $NT3^{+/+}$ mice).

However, it is interesting to remark that we have observed significant differences in β_3-AR-mediated relaxation.

As occurred in rat, curves of relaxation to the selective β_3-AR agonist SR58611A were biphasic in mouse aorta and discriminated two populations of β-ARs with a high and low potency, indicating that a mixed population of β_3- (high potency) and β_1-/ β_2-AR (low potency) play a functional role in this vessel. In aortic rings from $eNT3^{-}$ mice, a dramatic decrease in the fraction of the response dependent on β_3–AR activation was observed. These findings are directly in line with previous results in our laboratory where we observed a lack of β_3-AR function in $NT3^{+/-}$ *vs* $NT3^{+/+}$ mice.

Therefore, deficit in NT-3 expression in vessels conducts to an impaired β_3-AR function that could be due to a decreased expression or an altered function of this subtype. Further investigations are needed to clarify this aspect, and to determine the importance of the relationship between NT-3 and β_3-AR, but preliminary data obtained in heart from mice with a partial deficit in NT-3 expression showed a decreased expression of the β_3-AR subtype whereas no changes in the expression of the β_1 and β_2 subtypes were found. This observation needs confirmation in other tissues, especially in vessels, but implies that NT-3 modulates β_3-AR expression in the cardiovascular system and the consequence of this modulation was a functional change associated to a poor β_3-AR response in vessels as aorta, where this subtype is expressed and exerts a vasodilator activity.

The β_3-AR is a novel and intriguing receptor, with multiple functions within the cardiovascular system. This becomes critically crucial in cardiac diseases such as HF, and represents an emerging attractive target for pharmacological modulation in the injured heart.

Importantly, to preserve cardiac output in HF, there is an increase in sympathetic activity and catecholamine release to stimulate β-ARs mediated inotropic capacity. However, chronic exposure of the heart to high levels of catecholamine

can lead to further pathologic changes that include a progressive deterioration of cardiac function and structure (Cannavo & Koch, 2017). Enhancement of β_3-ARs could represent either a protective or a detrimental mechanism that may lead to further deterioration of HF (Cannavo & Koch, 2017). In this regard, the role of this receptor in the heart has been debated for years.

Some reports have suggested that due to its cardiodepressant effect, sustained activation of β_3-AR in HF could contribute to impaired cardiac function whereas the antagonism of this receptor has been proposed as a potential strategy against HF development (Masutani et al., 2013; Moniotte & Balligand, 2002).
However, by contrast with this hypothesis, other studies strongly support the idea that overexpression or persistent activation of β_3-AR is cardio-protective and can attenuate pathological LV hypertrophy acting against the detrimental effects of chronic β-ARs stimulation for its compensatory actions that prevents the effects of excessive catecholamines stimulation on the heart (Belge et al., 2014; Niu et al., 2012). Importantly, as shown in these studies, the activation of NOS and subsequent NO generation represent the main mechanism responsible for β_3-ARs-induced cardio protection (Cannavo & Koch, 2017) Therefore, the β_3-AR represents an emerging attractive target for pharmacological modulation in the injured heart.

As our results show, there is a close relationship between β_3-AR function and NT-3 expression, therefore if this relationship could be confirmed in human cardiovascular system, NT-3 could become an interesting pharmacological target to modulate β_3-ARs function in cardiovascular pathologies. For this reason, our next step was to analyse changes in the expression of β-ARs, NT-3 and TrkC in the human failing heart.

4. CHANGES OF THE NT-3/TRKC PATHWAY IN HUMAN HEART FAILURE AND HYPERTENSION

The role of NT has not been extensively studied in the context of hypertension, atherosclerosis, acute myocardial infarction, HF or cardiac hypertrophy, and little is known about the role for NT-3 and TrkC in cardiovascular diseases.

Human heart failure

Human HF is recognized as a major public health problem arising from multiple causes that will affect one in five adults, conferring elevated mortality rates. Regardless of the cause, multiple organ systems attempt to compensate for the deteriorating heart and the sympathetic nervous system responds to HF with increased activity. Consequently, catecholamines powerfully stimulate the heart function at the expense of over-proportional increases in energy consumption. This is a no rigid signalling system that adapts to continuous stimulation by reducing the abundance of β_1-ARs (Montó et al., 2012). As we have shown in genetically engineered mice, there is a relationship between NT-3 and β_3-AR expression therefore, a question that remains unanswered is the role that the NT-3/TrkC pathway plays in this adaptation.

In this way, in a model of rat HF (salt-sensitive Dhal rats), which presents profound alterations of sympathetic cardiac endings, a correlation was also observed between these alterations and the decreased expression of NT-3 in the heart (Kreusser et al., 2008), confirming the relationship between these parameters.

To study what happens in human HF, we quantified mRNA and protein expression of NT-3 and TrkC, as well as mRNA expression of the β_1, β_2, and β_3–ARs in no failing hearts obtained from donors and in failing hearts from patients with end-stage HF who had undergone a cardiac transplant. The group included patients with dilated cardiomyopathy or ischemic cardiomyopathy and patients with other forms of cardiomyopathy (nonischemic, nondilated). We analysed the functional significance of the changes in the expression by correlating them with the clinical variables related to the cardiac function such as left ventricular ejection fraction (LVEF), left ventricular end-systolic diameter (LVESD), and left ventricular end-diastolic diameter (LVEDD) among others.

Our results show that gene and protein levels of NT-3 and TrkC, are similar in men and women, but significantly increased in the LV of patients with HF compared to non-failing hearts. Moreover, in the failing hearts, a positive correlation exists between mRNA levels of NT-3 and TrkC and a similar correlation was found between the mRNA levels of NT-3 and the three β-ARs.

These correlations indicate that a common mechanism regulated all genes or, more probably, that NT-3 controls the expression of the other four genes. If this is the case, the increase in the expression of NT-3 could exert a control of β_1, β_2, and β_3-ARs expression in the failing heart that partially counteract the dramatic downregulation of the β_1-AR characteristic of the HF (Monto et al., 2012). Our results confirm the lower expression of β_1-AR in the deficient heart, and show that β_2, and β_3 expression did not decrease but slightly increased, although these changes did not reach statistical significance.

Present results provide new data about the role of the NT-3/TrkC pathway in the context of cardiovascular disease. However, they contrast to evidences obtained by other authors as Hiltunen et al., (2001) who have addressed this question and found that NGF mRNA is elevated in the infarcted area following ischemia-reperfusion in rat heart, BDNF mRNA is transiently expressed in myocytes at the border of the infarcted area, while NT-3 mRNA changes little. However, if we consider that in this experimental approach NT-3 levels were immediately determined after the injury, the results could be different to that observed in patients with an advanced stage of HF.

NT-3 strongly increased cardiomyocite size, expression of cardiac hypertrophic markers as well as [3H]-phenylalanine uptake and myofilament reorganization of cardiomyocytes (Kawaguchi-Manabe et al., 2007; Saygili et al., 2010), indicating that NT-3 is a novel cardiac hypertrophic factor that could be involved in the cardiac hypertrophy characteristic of the failing heart. However, NT-3 was downregulated in cardiac hypertrophy induced in rat by pressure overload (*in vivo*), and in cardiomyocyte hypertrophy evoked by endothelin-1 stimulation (*in vitro*) (Kawaguchi-Manabe et al., 2007). The increased expression of NT-3 observed in our group of failing heart patients did not confirm the decrease observed in rats, but could be involved in the cardiac hypertrophy characteristic of HF. According to this hypothesis, NT-3 would play a detrimental role in human HF.

The role of NT-3 has been also analysed after a process of cerebral ischemia, showing a decrease in its expression as well as a protective action when it is exogenously provided (Galvin & Oorschot, 2003; Lindvall et al., 1992; Zhang et al., 1999). This protective role could also be invoked in our group of patients since

there is a direct correlation between NT-3 expression and the LVEF which indicates that higher levels of NT-3 are directly related to a better cardiac functionality.

Considering these paradoxical evidences, we can propose that an initial decrease in NT-3 expression after a cardiac injury (no detected in our advanced HF patients), could be followed by a counteracting mechanism consistent in an increased NT-3 expression to favour tissue and neuronal regeneration. In our patients, with an advanced stage of HF (class III-IV), this cardioprotective mechanism is present.

According to this proposal, we found a significant correlation between NT-3 expression and the LVEF in failing hearts. This correlation, not previously described, suggests that increased NT-3 expression in the left ventricle could be associated with cardioprotection. This beneficial mechanism could be related to a direct activity of NT-3 on cardiac function or, to an indirect action regulating the expression of β_2 and β_3-ARs with beneficial consequences in HF.

A complementary analysis of data gives us information about the influence of pharmacological treatments in the expression of NT-3 and TrkC in human LV. In the group of HF patients, chronic treatment with dobutamine (β_1-AR agonist), spironolactone and ACE inhibitors did not change mRNA levels of NT-3 or TrkC. Only carvedilol treatment significantly decreases NT-3 expression, and this observation deserver further investigation to clarify its role in the clinical benefit of carvedilol treatment in HF.

Human Hypertension

As it has been previously discussed, in genetically engineered mice with partial or endothelial deletion of NT-3 we found lower values of arterial pressure compared to their respective controls. To deepen this finding, we have analysed in the group of HF patients, the influence of hypertension on NT-3 and TrkC expression. Our results show that, in the LV, not significant changes in NT-3 nor TrkC expression were found in hypertensive *vs* normotensive patients.

To our knowledge, no previous studies in human had addressed this question, but Zhang and Rush (2001) have demonstrated increased NT-3 levels in superior

cervical ganglia, heart and mesenteric artery of SHR. The authors propose that the elevated NT3 found in the sympathetic ganglia and hyperinnervated organs of SHR animals could indicate that NT3 may play a role in the development of hyperinnervation, possibly by enhancing the survival and/or nerve sprouting of sympathetic neurons.

Furthermore, our studies with genetically engineered mice showed that partial deletion of NT-3 or repressed NT-3 expression in endothelium conducts to animals with a decreased blood pressure compared to their respective controls.

To clarify the apparent discrepancy observed in our results in human heart and rats, we analysed changes in the gene expression of NT-3 and TrkC in two different hypertensive models: genetically induced hypertension (SHR), the same animal model used in the previous study (Zhang and Rush, 2001), and hypertension induced by endothelial dysfunction (NO depletion after chronic L – NAME treatment) (Oliver et al., 2014).

No significant differences in the cardiac NT-3 and TrkC expression were found in the heart from SHR animals compared with its Wistar-Kyoto controls, which agree with our data in human heart from hypertensive patients, but does not confirm the results previously obtained by Zhang and Rush (2001) respect to NT-3 levels in SHR. A possible explanation for this discrepancy could be the different method used to determine NT-3 expression: qRT-PCR and immunoblot in the present work and ELISA in previous study. Another possible reason for the discrepancy could be the age of animals, 12 weeks in the previous *vs* 20 weeks in the present study, since the NT-3 expression in these rats decreases with age (Maisonpierre et al., 1990; Zhang & Rush, 2001).

In the same way, in the L-NAME induced model of hypertension, similar levels of NT-3 were found in hearts from hypertensive *vs* normotensive animals but, in this case, a significant increase in the TrkC expression was evidenced. The significance of this change deserves further investigation, but could have the same consequences on blood pressure than an increased expression of NT-3.

Taken together, observations in genetically engineered mice permit to establish that NT-3 could play a role in the control of blood pressure, but changes in its cardiac expression are not involved in the elevated arterial pressure observed in

the group of hypertensive HF patients, nor in SHR or L-NAME-induced hypertensive rats.

5. CORRELATION BETWEEN NT-3 EXPRESSION AND BMI IN HUMAN HEART FAILURE

Finally, another interesting result obtained in the present work was the significant and negative correlation found between NT-3 expression in LV of HF patients and BMI.

Previous findings have demonstrated that levels of NGF and BDNF are reduced in patients with metabolic syndrome associated with acute coronary syndromes (Chaldakov et al., 2004; 2009). However, evidence does not exist, until now, for the involvement of NT-3 in cardiometabolic diseases.

Our observation was casual, and did not constitute an initial objective of our study, but merits further attention. Therefore, the next step in our work was to analyse the expression of NT-3 and TrkC in tissues obtained from Zucker rats, the best-known and most widely used rat model of genetic obesity.

Genetically obese animals have been characterized following spontaneously occurring single gene mutations and are widely used as animal models of obesity include the ob/ob mouse, db/db mouse and the Zucker fa/fa rat (Ingalls et al., 1950; Zucker and Zucker, 1961; Coleman, 1978). All three models display hyperphagia, hyperinsulinaemia, and hyperlipidaemia but differ in the degree of hyperglycaemia. Thus, db/db mice have markedly elevated plasma glucose levels and are often used as a model of diabetes whereas ob/ob mice display mild to moderate hyperglycaemia and Zucker fa/fa rats are not hyperglycaemic but are insulin-resistant (Vickers et al., 2011). This monogenetic model of obesity exhibits deficits in the signalling pathways involving the pleiotropic adipokine, leptin. The mutation in Zucker fa/fa rats has marked elevations in circulating leptin but has deficient leptin receptors. As occurs in man, where circulating leptin levels correlate closely with the degree of adiposity (Maffei et al., 1995). For this reason, we have chosen the Zucker rats to analyse changes in the expression of NT-3/TrkC related to obesity.

Our preliminary results obtained in this animal model show markedly decreased expression of NT-3 in kidneys and slightly decreased expression in hearts from obese *vs* non obese Zucker rats. No changes in TrkC expression were found in heart from obese *vs* lean Zucker rats, but a significant increase in the expression of this receptor was found in kidney from obese animals.

This result reaches more interest if we realize that changes in NT-3 expression were mimicked by β_3-AR expression in human and rat tissues, and that a reduction of NT-3 expression was associated with increased BMI.

The β_3-AR mainly exists in white (WAT) and brown (BAT) adipose tissue and it plays roles in lipolysis in WAT and in thermogenesis in BAT (Arch, 2002). Whereas rodent species possess abundant levels of the adipocyte-specific β_3-AR and lesser amounts of the two other subtypes, the reverse is generally the case in humans. Since there is a genetic correlation between the β_3-AR and the states of obesity, hyperinsulinemia, and insulin resistance, much interest has focused on the mechanisms by which a decreased function of the β_3-AR might result in such phenotypes. Already, some reports have demonstrated that β_3-AR agonists have the ability to improve both obesity and insulin resistance in rodent models, with increases in energy expenditure in WAT and BAT (Matsuda et al., 2002; Oana et al., 2005; Okamoto et al., 2000).

Since these early days, many pharmaceutical companies have attempted to develop β_3-AR agonists for the treatment of human obesity, but there is no report that a compound has progressed beyond phase II clinical trials. The fundamental problem is that the β_3-AR is less important as a regulator of energy balance in humans than in rodents (Barbe et al., 1996; Deng et al., 1997; Sennitt et al., 1998) Nevertheless, there is evidence that it plays a significant role in the regulation of energy balance in humans (Arch, 2002). Moreover, recent evidence that there is a significant amount of brown adipose tissue, which expresses the β_3-AR, in many adult humans (Nedergaard et al., 2007) and treatment with β_3-AR agonists may increase the amount and activity of this brown adipose tissue (Arch, 2008), offers new hope about the role of β_3-AR in the control of adipose tissue physiology.

The fact that changes in NT-3 and β_3-AR expression are parallel and related to BMI, opens new possibilities to analyse this relationship in order to look for new therapeutic targets in obesity. In addition, in human heart, a close correlation was also found between NT-3 and the other two adrenoceptor subtypes, β_1 and β_2, who has the main role in controlling human lipolitic activity. Therefore, at present a new study is conducting in our laboratory and its objective is to study the relation that exists between the NT-3/TrkC pathway and β-ARs, specially β_3, in adipose tissue.

VI CONCLUSIONS

1. Human and rodent vascular territories express high levels of NT-3 and its receptor TrkC. Immunoblotting in different rat tissues, detected several isoforms of NT-3 and TrkC and the relative expression of these forms varies depending on the tissue analysed.

2. Exogenous NT-3 did not significantly modify the migration or tubular network formation in different lines of human endothelial cells (aorta, coronary artery and coronary microvasculature), nor the angiogenic process determined in rat aortic rings. The lack of response to NT-3 could be attributed to a loss of TrkC expression during culture.

3. A partial vasodilatory response of exogenous NT-3, which depends on endothelial NO release, has been demonstrated in rat aorta but not in rat tail artery. The inhibitor of Trk receptor, K252a, did not modify the NT-3 mediated vasodilatory response nor the α_1-adrenoceptor induced contractile response, indicating that exogenous or endogenous NT-3 does not act trough TrkC receptors to modulate the vascular tone.

4. Using genetically engineered mice with a reduced expression of NT-3 and mice in which the expression of endothelial NT-3 is suppressed, we found a significant decrease in systolic blood pressure, providing evidence that NT-3 could play a role in the control of arterial blood pressure. However, in a group of hypertensive heart failure patients, or in SHR or L-NAME-induced hypertensive rats, changes in cardiac expression of NT-3 were not observed.

5. Changes in the expression of β_3-adrenoceptors were observed in the cardiovascular system of these models of genetically engineered mice with a partial expression of NT-3 or suppressed NT-3 expression in endothelium. In mouse aorta, this change conducts to a loss of β_3-adrenoceptor-mediated relaxant response

6. In left ventricle from human failing heart, higher gene and protein expression of NT-3 and TrkC was observed, as well as a positive correlation between mRNA levels of NT-3 and the three β-adrenoceptor subtypes, confirming the relationship between NT-3 and β- adrenoceptor observed in genetically engineered mice.

7. In heart failure patients a positive correlation between NT-3 gene expression and left ventricle ejection fraction was observed which evidences a possible cardiovascular protective effect of NT-3 in heart.

8. A significant and negative correlation was observed between NT-3 gene expression in left ventricle of heart failure patients and body mass index. Moreover, reduced NT-3 and β_3-adrenoceptor mRNA levels were found in kidney from obese compared to not obese Zucker rats, showing that changes in NT-3 and β_3-adrenoceptor expression occurs in parallel also in this rat model of obesity. This observation supposes an initial attempt to investigate the relationship between NT-3 and obesity, and opens new possibilities to look for new therapeutic targets in obesity.

VII RESUMEN

INTRODUCCIÓN

Las neurotrofinas (NT) o factores neurotróficos promueven la proliferación, supervivencia y diferenciación de diferentes poblaciones celulares. Esta familia incluye el factor de crecimiento nervioso (NGF), el factor neurotrófico derivado del cerebro (BDNF), la neurotrofina-3 (NT-3) y la neurotrofina-4 (NT-4) (Caporali & Emanueli, 2009; Tessarollo, 1998). Todas las NT son sintetizadas inicialmente en el retículo endoplasmático rugoso como pro-neurotrofinas (Bothwell, 2014; Caporali & Emanueli, 2009).

Las NT se unen a dos tipos de receptores de membrana con diferentes selectividades: la familia de los receptores tirosina cinasa (Trk) y el receptor $p75^{NTR}$ (Longo & Massa, 2013; Zanin et al., 2013; 2016). Los receptores Trk (TrkA, TrkB y TrkC) son glicoproteínas transmembrana de aproximadamente 140 kDa con un dominio tirosina cinasa intracelular (Deinhardt & Chao, 2014).

NT-3 se une selectivamente y con elevada afinidad al receptor TrkC, pero también, con menor afinidad, a los receptores TrkA, TrkB y $p75^{NTR}$ (Donovan et al., 2000; Gibon & Barker, 2017; Ivanov et al., 2013; Longo & Massa, 2013; Tessarollo et al., 1997). NT-3 puede encontrarse en forma de monómeros (21kDa) o dímeros (40kDa). La actividad biológica de los monómeros es hasta 1000 menor, probablemente por una interacción menos eficiente con su receptor TrkC (Chung et al., 2017; Kolbeck et al., 1994). En humanos, TrkC presenta al menos tres isoformas: (i) Una isoforma de 145–150 kDa con glicosilación variable, que corresponde al receptor TrkC completo. Esta isoforma, con actividad catalítica, es responsable de las principales vías de señalización (Elkabes et al., 1995; Menn et al., 2000; Tesarollo et al., 1997; Tsoulfas et al., 1993). (ii) Otra isoforma truncada no catalítica de 50-60 kDa, que carece del dominio tirosina quinasa (Menn et al., 1998; Shelton et al., 1995) y, finalmente, una tercera isoforma truncada de aproximadamente 110 kDa que carece de porciones en el dominio citoplásmico (Donovan et al., 1995; Tesarollo et al., 1997).

La activación de TrkC está mediada por la dimerización, fosforilación y posterior endocitosis del complejo ligando-receptor (Deinhardt & Chao, 2014). Los

receptores Trk activan tres vías de señalización intercelular: (i) vía MAPK/ERK1/2, (ii) vía PI3K/Akt/NO, y (iii) la vía PLCγ1/PKC (Caporali & Emanueli, 2009; Chao, 2003; Longo & Massa, 2013).

NT-3 se expresa de forma abundante en tejidos neuronales durante el desarrollo embionario, pero su expresión disminuye en el adulto (Hohn et al., 1990; Lamballe et al., 1994; Maisonpierre et al., 1990). NT-3 y TrkC también se encuentran ampliamente distribuidos en tejidos periféricos como músculo esquelético, corazón, pulmón, intestino e hígado (Donovan et al., 1995; Gibon & Barker, 2017; Su et al., 2016; Tessarollo et al., 1994; Yano at al., 2009).

En el sistema cardiovascular, la expresión de NT-3 y sus receptores permanece constante desde el desarrollo embrionario hasta la edad adulta, aunque se conoce poco su papel funcional (Scarisbrick y cols., 1993). Así, se ha detectado NT-3 en anillos de aorta de rata, corazón, células endoteliales del cerebro y células del músculo liso vascular (Damon, 2008; Donovan et al., 1995; Kawaguchi-Manabe et al., 2007).

NT-3 y TrkC son puntos clave en la función y el desarrollo de la inervación simpática cardiovascular (Scarisbrick et al., 1999) y en la formación del corazón y los vasos durante la etapa embrionaria (Lin et al., 2000; Saygili et al., 2010; Tesarollo et al.,1993). El déficit de NT-3 durante el desarrollo embrionario conduce a malformaciones cardíacas letales, que imitan las alteraciones características de la tetralogía de Fallot (Donovan y cols., 1996, Meuchel et al., 2011; Werner et al., 2014). La eliminación genética de NT-3 promueve anomalías cardiovasculares graves, como defectos del tabique auricular y ventricular, así como estenosis pulmonar, provocada por déficits en la población de células derivadas de la cresta neural (Donovan et al., 1996; Palko et al., 1999; Srivastava & Olson, 1996). Otros estudios indican que los ratones que sobreexpresan la isoforma truncada de TrkC presentan diversas anomalías cardíacas (Emanueli et al., 2014; Palko y cols., 1999).

En el sistema cardiovascular adulto, la NT-3 sintetizada en los vasos sanguíneos favorece el crecimiento de los axones (Emanuelli et al., 2014), y estudios recientes indican que la NT-3 presente en los tejidos vasculares induce la fosforilación de eNOS presente en las células madre neurales a través de la

activación de TrkC. lo que conduce a la producción de NO (Delgado et al., 2014). Además, NT-3 parece ejercer una acción hipertrófica sobre los cardiomiocitos (Kawaguchi-Manabe et al., 2007; Saygili et al., 2010), promueve la neovascularización terapéutica, como la que se produce en tejido isquémico (Caporali et al., 2012; Cristofaro et al., 2010b; Donovan et al., 1996; Tessarollo et al., 1997) e induce la producción de NO en las células endoteliales de la arteria pulmonar, de aorta y de cerebro (Meuchel et al, 2011).

Las NT y sus receptores no solo están involucradas en la funcionalidad del corazón y los vasos sanguíneos en condiciones fisiológicas, sino también en condiciones patológicas. Múltiples estudios han relacionado cambios en la expresión o actividad de las NT con la patogénesis de varias enfermedades cardiovasculares como el infarto de miocardio (Meloni et al., 2010, 2012), hipertensión (Zhang & Rush, 2001), arteriosclerosis (Donovan et al., 1995; Kraemer et al., 1999), síndrome metabólico Chaldakov et al., 2004; 2009 o insuficiencia cardíaca (Kawaguchi-Manabe, et al, 2007).

OBJETIVOS

Con estos antecedentes, el objetivo de la presente tesis es determinar la expresión de NT-3 y TrkC en el sistema cardiovascular de humanos y roedores, así como el papel de la vía NT-3/TrkC como moduladora de las funciones cardiovasculares y su relación con las enfermedades a este nivel.

Este objetivo general se desarrolla en los siguientes objetivos específicos:

• Determinar la expresión (génica y/o proteica) de NT-3 y TrkC en ventrículo izquierdo, riñón, cerebro y vasos de humanos y/o roedores, así como en líneas celulares humanas de aorta y corazón o cultivos celulares primarios de rata.

• Estudiar el papel de NT-3/TrkC en el proceso de migración en tres líneas celulares endoteliales humanas diferentes: aorta, arteria coronaria y microvasculatura coronaria.

• Analizar el papel de NT-3/TrkC en el proceso angiogénico tanto en modelos *in vitro* en líneas celulares endoteliales humanas, como en modelos *ex vivo* en anillos de aorta aislada de rata.

• Analizar el papel de NT-3 en anillos de aorta y en arteria caudal de rata, y la participación del NO en su mecanismo de acción; determinando la influencia del endotelio o del tejido adiposo perivascular.

• Determinar las consecuencias de los cambios en la expresión de NT-3 a nivel cardiovascular, mediante el uso de ratones genéticamente modificados con expresión parcial o eliminación endotelial de NT-3.

• Analizar los cambios en la expresión de NT-3/TrkC que ocurren en el miocardio de pacientes con insuficiencia cardíaca sometidos a diferentes tratamientos farmacológicos, y en tejidos cardiovasculares de modelos animales con hipertensión u obesidad, para establecer si existe un paralelismo entre éstos últimos y los determinados en patologías humanas.

MATERIAL Y MÉTODOS

Modelos experimentales:

Humanos: Las muestras humanas proceden de pacientes del Servicio de Cardiología del Hospital Universitario “La Fe” (Valencia, España). Los protocolos utilizados fueron aprobados por el Comité Ético de Investigación Clínica de la Universidad de Valencia, así como por el Comité Ético del Hospital La Fe, obteniendo en cada caso el consentimiento informado de los pacientes.

Las muestras de miocardio insuficiente se obtuvieron de pacientes con insuficiencia cardiaca (38 pacientes), sometidos a diferentes tratamientos farmacológicos. Como control se obtuvieron un total de 4 muestras de explantes de corazón, que no pudieron ser aprovechados en trasplante cardiaco, procedentes de donantes sin enfermedad cardiovascular diagnosticada y con un perfil bioquímico dentro de la normalidad. A todos ellos se les determinaron variables antropométricas, hemodinámicas y perfiles bioquímicos en sangre. Inmediatamente tras la extracción del órgano, se deposita en suero fisiológico a 4°C y, tras la obtención de la fracción deseada del ventrículo izquierdo, se congela en nitrógeno líquido y se almacena a -80°C hasta su procesado. La arteria aorta se obtuvo de 4 pacientes sometidos previamente a cirugía aortica.

Ratas de 15-20 semanas: (i) ratas Wistar (250-300g); (ii) ratas Wistar hipertensas por tratamiento con L-NAME (80 mg/kg/día en agua de bebida

durante 4 semanas); (iii) ratas espontáneamente hipertensas (SHR) y sus controles (WKY) y (iv) ratas Zucker obesas (550- 680 g) y sus controles.

Ratones manipulados genéticamente para modificar la vía NT-3/TrkC (Fariñas et al., 1994): (i) ratones en los que se suprime la expresión de NT-3 endotelial (*Ntf3$^{flox\ 1/flox2}$*; *Tie2-cre$^{+/0}$*; **eNT3^{-}**) y sus controles (*Ntf3$^{flox\ 1/flox2}$*; *Tie2-cre$^{0/0}$*; **eNT3^{+}**); (ii) ratones con expresión parcial de NT-3 (*Nft3$^{+/lacZneo}$*; **NT3$^{+/-}$**) y sus controles (*Ntf3$^{+/+}$*; **NT3$^{+/+}$**).

La medida de presión arterial en los animales se realizó por el método no invasivo de medida con pletismógrafo en cola del animal consciente.

El cuidado y tratamiento de los animales se llevó a cabo siguiendo la legislación española recogida en el Real Decreto 53/2013, de 1 de febrero. Además, todos los protocolos utilizados han sido aprobados por el Comité Ético de Experimentación Animal de la Universidad de Valencia. Lo animales fueron anestesiados con isofluorano y sacrificados por dislocación cervical (ratones) o por decapitación (ratas), teniendo en cuenta las recomendaciones para eutanasia de los animales.

Una vez sacrificado el animal se aislaron los tejidos, incluyendo aorta torácica, arteria caudal, corazón, cerebro y riñón. Los tejidos fueron extraídos y puestos en una solución de Krebs. Aquellos que se vayan a utilizar para estudiar expresión génica y/o proteica se almacenan inmediatamente en nitrógeno líquido a -80ºC.

Líneas celulares humanas: células endoteliales de aorta (HAoEC), de arteria coronaria (HCAEC) y de microvasculatura cardiaca (HCMEC); células de musculo liso de aorta (HAoSMC); fibroblastos de aorta (HAoAF); cardiomiocitos (HCM); y fibroblastos de corazón (HCF). Las líneas celulares fueron cultivadas en su medio correspondiente suplementado con suero bovino fetal (5%) y factores de crecimiento (medio completo). En algunos experimentos no se añadió suero bovino fetal ni factores de crecimiento (medio basal) o se añadió 0.5% de suero (medio basal con 0.5% de suero).

Las células crioconservadas se descongelaron siguiendo las instrucciones de la casa comercial (Promocell) y se fueron realizando los subcultivos una vez

alcanzado el 80% de confluencia. Periódicamente se congelaron células en nitrógeno líquido a -80ºC, a diferentes pases, para mantener un stock.

Cultivos primarios de fibroblastos de corazón y células de musculo liso de la aorta de rata. Las células se cultivaron hasta alcanzar aproximadamente un 75% de confluencia (células cultivadas). En otros casos, las células se congelaron inmediatamente después de aislarse del tejido (células frescas).

Protocolos experimentales:

Ensayo de la β-galactosidasa en aorta, caudal, ventrículo izquierdo, riñón y cerebro de ratones en los que el gen NT-3 fue reemplazado por el gen *lacZ*, que codifica la enzima β-galactosidasa integrada en el locus de la NT-3 (*Ntf3*$^{+/lacZneo}$). Los órganos fueron extraídos del animal e inmediatamente incubados en el medio correspondiente durante una hora (vasos) o dos horas para el resto de tejidos. La enzima β-galactosidasa hidroliza β-galactósidos como el X-gal, generando un producto final de color azul intenso. Por tanto, las muestras teñidas de azul indican expresión del gen *lacZ*. Las imágenes fueron obtenidas con un microscopio LEICA.

Cuantificación de la expresión génica y proteica de NT-3, TrkC, adrenoceptores β y GAPDH (control) en tejidos extraídos de animales y/o humanos y en líneas celulares humanas o cultivos celulares primarios de rata.

La cuantificación de la expresión génica, se realizó mediante la reacción en cadena de la polimerasa a tiempo real (qPCR) a partir del RNA total, aislado y purificado de las muestras previamente disueltas en Tripure. A continuación, los mRNA codificantes para cada uno de los genes de interés se cuantificaron mediante la reacción de la transcripción reversa (RT-PCR) utilizando sondas Taqman® y siguiendo los protocolos previamente establecidos en nuestro laboratorio (Monto et al., 2012; Oliver et al., 2010).

La cuantificación de la expresión proteica se realizó mediante Western blot y posterior análisis densitométrico a partir de las muestras homogeneizadas en un tampón de lisis (RIPA) (Monto et al., 2012; Oliver et al., 2010). La concentración de proteínas se determinó previamente por el método Bradford.

Migración celular mediante la puesta a punto en nuestro laboratorio del protocolo del ensayo de herida o "*scratch*" en cultivos de células endoteliales humanas (HAoEC; HCAEC y HCMEC). Las células se sembraron en placas de 24 pocillos y se incubaron hasta confluencia. A continuación, se realizó la herida manualmente rascando la monocapa celular con una punta de pipeta. Previamente se analizaron las condiciones óptimas (concentración de suero y tiempo de migración) para prevenir la proliferación y el daño celular: HAoEC y HCAEC se incubaron en medio basal (sin suero ni factores de crecimiento) después de realizar la herida; mientras que HCMEC se mantuvieron en medio basal suplementado con suero (0,5%). Para estudiar el papel de NT-3 en la migración celular, las células endoteliales se incubaron durante 8h en presencia de DMSO (0.01%; control), NT-3 (32ng/ml), K252a (0.2 μM) o NT-3 + K252a en los medios correspondientes a 37ºC y 5% CO2. La tasa de migración fue analizada midiendo el área de la herida a las 0h y 8h con un microscopio invertido Leica DM IL LED.

Angiogénesis ensayada en dos modelos experimentales: *in vitro* en células endoteliales humanas (HAoEC; HCAEC y HCMEC) y *ex vivo* en aorta aislada de rata según el protocolo establecido en nuestro laboratorio (Vicente et al., 2013), utilizando en ambos casos una matriz tridimensional en Matrigel™.

En estudios *in vitro* las células fueron incubadas en placas de 96 pocillos en condiciones habituales de cultivo (medio completo) durante 18 horas en presencia de los mismos estímulos empleados en el ensayo de migración.

En los ensayos *ex vivo* los anillos de aorta de 1mm de grosor se sembraron embebidos en Matrigel™ y se mantuvieron incubados en medio basal suplementado con suero bovino fetal (5%) durante 7 días en presencia de los estímulos.

Se tomaron fotos del crecimiento de los vasos: número de nuevas estructuras tubulares formadas (ensayos *in vitro* en células) o longitud del crecimiento del vaso (ensayos *ex vivo* en anillos de aorta) utilizando un microscopio Leica.

Ensayo de viabilidad celular mediante el método de MTT descrito por Mossman (1983) para descartar citotoxicidad de los productos ensayados en las condiciones experimentales descritas en ensayos de migración y angiogénesis.

Anillos quiescentes: la aorta aislada de rata se dividió en dos segmentos, uno de ellos fue incubado a 37ºC y 5% CO2 durante 7 días en medio basal (anillo quiescente) y el otro fue congelado inmediatamente a -80ºC (anillo fresco). Los niveles de mRNA de TrkC se analizaron por qPCR en vasos quiescentes y frescos.

Estudios funcionales en baño de órganos en anillos de 4-5 mm de longitud de aorta y/o arteria caudal de rata y ratón. En todos los casos se comprobó la funcionalidad del vaso mediante la contracción con KCl (80 mM) y la integridad del endotelio vascular realizando curvas concentración respuesta (CCR) de relajación con acetilcolina (10nM-100µM) sobre la meseta de contracción inducida por fenilefrina (aorta: 1µM, arteria caudal: 10µM).

Efecto de NT-3 sobre el tono vascular mediante la realización de CCR de relajación de NT-3 (2,4,8,16 and 32 ng/ml) sobre la contracción inducida por concentración única (1µM o 10µM; esquema 1) o CCR (10nM-1µM o 10nM-10µM; esquema 4) de fenilefrina en aorta o arteria caudal, respectivamente. En algunos experimentos se determinó la influencia del endotelio (anillos con o sin endotelio) o la implicación del NO (anillos en presencia o no de L-NAME 100µM) sobre la vasoconstricción inducida por fenilefrina y la vasodilatación mediada por NT-3. En otros casos se realizaron experimentos en presencia o ausencia de un inhibidor de Trk (K252a 0.2 µM) para estudiar la implicación de TrkC en el tono vascular.

Se analizó la influencia del tejido adiposo perivascular (anillos de aorta con o sin tejido adiposo) sobre la vasoconstricción inducida por fenilefrina (10nM-10µM) y la vasodilatación mediada por NT-3 (2,4,8,16 and 32 ng/ml) o por acetilcolina (10nM-100µM), o por los adrenoceptores β, utilizando isoprenalina (1nM-100µM; agonista no-selectivo β_1 y β_2) y un agonista selectivo del subtipo β_3 (SR58611A, 1nM-100µM) (Esquema 4).

Influencia de la inhibición de la expresión de NT-3 endotelial, en ratones modificados genéticamente, sobre el tono vascular siguiendo el protocolo descrito en el esquema 4. Se emplearon anillos de aorta con endotelio de ratones en los que la expresión endotelial de NT-3 fue suprimida (eNT3-) y sus

correspondientes ratones control con niveles normales de expresión de NT-3 (eNT3 +).

Análisis estadístico utilizando el test *t Student* y análisis de varianza (ANOVA) para la comparación de medias múltiples (GraphPad Prism 4.0). Para las correlaciones entre variables analizadas se utilizó el análisis de regresión lineal y se evaluó el coeficiente de correlación de Pearson.

RESULTADOS Y DISCUSIÓN

Expresión de NT-3 y TrkC en el sistema cardiovascular humano y de rata

Se determinó la expresión génica de NT-3 y de su receptor, TrkC en explantes de ventrículo izquierdo de individuos sanos y en aorta de sujetos que fueron sometidos a cirugía. Los resultados obtenidos evidencian expresión génica de NT-3 y TrkC en ambos territorios, siendo mucha mayor en aorta que en el corazón (Figura 1). Resultados previos habían puesto de manifiesto en roedores que el lecho vascular produce cantidades elevadas de NT-3 que facilitan el crecimiento de los axones (Emanueili et al., 2014). Nuestros resultados demuestran también una expresión elevada de TrkC en aorta siendo mucho mayor que en corazón lo que sugiere que la NT-3 puede actuar en los vasos no solo facilitando el desarrollo neuronal, sino también localmente de forma autocrina o paracrina.

Es por ello que nos pareció interesante determinar cuáles son los tipos celulares de estos tejidos que expresan principalmente NT-3 y TrkC y, por tanto, se analizó su expresión génica en diferentes tipos de células humanas aórticas comparándolas con cardiacas. Los resultados obtenidos nos muestran que en las células humanas cardíacas se detectó expresión de NT-3 y TrkC, siendo mayor la expresión de TrkC en cardiomiocitos (HCM) que en fibroblastos (HCF) (Figura 2A y B). En células aórticas humanas se detectó una mayor expresión de NT-3 en células musculares lisas (HAoSMC) y fibroblastos (HAoAF) respecto a la obtenida en células endoteliales (HAoEC), mientras que la expresión de TrkC fue mayor en fibroblastos respecto a los otros dos tipos celulares (Figura 2C y D). Es de destacar el hecho de que los niveles de expresión de NT-3 y TrkC obtenidos en las células aórticas humanas fueron mucho menores que los obtenidos en el tejido entero sugiriendo una pérdida de expresión derivada del

aislamiento de las células o del cultivo de las mismas. Este punto se analizó con más detalle utilizando vasos de ratas y se discutirá más adelante.

Estudios anteriores han puesto en evidencia la expresión de NT-3 y TrkC en aorta y corazón de rata, pero existen discrepancias respecto a los niveles relativos de ambos genes en la edad adulta. Así, algunos autores describen niveles más altos de expresión de NT-3 en vasos respecto al corazón (Scarisbrick et al., 1993) mientras que otros autores describen que NT-3 se expresa al mismo nivel en aorta y corazón y TrkC se expresa en mayor proporción en el corazón que en la aorta (Kawaguchi-Manabe et al., 2007).

Con objeto de aclarar estas discrepancias se realizó un análisis comparativo de la expresión génica y proteica de NT-3 y TrkC en diferentes territorios de ratas Wistar adultas: territorios vasculares representantes de vasos de conductancia (aorta) y de distribución (caudal), así como en ventrículo izquierdo, riñón y córtex cerebral. Los resultados obtenidos muestran que existe una elevada expresión génica de NT-3 en los vasos (aorta y arteria caudal) que fue significativamente mayor que la obtenida en los otros territorios (Figura 3A). Respecto al TrkC se detectaron niveles de expresión elevados y similares en los vasos y cortex cerebral, sin embargo, en corazón y riñón los niveles de expresión fueron muy bajos (Figura 3B).

En cuanto a la expresión proteica se detectaron varias isoformas de NT-3 y TrkC en los diferentes tejidos de rata, observando que la expresión relativa de estas isoformas varía dependiendo del tejido analizado (Figura 4 y 5).

Localización de la expresión de NT-3 en distintos tejidos de ratón

Se utilizaron ratones en los que el gen NT-3 fue reemplazado por el gen *lacZ*, expresando la enzima β-galactosidasa, (*Ntf3*$^{+/lacZneo}$; NT3$^{+/-}$). Se confirmó en estos ratones la disminución de la expresión génica de NT-3 en aorta y ventrículo izquierdo respecto a los ratones control NT3$^{+/+}$. La pérdida de expresión de NT-3 en estos ratones heterocigotos era predecible, pero se demostró además que los niveles de expresión de su receptor TrkC no fueron modificados (Figura 6).

La tinción histoquímica de la β-galactosidasa en los ratones NT3$^{+/-}$ reveló una expresión de NT-3 limitada en determinadas regiones del cerebro adulto

coincidiendo con los resultados descritos por Vigers et al (2000). Es de destacar que se observó una expresión elevada de NT-3 en aorta y arteria caudal, así como en los vasos del cerebro y en la vasculatura de las zonas más irrigadas de tejidos periféricos como corazón y riñón (Figuras 7 y 8).

Estos resultados demuestran la abundante presencia de NT-3 en los vasos sanguíneos de ratones adultos, y confirman los resultados obtenidos en esta Tesis en vasos de rata y humanos, así como los descritos por otros autores (Delgado et al., 2014, Meuchel et al., 2011, Scarisbrick et al., 1993)

Por ello, el siguiente objetivo de la Tesis fue investigar el papel funcional de la vía NT-3/TrkC en vasos.

Papel funcional de la vía NT-3/TrkC en vasos

Se analizó el papel de la NT-3 exógena en dos escenarios funcionales:

A. Estudios preliminares indican que la NT-3 es un factor de crecimiento neuronal capaz de inducir proliferación y migración de diferentes tipos celulares (Caporali & Emanueli, 2009), por lo que podría promover la migración y angiogénesis.

B. NT-3 podría modular el tono vascular ya que se ha descrito que produce una fosforilación de la eNOS con la subsiguiente formación de NO en células endoteliales (Meuchel et al, 2011; Delgado et al., 2014).

A. NT-3 como un factor angiogénico

Se examinó el efecto de la NT-3 exógena en presencia y ausencia del inhibidor del Trk, K252a, en la migración celular y en la formación de nuevos túbulos en diferentes líneas de células endoteliales humanas (aorta, arteria coronaria y microvasculatura coronaria). También se estudió el proceso angiogénico *ex vivo* utilizando anillos aórticos de rata.

NT-3 (32 ng/ml), K252a (0.2 µM) o NT-3 en presencia de K252a no modificaron significativamente la migración (Tabla 2, Figura 11) o la formación de nuevos túbulos (Tabla 3, Figura 12) en las diferentes líneas de células endoteliales humanas ensayadas. Tampoco se observaron cambios en el proceso angiogénico determinado en anillos aórticos de rata (Figura 13).

Sin embargo, resultados previos obtenidos por Cristofano et al. (2010), han descrito un papel pro-angiogénico de la NT-3 recombinante *in vitro* (cultivos de células endoteliales de músculo esquelético de ratón y HUVEC transfectadas con TrkC) y de la transferencia de NT-3 *in vivo* (la sobreexpresión de NT-3 induce una neovascularización utilizando el ensayo de angiogénesis mesénterica de rata).

Teniendo en cuenta la falta de respuesta a la NT-3 en nuestras condiciones experimentales y la disminución drástica en la expresión génica de NT-3 y TrkC en las diferentes líneas celulares humanas de aorta ensayadas (endoteliales, músculo liso y fibroblastos) respecto a la aorta humana, descrita con anterioridad en la presente Tesis, nos hizo pensar que una pérdida del receptor de NT-3 durante el cultivo de las células o la incubación de la aorta podría ser responsable de esta falta de actividad.

Con objeto de confirmar esta hipótesis, se prepararon anillos de aorta de rata Wistar quiescentes y se determinaron los niveles de mRNA de TrkC en este tejido. Los resultados obtenidos muestran una pérdida significativa de la expresión génica de TrkC en los anillos quiescentes frente a los recién aislados. Resultados similares se obtuvieron utilizando células de músculo liso aisladas de aorta de rata y fibroblastos aislados de corazón de rata, que se cultivaron hasta confluencia. Se observó una reducción significativa en la expresión génica de NT-3 y TrkC después del cultivo comparándola con la obtenida en células recién aisladas (frescas) (Figura 14).

Esta observación explica la baja expresión de NT-3 y TrkC en células cultivadas de humanos, y dificulta el estudio *in vitro* de la actividad de NT-3.

B. NT-3 como modulador del tono vascular

En el presente trabajo se analizó el efecto de la NT-3 exógena sobre el tono vascular de la aorta y la arteria caudal de rata Wistar, dos territorios representativos de vasos de conductancia o de distribución, respectivamente. Se realizaron diferentes protocolos experimentales para determinar la influencia del endotelio o del tejido adiposo perivascular (PVAT) en la actividad de la vía NT-3/TrkC en el tono vascular.

Para determinar ***la influencia del endotelio*** se utilizaron anillos con y sin endotelio o pre-incubados en presencia o ausencia del inhibidor de la NOS, L-NAME (100 µM).

Los resultados obtenidos muestran que, en la aorta aislada, la adición de concentraciones acumulativas de NT-3 sobre la meseta de contracción inducida por fenilefrina1 µM, agonista α_1, provocó una curva concentración-respuesta de relajación que no se observó en los vasos desprovistos de endotelio ni en los pre-incubados con L-NAME (Figura 15A, Tabla 5). Estos resultados nos indican que NT-3 ejerce una acción relajante en aorta de rata dependiente de la liberación de NO endotelial y concuerdan con los obtenidos por Meuchel et al. (2010) en la arteria pulmonar.

Sin embargo, en la arteria caudal, NT-3 indujo una respuesta relajante no significativa y que, además, no se vio modificada en los vasos pre-incubados con L-NAME (Figura 15B, Tabla 5). Por tanto, vemos una clara diferencia en las respuestas vasculares a NT-3 dependiendo del tipo de vaso y su dependencia de la liberación de NO para modular el tono contráctil. En la aorta, un vaso de conductancia con una alta modulación de la respuesta contráctil por diferentes mecanismos dependientes de NO (Arce et al., 2017), el efecto de NT-3 en el endotelio promueve la síntesis y liberación de NO que induce vasodilatación de forma similar a lo que ocurre con acetilcolina. En la arteria caudal, NT-3 no ejerce ninguna actividad vasodilatadora significativa, como también ocurre con la acetilcolina.

Además, los resultados obtenidos descartan la intervención de los receptores TrkC en la modulación del tono vascular de NT-3 en la aorta o la arteria caudal, ya que la pre-incubación con K252a no modificó la respuesta relajante inducida por NT-3 (Figura 16, Tabla 6). Asimismo, la respuesta vasoconstrictora a fenilefrina (agonista α_1 adrenérgico) en la aorta o la arteria caudal (Figura 17, Tabla 7), no se modificó tras pre-incubación con el inhibidor de Trk, lo que indica que NT-3 exógena o las NT endógenas no activan estos receptores para modular el tono vascular.

En otro grupo de experimentos ***analizamos la influencia del PVAT*** en la vasodilatación inducida por NT-3 en aorta de rata. Actualmente se ha

demostrado que el PVAT es un depósito de grasa especializado que rodea la mayoría de los vasos sanguíneos, liberando factores difusibles que modulan la reactividad vascular local y el estado inflamatorio y, como resultado, pueden contribuir a los cambios fisiopatológicos observados en las enfermedades cardiovasculares, la diabetes y la obesidad (Ramírez et al., 2017). Se ha descrito que el PVAT ejerce propiedades anti-contráctiles, pero también pro-contráctiles (Ramírez et al., 2017).

Por este motivo, analizamos la actividad de NT-3 en anillos aórticos con o sin PVAT, realizando además un estudio previo del papel modulador del PVAT en las respuestas mediadas por diferentes agonistas con actividades contráctiles o relajantes.

En primer lugar, se estudió la influencia del PVAT en la respuesta contráctil sostenida provocada por una solución despolarizante (KCl 80 mM) o una concentración máxima del agonista α_1 adrenérgico fenilefrina, y observamos que, en ambos casos, la contracción obtenida en anillos de aorta con PVAT (+ PVAT) fue significativamente menor que la obtenida en anillos sin PVAT (-PVAT) (Figura 18). De forma similar, los parámetros de la curvas concentración-respuesta a fenilefrina en los anillos aórticos + PVAT o -PVAT (Emax y pEC50) disminuyeron significativamente en los anillos + PVAT (Figura 19, Tabla 8). Por lo tanto, nuestros datos corroboran la existencia de un mecanismo anti-contráctil mediado por PVAT en la aorta de rata.

Para aclarar el papel pro-contráctil del PVAT, probamos su efecto sobre la vasodilatación inducida por acetilcolina y por la activación de los adrenoceptores β. Nuestros resultados confirman que el PVAT afecta negativamente a la relajación inducida por la acetilcolina tal como ha sido descrito por otros autores en aorta (Lee et al., 2014; Mikolajczyk et al., 2016) y en otros territorios vasculares (Aalbaek et al., 2015; Vallejo et., 2011). Además, encontramos que el PVAT tiene un efecto inhibitorio similar sobre la vasodilatación inducida por isoprenalina, agonista selectivo de los adrenoceptores β_1 y β_2 o SR58611A, agonista β_3, aunque en este último caso, la inhibición inducida por PVAT no alcanzó significación estadística (Figura 20, Tabla 9). En ambos casos, las curvas de relajación del agonista selectivo β_3 (SR5811A) fueron bifásicas, discriminando dos poblaciones de adrenoceptores β, una de alta potencia que

corresponde a los adrenoceptores β_3 y otra de baja potencia que corresponde a los adrenoceptores β_1 y/o β_2.

En conjunto, nuestros hallazgos indican que el equilibrio entre mediadores vasodilatadores y vasoconstrictores liberados por PVAT fue favorable para los mediadores vasodilatadores, ya que el efecto sobre las respuestas contráctiles fue más marcado que el observado sobre los agentes vasodilatadores.

La actividad anti-contráctil mostrada por PVAT frente a la vasodilatación provocada por la acetilcolina y los agonistas β también se observó cuando la relajación se produjo por NT-3, aunque las diferencias no alcanzaron significación estadística (Figura 21, Tabla 10). Teniendo en cuenta la implicación del NO en las respuestas relajantes de acetilcolina (Furchgott & Zawadzki, 1980), los agonistas β (Flacco et al., 2013) y la NT-3 (presente trabajo) podemos suponer que una disminución en la liberación de NO o en su biodisponibilidad puede estar involucrado en la menor vasodilatación observada en presencia de PVAT.

En cualquier caso, la actividad relajante de NT-3 en la aorta no es notable, y carece de acción en la arteria caudal, lo que indica que depende del tipo de vaso. Teniendo en cuenta estos resultados, la existencia de una expresión abundante de NT-3 y TrkC en los vasos no siempre puede explicarse por un papel significativo de esta NT en el tono vascular y abre nuevas preguntas sobre su papel fisiológico en los vasos. Para aclarar este punto, el siguiente paso en nuestro trabajo fue proponer un estudio con un enfoque diferente, en el que analizamos las consecuencias de un déficit de NT-3 a nivel vascular, y para este fin, trabajamos con dos modelos de ratones genéticamente modificados.

Consecuencias de una expresión reducida de NT-3 en ratones genéticamente manipulados a nivel cardiovascular

Se trabajó con dos grupos de ratones modificados genéticamente:

-Ratones ($NT3^{+/-}$), que expresan niveles reducidos de NT-3 sin cambiar la expresión del receptor TrkC y sus controles, ratones salvajes ($NT3^{+/+}$).

-Ratones que no expresan NT-3 en el endotelio ($eNT3^-$) y sus controles ($eNT3^+$). Esta eliminación de la NT-3 no cambia el crecimiento o morfometría de la vasculatura.

Los resultados en ratones $NT\text{-}3^{+/-}$, obtenidos mediante tinción immunohistoquímica con β-galactosidasa, confirman que NT-3 se encuentra abundantemente expresada en los vasos, pero la reducción de su expresión o la inhibición de su expresión en el endotelio no conduce a alteraciones en el peso corporal, el peso del corazón o en el ratio peso corazón/peso corporal (Tabla 11).

Por lo que respecta a la presión arterial, se observó una disminución de la presión sanguínea en estos ratones al compararlos con sus grupos control (Tabla 12, Figura 22) lo que sugiere un papel de la NT-3 en el control de la presión arterial que se debe a su presencia en el endotelio vascular, ya que los cambios observados son similares en ambos grupos de ratones.

Analizamos también la influencia que tiene en la función vascular la inhibición de la expresión endotelial de NT-3. Estudiamos diferentes agentes que modulan el tono vascular en la aorta de ratón como son un agente despolarizante, KCl 80mM, un agente que induce la liberación endotelial de NO, la acetilcolina, o agentes que activan los adrenoceptores como fenilefrina (adrenoceptores α1) o isoprenalina (adrenoceptores β1, β2) y SR5811A (adrenoceptores β3).

Todos los experimentos fueron realizados en aortas con endotelio intacto, en las que se ha eliminado el tejido adiposo perivascular. En todos los vasos ensayados, se determinó la respuesta a KCl 80mM encontrando que no se ve alterada por la falta de NT-3 endotelial. Lo mismo ocurre cuando estudiamos la contracción inducida por estimulación de adrenoceptores α1. Las CCR a fenilefrina son similares en ratones con y sin NT-3 endotelial (Figura 23, Tabla 13). Cuando se realiza una curva de relajación con acetilcolina sobre la meseta de contracción inducida por fenilefrina 1 μM, tampoco observamos diferencias significativas en la respuesta vasodilatadora, mediada en este caso por la liberación de NO endotelial (Figura 25, Tabla 15). Estos resultados evidencian que en los ratones en los que se elimina la expresión de NT-3 en el endotelio no se modifica la respuesta contráctil inducida por una solución despolarizante o por la activación de adrenoceptores α_1, ni tampoco la respuesta vasodilatadora

mediada por NO. Sin embargo, cuando la respuesta vasodilatadora esta inducida por activación de adrenoceptores β, los resultados no son iguales. La adición de concentraciones acumulativas crecientes de isoprenalina (agonista selectivo de adrenoceptores β_1, β_2) produjo una respuesta vasodilatadora concentración-dependiente igual en los dos grupos de ratones mientras que la adición de SR58611A, (agonista selectivo β_3) dio resultados diferentes (Figura 24, Tabla 14). En los ratones control ($eNT3^+$), se obtuvieron curvas bifásicas, discriminando dos sitios o poblaciones de receptores de alta y baja potencia: uno que correspondería a los adrenoceptores β_3 (elevada potencia) cuyo porcentaje fue de 26%, y otro que correspondería a los adrenoceptores β_1 y/o β_2. Sin embargo, en los ratones que no tienen NT-3 en el endotelio ($eNT3^-$), se observó una disminución drástica en la población de elevada potencia, es decir, en la población de adrenoceptores β_3 (Figura 24B, Tabla 14B). Estos resultados confirman los que anteriormente se habían realizado en el laboratorio con ratones en los que la expresión de NT-3 había sido parcialmente reducida (ratones $NT\text{-}3^{+/-}$), evidenciando que un déficit en la expresión de la NT-3 en los vasos conduce a una alteración en la función del adrenoceptor β_3 que se puede explicar bien por una expresión disminuida o bien por una función alterada de este subtipo.

Analizando la expresión de NT-3, TrkC y los tres subtipos de adrenoceptores β en el ventrículo izquierdo de los ratones con una expresión reducida de NT-3 ($NT3^{+/-}$) observamos que tanto la expresión de NT-3 como la del subtipo β_3 están significativamente disminuidas, sin que cambie la expresión de los otros tres genes estudiados (Figure 26).

Aunque estos resultados se deben confirmar en otros tejidos, podemos asumir que hay una estrecha relación entre la expresión de NT-3 y del adrenoceptor β_3, por lo que este factor neurotrófico podría ser una diana terapéutica para modular la función del adrenoceptor β_3 en patologías cardiovasculares. Hasta el momento, el papel de este subtipo en patología cardiovascular es controvertido, existiendo datos que apoyan tanto un papel protector como deletéreo en patologías como la insuficiencia cardiaca (Cannavo & Koch, 2017)

Por esta razón, nuestro siguiente paso ha sido analizar los cambios de expresión de adrenoceptor β_3, NT-3 y TrkC en pacientes con insuficiencia cardiaca.

Cambios en la vía NT-3/TrkC en patologías cardiovasculares

Nuestro último objetivo fue analizar los cambios de expresión de NT-3 y TrkC en patologías cardiovasculares humanas como la hipertensión y la insuficiencia cardiacas

Se analizaron los niveles de expresión génica y proteica de NT-3 y TrkC en muestras de ventrículo izquierdo en sujetos control y en pacientes con insuficiencia cardiaca en fase terminal sometidos a trasplante cardiaco. Dentro de estos últimos se incluyen pacientes con cardiopatía isquémica y con miocardiopatía dilatada, en tratamiento con estimulantes cardiacos como dopamina, noradrenalina y dobutamina; antagonistas del receptor mineralcorticoide como espironolactona; β-bloqueantes como carvedilol; inhibidores de la enzima convertidora de la angiotensina; fármacos antiarrítmicos como amiodarona o con digoxina, en función del estado hemodinámico de los pacientes (Tabla 16).

Determinamos los niveles de mRNA de NT-3 y TrkC, encontrando que aumentan en pacientes con insuficiencia cardiaca respecto a los sujetos control (Figura 27 A y B). Tras el análisis de la expresión génica, se determinó la expresión proteica utilizando la técnica de Western blot. Se detectaron dos isoformas de la proteína NT-3, a 20 kDa y a 25 kDa en ventrículo izquierdo. El análisis densitométrico muestra un aumento significativo en la banda de 25 kDa en pacientes con insuficiencia respecto a los sujetos sanos, mientras que no se observaron diferencias en la banda de 20 kDa. Por otro lado, también aparecen dos isoformas de TrkC a 50 kDa y 110 kDa, y en ambos casos se aprecia aumento en la expresión de TrkC en el miocardio enfermo respecto al control (Figura 27 F y G).

Cabe destacar que la expresión génica de NT-3 y TrkC en pacientes con insuficiencia cardiaca no depende del sexo, ya que se observaron valores similares de mRNA en muestras de miocardio enfermo de hombres y mujeres (Figura 29 A y B).

Es interesante señalar que cuando establecemos si existe una correlación estadística entre la expresión de NT-3 o TrkC y las variables clínicas características de la insuficiencia cardiaca encontramos que la correlación de

Pearson evidencia una asociación significativa y positiva entre los niveles de mRNA de NT-3 y la fracción de eyección del ventrículo izquierdo (LVEF) de los pacientes con insuficiencia cardiaca (Figura 30A). Estos resultados indican, por primera vez, la posibilidad de que la función de NT-3 en el ventrículo izquierdo podría estar asociada a la cardioprotección, que bien puede estar relacionada directamente con la actividad de NT-3 en la funcionalidad cardiaca o bien puede deberse a una acción indirecta de NT-3 regulando la expresión de los adrenoceptores β con efectos beneficiosos en insuficiencia cardiaca. El papel protector de NT-3 también se había puesto de manifiesto tras un proceso de isquemia cerebral cuando se administra de forma exógena, aunque, tras el proceso, se observa un descenso en su expresión (Galvin & Oorschot., 2003; Lindvall et al., 1992; Zhang et al., 1999).

Para confirmar esta hipótesis, determinamos la expresión génica de los adrenoceptores β en el ventrículo izquierdo de los pacientes con insuficiencia cardiaca y los comparamos con los donantes control. Los resultados indican una disminución significativa del subtipo β_1 en el ventrículo izquierdo insuficiente (Figura 27C), lo que corrobora estudios anteriores (Monto et al., 2012). Esta disminución no se observa cuando analizamos la expresión de los subtipos β_2 y β_3 (Figura 27D y E). Además, se realizó una correlación de Pearson para determinar si existe una asociación estadísticamente significativa entre los niveles de expresión génica de NT-3 o TrkC y la expresión de los adrenoceptores β en muestras de miocardio. Encontramos que existe una correlación significativa y positiva entre los niveles de expresión de NT-3 y los tres subtipos de adrenoceptores β (Figura 28). Esta correlación indica dos posibilidades, la primera sería la existencia de un mecanismo común que regula estos genes y la segunda es que la NT-3 controla la expresión de los adrenoceptores β. Si éste es el caso, el aumento de expresión de NT-3 observado en corazón insuficiente, puede ejercer un control positivo en la expresión de los adrenoceptores β y podría contrarrestar parcialmente la regulación a la baja del adrenoceptor β_1, característica de la insuficiencia cardiaca. Esta hipótesis explicaría también la relación positiva encontrada entre la expresión de NT-3 y la fracción de eyección del ventrículo izquierdo.

Es interesante destacar que también existe una correlación positiva y significativa entre la expresión génica de NT-3 y TrkC en miocardio (Figura 28A), lo que podría interpretarse en el mismo sentido comentado anteriormente, o bien como la existencia de un mecanismo regulador común, o bien que uno de ellos modula la expresión del otro. Sin embargo, no se observa relación entre la expresión de TrkC y otras variables clínicas, lo que confiere un papel preponderante a la NT-3 en cuanto a la funcionalidad cardiaca.

Estos resultados dan nueva información sobre el papel de la NT-3 y TrkC en el contexto de las enfermedades cardiovasculares. Sin embargo, el aumento de expresión de la NT-3 observado en nuestro grupo con pacientes enfermos contrasta con los resultados de Hiltunen et al., (2001) que no encuentran diferencias en la expresión de NT-3 en el área infartada del corazón de rata, y contrasta también con la disminución en la expresión de NT-3 que aparece en la hipertrofia cardiaca inducida en rata (Kawaguchi-Manabe et al., 2007) aunque, a su vez, hay que tener en cuenta que NT-3 es un factor hipertrófico cardiaco (Kawaguchi-Manabe et al., 2007; Saygili & cols., 2010). Hay que tener en cuenta que en estos casos la determinación de NT-3 se hace inmediatamente tras la inducción de la patología.

Considerando estas evidencias paradójicas, proponemos que tras un proceso de daño cardiaco se puede producir un descenso en la expresión de NT-3, no detectado en nuestros pacientes que se encuentran en un estado avanzado de insuficiencia cardiaca. Esta disminución inicial sería contrarrestada por un aumento en la expresión de NT-3 como mecanismo compensador que favorece la regeneración tisular y neuronal.

Asimismo, también se analizó la influencia de la vía NT-3/TrkC en la hipertensión, ya que la eliminación de la NT-3 en el endotelio o la expresión parcial de NT-3 conduce a la disminución de la presión sanguínea en ratones transgénicos comparado con sus respectivos controles. En el grupo de los pacientes con insuficiencia cardiaca, sin embargo, no se observaron diferencias estadísticamente significativas en los niveles de expresión de NT-3 o TrkC entre pacientes hipertensos respecto a los normotensos (Figura 29C y D).

Complementamos este estudio en dos modelos de ratas hipertensas. El primer modelo utilizado es el de ratas espontáneamente hipertensas (SHR) que muestran valores elevados de presión arterial con respecto a sus controles, las ratas Wistar-Kyoto (WKY). El segundo modelo fue el de ratas Wistar tratadas crónicamente con L-NAME, un inhibidor de la sintasa de NO (NOS), que conduce a una elevación de las cifras de presión arterial similar a la encontrada en ratas SHR. Los resultados demostraron que no aparecen cambios significativos en la expresión génica y proteica de NT-3 y TrkC en el ventrículo izquierdo de ratas SHR comparado con el de ratas WKY (Figura 32), resultados que coinciden con los obtenidos en corazón de pacientes hipertensos con insuficiencia cardiaca respecto a los normotensos, pero no coinciden con resultados previos en ratas más jóvenes (Maisonpierre et al., 1990; Zhang & Rush, 2001).

En las ratas tratadas con L-NAME no aparecen cambios significativos en la expresión génica de NT-3, pero se observa un aumento significativo de la expresión de TrkC en ventrículo izquierdo (Figura 33).

Considerando en conjunto los resultados obtenidos en animales genéticamente manipulados, en pacientes y en modelos animales de hipertensión, podemos establecer que NT-3 puede ejercer un papel en el control de la presión arterial, pero que este papel no se debe a cambios en su expresión cardiaca.

Relación entre la vía NT-3/TrkC y el índice de masa corporal

Finalmente, otro resultado interesante obtenido en el presente trabajo es la correlación inversa obtenida entre la expresión de NT-3 en ventrículo izquierdo de pacientes con insuficiencia cardiaca y el índice de masa corporal (BMI) (Figura 30B), pues hasta ahora, otras neurotrofinas se habían relacionado con la obesidad (Chaldakov et al., 2004; 2009) pero no la NT-3.

Ante esta observación, el siguiente y último paso fue analizar la expresión de NT-3 y TrkC en tejidos obtenidos de un modelo de rata Zucker obesa, y compararlos con su cepa control. Los resultados indican que la expresión de la NT-3 se encuentra significativamente disminuida en el riñón y presenta una leve disminución, pero no significativa, en el corazón de ratas obesas en comparación con las ratas control. Mientras que la expresión de TrkC aumenta significativamente en el riñón, en el corazón no se encuentran diferencias de

expresión entre las ratas Zucker y control (Figura 34A y B). Se demostró además una disminución paralela en la expresión del adrenoceptor β_3 en riñón y corazón, siendo significativa en el riñón (Figura 34C). Sin embargo, no se observaron cambios en la expresión de los subtipos β_1 y β_2 entre las ratas Zucker obesas y sus controles (Figura 34D y E)

Dada la estrecha relación encontrada entre la expresión de NT-3 y los adrenoceptores β, y considerando el papel que los subtipos β (Arch, 2002), y especialmente el β_3 (Barbe et al., 1996; Deng et al., 1997; Sennitt et al., 1998), juegan en el control metabólico del tejido adiposo, estos resultados, aunque preliminares, abren una nueva vía de investigación para tratar de determinar la relación entre NT-3/TrkC y adrenoceptores β en tejido adiposo.

CONCLUSIONES

Con todos lo anteriormente descrito llegamos a las siguientes conclusiones:

1.Vasos humanos y de roedores expresan niveles elevados de NT-3 y su receptor TrkC. Mediante inmunotransferencia, se detectaron varias isoformas de NT-3 y TrkC en diferentes tejidos de rata, observando que la expresión relativa de estas isoformas varía dependiendo del tejido analizado.

2. La NT-3 exógena no modifica significativamente la migración o la formación de nuevos túbulos en diferentes líneas de células endoteliales humanas (aorta, arteria coronaria y microvasculatura coronaria), ni el proceso angiogénico determinado en anillos aórticos de rata. La falta de respuesta a NT-3 podría atribuirse a una pérdida de expresión de TrkC durante el cultivo.

3. Se ha demostrado una respuesta vasodilatadora parcial de NT-3 exógena, que depende de la liberación endotelial de NO en la aorta, pero no en la arteria caudal de rata. El inhibidor del receptor Trk, K252a, no modifica la respuesta vasodilatadora mediada por NT-3 ni la respuesta contráctil inducida por adrenoceptores α_1, lo que indica que la NT-3 exógena o endógena no actúa a través de los receptores TrkC para modular el tono vascular.

4. Usando ratones genéticamente modificados, con una expresión reducida de NT-3 o en los que se suprime la expresión de NT-3 endotelial, encontramos una disminución significativa en la presión arterial sistólica, proporcionando evidencia de que NT-3 podría desempeñar un papel en el control de la presión arterial. Sin embargo, en un grupo de pacientes con insuficiencia cardíaca hipertensiva o en ratas hipertensas inducidas por SHR o L-NAME, no se observaron cambios en la expresión cardíaca de NT-3.

5. Se observaron cambios en la expresión de adrenoceptores β_3 en el sistema cardiovascular de los mismos modelos de ratones genéticamente modificados, con expresión parcial de NT-3 o con expresión suprimida de NT-3 en el endotelio. En la aorta de ratón, estas modificaciones conducen a una pérdida de la respuesta relajante mediada por los adrenoceptores β_3

6. En el ventrículo izquierdo de pacientes con insuficiencia cardíaca, se observó una mayor expresión génica y proteica de NT-3 y TrkC, así como una correlación positiva entre los niveles de mRNA de NT-3 y los tres subtipos de adrenoceptores β, lo que confirma la relación entre NT-3 y los adrenoceptores β observada en ratones genéticamente modificados.

7. En pacientes con insuficiencia cardíaca, existe una correlación positiva entre la expresión del gen NT-3 y la fracción de eyección del ventrículo izquierdo, lo que evidencia un posible efecto protector cardiovascular de la NT-3 en el corazón.

8. En el ventrículo izquierdo de los pacientes con insuficiencia cardíaca, existe una correlación inversa entre la expresión del gen NT-3 y el índice de masa corporal. Además, se encontraron niveles reducidos de mRNA de NT-3 y adrenoceptor β_3 en riñones de ratas Zucker obesas, en comparación con las no obesas. Esto demuestra que los cambios en la expresión de NT-3 y β_3-AR se producen en paralelo también en este modelo de obesidad en ratas, y supone un paso inicial para investigar la relación entre la NT-3 y la obesidad, abriendo vías alternativas para buscar nuevas dianas terapéuticas en la obesidad.

VIII REFERENCES

Aalbaek, F., Bonde, L., Kim, S., & Boedtkjer, E. (2015). Perivascular tissue inhibits rho-kinase-dependent smooth muscle Ca(2+) sensitivity and endothelium-dependent H2 S signalling in rat coronary arteries. *J Physiol*, *593*(21), 4747–4764.

Adair, T., & Montani, J. (2010). *Angiogenesis Assay*. *Angiogenesis*. San Rafael (CA). Retrieved from www.ncbi.nlm.nih.gov/books/NBK53241/

Aghamohammadzadeh, R Unwin, R., Greenstein, A., & Heagerty, A. (2015). Effects of Obesity on Perivascular Adipose Tissue Vasorelaxant Function: Nitric Oxide, Inflammation and Elevated Systemic Blood Pressure. *J Vas Res*, *52*(5), 299–305.

Agüero, J., Almenar, L., D'Ocon, P., Oliver, E., Montó, F., Rueda, J., … Salvador, A. (2009). Myocardial and peripheral lymphocytic transcriptomic dissociation of beta-adrenoceptors and G protein-coupled receptor kinases in heart transplantation. *J Hear Lung Transpl*, *28*(11), 1166–1171.

Ahima, R., & Flier, J. (2000). Adipose tissue as an endocrine organ. *Trends Endocrinol Metab*, *11*(8), 327–332.

Aird, W. C. (2007). Phenotypic heterogeneity of the endothelium: I. Structure, function, and mechanisms. *Circ Res*, *100*(2), 158–173.

Al-Qudah, M. A., & Al-Dwairi, A. (2016). Mechanisms and regulation of neurotrophin synthesis and secretion. *Neurosciences*, *21*(4), 306–313.

Almabrouk, T., Ewart, M., Salt, I., & Kennedy, S. (2014). Perivascular fat, AMP-activated protein kinase and vascular diseases. *Br J Pharmacol*, *171*, 595–617.

Aplin, A. C., Fogel, E., Zorzi, P., & Nicosia, R. F. (2008). Chapter 7 The Aortic Ring Model of Angiogenesis. *Methods Enzymol*, *443*(08), 119–136.

Arcamone, N., Lucini, C., Borzacchiello, G., Castaldo, L., Gargiulo, G., & De Girolamo, P. (2005). Distribution of NGF and NT-3-like protein immunoreactivity in the teleost kidney. *Microsc Res Tech*, *66*(1), 17–24.

Arce, C., Vicente, D., Segura, V., Flacco, N., Montó, F., Almenar, L., … Ivorra, M. D. (2017). Activation of α1A-adrenoceptors desensitizes the rat aorta

response to phenylephrine through a neuronal NOS pathway, a mechanism lost with ageing. *Br J Pharmacol*, *174*(13), 2015–2030.

Arch, J. (2008). The discovery of drugs for obesity, the metabolic effects of leptin and variable receptor pharmacology: perspectives from beta3-adrenoceptor agonists. *Naunyn Schmiedebergs Arch Pharmacol*, *378*(2), 225–240.

Arch, J. R. S. (2002). β3-adrenoceptor agonists: Potential, pitfalls and progress. *Eur J Pharmacol*, *440*(2–3), 99–107.

Arévalo, J. C., & Wu, S. H. (2006). Neurotrophin signaling: Many exciting surprises! *Cell Mol Life Sci*, *63*(13), 1523–1537.

Ayala-Lopez, N., Martini, M., Jackson, W. F., Darios, E., Burnett, R., Seitz, B., … Watts, S. W. (2014). Perivascular adipose tissue contains functional catecholamines. *Pharmacol Res Perspect*, *2*(3), 1–12.

Barbacid, M. (1994). The Trk family of neurotrophin receptors. *J Neurobiol*, *25*(11), 1386–1403.

Barbe, P., Millet, L., Galitzky, J., Lafontan, M., & Berlan, M. (1996). In situ assessment of the role of the β1-, β2- and β3-adrenoceptors in the control of lipolysis and nutritive blood flow in human subcutaneous adipose tissue. *Br J Pharmacol*, *117*, 907–913.

Bartkowska, K., Gajerska, M., Turlejski, K., & Djavadian, R. L. (2013). Expression of TrkC Receptors in the Developing Brain of the Monodelphis opossum and Its Effect on the Development of Cortical Cells. *PLoS One*, *8*(9), 1–14.

Bates, D. O., & Harper, S. J. (2002). Regulation of vascular permeability by vascular endothelial growth factors. *Vascul Pharmacol*, *39*(4–5), 225–237.

Baxter, G. T., Radeke, M. J., Kuo, R. C., Makrides, V., Hinkle, B., Hoang, R., … Feinstein, S. C. (1997). Signal transduction mediated by the truncated trkB receptor isoforms, trkB.T1 and trkB.T2. *J Neurosci*, *17*(8), 2683–2690.

Belge, C., Hammond, J., Dubois-Deruv, E., Manoury, B., Hamelet, J., Beauloye, C., … Balligand, J. (2014). Enhanced expression of β3-adrenoceptors in cardiac myocytes attenuates neurohormone-induced hypertrophic remodeling through nitric oxide synthase. *Circulation*, *129*(4), 451–462.

Belmonte, S., & Blaxall, B. (2011). G protein coupled receptor kinases as therapeutic targets in cardiovascular disease. *Circ Res*, *109*, 309–319.

Beltaifa, S., Webster, M. J., Ligons, D. L., Fatula, R. J., Herman, M. M., Kleinman, J. E., & Weickert, C. S. (2005). Discordant changes in cortical TrkC mRNA and protein during the human lifespan. *Eur J Neurosci*, *21*(9), 2433–2444.

Benjamin, E. J., Virani, S. S., Callaway, C. W., Chamberlain, A. M., Chang, A. R., Cheng, S., … Muntner, P. (2018). *Heart disease and stroke statistics - 2018 update: A report from the American Heart Association*. *Circulation* (Vol. 137).

Berkemeier, L. R., Winslow, J. W., Kaplan, D. R., Nikolics, K., Goeddel, D. V., & Rosenthal, A. (1991). Neurotrophin-5: A novel neurotrophic factor that activates trk and trkB. *Neuron*, *7*(5), 857–866.

Bianchi, E., Artico, M., Di Cristofano, C., Leopizzi, M., Taurone, S., Pucci, M., … Della Rocca, C. (2013). Growth factors, their receptor expression and markers for proliferation of endothelial and neoplastic cells in human osteosarcoma. *Int J Immunopathol Pharmacol*, *26*(3), 621–632.

Bierl, M. A., Jones, E. E., Crutcher, K. A., & Isaacson, L. G. (2005). “Mature” nerve growth factor is a minor species in most peripheral tissues. *Neurosci Lett*, *380*(1–2), 133–137.

Bir, S. C., Xiong, Y., Kevil, C. G., & Luo, J. (2012). Emerging role of PKA/eNOS pathway in therapeutic angiogenesis for ischaemic tissue diseases. *Cardiovasc Res*, *95*(1), 7–18.

Birnbaum, T., Roider, J., Schankin, C. J., Padovan, C. S., Schichor, C., Goldbrunner, R., & Straube, A. (2007). Malignant gliomas actively recruit bone marrow stromal cells by secreting angiogenic cytokines. *J Neurooncol*, *83*(3), 241–247.

Black, E. A. E., Smith, P. M., McIsaac, W., & Ferguson, A. V. (2018). Brain-derived neurotrophic factor acts at neurons of the subfornical organ to influence cardiovascular function. *Physiol Rep*, *6*(10), 1–10.

Blais, M., Lévesque, P., Bellenfant, S., & Berthod, F. (2013). Nerve Growth Factor, Brain-Derived Neurotrophic Factor, Neurotrophin-3 and Glial-Derived

Neurotrophic Factor Enhance Angiogenesis in a Tissue-Engineered *In Vitro* Model. *Tissue Eng Part A*, *19*(15–16), 1655–1664.

Bothwell, M. (2014). NGF, BDNF, NT3, and NT4. In *Neurotrophic factors* (pp. 3–15).

Bothwell, M. (2016). Recent advances in understanding neurotrophin signaling. *F1000Research*, *5*(0), 1885.

Bouïs, D., Hospers, G. A. P., Meijer, C., Molema, G., & Mulder, N. H. (2001). Endothelium in vitro: A review of human vascular endothelial cell lines for blood vessel-related research. *Angiogenesis*, *4*(2), 91–102.

Bowers, S. L. K., & Baudino, T. A. (2010). Laying the groundwork for growth: Cell-cell and cell-ECM interactions in cardiovascular development. *Birth Defects Res Part C - Embryo Today Rev*, *90*(1), 1–7.

Bradley, E., Law, A., Bell, D., & Johnson, C. D. (2003). Effects of varying impulse number on cotransmitter contributions to sympathetic vasoconstriction in rat tail artery. *Am J Physiol Hear Circ Physiol*, *284*(6), H2007-14.

Brahimi, F., Maira, M., Barcelona, P. F., Galan, A., Aboulkassim, T., Teske, K., … Saragovi, H. U. (2016). The paradoxical signals of two TrkC receptor isoforms supports a rationale for novel therapeutic strategies in ALS. *PLoS One*, *11*(10), 1–25.

Britton, K., Pedley, A., Massaro, J., Corsini, E., Murabito, J., Hoffmann, U., & Fox, C. (2012). Prevalence, distribution, and risk factor correlates of high thoracic periaortic fat in the Framingham Heart Study. *J AM Hear Assoc*, *0:e004200*, 1–10.

Brodski, C., Schnurch, H., & Dechant, G. (2000). Neurotrophin-3 promotes the cholinergic differentiation of sympathetic neurons. *Proc Natl Acad Sci U S A*, *97*(17), 9683–9688.

Bulloch, J., & Daly, C. (2014). Autonomic nerves and perivascular fat: interactive mechanisms. *Pharmacol Ther*, *143*, 61–73.

Cannavo, A., & Koch, W. (2017). Targeting β3-Adrenergic Receptors in the Heart: Selective Agonism and β-Blockade. *J Cardiovasc Pharmacol*, *69*(2), 71–78.

Cannon, R. O. (1998). Role of nitric oxide in cardiovascular disease: Focus on the endothelium. *Clin Chem*, *44*(8 II), 1809–1819.

Caporali, A., & Emanueli, C. (2009). Cardiovascular actions of neurotrophins. *Physiol Rev*, *89*(1), 279–308.

Caporali, A., & Emanueli, C. (2012). MicroRNAs in Postischemic Vascular Repair. *Cardiol Res Pract*, *2012*, 486702.

Caporali, A., Meloni, M., Miller, A. M., Vierlinger, K., Cardinali, A., Spinetti, G., … Emanueli, C. (2012). Soluble ST2 is regulated by p75 neurotrophin receptor and predicts mortality in diabetic patients with critical limb ischemia. *Arterioscler Thromb Vasc Biol*, *32*(12), e149-60.

Caporali, A., Sala-Newby, G. B., Meloni, M., Graiani, G., Pani, E., Cristofaro, B., … Emanueli, C. (2008). Identification of the prosurvival activity of nerve growth factor on cardiac myocytes. *Cell Death Differ*, *15*(2), 299–311.

Carmeliet, P. (2005). Angiogenesis in life, disease and medicine. *Nature*, *438*(7070), 932–936.

Carmeliet, P., & Jain, R. K. (2011). Molecular mechanisms and clinical applications of angiogenesis. *Nature*, *473*(7347), 298–307.

Cassis, L., Lynch, K., & Peach, M. (1988). Localization of angiotensinogen messenger RNA in rat aorta. *Circ Res*, *62*, 1259–1262.

Cassis, L., Police, S., Yiannikouris, F., & Thatcher, S. (2008). Local adipose tissue renin-angiotensin system. *Curr Hypertens Rep*, *10*(2), 93–98.

Chaldakov, G. N., Fiore, M., Ghenev, P. I., Beltowski, J., Rančić, G., Tunçel, N., & Aloe, L. (2014). Triactome: Neuro-immune-adipose interactions. Implication in vascular biology. *Front Immunol*, *5*(APR), 1–9.

Chaldakov, G. N., Fiore, M., Hristova, M. G., & Aloe, L. (2003). Metabotrophic potential of neurotrophins:implication in obesity and related diseases? *Med Sci Monit*, *9*(10), HY19-21.

Chaldakov, G. N., Fiore, M., Stankulov, I. S., Manni, L., Hristova, M. G., Antonelli, A., … Aloe, L. (2004). Neurotrophin presence in human coronary

atherosclerosis and metabolic syndrome: A role for NGF and BDNF in cardiovascular disease? *Prog Brain Res*, *146*, 279–289.

Chaldakov, G. N., Tonchev, A. B., & Aloe, L. (2009). NGF and BDNF: from nerves to adipose tissue, from neurokines to metabokines. *Riv Psichiatr*, *44*(2), 79–87.

Chartterjee, T., Stoll, L., Denning, G., Harrelson, A., Blomkalns, A., Idelman, G., & et al. (2009). Proinflammatory phenotype of perivascular adipocytes. *Circ Res*, *104*, 541–549.

Chen, Y. (2013). Scratch Wound Healing Assay. *J Chem Inf Model*, *53*(1 ml), 1689–1699.

Chester, A. H., Yacoub, M. H., & Moncada, S. (2017). Nitric oxide and pulmonary arterial hypertension. *Glob Cardiol Sci Pract*, *2017*(2), 1–16.

Chung, J.-Y., Kim, M.-W., Im, W., Hwang, I. K., Bang, M.-S., & Kim, M. (2017). Expression of Neurotrophin-3 and trkC following Focal Cerebral Ischemia in Adult Rat Brain with Treadmill Exercise. *Biomed Res Int*, *2017*, 1–6.

Close, B., Banister, K., Baumans, V., Bernoth, E., Bromage, N., Bunyan, J., … Warwick, C. (1996). Recommendations for euthanasia of experimental animals: Part 1. *Lab Anim*, *30*, 293–316.

Cressman, M., Gifford, D., & Facc, M. (1983). Hypertension and stroke. *J AM COLL CARDIOL*, 521–527.

Cristofaro, B., Stone, O. A., Caporali, A., Dawbarn, D., Ieronimakis, N., Reyes, M., … Emanueli, C. (2010). Neurotrophin-3 is a novel angiogenic factor capable of therapeutic neovascularization in a mouse model of limb ischemia. *Arterioscler Thromb Vasc Biol*, *30*(6), 1143–1150.

Damon, D. H. (2008). TH and NPY in sympathetic neurovascular cultures: role of LIF and NT-3. *Am J Physiol Cell Physiol*, *294*, C306–C312.

Daniel J. Belliveau,* Irena Krivko,* Judi Kohn,* Christian Lachance,* Christine Pozniak,* Dmitri Rusakov, § David Kaplan, * ‡ and Freda D. Miller*. (1997). NGF and neurotrophin-3 both activate TrkA on sympathetic neurons but differentially regulate survival and neuritogenesis. *J Cell Biol*, *136*(2), 375–

388.

Darios, E., Winner, B., Charvat, T., Krasinksi, A., Punna, S., & Watts, S. (2016). The adipokine chemerin amplifies electrical field-stimulated contraction in the isolated rat superior mesenteric artery. *Am J Physiol Hear Circ Physiol*, *311*, H498–H507.

Delgado, A. C., Ferrón, S. R., Vicente, D., Porlan, E., Perez-Villalba, A., Trujillo, C. M., … Fariñas, I. (2014). Endothelial NT-3 Delivered by Vasculature and CSF Promotes Quiescence of Subependymal Neural Stem Cells through Nitric Oxide Induction. *Neuron*, *83*(3), 572–585.

Deng, C., Paoloni-Giacobino, A., Kuehne, F., Boss, O., Revelli, J., Moinat, M., … Giacobino, J. (1997). Respective degree of expression of β1-, β2- and β3-adrenoceptors in human brown and white adipose tissues. *Br J Pharmacol*, *118*, 929–934.

Descamps, B., Saif, J., Benest, A. V., Biglino, G., Bates, D. O., Chamorro-Jorganes, A., & Emanueli, C. (2018). BDNF (Brain-Derived Neurotrophic Factor) Promotes Embryonic Stem Cells Differentiation to Endothelial Cells Via a Molecular Pathway, Including MicroRNA-214, EZH2 (Enhancer of Zeste Homolog 2), and eNOS (Endothelial Nitric Oxide Synthase). *Arterioscler Thromb Vasc Biol*, *38*(9), 2117–2125.

Dias, R. G., Negrão, C. E., & Krieger, M. H. (2011). Nitric oxide and the cardiovascular system: cell activation, vascular reactivity and genetic variant. *Arq Bras Cardiol*, *96*(1), 68–75.

Dolle, J., Rezvan, A., Allen, F. D., Lazarovici, P., & Lelkes, P. I. (2005). Nerve Growth Factor-Induced Migration of Endothelial Cells. *J Pharmacol Exp Ther*, *315*(3), 1220–1227.

Donovan, M., Hahn, R., Tesarollo, L., & Hempstead, B. (1996). Identification of an essential noneuronal function of neurotrophin 3 in mammalian cardiad development. *Nat Genet*, *14*(3), 210–213.

Donovan, M. J., Hahn, R., Tesarollo, L., & Hempstead, B. L. (1996). Identification of an essential nonneuronal function of neurotrophin 3 in mammalian cardiac development. *Nat Genet*, *14*(3), 210–213.

Donovan, M. J., Lin, M. I., Wiegn, P., Ringstedt, T., Kraemer, R., Hahn, R., … Hempstead, B. L. (2000). Brain derived neurotrophic factor is an endothelial cell survival factor required for intramyocardial vessel stabilization. *Development*, *127*(21), 4531–4540.

Donovan, M. J., Miranda, R. C., Kraemer, R., McCaffrey, T. A., Tessarollo, L., Mahadeo, D., … Parada, L. (1995). Neurotrophin and neurotrophin receptors in vascular smooth muscle cells. Regulation of expression in response to injury. *Am J Pathol*, *147*(2), 309–324. Retrieved from http://www.pubmedcentral.nih.gov/articlerender.fcgi?artid=1869811&tool=pmcentrez&rendertype=abstract

Dubrovska, G., Verlohren, S., Luft, F. C., & Gollasch, M. (2004). Mechanisms of ADRF release from rat aortic adventitial adipose tissue. *Am J Physiol Hear Circ Physiol*, *286*(3), H1107-13.

Ebrahim, H. Y., & El Sayed, K. A. (2016). Discovery of novel antiangiogenic marine natural product scaffolds. *Mar Drugs*, *14*(3).

Elkabes, S., Schaar, D. ., Dreyfus, C. ., & Black, I. . (1995). Developmental regulation of neurotrophin-3 and TrkC splice variants in optic nerve glia in vivo, *66*(4), 879–889.

Elshamy, W. M., Linnarsson, S., Lee, K. F., Jaenisch, R., & Ernfors, P. (1996). Prenatal and postnatal requirements of NT-3 for sympathetic neuroblast survival and innervation of specific targets. *Development*, *122*(2), 491–500.

Emanueli, C., Meloni, M., Hasan, W., & Habecker, B. A. (2014). The biology of neurotrophins: Cardiovascular Function. In G. R. Lewin & B. D. Carter (Eds.), *Neurotrophic factors* (Handbook o, pp. 309–328). Berlin Heidelberg: Springer-Verlag.

Emanueli, C., Salis, M. B., Pinna, A., Graiani, G., Manni, L., & Madeddu, P. (2002). Nerve growth factor promotes angiogenesis and arteriogenesis in ischemic hindlimbs. *Circulation*, *106*(17), 2257–2262.

Engeli, S., Gorszelnialk, K., Kreutz, R., Runkel, N., Distler, A., & Sharma, A. (1999). Co-expression of renin–angiotensin system genes in human adipose tissue. *J Hypertens*, *17*, 555–560.

Ernfors, P., Ibáñez, C. F., Ebendal, T., Olson, L., & Persson, H. (1990). Molecular cloning and neurotrophic activities of a protein with structural similarities to nerve growth factor: developmental and topographical expression in the brain. *Proc Natl Acad Sci U S A*, *87*(14), 5454–5458.

Esteban, P. F., Yoon, H. Y., Becker, J., Dorsey, S. G., Caprari, P., Palko, M. E., … Tessarollo, L. (2006). A kinase-deficient TrkC receptor isoform activates Arf6-Rac1 signaling through the scaffold protein tamalin. *J Cell Biol*, *173*(2), 291–299.

Farhadi, H. F., Mowla, S. J., Petrecca, K., Morris, S. J., Seidah, N. G., & Murphy, R. A. (2000). Neurotrophin-3 sorts to the constitutive secretory pathway of hippocampal neurons and is diverted to the regulated secretory pathway by coexpression with brain-derived neurotrophic factor. *J Neurosci*, *20*(11), 4059–4068.

Fariñas, I., Jones, K., Backus, C., Wang, X.-Y., & Reichardt, L. F. (1994). Severe sensory and sympathethic deficits in mice lacking neurotrophin-3. *Nature*, *368*, 658–661.

Femminella, G. D., Candido, C., Conte, M., Provenzano, S., Rengo, C., Coscioni, E., & Ferrara, N. (2016). Cognitive Function and Heart Failure: The Role of the Adrenergic System. *Recent Patents Endocr Metab Immune Drug Discov*, *10*(1), 40–49.

Fenner, B. M. (2012). Truncated TrkB: Beyond a dominant negative receptor. *Cytokine Growth Factor Rev*, *23*(1–2), 15–24.

Ferrara, N., & Kerbel, R. S. (2005). Angiogenesis as a therapeutic target. *Nature*, *438*(7070), 967–974.

Flacco, N., Segura, V., Perez-Aso, M., Estrada, S., Seller, J. F., Jiménez-Altayõ, F., … Ivorra, M. D. (2013). Different β-adrenoceptor subtypes coupling to cAMP or NO/cGMP pathways: Implications in the relaxant response of rat conductance and resistance vessels. *Br J Pharmacol*, *169*(2), 413–425.

Folkman, J. (1997). *Regulation of Angiogenesis*. (I. D. Goldgerb & E. M. Rosen, Eds.), *Angiogenesis and angiogenesis inhibition: An overview*. Berlin.

Fox, E. A., & McAdams, J. (2010). Smooth-muscle-specific expression of neurotrophin-3 in mouse embryonic and neonatal gastrointestinal tract. *Cell Tissue Res*, *340*(2), 267–286.

Francis, N., Farinas, I., Brennan, C., Rivas-Plata, K., Backus, C., Reichardt, L., & Landis, S. (1999). NT-3, like NGF, is required for survival of sympathetic neurons, but not their precursors. *Dev Biol*, *210*(2), 411–427.

Freedman, S. B., & Isner, J. M. (2001). Therapeutic angiogenesis for ischemic cardiovascular disease. *J Mol Cell Cardiol*, *33*(3), 379–393.

Fulgenzi, G., Tomassoni-Ardori, F., Babini, L., Becker, J., Barrick, C., Puverel, S., & Tessarollo, L. (2015). BDNF modulates heart contraction force and long-term homeostasis through truncated TrkB.T1 receptor activation. *J Cell Biol*, *210*(6), 1003–1012.

Furchgott, R. (1988). Studies on relaxation of rabbit aorta by sodium nitrate: the basis for the proposal that the acid-activatable inhibitory factor from bovine retractor penis is inorganic nitrite and the endothelium-derived relaxing factor is nitric oxide. In P. M. Vanhoutte (Ed.), *Vasodilatation: Vascular Smooth Muscle, Peptides, Autonomic Nerves, and endothelium* (pp. 401–404). New York: Raven Press.

Furchgott, R., & Zawadzki, J. (1980). The obligatory role of endothelial cells in the relaxation of arterial smooth muscle by acetylcholine, *288*(27), 373–376.

Gálvez, B., De Castro, J., Herold, D., Dubrovska, G., Arribas, S., González, M. C., … Alfonso, M. S. F. (2006). Perivascular adipose tissue and mesenteric vascular function in spontaneously hypertensive rats. *Arterioscler Thromb Vasc Biol*, *26*(6), 1297–1302.

Galvin, K., & Oorschot, D. (2003). Continuous low-dose treatment with brain-derived neurotrophic factor or neurotrophin-3 protects striatal medium spiny neurons from mild neonatal hypoxia/ischemia: a stereological study. *Neuroscience*, *118*(4), 1023–1032.

Gao, Y. (2007). Dual modulation of vascular function by perivascular adipose tissue and its potential correlation with adiposity/lipoatrophy-related vascular dysfunction. *Curr Pharm Des*, *13*, 2185–2192.

Gao, Y. J., Zeng, Z. H., Teoh, K., Sharma, A. M., Abouzahr, L., Cybulsky, I., … Lee, R. M. K. W. (2005). Perivascular adipose tissue modulates vascular function in the human internal thoracic artery. *J Thorac Cardiovasc Surg*, *130*(4), 1130–1136.

Gao, Y., Lu, C., Su, L., Sharma, A., & Lee, R. (2007). Modulation of vascular function by perivascular adipose tissue: the role of endothelium and hydrogen peroxide. *Br J Pharmacol*, *3*, 323–331.

Gao, Y., Takemori, K., Su, L., An, W., Lu, C., Sharma, A., & et al. (2006). Perivascular adipose tissue promotes vasoconstriction: the role of superoxide anion. *Cardiovasc Res*, *71*, 363–373.

Gelati, M., Aplin, A. C., Fogel, E., Smith, K. D., & Nicosia, R. F. (2008). The angiogenic response of the aorta to injury and inflammatory cytokines requires macrophages. *J Immunol*, *181*(8), 5711–5719.

Gibon, J., & Barker, P. A. (2017a). Neurotrophins and Proneurotrophins: Focus on Synaptic Activity and Plasticity in the Brain. *Neuroscientist*, *23*(6), 587–604.

Gibon, J., & Barker, P. A. (2017b). Neurotrophins and Proneurotrophins. *Neurosci*, 107385841769703.

Gil-Ortega, M., Somoza, B., Huang, Y., Gollasch, M., & Fernández-Alfonso, M. S. (2015). Regional differences in perivascular adipose tissue impacting vascular homeostasis. *Trends Endocrinol Metab*, *26*(7), 367–375.

Gil-Ortega, M., Stucchi, P., Guzmán-Ruiz, R., Cano, V., Arribas, S., González, M., … Somoza, B. (2010). Adaptative nitric oxide overproduction in perivascular adipose tissue during early diet-induced obesity. *Endocrinology*, *151*(7), 3299–3306.

Gisbert, R., Noguera, M. A., Ivorra, M. D., & D'Ocon, P. (2000). Functional Evidence of a Constitutively Active Population of α1D-Adrenoceptors in Rat Aorta. *J Pharmacol Exp Ther*, *295*(2), 810–817.

Glerup, S., Nykjaer, A., & Vaegter, C. (2014). Sortilin in Neurotrophic Factor Signaling. In *Neurotrophic factors* (pp. 165–189).

Gollasch, M. (2012). Vasodilator signals from perivascular adipose tissue. *Br J Pharmacol*, *3*, 633–642.

Gollasch, M., & Dubrovska, G. (2004). Paracrine role for periadventitial adipose tissue in the regulation of arterial tone. *Trends Pharmacol Sci*, *25*(12), 647–653.

Govoni, S., Pascale, A., Amadio, M., Calvillo, L., D'Elia, E., Cereda, C., … Vanoli, E. (2011). NGF and heart: Is there a role in heart disease? *Pharmacol Res*, *63*(4), 266–277.

Greenberg, S., Xie, J., Wang, Y., Cai, B., Kolls, J., Nelson, S., & et al. (1985). Tumor necrosis factor-alpha inhibits endothelium-dependent relaxation. *J App Physiol*, *74*, 2394–2403.

Greenstein, A., Khavandi, K., Withers, S., Sonoyama, K., Clancy, O., Jeziorska, M., … Heagerty, A. (2009). Local inflammation and hypoxia abolish theprotective anticontractile properties of perivascular fat in obesepatients. *Circulation*, *119*, 1661–1670.

Groneberg, D. A., Peiser, C., Eynott, P. R., Welker, P., Erbes, R., Witt, C., … Fischer, A. (2005). Transcriptional down-regulation of neurotrophin-3 in chronic obstructive pulmonary disease. *Biol Chem*, *386*(1), 53–59.

Guo, D. Q., Zhang, H., Tan, S. J., & Gu, Y. C. (2014). Nifedipine promotes the proliferation and migration of breast cancer cells. *PLoS One*, *9*(12), 1–20.

Gustafson, B., Hammarstedt, A., Andersson, C., & Smith, U. (2007). Inflamed Adipose Tissue : A Culprit Underlying the Metabolic Syndrome and. *J Am Heart Assoc*, *27*, 2276–2283.

Guzik, T. J., Marvar, P. J., Czesnikiewicz-Guzik, M., & Korbut, R. (2007). Perivascular adipose tissue as a messenger of the brain-vessel axis: Role in vascular inflammation and dysfunction. *J Physiol Pharmacol*, *58*(4), 591–610.

Habecker, B. A., Bilimoria, P., Linick, C., Gritman, K., Lorentz, C., Woodward, W., & Birren, S. (2008). Regulation of cardiac innervation and function via the p75 neurotrophin receptor. *Aut Neurosci*, *140*(1–2), 40–48.

Hallböök, F., Ibáñez, C. F., & Persson, H. (1991). Evolutionary studies of the nerve growth factor family reveal a novel member abundantly expressed in xenopus ovary. *Neuron*, *6*(5), 845–858.

Hapner, S. J., Boeshore, K. L., Large, T. H., & Lefcort, F. (1998). Neural differentiation promoted by truncated trkC receptors in collaboration with p75(NTR). *Dev Biol*, *201*(1), 90–100.

Hassankhani, A., Steinhelper, M. E., Soonpaa, M. H., Katz, E. B., Taylor, D. A., Andrade-Rozental, A., … Federoff, H. J. (1995). Overexpression of NGF within the Heart of Transgenic Mice Causes Hyperinnervation, Cardiac Enlargement, and Hyperplasia of Ectopic Cells. *Dev Biol*, *169*(1), 309–321.

Head, R. (1989). Hypernoradrenergic innervation: its relationship to functional and hyperplastic changes in the vasculature of the spontaneously hypertensive rat. *Blood Vessels*, *26*(1), 1–20.

Heil, M., Eitenmüller, I., Schmitz-Rixen, T., & Schaper, W. (2006). Arteriogenesis versus angiogenesis: Similarities and differences. *J Cell Mol Med*, *10*(1), 45–55.

Henrichot, E., Juge-Aubry, C., Pernin, A., Pache, J., Velebit, V., & Dayer, J. (2005). Production of chemokines by perivascular adipose tissue. *Arter Thromb Vasc Biol*, *25*, 2594–2599.

Hiltunen, J., Arumäe, U., Moshnyakov, M., & Saarma, M. (1996). Expression of mRNAs for neurotrophins and their receptors in developing rat heart. *Circ Res*, *79*(5), 930–939.

Hiltunen, J., Laurikainen, A., Vakeva, A., Meri, S., & Saarma, M. (2001). Nerve growth factor and brain-derived neurotrophic factor mRNAs are regulated in distinct cell populations of rat heart after ischaemia and reperfusion. *J Pathol*, *194*(2), 247–253.

Hiroko Yano, Risa Torkin, Laura Andres Martin, Moses V. Chao, and K. K. T. (2009). Proneurotrophin-3 is a neuronal apoptotic ligand: evidence for retrograde-directed cell killing. *J Neurosci*, *25*(5), 14790–14802.

Hoeben, A., Landuyt, B., Highley, M., Wildiers, H., Van Oosterom, A., & De

Bruijin, E. (2004). Vascular Endothelial Growth Factor and Angiogenesis, *56*(4), 549–580.

Hohn, A., Leibrock, J., Bailey, K., & Barde, Y.-A. (1990). Identification and characterization of a novel member of the nerve growth factor/brain-derived neurotrophic factor family. *Nature*.

Howe, C. L., & Mobley, W. C. (2005). Long-distance retrograde neurotrophic signaling. *Curr Opin Neurobiol*, *15*(1), 40–48.

Hoyle, G. W. (2003). Neurotrophins and lung disease. *Cytokine Growth Factor Rev*, *14*(6), 551–558.

Huang, Eric, J., & Reichardt, Louis, F. (2001). Neurotrophins: Roles in Neuronal Development and Function. *Annu Rev Neurosci*, *24*, 677–736.

Huang, E. J., & Reichardt, L. F. (2003). Trk Receptors: Roles in Neuronal Signal Transduction. *Annu Rev Biochem*, *72*(1), 609–642.

Ieda, M., Kanazawa, H., Ieda, Y., Kimura, K., Matsumura, K., Tomita, Y., … Fukuda, K. (2006). Nerve growth factor is critical for cardiac sensory innervation and rescues neuropathy in diabetic hearts. *Circulation*, *114*(22), 2351–2363.

Ignarro, L. J., Buga, G. M., Byrns, R. E., Wood, K. S., & Chaudhuri, G. (1988). Endothelium-derived relaxing factor and nitric oxide possess identical pharmacologic properties as relaxants of bovine arterial and venous smooth muscle. *J Pharmacol Exp Ther*, *246*(1), 218–226.

Ivanov, S. V., Panaccione, A., Brown, B., Guo, Y., Moskaluk, C. A., Wick, M. J., … Yarbrough, W. G. (2013). TrkC signaling is activated in adenoid cystic carcinoma and requires NT-3 to stimulate invasive behavior. *Oncogene*, *32*(32), 3698–3710.

Jaffe, E. A., Nachman, R. L., Becker, C. G., & Minick, C. R. (1973). Culture of human endothelial cells derived from umbilical veins. Identification by morphologic and immunologic criteria. *J Clin Invest*, *52*(11), 2745–2756.

Jane de Lartigue. (2017). TRK Inhibitors Advance Rapidly in “Tumor-Agnostic” Paradigm. *Oncol Live*, 1–3. Retrieved from

https://www.onclive.com/publications/oncology-live/2017/vol-18-no-15/trk-inhibitors-advance-rapidly-in-tumoragnostic-paradigm

Justus, C., Leffler, N., Ruiz-Echevarria, M., & Yang, L. (2014). In vitro cell migration and invasion assays. *J Vis Exp*, *88*, 1–8.

Kaisho, Y., Shintani, A., Nishida, M., Fukumoto, H., & Igarashi, K. (1994). Developmental changes of neurotrophin-3 level in the mouse brain detected by a highly sensitive enzyme immunoassay. *Brain Res*, *666*(1), 143–146.

Karlsson, C., Lindell, K., Ottosson, M., Sjöström, L., Carlsson, B., & Carlsson, L. (1998). Human adipose tissue expresses angiotensinogen and enzymes required for its conversion to angiotensin II. *J Clin Endocrinol Metab*, *83*(11), 3925–3929.

Kawaguchi-Manabe, H., Ieda, M., Kimura, K., Manabe, T., Miyatake, S., Kanazawa, H., … Fukuda, K. (2007). A novel cardiac hypertrophic factor, neurotrophin-3, is paradoxically downregulated in cardiac hypertrophy. *Life Sci*, *81*(5), 385–392.

Keeler, A. B., & Deppmann, C. D. (2017). The evolutionary origins of antagonistic neurotrophin signaling, 3–5.

Kermani, P. & B. H. (2007). Kermani, *17*(4), 140–143.

Kermani, P., Rafii, D., Jin, D. K., Whitlock, P., Schaffer, W., Chiang, A., … Hempstead, B. L. (2005). Neurotrophins promote revascularization by local recruitment of TrkB+endothelial cells and systemic mobilization of hematopoietic progenitors. *J Clin Invest*, *115*(3), 653–663.

Ketonen, J., Shi, J., Martonen, E., & Mervaala, E. (2010). Periadventitial adipose tissue promotes endothelial dysfunction via oxidative stress in diet-induced obese C57Bl/6 mice. *Circ J*, *74*(7), 1479–1487.

Kisanuki, Y., Hammer, R., Miyasaki, J., Williams, S., Richardson, J., & Yanagisawa, M. (2001). Tie2-Cre transgenic mice: a new model for endothelial cell-lineage analysis in vivo. *Dev Biol*, *230*(2), 230–242.

Kolbeck, R., Jungbluth, S., & Barde, Y.-A. (1994). Characterisation of Neurotrophin Dimers and Monomers. *Eur J Biochem*, *225*(3), 995–1003.

Kraemer, R., Nguyen, H., March, K., & Hempstead, B. (1999). NGF activates similar intracellular signaling pathways in vascular smooth muscle cells as PDGF-BB but elicits different biological responses. *Arterioscler Thromb Vasc Biol*, *19*(4), 1041–1050.

Kreusser, M., Buss, S., Krebs, J., Kinscherf, R., Metz, J., Katus, H., … Backs, J. (2008). Differential expression of cardiac neurotrophic factors and sympathetic nerve ending abnormalities within the failing heart. *J Mol Cell Cardiol*, *44*(2), 380–387.

Krishna, M., & Narang, H. (2008). The complexity of mitogen-activated protein kinases (MAPKs) made simple. *Cell Mol Life Sci*, *65*(22), 3525–3544.

Lamballe, F., Smeyne, R. J., & Barbacid, M. (1994). Developmental expression of trkC, the neurotrophin-3 receptor, in the mammalian nervous system. *J Neurosci*, *14*(1), 14–28. Retrieved from http://www.ncbi.nlm.nih.gov/pubmed/8283230

Lamballe, F., Tapley, P., & Barbacid, M. (1993). trkC encodes multiple neurotrophin-3 receptors with distinct biological properties and substrate specificities. *EMBO J*, *12*(8), 3083–3094.

Lazarovici, P., Lahiani, A., Gincberg, G., Haham, D., Fluksman, A., Benny, O., … Lelkes, P. I. (2018). Nerve growth factor-induced angiogenesis: 1. Endothelial cell tube formation assay. *Methods Mol Biol*, *1727*, 239–250.

Lee, M., Chen, S., Tsao, C., & Wu, C. (2014). Perivascular Adipose Tissue Inhibits Endothelial Function of Rat Aortas via Caveolin-1. *PLoS One*, *9*(6), e99947.

Lee, R., Kermani, P., Teng, K. K., & Hempstead, B. L. (2001). Regulation of {Cell} {Survival} by {Secreted} {Proneurotrophins}. *Science (80-)*, *294*(5548), 1945–1948.

Lee, R., Kermani, P., Teng, K. K., & Hempstead, B. L. (2001). Regulation of cell survival by secreted proneurotrophins. *Science (80-)*, *294*(5548), 1945–1948.

Lee, R., Lu, C., Su, L., & Gao, Y. (2009). Endothelium-dependent relaxation factor

released by perivascular adipose tissue. *J Hypertens*, *27*(4), 782–790.

Lehman, S., Massaro, J., Schlett, C., O'Donnell, C., Hoffmann, U., & Fox, C. (2010). Peri-aortic fat, cardiovascular disease risk factors, andaortic calcification: the Framingham heart study. *Atherosclerosis*, *210*(2), 656–661.

Leßmann, V., & Brigadski, T. (2009). Mechanisms, locations, and kinetics of synaptic BDNF secretion: An update. *Neurosci Res*, *65*(1), 11–22.

Lewin, G. R., & Nykjaer, A. (2014). Pro-neurotrophins, sortilin, and nociception. *Eur J Neurosci*, *39*(3), 363–374.

Li, R., Andersen, I., Aleke, J., Golubinskaya, V., Gustafsson, H., & Nilsson, H. (2013). Reduced anti-contractile effect of perivascular adipose tissue on mesenteric small arteries from spontaneously hypertensive rats: role of Kv7 channels. *Eur J Pharmacol*, *698*, 310–315.

Liang, C. C., Park, A. Y., & Guan, J. L. (2007). In vitro scratch assay: A convenient and inexpensive method for analysis of cell migration in vitro. *Nat Protoc*, *2*(2), 329–333.

Lin, B., Pirrung, M. C., Deng, L., Li, Z., Liu, Y., & Webster, N. J. G. (2007). Neuroprotection by Small Molecule Activators of the, *322*(1), 59–69.

Lin, M. I., Das, I., Schwartz, G. M., Tsoulfas, P., Mikawa, T., & Hempstead, B. L. (2000). Trk C receptor signaling regulates cardiac myocyte proliferation during early heart development in vivo. *Dev Biol*, *226*(2), 180–191.

Lindvall, O., Ernfors, P., Bengzon, J., Kokaia, Z., Smith, M., Siesjö, B., & Persson, H. (1992). Differential regulation of mRNAs for nerve growth factor, brain-derived neurotrophic factor, and neurotrophin 3 in the adult rat brain following cerebral ischemia and hypoglycemic coma. *Proc Natl Acad Sci U S A*, *89*(2), 648–652.

Livak, K., & Schmittgen, T. (2001). Analysis of relative gene expression data using real-time quantitative PCR and the 2(-Delta Delta C(T)) Method. *Methods*, *25*(4), 402–408.

Lobato, N., Neves, K., Filgueira, F., Fortes, Z., Carvalho, M., Webb, R., & et al. (2012). The adipokine chemerin augments vascular reactivity to contractile

stimuli via activation of the MEK-ERK1/2 pathway. *Life Sci*, 600–606.

Lockhart, S., Mead, J., Pisano, J., Slonimsky, J., & Birren, S. (2000). Nerve growth factor collaborates with myocyte-derived factors to promote development of presynaptic sites in cultured sympathetic neurons. *J Neurobiol*, *42*(4), 460–476.

Lohn, M., Dubrovska, G., Lauterbach, B., Luft, F. C., Gollasch, M., & Sharma, A. M. (2002). Periadventitial fat releases a vascular relaxing factor. *FASEB J*, *16*, 1057–1063.

Longo, F. M., & Massa, S. M. (2013). Small-molecule modulation of neurotrophin receptors: a strategy for the treatment of neurological disease. *Nat Rev Drug Discov*, *12*(7), 507–525.

Lu, C., Su, L., Lee, R., & Gao, Y. (2010a).). Mechanisms for perivascular adiposetissue-mediated potentiation of vascular contraction to perivascularneuronal stimulation: the role of adipocyte-derived angiotensin II. *Eur J Pharmacol*, *635*(1–3), 107–112.

Lu, C., Su, L., Lee, R., & Gao, Y. (2010b). Mechanisms for perivascular adipose tissue-mediated potentiation of vascular contraction to perivascular neuronal stimulation: the role of adipocyte-derived angiotensin II. *Eur J Pharmacol*, *634*, 107–112.

Lumeng, C., Bodzin, I., & Saltiel, A. (2007). Obesity induces a phenotypic switch in adipose tissue macrophage polarization. *J Clin Invest*, *117*, 175–184.

Luther, J., & Birren, S. (2009). p75 and TrkA signaling regulates sympathetic neuronal firing patterns via differential modulation of voltage-gated currents. *J Neurosci*, *29*(17), 5411–5424.

Ly, K., Régent, A., Molina, E., Saada, S., Sindou, P., Le-Jeunne, C., … Jauberteau, M.-O. (2014). Neurotrophins are expressed in giant-cell arteritis lesions and may contribute to vascular remodeling. *Arthritis Res Ther*, *16*(6), 487.

Ma, L., Ma, S., He, H., Yang, D., Chen, X., Luo, Z., … Zhu, Z. (2010). Perivascular fat-mediated vascular dysfunction and remodeling through the AMPK/mTOR

pathway in high-fat diet-induced obese rats. *Hypertens Res*, *33*(5), 446–453.

Maisonpierre, P. C., Belluscio, L., Friedman, B., Alderson, R. F., Wiegand, S. J., Furth, M. E., … Yancopoulos, G. D. (1990). NT-3, BDNF, and NGF in the developing rat nervous system: Parallel as well as reciprocal patterns of expression. *Neuron*, *5*(4), 501–509.

Manning, B and Cantley, L. (2007). AKT/PBK signaling: Navigating Downstream. *Cell*, *129*(7), 1261–1274.

Marchesi, C., Ebrahimian, T., Angulo, O., Paradis, P., & Schiffrin, E. (2009). Endothelial nitric oxide synthase uncoupling and perivascularadipose oxidative stress and inflammation contribute to vasculardysfunction in a rodent model of metabolic syndrome. *Hypertension*, *54*, 1–18.

Martin-Zanca, D., Barbacid, M., & Parada, L. F. (1990). Expression of the trk proto-oncogene is restricted to the sensory cranial and spinal ganglia of neural crest origin in mouse development. *Genes Dev*, *4*(5), 683–694.

Martinelli, P. M., & Ribeiro, E. (2016). Neurotrophic Factors and Heart Diseases, *3*(1), 483–491.

Masutani, S., Cheng, H., Morimoto, A., Hasegawa, H., Han, Q., Little, W., & Cheng, C. (2013). β3-Adrenergic receptor antagonist improves exercise performance in pacing-induced heart failure. *Am J Physiol Hear Circ Physiol*, *305*(6), H923-30.

Matsuda, M., Shimomura, I., Sata, M., & et al. (2002). Role of adiponectin in preventing vascular stenosis. The missing link of adipo-vascular axis. *J Biol Chem*, *277*, 37487–37491.

Meloni, M., Caporali, A., Graiani, G., Lagrasta, C., Katare, R., Linthout, V., … Quaini, F. (2010). UKPMC Funders Group Nerve Growth Factor Promotes Cardiac Repair following Myocardial Infarction, *106*(7), 1275–1284.

Meloni, M., Cesselli, D., Caporali, A., Mangialardi, G., Avolio, E., Reni, C., … Emanueli, C. (2015). Cardiac nerve growth factor overexpression induces bone marrow-derived progenitor cells mobilization and homing to the infarcted heart. *Mol Ther*, *23*(12), 1854–1866.

Meloni, M., Descamps, B., Caporali, A., Zentilin, L., Floris, I., Giacca, M., & Emanueli, C. (2012). Nerve growth factor gene therapy using adeno-associated viral vectors prevents cardiomyopathy in type 1 diabetic mice. *Diabetes*, *61*(1), 229–240.

Mendizábal, Y., Llorens, S., & Nava, E. (2013). Vasoactive effects of prostaglandins from the perivascular fat of mesenteric resistance arteries in WKY and SHROB rats. *Life Sci*, *93*(25–26), 1023–1032.

Menn, B., Timsit, S., Calothy, G., & Lamballe, F. (1998). Differential Expression of TrkC Catalytic and Noncatalytic Isoforms Suggests That They Act Independently or in Association. *J Comp Neurol*, *401*, 47–64.

Menn, B., Timsit, S., Represa, A., Mateos, S., Calothy, G., & Lamballe, F. (2000). Spatiotemporal expression of noncatalytic TrkC NC2 isoform during early and late CNS neurogenesis: A comparative study with TrkC catalytic and p75(NTR) receptors. *Eur J Neurosci*, *12*(9), 3211–3223.

Meuchel, L., Townsend, E., Thompson, M., Pabelick, C., & Prakash, Y. (2010). *Effect of neurotrophin on NO generation in airway epithelial cells*. New Orleans, LA.

Meuchel, L. W., Thompson, M. A., Cassivi, S. D., Pabelick, C. M., & Prakash, Y. S. (2011). Neurotrophins induce nitric oxide generation in human pulmonary artery endothelial cells. *Cardiovasc Res*, *91*(4), 668–676.

Meyer, L., Ciaraldi, T., Henry, R., Wittgrove, A., & Phillips, S. (2013). Adipose tissue depot and cell size dependency of adiponectin synthesis and secretion in human obesity. *Adipocyte*, *2*(4), 217–226.

Meyer, M., Fredette, N., Barton, M., & Prossnitz, E. (2013). Regulation of vascular smooth muscle tone by adipose-derived contracting factor. *PLoS One*, *8*, e79245.

Mikolajczyk, T., Nosalski, R., Szczepaniak, P., Budzyn, K., Osmenda, G., Skiba, D., & et al. (2016). Role of chemokine RANTES in the regulation of perivascular inflammation, T-cell accumulation, and vascular dysfunction in hypertension. *FASEB J*, *30*, 1987–1999.

Mikolajczyk, T., Nosalski, R., Szczepaniak, P., Budzyn, K., Osmenda, G., Skiba, D., … Guzik, T. (2016). Role of chemokine RANTES in the regulation of perivascular inflammation, T-cell accumulation, and vascular dysfunction in hypertension. *FASEB J*, *30*(5), 1987–1999.

Moncada, S., Palmer, R., & Higgs, E. A. (1988). The discovery of nitric oxide as the endogenous nitrovasodilator, *12*(4), 365–372.

Moniotte, S., & Balligand, J. (2002). Potential use of beta(3)-adrenoceptor antagonists in heart failure therapy. *Cardiovasc Drug Rev*, *20*, 19–26.

Montesano, R., Orci, L., & Vassalli, P. (1983). In Vitro Rapid Organization of Endothelial Cells into Capillary-like Networks Is Promoted by Collagen Matrices. *J Cell Biol*, *97*, 1648–1652.

Montó, F., Oliver, E., Vicente, D., Rueda, J., Agüero, J., Almenar, L., … D'Ocon, P. (2012). Different expression of adrenoceptors and GRKs in the human myocardium depends on heart failure etiology and correlates to clinical variables. *Am J Physiol Hear Circ Physiol*, *303*(3), H368-76.

Morotti, A., Mila, S., Accornero, P., Tagliabue, E., & Ponzetto, C. (2002). K252a inhibits the oncogenic properties of Met, the HGF receptor. *Oncogene*, *21*(32), 4885–4893.

Mossman, T. (1983). Rapid colorimetric assay for cellular growth and survival: Application to proliferation and cytotoxicity assays. *J Inmunol Methods*, *65*(1–2), 55–63.

Murohara, T., Witzenbichler, B., Spyridopoulos, I., Asahara, T., Ding, B., Sullivan, A., … Isner, J. M. (1999). Endothelial Cell Migration.

Narisawa-Saito, M., & Nawa, H. (1996). Differential Regulation of Hippocampal Neurotrophins During Aging in Rats. *J Neurochem*, *67*(3), 1124–1131.

Nawa, H., Carnahan, J., & Gall, C. (1995). BDNF Protein Measured by a Novel Enzyme Immunoassay in Normal Brain and after Seizure: Partial Disagreement with mRNA Levels. *Eur J Neurosci*, *7*(7), 1527–1535.

Nedergaard, J., Bengtsson, T., & Cannon, B. (2007). Unexpected evidence for active brown adipose tissue in adult humans. *Am J Physiol Endocrinol*

Metab, *293*, E444-452.

Nemoto, K., Fukamachi, K., Nemoto, F., Miyata, S., Hamada, M., Nakamura, Y., … Ueyama, T. (1998). Gene expression of neurotrophins and their receptors in cultured rat vascular smooth muscle cells. *Biochem Biophys Res Commun*, *245*(1), 284–288.

Nicosia, R. F. (2009). The aortic ring model of angiogenesis: A quarter century of search and discovery. *J Cell Mol Med*, *13*(10), 4113–4136.

Nikolics, K. (1993). Identification of Neurotrophic Factors by Molecular Biological Techniques. In A. Boulton, G. Bake, & F. Hefti (Eds.), *Neurotrophic Factors* (pp. 25–55). Totowa, New Jersey: The Humana Press Inc.

Niu, X., Watts, V., Cingolani, O., Sivakumaran, V., Leyton-Mange, J., Ellis, C., … Barouch, L. (2012). Cardioprotective effect of beta-3 adrenergic receptor agonism: role of neuronal nitric oxide synthase. *J Am Coll Cardiol*, *59*(22), 1979–1987.

Nockher, W. A., & Renz, H. (2002). The role of neurotrophins in the pathogenesis of asthma and related diseases: Allergy and asthma as prototypic neuro-immune diseases? *Clin Exp Allergy*, *32*(9), 1266–1268.

Oana, F., Takeda, H., Hayakawa, K., Matsuzawa, A., Akahane, S., Isaji, M., & Akahane, M. (2005). Physiological difference between obese (fa/fa) Zucker rats and lean Zucker rats concerning adiponectin. *Metabolism*, *54*(8), 995–1001.

Okamoto, Y., Arita, Y., Nishida, M., & et al. (2000). An adipocyte-derived plasma protein, adiponectin, adheres to injured vascular walls. *Horm Metab Res*, *32*, 47–50.

Oliver, E., Flacco, N., Arce, C., Ivorra, M., D'Ocon, P., & Noguera, M. A. (2014). Changes in adrenoceptors and G-protein-coupled receptor kinase 2 in L-NAME-induced hypertension compared to spontaneous hypertension in rats. *J Vas Res*, *51*(3), 209–220.

Oliver, E., Rovira, E., Montó, F., Valldecabres, C., Julve, R., Muedra, V., … D'Ocon, P. (2010). beta-Adrenoceptor and GRK3 expression in human

lymphocytes is related to blood pressure and urinary albumin excretion. *J Hypertens*, *28*(6), 1281–1289.

Orshal, J., & Khalil, R. (2004). Interleukin-6 impairs endotheliumdependent NO–cGMP-mediated relaxation and enhances contraction in systemic vessels of pregnant rats. *Integr Comp Physiol*, *286*, R1013–R1023.

Ozen, G., Topal, G., Gomez, I., Ghorreshi, A., Boukais, K., Benyahia, C., … Norel, X. (2013). Control of human vascular tone by prostanoids derived from perivascular adipose tissue. *Prostaglandins Other Lipid Mediat*, *107*, 13–17.

Padilla, J., Jenkins, N. T., Vieira-Potter, V. J., & Laughlin, M. H. (2013). Divergent phenotype of rat thoracic and abdominal perivascular adipose tissues. *AJP Regul Integr Comp Physiol*, *304*(7), R543–R552.

Palko, M. E., Coppola, V., & Tessarollo, L. (1999). Evidence for a role of truncated trkC receptor isoforms in mouse development. *J Neurosci*, *19*(2), 775–782. Retrieved from http://www.ncbi.nlm.nih.gov/pubmed/9880597

Payne, G., Borbouse, L., Kumar, S., Neeb, Z., Alloosh, M., Sturek, M., & Tune, J. (2010). Epicardial perivascular adipose-derived leptin exacerbates coronary endothelial dysfunction in metabolic syndrome via a protein kinase C-beta pathway. *Arterioscler Thromb Vasc Biol*, *30*(9), 1711–1717.

Paz, N. G., & Amore, P. A. D. (2014). NIH Public Access, *335*(1), 5–16.

Peak, C., Cross, L., Shingh, A., & Gaharwar, A. (2015). Microscale Technologies for Engineering Complex Tissue Structures. In A. Singh & A. K. Gaharwar (Eds.), *MicroscaleTechnologies for Cell Engineering* (pp. 3–25).

Pepper, M. S. (1997). Transforming growth factor-beta: Vasculogenesis, angiogenesis, and vessel wall integrity. *Cytokine Growth Factor Rev*, *8*(1), 21–43.

Phillips, S. A., & Guazzi, M. (2015). The vasculature in cardiovascular diseases: Will the vasculature tell us what the future holds? *Prog Cardiovasc Dis*, *57*(5), 407–408.

Pius-Sadowska, E., & Machaliński, B. (2017). BDNF – A key player in cardiovascular system. *J Mol Cell Cardiol*, *110*, 54–60.

Plehm, R., Barbosa, M., & Bader, M. (2006). Animal models for hypertension/blood pressure recording. *Methods Mol Med*, *129*, 115–126.

Poelmann, R., & Gittenberger-de Groot, A. (2018). Hemodynamics in Cardiac Development. *J Cardiovasc Dev Dis*, *5*(4), 54.

Prakash, Y., Thompson, M., Meuchel, L., Pabelick, C., Mantilla, C., Zaidi, S., & Martin, R. (2010). Neurotrophins in lung health and disease. *Expert Rev Respir Med*, *4*(3), 395–411.

Quartu, M., Serra, M. P., Manca, A., Follesa, P., Ambu, R., & Del Fiacco, M. (2003). High affinity neurotrophin receptors in the human pre-term newborn, infant, and adult cerebellum. *Int J Dev Neurosci*, *21*(6), 309–320.

Rafii, S., Butler, J. M., & Ding, B. Sen. (2016). Angiocrine functions of organ-specific endothelial cells. *Nature*, *529*, 316–325.

Rajendran, P., Rengarajan, T., Thangavel, J., Nishigaki, Y., Sakthisekaran, D., Sethi, G., & Nishigaki, I. (2013). The vascular endothelium and human diseases. *Int J Biol Sci*, *9*(10), 1057–1069.

Ramirez, J., O'Malley, E., & Ho, W. (2017). Pro-contractile effects of perivascular fat inhealth and disease. *Br J Pharmacol*, *174*, 3482–3495.

Ramos-Ruiz, R., Penela, P., Penn, R., & Al, E. (2000). Analysis of the human G protein-coupled receptor kinase 2 (GRK2) gene promoter. Regulation by signal transduction systems in aortic smooth muscle cells. *Circulation*, *101*, 2083–2089.

Reichardt, L. F. (2006). Neurotrophin-regulated signalling pathways. *Philos Trans R Soc*, *361*, 1545–1564.

Rengo, G., Lymperopoulus, A., Leosco, D., & Koch, W. (2011). GRK2 as a novel gene therapy target in heart failure. *J Mol Cell Cardiol*, *50*, 785–792.

Ricci, A., Bronzetti, E., Mannino, F., Felici, L., Terzano, C., & Mariotta, S. (2004). Elevated neurotrophin and neurotrophin receptor expression in spontaneously hypertensive rat lungs. *Growth Factors*, *22*(3), 195–205.

Riedel, J., Badewien-Rentzsch, B., Kohn, B., Hoeke, L., & Einspanier, R. (2016).

Characterization of key genes of the renin-angiotensin system in mature feline adipocytes and during in vitro adipogenesis. *Physiol Anim Nutr*, *100*, 1139–1148.

Rodriguez, E. R., & Tan, C. D. (2017). Structure and Anatomy of the Human Pericardium. *Prog Cardiovasc Dis*, *59*(4), 327–340.

Roskoski, R. (2007). Vascular endothelial growth factor (VEGF) signaling in tumor progression. *Crit Rev Oncol Hematol*, *62*(3), 179–213.

Rudge, J. S., Li, Y., Pasnikowski, E. M., Mattsson, K., Pan, L., Yancopoulos, G. D., … Ip, N. Y. (1994). Neurotrophic Factor Receptors and Their Signal Transduction Capabilities in Rat Astrocytes. *Eur J Neurosci*, *6*(5), 693–705.

Sayago-Silva, I., Garcia-Lopez, F., & Segovia-Cubero, J. (2013). Epidemiology of heart failure in Spain over the last 20 years. *Rev Esp Cardiol*, *66*(8), 649–656.

Saygili, E., Schauerte, P., Küppers, F., Heck, L., Weis, J., Weber, C., … Rana, O. R. (2010). Electrical stimulation of sympathetic neurons induces autocrine/paracrine effects of NGF mediated by TrkA. *J Mol Cell Cardiol*, *49*(1), 79–87.

Scarisbrick, I. A., Jones, E. G., & Isackson, P. J. (1993). Coexpression of mRNAs for NGF, BDNF, and NT-3 in the cardiovascular system of the pre- and postnatal rat. *J Neurosci*, *13*(3), 875–893.

Schleifenbaum, J., Köhn, C., Voblova, N., Dubrovska, G., Zavarirskaya, O., Gloe, T., … Gollasch, M. (2010). Systemic peripheral artery relaxation by KCNQ channel openers and hydrogen sulfide. *J Hypertens*, *28*(9), 1875–1882.

Sennitt, M., Kaumann, A., Molenaar, P., Beeley, L., Young, P., Kelly, J., … Arch, J. (1998). The contribution of classical (beta1/2-) and atypical beta-adrenoceptors to the stimulation of human white adipocyte lipolysis and right atrial appendage contraction by novel beta3-adrenoceptor agonists of differing selectivities. *J Pharmacol Exp*, *285*(3), 1084–1095.

Shadiack, A., Sun, Y., & Zigmond, R. (2001). Nerve growth factor antiserum induces axotomy-like changes in neuropeptide expression in intact

sympathetic and sensory neurons. *J Neurosci*, *21*, 363–371.

Sharma, N., Deppmann, C., Harrington, A., St Hillaire, C., Chen, Z., Lee, F., & Ginty, D. (2010). Long-distance control of synapse assembly by target-derived NGF. *Neuron*, *67*(3), 422–434.

Sharma, N., & Waymack, J. (2018). Acute Cardiac Tamponade. Retrieved from www.ncbi.nlm.nih.gov/books/NBK534806/

Shelton, D. L., Sutherland, J., Gripp, J., Camerato, T., Armanini, M. P., Phillips, H. S., … Levinson3, A. D. (1995). Human trks: Molecular Cloning, Tissue Distribution, and Expression of Extracellular Domain Immunoadhesins. *J Neurosci*, *15*(l), 477–491.

Shen, L., Zeng, W., Wu, Y. X., Hou, C. L., Chen, W., Yang, M. C., … Zhu, C. H. (2013). Neurotrophin-3 accelerates wound healing in diabetic mice by promoting a paracrine response in mesenchymal stem cells. *Cell Transplant*, *22*(6), 1011–1021.

Shimazu, K., Zhao, M., Sakata, K., Akbarian, S., Bates, B., Jaenisch, R., & Lu, B. (2006). NT-3 facilitates hippocampal plasticity and learning and memory by regulating neurogenesis. *Learn Mem*, *13*(3), 307–315.

Sinha, S., Sridhara, S. R. C., Srinivasan, S., Muley, A., Majumder, S., Kuppusamy, M., … Chatterjee, S. (2011). NO (nitric oxide): The ring master. *Eur J Cell Biol*, *90*(1), 58–71.

Soltis, E. E., & Cassis, L. A. (1991). Influence of perivascular adipose tissue on rat aortic smooth muscle responsiveness. *Clin Exp Hypertens A*, *13*(2), 277–296. Retrieved from http://www.ncbi.nlm.nih.gov/pubmed/2065467

Song, W., Volosin, M., Cragnolini, A. B., Hempstead, B. L., & Friedman, W. J. (2010). ProNGF Induces PTEN via p75NTR to Suppress Trk-Mediated Survival Signaling in Brain Neurons. *J Neurosci*, *30*(46), 15608–15615.

Sornelli, F., Fiore, M., Chaldakov, G. N., & Aloe, L. (2009). Adipose tissue-derived nerve growth factor and brain-derived neurotrophic factor : results from experimental stress and diabetes. *Neurobiology*, *1*, 179–183.

Srivastava, D., & Olson, E. (1996). Neurotrophin-3 knocks heart off Trk. *Nat Med*,

2, 1069–1071.

Staton, C. A., Reed, M. W. R., & Brown, N. J. (2009). A critical analysis of current in vitro and in vivo angiogenesis assays. *Int J Exp Pathol*, *90*(3), 195–221.

Story, G., Dicarlo, S., Rodenbaugh, D., Dluzen, D., Kucera, J., Maron, M., & Walro, J. (2000). Inactivation of one copy of the mouse neurotrophin-3 gene induces cardiac sympathetic deficits. *Physiol Genomics*, *2*(3), 129–136.

Su, Y. W., Chung, R., Ruan, C. S., Chim, S. M., Kuek, V., Dwivedi, P. P., … Xian, C. J. (2016). Neurotrophin-3 Induces BMP-2 and VEGF Activities and Promotes the Bony Repair of Injured Growth Plate Cartilage and Bone in Rats. *J Bone Miner Res*, *31*(6), 1258–1274.

Subalakshmi, M., Saranya, A., Uma, M., Jarina, A., Kavimani, S., & Mural, R. (2014). an Overview of the Current Methodologies Used for Activity. *Int J Exp Pharmacol*, *4*(2), 127–131.

Sukhovershin, R. A., Yepuri, G., & Ghebremariam, Y. T. (2015). Endothelium-Derived Nitric Oxide as an Antiatherogenic Mechanism: Implications for Therapy. *Methodist Debakey Cardiovasc J*, *11*(3), 166–171.

Takeo, C., Nakamura, S., Tanaka, T., Uchida, D., Noguchi, Y., Nagao, T., … Tatsuno, I. (2003). Rat cerebral endothelial cells express trk C and are regulated by neurotrophin-3. *Biochem Biophys Res Commun*, *305*(2), 400–406.

Tanai, E., & Frantz, S. (2015). Pathophysiology of Heart Failure. *Compr Physiol*, *6*(1), 187–214.

Tessarollo, L. (1998). Pleiotropic functions of neurotrophins in development. *Cytokine Growth Factor Rev*, *9*(2), 125–137.

Tessarollo, L., Tsoulfas, P., Donovan, M. J., Palko, M. E., Blair-Flynn, J., Hempstead, B. L., & Parada, L. F. (1997). Targeted deletion of all isoforms of the trkC gene suggests the use of alternate receptors by its ligand neurotrophin-3 in neuronal development and implicates trkC in normal cardiogenesis. *Proc Natl Acad Sci U S A*, *94*(26), 14776–14781.

Tessarollo, L., Tsoulfas, P., Martin-Zanca, D., Gilbert, D. J., Jenkins, N. A.,

Copeland, N. G., & Parada, L. F. (1993). trkC, a receptor for neurotrophin-3, is widely expressed in the developing nervous system and in non-neuronal tissues. *Development*, *118*(2), 463–475.

Tessarollo, L., Vogel, K. S., Palko, M. E., Reid, S. W., & Parada, L. F. (1994). Targeted mutation in the neurotrophin-3 gene results in loss of muscle sensory neurons. *Proc Natl Acad Sci*, *91*(25), 11844–11848.

Thoenen, H. (1972). Comparison between the effect of neuronal activity and nerve growth factor on the enzymes involved in the synthesis of norepinephrine. *Pharmacol Rev*, *24*(2), 255–267.

Timsit, S., Calothy, G., & Lamballe, F. (1998). Differential Expression of TrkC Catalytic and Noncatalytic Isoforms Suggests That. *J Comp Neurol*, *64*(July), 47–64.

Tousoulis, D., Kampoli, A.-M., Tentolouris, C., Papageorgiou, N., & Stefanadis, C. (2012). The role of nitric oxide on endothelial function. *Curr Vasc Pharmacol*, *10*(1), 4–18.

Tremel, A., Cai, A., Tirtaatmadja, N., Hughes, B. D., Stevens, G. W., Landman, K. A., & O'Connor, A. J. (2009). Cell migration and proliferation during monolayer formation and wound healing. *Chem Eng Sci*, *64*(2), 247–253.

Truzzi, F., Marconi, A., Lotti, R., Dallaglio, K., French, L. E., Hempstead, B. L., & Pincelli, C. (2008). Neurotrophins and their receptors stimulate melanoma cell proliferation and migration. *J Invest Dermatol*, *128*(8), 2031–2040.

Tsoulfas, P., Soppet, D., Escandon, E., Tessarollo, L., Mendoza-Ramirez, J. L., Rosenthal, A., … Parada, L. F. (1993). The rat trkC locus encodes multiple neurogenic receptors that exhibit differential response to neurotrophin-3 in PC12 cells. *Neuron*, *10*(5), 975–990.

Valenzuela, D. M., Maisonpierre, P. C., Glass, D. J., Rojas, E., Nuñez, L., Kong, Y., … Yancopoulos, G. D. (1993). Alternative forms of rat TrkC with different functional capabilities. *Neuron*, *10*(5), 963–974.

Vallejo, S., Romancho, T., Angulo, J., Villalobos, L., Cercas, E., & Leivas, A. (2011). Visfatin impairs endothelium-dependent relaxation inrat and human

mesenteric microvessels through nicotinamidephosphoribosyltransferase activity. *PLoS One*, *6*(11), e27299.

Verlohren, S., Dubrovska, G., Tsang, S. Y., Essin, K., Luft, F. C., Huang, Y., & Gollasch, M. (2004). Visceral periadventitial adipose tissue regulates arterial tone of mesenteric arteries. *Hypertension*, *44*(3), 271–276.

Vicente, D., Hernandez, B., Segura, V., Pascual, D., Fornaciari, G., Monto, F., … D'oco. (2016). Methodological Approach to Use Fresh and Cryopreserved Vessels as Tools to Analyze Pharmacological Modulation of the Angiogenic Growth. *J Cardiovasc Pharmacol*, *68*(3), 230–240.

Vicente, D., Montó, F., Oliver, E., Buendía, F., Rueda, J., Agüero, J., … D'Ocon, P. (2013). Myocardial and lymphocytic expression of eNOS and nNOS before and after heart transplantation: relationship to clinical status. *Life Sci*, *93*, 108–115.

Vigers, A. J., Baquet, Z. C., & Jones, K. R. (2000). Expression of neurotrophin-3 in the mouse forebrain: Insights from a targeted lacZ reporter. *J Comp Neurol*, *416*(3), 398–415.

Villacorta, L., Arbor, A., Campus, N., & Arbor, A. (2015). HHS Public Access, *21*(2), 137–147.

Virdis, A., Duranti, F., Rossi, C., Dell'Agnello, U., Santini, E., Anselmino, M., & et al. (2015). Tumour necrosis factor-alpha participates on the endothelin-1/nitric oxide imbalance in small arteries from obese patients: role of perivascular adipose tissue. *Eur Hear J*, (36), 784–794.

Wang, S., Bray, P., McCaffrey, T., March, K., Hempstead, B. L., & Kraemer, R. (2000). p75(NTR) mediates neurotrophin-induced apoptosis of vascular smooth muscle cells. *Am J Pathol*, *157*(4), 1247–1258.

Watts, S., Dorrance, A., Penfold, M., Rourke, J., Sinal, C., Seitz, B., & et al. (2013). Chemerin connects fat to arterial contraction. *Arter Thromb Vasc Biol*, *33*, 1320–1328.

Werner, P., Paluru, P., Simpson, A., Latney, B., Iyer, R., Brodeur, G., & Goldmuntz, E. (2014). Mutations in NTRK3 suggest a novel signaling

pathway in human congenital heart disease. *Hum Mutat*, *35*, 1459–1468.

Werner, P., Paluru, P., Simpson, A. M., Latney, B., Iyer, R., Brodeur, G. M., & Goldmuntz, E. (2015). NIH Public Access, *35*(12), 1459–1468.

Withers, S., Bussey, C., Saxton, S., Melrose, H., Watkins, A., & Heagerly, A. (2014). Mechanisms of adiponectin-associated perivascular function in vascular disease. *Arterioscler Thromb Vasc Biol*, *34*(8), 1637–1642.

Xie, D., Ju, D., Speyer, C., Gorski, D., & Kosir, M. A. (2016). Strategic Endothelial Cell Tube Formation Assay: Comparing Extracellular Matrix and Growth Factor Reduced Extracellular Matrix. *J Vis Exp*, (114), 1–5.

Xiong, H., Yamada, K., Han, D., Nabeshima, T., Enikolopov, G., Carnahan, J., & Nawa, H. (1999). Mutual regulation between the intercellular messengers nitric oxide and brain-derived neurotrophic factor in rodent neocortical neurons. *Eur J Neurosci*, *11*(5), 1567–1576.

Xu, M., Remillard, C. V, Sachs, B. D., Makino, A., Yao, W., Dillmann, W. H., … Yuan, J. X. (2008). P75 Neurotrophin Receptor Regulates Agonist-Induced Pulmonary Vasoconstriction Pulmonary Vasoconstriction. *Am J Physiol Hear Circ Physiol*, *295*(August 2008), 1529–1539.

Yamauchi, J., Chan, J. R., & Shooter, E. M. (2004). Neurotrophins regulate Schwann cell migration by activating divergent signaling pathways dependent on Rho GTPases. *Proc Natl Acad Sci U S A*, *101*(23), 8774–8779.

Yao, Q., Song, R., Ao, L., Zhan, Q., Cleveland, J. C., Yu, X., … Meng, X. (2015). Over-expression of neurotrophin 3 in human aortic valves affected by calcific disease induces the osteogenic responses via the Trk-Akt pathway. *Biochim Biophys Acta - Mol Basis Dis*, *1852*(9), 1940–1949.

Youn, Y. H., Feng, J., Tessarollo, L., Ito, K., & Sieber-Blum, M. (2003). Neural crest stem cell and cardiac endothelium defects in the TrkC null mouse. *Mol Cell Neurosci*, *24*(1), 160–170.

Zanin, J. P., Abercrombie, E., & Friedman, W. J. (2016). Proneurotrophin-3 promotes cell cycle withdrawal of developing cerebellar granule cell

progenitors via the p75 neurotrophin receptor. *Elife*, *5*(JULY), 1–21.

Zanin, J. P., Battiato, N. L., & Rovasio, R. A. (2013). Neurotrophic factor NT-3 displays a non-canonical cell guidance signaling function for cephalic neural crest cells. *Eur J Cell Biol*, *92*(8–9), 264–279.

Zhang, J., Shi, Q., Yang, P., Xu, X., Chen, X., Qi, C., … Liu, Y. (2012). Neuroprotection of neurotrophin-3 against focal cerebral ischemia/reperfusion injury is regulated by hypoxia-responsive element in rats. *Neuroscience*, *222*, 1–9.

Zhang, S. H., & Rush, R. A. (2001). Neurotrophin 3 is increased in the spontaneously hypertensive rat. *J Hypertens*, *19*(12), 2251–2256.

Zhang, W., Kitagawa, H., Hayashi, T., Sasaki, C., Sakai, K., Warita, H., … Abe, K. (1999). Topical application of neurotrophin-3 attenuates ischemic brain injury after transient middle cerebral artery occlusion in rats. *Brain Res*, *842*(1), 211–214.

Zhao, Y., Vanhoutte, P. M., & Leung, S. W. S. (2015). Vascular nitric oxide: Beyond eNOS. *J Pharmacol Sci*, *129*(2), 83–94.

Zhou, X. F., & Rush, R. (1995). Sympathetic neurons in neonatal rats require endogenous neurotrophin-3 for survival. *J Neurosci*, *15*(10), 6521–6530.

Zhou, X. F., & Rush, R. A. (1996). Functional roles of neurotrophin 3 in the developing and mature sympathetic nervous system. *Mol Neurobiol*, *13*(3), 185–197.

VIII APPENDIX